The Involvement of CaMKII in Myocardial Ischaemia-Reperfusion Injury

Osian Llwyd

2012

A thesis submitted in partial fulfillment of the requirements
for the degree of Doctor of Philosophy

Declaration

This work has not been submitted in substance for any other degree or award at this or any other university or place of learning, nor is being submitted concurrently in candidature for any degree or other award.

Signed:

STATEMENT 1

This thesis is being submitted in partial fulfillment of the requirements for the degree of PhD

Signed:

STATEMENT 2

This thesis is the result of my own independent work/investigation, except where otherwise stated. Other sources are acknowledged by explicit references. The views expressed are my own.

Signed:

STATEMENT 3

I hereby give consent for my thesis, if accepted, to be available for photocopying and for inter-library loan, and for the title and summary to be made available to outside organisations.

Signed:

Abstract

CaMKII acts as a second messenger to Ca^{2+} signals within the cardiac myocyte. Cellular stresses such as ischaemia and subsequent reperfusion perturb the normal physiological oscillations of Ca^{2+} to cause an escalating concentration which damages the cell. CaMKII has been implicated as an injury signal during such cellular conditions. However, there are discrepancies as to whether CaMKII is a possible mechanism of ischaemic preconditioning as its inhibition can abrogate or improve the protective effect of preconditioning. This thesis investigated the effects of CaMKII inhibition in models of ischaemia-reperfusion (I-R) injury. It was hypothesised that CaMKII promotes irreversible injury caused by acute myocardial infarction (AMI), but would also have a beneficial role in mediating cardioprotection by ischaemic preconditioning. This work has demonstrated that: i) in an *ex vivo* rat heart model of regional I-R injury, CaMKII promoted irreversible injury but is not a feasible target for reperfusion therapy as only a pre-ischaemic intervention reduced myocardial infarction; ii) CaMKII activation was not a pre-requisite for protection with ischaemic preconditioning, although an additive protective effect of CaMKII inhibition and ischaemic preconditioning was possible; iii) models of simulated I-R or oxidative stress in the H9c2 cells did not involve CaMKII activity; iv) isolated cardiac myocytes paced at 1Hz and subjected to simulated I-R do not engage a significant amount of CaMKII activity. These studies substantiate the involvement of CaMKII during ischaemic injury and establish that it does not play a substantial role in ischaemic preconditioning. It highlights the characteristics of the kinase within *in vitro* models of I-R injury. Understanding CaMKII role in I-R may underpin the development of future therapeutic strategies for the management of AMI.

Acknowledgments

A big *diolch* to everyone that has been involved with this thesis.

Diolch o galon to Gary, for opening the door to new opportunities within the field of I-R injury, and giving me the competence to delve further into the subject. This is also extended to everyone (past and present) in team GB, but in particular top boy Dwaine for passing on his Langendorff skills. *Diolch* to everyone within the Tenovus research group for letting me use their cell culture facilities and making it so enjoyable. *Diolch* also to Chris George, for your time, expertise and showing me the other dimension to calcium signaling.

Diolch yn arbennig i Dad a Mam, am eu cariad a'u cefnogaeth, nid yn unig dros y cyfnod diweddar ond ar hyd y blynyddoedd. A Rhun, ti'n gwbod bod fi'n gwerthfawrogi fe bra.

Ελένη, ευχαριστώ πολύ, που μου έδωσες μια άλλη ζωή!

And last but not least, a big *diolch* to Henning Wackerhage for rekindling my appetite for research.

Nid wy'n gofyn bywyd moethus, / I’d not ask a life that’s easy,
Aur y byd na'i berlau mân: / Gold and pearls so little mean,
Gofyn wyf am galon hapus, / Rather seek a heart that’s joyful,
Calon onest, calon lân. / Heart that’s honest, heart that’s clean.
Daniel James (1848-1920) / translated by Daniel Cowen

Table of Contents

List of Abbreviations

$[ion]_i$ - Intracellular ion concentration

$[ion]_0$ - Extracellular ion concentration

2-DG - 2-Deoxyglucose

AIP - Autocamtide-2 related inhibitory peptide

AMI - Acute Myocardial Infarction

ATP - Adenosine Triphosphate

CaM - Calmodulin

CaMKII - Ca^{2+}/Calmodulin Dependant Protein Kinase II

CAO - Coronary Artery Occlusion

CaV - Voltage-gated Ca^{2+} channels

CFR - Coronary Flow Rate

cGMP - Cyclic Guanosine Monophosphate

CHD - Coronary Heart Disease

CICR - Calcium Induced Calcium Release

CREB - Cyclic AMP response element-binding protein

CVD - Cardiovascular Disease

DAD - Delayed afterdepolarisation

EAD - Early afterdepolarisation

E-C coupling - Excitation-Contraction Coupling

ECG - Electrocardiogram

ER - Endoplasmic Reticulum

GM - Genetically Modified

GPCR - G-protein coupled receptors

HF - Heart Failure

HR - Heart Rate

$I_{Ca.L}$ - Ca^{2+} current

I_K - K^+ current

I_{Na} - Na^+ current

$InsP_3$ - Inositol 1,4,5-triphosphate

I-R - Ischaemia Reperfusion

IHA - Intermittent High Altitude Hypoxia

IP_3R - Inositol 1,4,5-triphosphate Receptor

IPC - Ischaemic Preconditioning

ITN - Inter Transient Noise

LDH - Lactate Dehydrogenase

LTCC - L-Type Ca^{2+} Channel

LVDP - Left Ventricle Developed Pressure

LVH - Left Ventricle Hypertrophy

MI - Myocardial Infarction

mPTP - Mitochondrial Permeability Transition Pore

NaV - Voltage-gated Na^{+} channels

NCX - Na^{+}/Ca^{2+} Exchanger

NFAT - Nuclear Factor of activated T cells

NHE - Na^{+} Hydrogen Exchange

NO - Nitric Oxide

NSTEMI - Non ST-Segment Elevation Myocardial Infarction

PBS - Phosphate Buffered Saline

PCI - Percutaneous Coronary Intervention

PKG - cGMP-dependant protein kinase

PLB - Phospholamban

Po - Open probability

PLC - Phospholipase C

PI3K - Phosphatidylinositol 3-kinases

PKC - Protein Kinase C

PKA - Protein Kinase A

RISK - Reperfusion Injury Salvageable Kinases

RYR2 - Ryanodine Receptor

ROS - Reactive Oxygen Species

ROI - Region of Interest

RPP - Rate Pressure Product

SERCA2a - Sarco/endoplasmic reticulum Ca^{2+}-ATPase pump

SR - Sarcoplasmic Reticulum

STEMI - ST-Segment Elevation Myocardial Infarction

TUNEL - Terminal deoxynucleotidyl transferase dUTP nick end labeling

Vfib - Ventricular Fibrillation

List of Figures & Tables

Figures

Tables

CHAPTER 1:
General Introduction

1.1. Ca^{2+} Signalling in the Cardiac Myocyte

Calcium is an alkaline earth metal that adopts a divalent cation (Ca^{2+}) when present freely in water. It binds readily to other molecules and has evolved into an intracellular signal that is essential and with diverse effects in all living cells. The cardiac myocyte provides an example of the varied signalling effects of Ca^{2+}. These signalling functions include: muscle contraction and mechanical movement of the cell (Bers, 2000); the stimulation of energy production to 'parallel' the cell's energy demand (Griffiths & Rutter, 2009); co-ordination and regulation of gene transcription and DNA synthesis (Bootman et al., 2009); instigation of auto digestion of organelles or promotion of cell death (Høyer-Hansen and Jääattelä, 2007).

In many cases, Ca^{2+} acts as an intracellular second messenger to the numerous ligands that target cell membranes. The cell receptors pick up and relay the distant hormonal or neuronal signals to specific molecules within the cytosol or organelles by means of Ca^{2+} signalling. As its cation properties allow a high affinity towards an array of intracellular proteins, it can influence several physiological activities. When bound to a protein Ca^{2+} can change the conformation of the molecule and thus alter its activity in a signalling cascade.

Ca^{2+} signalling is accomplished when the cells distinguish the change in intracellular Ca^{2+} concentration ($[Ca^{2+}]_i$) for a given location (Berridge, 2009). Whether the transient delivery of the ion is global or localised it can also provide a valuable electrochemical gradient that is used by the cells as a source of stored energy (Sheu and Fozzard, 1982). Recent advances have been made in understanding how the cell handles small and subtle localisation of $[Ca^{2+}]_i$ and the way this is interpreted by organelles to produce specific cellular effects (Laude and Simpson, 2009).

1.1.1. Excitation-Contraction Coupling

Cardiac myocytes are excitable cells since they respond to an electrical impulse (e.g. an action potential) with a rapid physical contraction. Broadly termed excitation-contraction coupling (Sandow, 1952), Ca^{2+} has two roles to play in this process. The first is during the excitation of the cells, when an action potential depolarises the intracellular space and allows extracellular Ca^{2+} to enter the cell via voltage-gated Ca^{2+} channels (CaV). The second action occurs in response to the influx of Ca^{2+}, which releases additional Ca^{2+} from the sarcoplasmic reticulum (SR). A global discharge of stored Ca^{2+} will then flood the myofilaments, leading to cell shortening and effecting systolic contraction of the myocardium. For relaxation of the muscle and diastolic filling to occur, removal of Ca^{2+} from the cytosol is necessary to complete the cycle, by activation of ionic pumps and exchangers positioned on the SR and sarcolemma.

1.1.1.2. The Cardiac Action Potential

The difference in ion concentration either side of the plasma membrane creates an intracellular potential within all cells. This electrical charge can fluctuate in excitable cells (figure 1.1) to form an action potential and provide a specific electrical stimulus. In ventricular myocytes, during diastolic relaxation, the resting membrane potential (termed phase 4) is around -80 to -90 mV (Zaza and Rosen, 2000).

Stimulated by an action potential (or a propagating impulse) that is conducted throughout the heart, a sufficient amount of voltage-gated Na^{+} channels (NaV) will allow Na^{+} ions to enter the cell down an electrochemical gradient (145 mM to 20 mM; Klabunde, 2011). This movement activates the remaining NaV to allow an inward Na^{+} current (I_{Na}), which rapidly depolarises (phase 0) the cell. CaV1.2 channels, also known as L-type Ca^{2+} channels (as it is a long lasting current, LTCC) have a threshold of

around -40 to -30 mV for opening and conducting an inward Ca^{2+} current ($I_{Ca.L}$). Also acting down an electrochemical gradient (from 2.5 mM to 0.1 µM), the $I_{Ca.L}$ is small enough for it not to be distinguishable in the large upward deflection of the I_{Na} (figure 1.1).

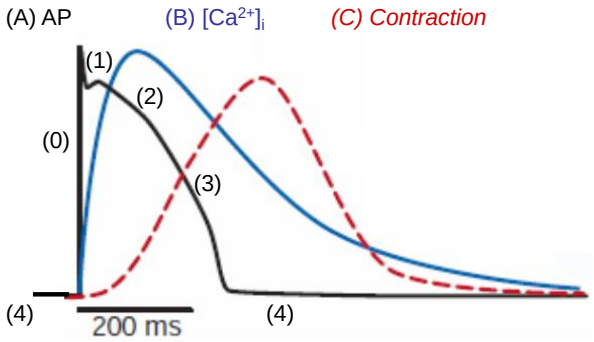

Figure 1.1: Time course of excitation-contraction coupling in a rabbit ventricular myocyte (adapted from Bers, 2002). *(A) The shape and five phases (0-4) of an action potential (AP): phase 0, rapid depolarisation; phase 1, early rapid repolarisation; phase 2, plateau; phase 3, final rapid repolarisation; phase 4, resting membrane potential. (B) The transient $[Ca^{2+}]_i$ instigated by the action potential. (C) Cell contraction and relaxation corresponding with the rise and fall of $[Ca^{2+}]_i$.*

An early notch (phase 1), that is particularly prominent in myocytes of subepicardial origin, is created by a combination of the inactivation of I_{Na} and the activation of several outward K^+ (particularly I_{to}) and Cl^- currents. This rapid repolarisation towards 0 mV is short lived as the action potential forms a plateau (phase 2). This can last for several hundred milliseconds as the combination of the outward current (mainly I_{to}) and the inward current $I_{Ca.L}$ equilibrate each other's charges.

The final rapid repolarisation (phase 3) is due to the inactivation of LTCC and the activation of other repolarising K^+ currents (Barry and Nerbonne, 1996). The K^+

currents vary in their characteristics and include: the slow and rapid components of the delayed rectifier K^+ current known as I_{Ks} and I_{Kr} respectively; and the inwardly rectifying K^+ currents, I_{K1} and I_{KAch}. The delayed rectifier K^+ currents (I_{Ks} and I_{Kr}) close at a threshold of -80 mV after repolarisation has occurred and there is a return towards the resting membrane potential (Phase 4). I_{K1} maintains the current towards the K^+ equilibrium potential and is absent from sinus node and AV node cells allowing them to spontaneously gradually depolarize (automaticity). I_{KAch} is however enriched in the nodal cells allowing them to hyperpolarize the cell and slow the activation of action potentials and heart rate. They also differ to the voltage-gated ion channels as they are activated by G-proteins. Here, a signalling cascade is regulated by membrane bound receptors (G-protein coupled receptors, GPCR) that regulate the release of G-protein subunits (in this case the Gβγ subtype) that target the ion channel.

Exchanging ions is another method for regulating ion currents. Exchange has the advantage of being activated at certain ionic thresholds during the action potential. The Na^+/Ca^{2+} exchanger (NCX) moves one Ca^{2+} ion across the cell membrane in exchange for three Na^+ ions. During phase 2, when there is a sudden rise in $[Ca^{2+}]_i$, Na^+ is exchanged for the internal Ca^{2+} via the NCX in its forward mode (Weber et al., 2003). A reverse mode also exists briefly during phase 1 when there is a spike in the intracellular Na^+ concentration. A Na^+/K^+-ATPase exists to exchange three Na^+ ions for two K^+ ions. This is dependent on ATP to concurrently pump Na^+ out of the cell in exchange for K^+ to enter the cell (Hilgemann et al., 2006). Working against their chemical gradients, this movement of ions maintains the resting potential and drives the difference in ionic concentrations across the cell membrane.

1.1.1.3. Calcium-Induced Calcium Release

A key feature of excitation-contraction coupling in cardiac myocytes is the way that the extracellular Ca^{2+} is used as a trigger for release of large pools of intracellular Ca^{2+} (figure 1.2; Fabiato, 1983). Known as calcium-induced calcium release (CICR), several possible mechanisms have been proposed. The most widely accepted hypothesis involves $I_{Ca.L}$ (Bers, 2002). Other possibilities, such as Ca^{2+} entry via the NCX, may have a modest effect, but are believed to be more prominent under abnormal conditions (Bers, 2000).

The localisation of the LTCC and the ryanodine receptor (RYR2; cardiac muscle ryanodine receptor isoform), which acts as a Ca^{2+} release channel for the SR, underpins one of the key arguments for the CICR (Orchard and Brette, 2008). Assisted by the T tubules that extend the extracellular matrix into the cell, each LTCC positioned on these tubules administers Ca^{2+} to 6-20 RYR2 (Bridge et al., 1999; Bers, 2002). The junctional regions between the T tubule and the SR allow a short and direct interaction of the Ca^{2+} that enters through the LTCC.

The RYR2 has been thoroughly characterised and revealed to make molecular conformational changes that release Ca^{2+} from the SR when activated by Ca^{2+} (Tunwell et al., 1996). Four RYR2 monomer proteins associate to form the Ca^{2+} release channel. The foot region acts as a scaffolding protein which allows the binding of other proteins such as kinases and phosphatases close to the junctional complexes. One of the proteins, called FKBP-12.6, acts to stabilise these regions. This allows 'coupled gating' of the numerous clusters of RYR2 that then co-ordinates the release of Ca^{2+} in synchrony (Marx et al., 2001). Collectively, a substantial discharge of stored Ca^{2+} results in a spike of $[Ca^{2+}]_i$. Contraction of the cell occurs when the surplus of Ca^{2+} binds to troponin C. This promotes the interaction between myosin heads and actin

filaments which results in rapid shortening of the sarcomere and a systolic contraction of the myocyte.

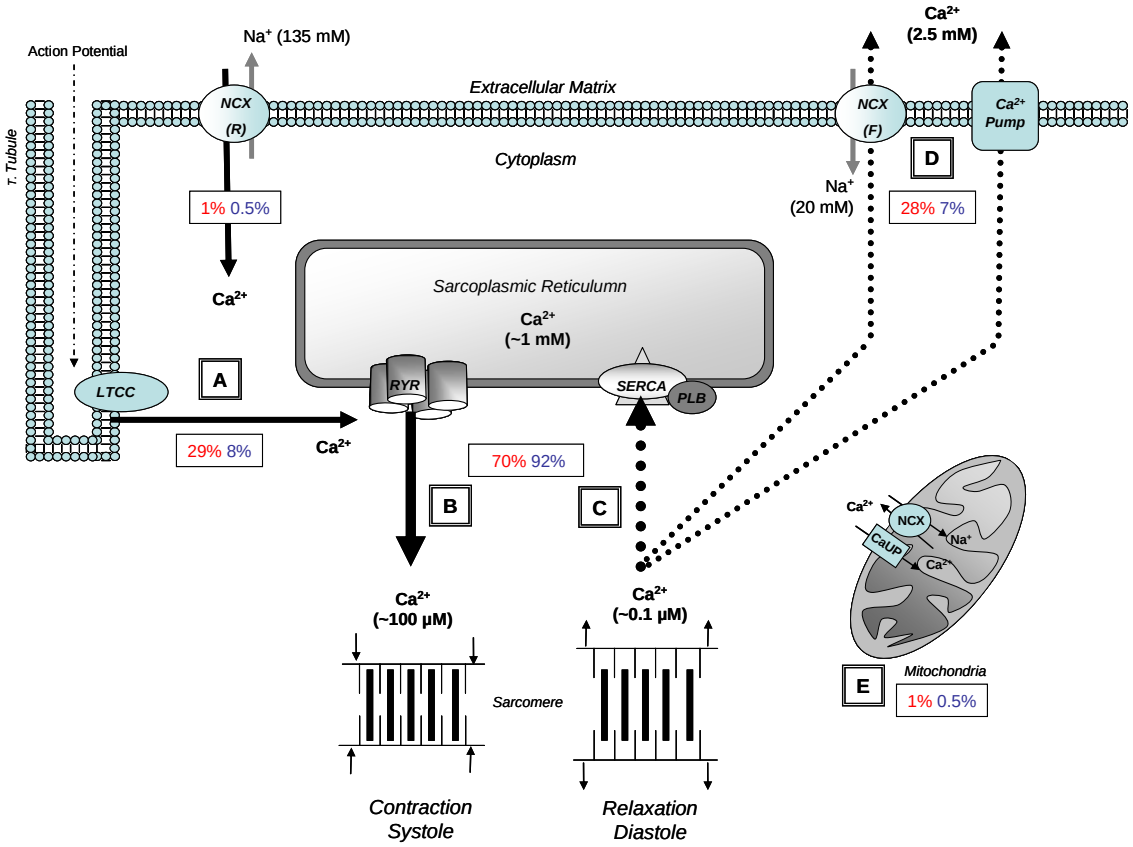

Figure 1.2: Contraction-relaxation cycle of a cardiac myocyte, with particular focus on the total Ca^{2+} movement and concentration of calcium-induced calcium release. *(A) The depolarising current travels down a T. tubule allowing the LTCC threshold to trigger Ca^{2+} entry. (B) Ca^{2+} entry triggers further release of Ca^{2+} from intracellular stores such as the SR, using RYR2 causing a flood of Ca^{2+} towards myofilaments.(C) Relaxation can only begin with the removal of Ca^{2+} back into the SR and (D) through sarcolemmal transporters. (E) Other organelles such as the mitochondria play a minor part in buffering any excess Ca^{2+} and use it to sense the altering transients to parallel production of ATP with contraction. The relative percentages of Ca^{2+} cycled per compartment for a human (red) and rat (blue) ventricle cell is also described (data taken from Bers, 2000). LTCC, L-type Ca^{2+} channel; RYR2, ryanodine receptor; PLB, phospholamban; SERCA2a, Sarco/Endoplasmic Reticulum Ca^{2+}-ATPase; NCX, Na^{+}/Ca^{2+} Exchanger in Forward (F) and Reverse (R) mode; CaUP, Ca^{2+} uniporter.*

There are many Ca^{2+} binding proteins and buffering systems within cells that compete for the binding of the ion (Bers, 2000). As such, the amount of Ca^{2+}/L cytosol to raise $[Ca^{2+}]_i$ to peak systolic concentrations of 1 µM exceeds 100 µM. The total amount of Ca^{2+} transported within the ventricular myocytes of rat and human are the same. However, there are significant differences between species in the extent to which each Ca^{2+} transport mechanism will be used. Figure 1.2 shows some of the key ion exchanges. Human and rat myocytes will cycle 70% and 92% respectively of their Ca^{2+} with the SR. Thus, the reduced SR Ca^{2+} uptake within the human cells will have consequences on their dependence for ion transporters such as the NCX to remove Ca^{2+} from the cytosol.

1.1.1.4. Cardiac Myocyte Relaxation

To allow diastolic filling, the cardiac myocytes must relax by reducing the $[Ca^{2+}]_i$. This requires removing the Ca^{2+} against its concentration gradient which is consequently reliant on ATP-dependent mechanisms (Bers, 2002). The slower rate of removal and prolonged decline in $[Ca^{2+}]_i$ (figure 1.1) demonstrates this effort.

The SR reabsorbs the same amount of Ca^{2+} that it has released through the sarco/endoplasmic reticulum Ca^{2+}-ATPase pump (SERCA2a, the predominant cardiac isoform) (Bers, 2000). For each ATP that is hydrolysed, two Ca^{2+} ions are taken up (Lee and East, 2001). A phosphate receiver known as phospholamban (PLB) can influence the activity of SERCA2a (Tada and Katz, 1982). Phosphorylation of PLB removes the natural inhibition that it has on the SERCA2a pump allowing a greater influx of Ca^{2+} and a faster rate of relaxation and diastolic filling (lusitropy). Storage of Ca^{2+} within the SR can reach concentrations of up to 20 mM (with 1 mM in free Ca^{2+})

and is aided by calsequestrin, a Ca^{2+} binding protein that can hold up to 50 Ca^{2+} ions (Beard et al., 2004).

The NCX is responsible for the majority of Ca^{2+} extrusion through the sarcolemma (Bers, 2000). The current matches the $I_{Ca.L}$ (Bridge et al., 1990) and is dependent on the $[Ca^{2+}]_i$ for activation and a stable and low $[Na^+]_i$ to maintain the ion gradient (Fearnley et al., 2011). As this relies on the Na^+/K^+-ATPase, the NCX is counted as having an energy consumption of 1 ATP molecule per Ca^{2+} ion that is extruded (Bers, 2000). Thus, it is less efficient than SERCA2a. A sarcolemmal Ca^{2+} pump also exists to drive Ca^{2+} out of the cell; but as its transport capability is much less than the NCX, its role is believed to be more to do with signal transduction than the contraction-relaxation cycle of the cell (Cartwright et al., 2005).

1.1.1.5. Modulation with β-Adrenergic Signalling

To modify the cells' contractile activity and cardiac output, Ca^{2+} handling proteins can be targeted by a variety of signalling pathways. One of the most notable pathways is the β-adrenergic system responsible for the heart's response to sympathetic stimulation. This enables the body to deal with increased demand by adapting the cardiac output with an increase in heart rate (chronotropy), contractile force (inotropy) and lusitropy.

Stimulated by the release of noradrenaline from the sympathetic nervous system, the β-adrenergic receptors are linked to GPCR. The Gαs subtype is responsible for the increased activity of another transmembrane protein, adenylyl cyclase (Buck et al., 1999). When activated, this enzyme converts ATP into the second messenger cyclic adenosine-3',5'-cyclic monophosphate (cAMP). This signalling messenger can interact with and release the active C subunit of protein kinase A (PKA), which phosphorylates many targets on Ca^{2+} handling proteins. These include: the LTCC (Yan et al., 2011)

and RYR2 (Shan et al., 2010) for greater peak force of contraction with augmented Ca^{2+} release; an increased Ca^{2+} to troponin-C interaction, that allows greater sensitivity for the ion (Layland et al., 2004); and Ser^{16} on PLB to increase the removal of Ca^{2+} ready for the next contracting cycle (Hagemann and Xiao, 2002).

A physiological response such as tachycardia can also stimulate a heart-rate induced increase in Ca^{2+} release (Grimm and Brown, 2010). Here, kinases sensitive to the repetitive release and increase in $[Ca^{2+}]_i$, known as Ca^{2+}/Calmodulin-dependent protein kinase II (CaMKII), target Ca^{2+} handling proteins to further augment the cycling of cytosolic Ca^{2+} (see section 1.2).

1.1.2. Gene Transcription and Regulation in Cardiac Myocytes

The Ca^{2+} signalling responsible for instigating the cell cycle and gene transcription in the nucleus operates differently to the prominent Ca^{2+} transients needed for cell contraction. Recent advances show that the nucleus has its own 'active' Ca^{2+} transient as well as having a 'passive' Ca^{2+} transient (Bootman et al., 2009; Ljubojevic et al., 2011). The passive diffusion of Ca^{2+} into the nucleus is a response to the high systolic $[Ca^{2+}]_i$ of E-C coupling. A minor restriction period delays the onset of the nuclear Ca^{2+} transient and helps protect against the constant sharp rises of Ca^{2+} overload particularly when the cell is stimulated by inotropic agents (Genka et al., 1999). The nucleus' own active Ca^{2+} transients are regulated by a series of Ca^{2+} regulating proteins (i.e. SERCA2a pump and Ca^{2+} release channels) present on the nuclear envelope. The Ca^{2+} release channel inositol 1,4,5-triphosphate receptor (IP_3R) has been shown to govern and mobilise independent nuclear Ca^{2+} transients (Rodrigues et al., 2009). Stimulated by the translocation of the second messenger inositol 1,4,5-triphosphate ($InsP_3$) from the cell membrane, the IP_3R will release Ca^{2+} and generate its own nuclear Ca^{2+} transient. Transcription factors such as cyclic AMP response element-binding protein (CREB), nuclear factor of activated T cells (NFAT) and numerous other kinases and phosphatases stimulate gene transcription in response to the oscillating Ca^{2+}, that help stimulate cell growth. This gives the ligands that target the cell membrane and its receptors (i.e. endothelin-1 via the Gαq-coupled receptors and $InsP_3$ release) their own elaborate signalling system for the mobilisation of nuclear Ca^{2+}.

1.1.3. Cell Death and Auto-digestion

Demaurex and Distelhorst (2003) stated "Organized life requires cell death, and execution of cell death relies on the very machinery of life." The execution of cell death was a reference to the cell's ability to induce cell suicide (apoptosis) or autophagy (catabolic digestion) in order to defend against pathogens or maintain homeostasis in injured cells. By using organelles such as the mitochondria and SR, cells have the machinery that will respond to genetic or environmental clues and trigger the necessary death signals. Apoptosis may be controlled by extrinsic death signals that are mediated by receptors on the cell membrane (e.g. Fas). However, the primary focus will be the intrinsic death pathway as it is regulated by the mitochondria and their regulation of Ca^{2+}. The mitochondria handle Ca^{2+} through the Ca^{2+} uniporter (for influx) and NCX (for efflux) which help stimulate energy production or buffer $[Ca^{2+}]_i$ during abnormal Ca^{2+} load (Griffiths and Rutter, 2009). When the sequestered Ca^{2+} reaches a threshold it acts as a death signal by releasing critical factors such as cytochrome c, which then activate proteases called caspases (Demaurex and Distelhorst, 2003). The Bcl-2/Bax family are other deaths signals that are important in deciding the mitochondrial tolerance to Ca^{2+} or permeability of cytochrome c (Harr and Distelhort, 2011). The significance and the interrelationships between the handling of Ca^{2+} by the SR, the mitochondria's tolerance to Ca^{2+} or the influence of signals such as the Bcl-2/Bax family are strongly debated. Autophagy, or the degradation of organelles, does not require caspase activation (Levine and Klionsky, 2004), but is associated with Ca^{2+} release from the endoplasmic reticulum (ER) or the IP_3R (Høyer-Hansen and Jääattelä, 2007). This release induces the autophagy signalling system that is usually triggered by the build up of misfolded proteins (ER stress) in order for them to be dealt with through a catabolic pathway.

1.2. Ca^{2+}/Calmodulin-Dependent Protein Kinase II

1.2.1. The CaMK Family

A family of Ser/Thr protein kinases called the CaMKs are responsible for transducing the diverse Ca^{2+} oscillations that occur in the cardiac myocyte, into physiological actions. The intermediary protein calmodulin (CaM) has a particular role in directing the activity of the CaMKs. This occurs when four Ca^{2+} ions first bind to CaM to form a Ca^{2+}/CaM complex. A 'dedicated' CaM exists on ion channels to sense and regulate Ca^{2+} in a direct manner, whilst a 'promiscuous' CaM exists to adjust the behaviour of other proteins such as the CaMKs (Saucerman and Bers, 2012).

The family of multifunctional kinases, CaMKII, CaMKK, CaMKI and CaMKIV have an immense number of duties to fulfil, with the latter three acting as part of a signalling cascade. Other members such as the myosin light chain kinase (MLCK), CaMKIII (also known as eEF2-kinase) and phosphorylase kinase act specifically on one substrate (Wayman et al., 2011). As they have different binding affinities for CaM, the kinases detect different levels of $[Ca^{2+}]_i$ and specific propagations of Ca^{2+}/CaM complexes (Song et al., 2008). Signalling involved with cell growth or specific targeting in the nucleus can then be differentiated from the global Ca^{2+} signals that are required for E-C coupling.

1.2.2. Biology of CaMKII

1.2.2.1. Isoforms and Gene Splicing

Mammalian cells possess four CaMKII gene products (α, β, γ, δ). The vasculature and cardiac muscle express the γ and δ subtypes, whilst the α and β are predominantly found in neuronal tissue (Schworer et al., 1993; Hudmon and Schulman, 2002). All four gene products share a high degree of homology, in particular at the N-terminal catalytic domain, where they have up to 92% similarity (Tobimatsu and Fujisawa, 1989). Gene splicing of seven exons in a central variable domain allows these four subtypes of CaMKII to diversify considerably both within and between the different organs and tissues (Tombes et al., 2003).

The δ isoform contains 15 known mammalian isozymes, of which seven are expressed in the heart (Tombes et al., 2003). Srinivasan et al. (1994) recognised that the δ_B isoform possessed a unique nuclear translocation sequence in the variable domain, speculating its activity might be for gene expression and cell proliferation. This was not apparent in the sequencing of the neuronal specific δ_A or the ubiquitously expressed δ_C subtype, which were confirmed to be contained within the cytosol by immunofluorescence. Other variants for the heart (δ_F, δ_G, δ_H, δ_I, δ_J) are thought to be only conserved for neonatal and stages of development (Hoch et al., 2000). Interestingly, extreme pathological stimuli can bring about non tissue specific variants. Colomer et al. (2003) detected, after seven days of transverse aortic constriction (TAC) in the mouse heart, the mRNA of the skeletal muscle specific δ_D isoform.

1.2.2.2. Structure and Functional Properties

The main domains that constitute the CaMKII monomer are illustrated in figure 1.3A. They are: the highly conserved N-terminal catalytic domain that contains the ATP binding site for its targeted proteins; the central regulatory domain that contains the binding site for Ca^{2+}/CaM; the C-terminal association domain that allows the union of a holoenzyme and the proximity for neighbouring kinase interactivity (Hudmon and Schulman, 2002). The monomers gather into a dodecameric holoenzyme (figure 1.3B(i)&(ii)) via the association domains' arrangement of two hexameric rings (Rosenberg et al., 2006). A combination of isozymes may compromise the holoenzyme, enabling varying lengths and properties (figure 1.3B(ii)) contributing to various amounts of allosteric control (Chao et al., 2011).

As shown in figure 1.4A, at low $[Ca^{2+}]_i$ a pseudosubstrate sequence located in the regulatory domain acts to auto-inhibit the kinase activity. This basal state also interferes with the ATP binding site on the catalytic domain (Hoffman et al., 2011). A rise in $[Ca^{2+}]_i$ and the binding of Ca^{2+}/CaM will render CaMKII active, as the α helix that arranges the kinase into an auto-inhibitory state is broken (Chao et al., 2011). A rearrangement of the regulatory domain will expose a Thr^{287} (Thr^{286} for CaMKIIα) phosphorylation site and the ATP binding site on the catalytic domain. Recent research suggests that at a high ATP concentration, it is possible that a 'primed' regulatory domain may be available to assist in the binding of Ca^{2+}/CaM (Hoffman et al., 2011).

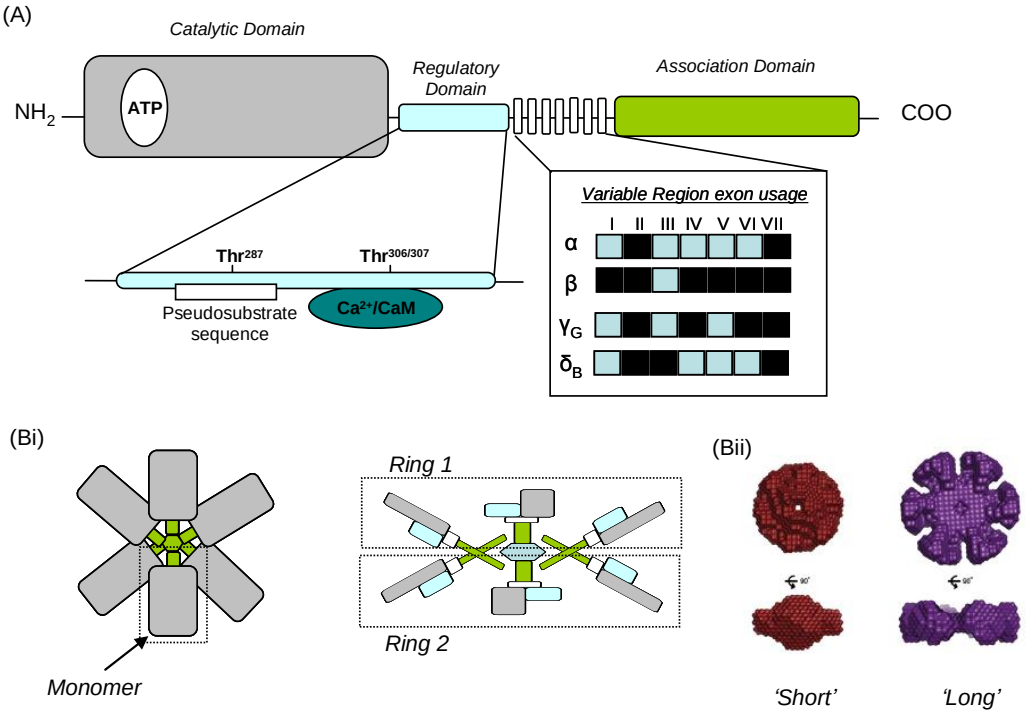

Figure 1.3: Biology of the CaMKII monomer and holoenzyme. *(A) The domains of a CaMKII monomer. The regulatory and variable domains are highlighted to depict key sites of activity and the possible variations in exon selection between each isoform. (Adapted from Tombes et al., 2003). (Bi) The CaMKII monomer forms two hexameric rings that combine into a dodecameric holoenzyme. (Bii) Examples of CaMKII holoenzyme with different combinations of short and long isozymes, that gives varying holoenzyme structures and activity (taken from Chao et al., 2011).*

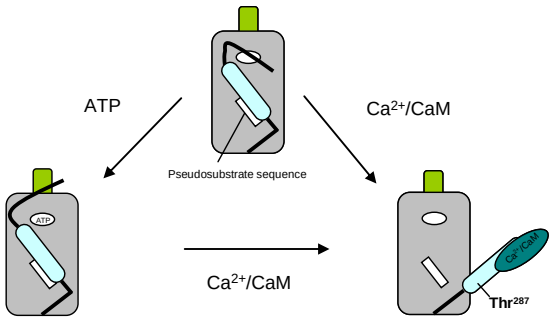

Figure 1.4A*: A cartoon of a CaMKII monomer transforming from an inactivated basal state to the primed and activated state in the presence of ATP, Ca^{2+}/CaM or both. Once activated with Ca^{2+}/CaM a Thr^{287} site on the regulatory domain is exposed. (Protein structure adapted from Hoffman et al., 2011.)*

If a Ca^{2+} transient increases in frequency, amplitude or duration (figure 1.4B) it will present two adjacent and 'Ca^{2+}/CaM active' CaMKII. This allows the newly exposed Thr^{287} site to be autophosphorylated (Meyer et al., 1992). Moreover, the kinase gains an improved association with Ca^{2+}/CaM, as its affinity increases by 1000 fold. Termed 'CaM trapping' this new affinity allows CaMKII to have an autonomously active status even in the presence of low $[Ca^{2+}]_i$ (Meyer et al., 1992; Singla et al., 2001). Even with the dissociation of Ca^{2+}/CaM, phosphorylation of Thr^{287} prevents the regulatory domain from returning to an auto-inhibitory state and have further autonomy in the absence of Ca^{2+} (Hoffman et al., 2011).

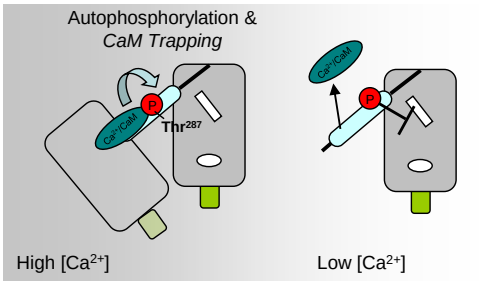

Figure 1.4B: *Further active states of CaMKII can be achieved with persistent Ca^{2+} transients allowing kinase-kinase activity at the Thr^{287} site. This slows the dissociation of Ca^{2+}/CaM (CaM trapping) from the kinase and the likelihood of it returning to an auto-inhibitory state. P, phosphorylation*

The phosphorylation of the $Thr^{306/307}$ sites within the regulatory domain allows CaMKII to be 'capped' and prevents Ca^{2+}/CaM from rebinding to the kinase (figure 1.4C). 'CaM capping' can only be done when Ca^{2+}/CaM is not associated to the region as they normally share a similar location (figure 1.3A). This has been proposed to be a mechanism that will differentiate between the stimulated and unstimulated kinases in order to maintain a balance between the reactions (Colbran, 1993; Hudmon and Schulman, 2002). Other states of activity have recently been discovered at the

Met$^{280/281}$ sites within the regulatory domain (Erickson et al., 2008). Oxidation of these sites when CaMKII is in the basal state would interfere with the binding of Ca^{2+}/CaM and the phosphorylation of Thr^{287} (Rellos et al., 2010). Thus, it is proposed that Ca^{2+} is not needed (or is required at a lower concentration) for this independent activity state of CaMKII.

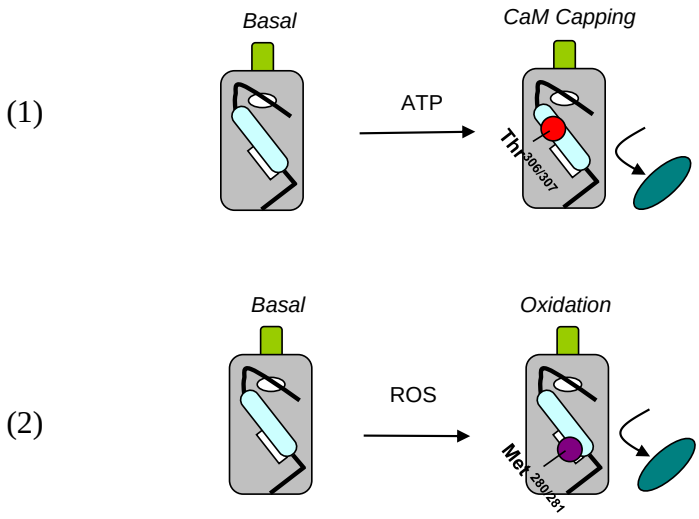

Figure 1.4C: *Further activity states of CaMKII. (1) 'CaM capping' of CaMKII may occur in the absence of Ca^{2+}/CaM and be a method of preventing its association with the kinase. (2) Oxidation of CaMKII at Met$^{280/281}$ gives further activity states in the absence of Ca^{2+}.*

For equilibrium, counteracting and deactivating CaMKII activity is achieved by phosphatases that dephosphorylate the kinase and its downstream targets (Ishida et al., 2008). These include the Ser/Thr protein phosphatases (classed as PPP), such as PP1 and PP2A. Although PP2B (calcineurin) can not directly dephosphorylate any CaMKII targets, an indirect relationship exists via PP2B influence on Inhibitor-1, which is a protein inhibitor of PP1. A more direct regulation of the kinase is believed to come

from a class of phosphatases called CaMK phosphatases, also expressed in a nuclear form (Ishida et al., 2008).

1.2.2.3. Pharmacological Manipulation

Many small molecule and peptide inhibitors have been devised to uncover the functional capacity of CaMKII. The organic small molecule inhibitors KN-62 and KN-93 compete for the Ca^{2+}/CaM binding site, but have been criticised for their non-specific ion channel activity (Ledoux et al., 1999; Gao et al., 2006; Rezazadeh et al., 2006). The inactive analog, KN-92, is reported to also have the same non-specific activity (Chelu et al., 2009, Said et al., 2008, Tsung et al., 2007). Thus, the inadequate association with CaMKII gives KN-92 an important role as a negative control for research within the field.

The auto-inhibitory substrate that lies within the kinase has been a target for many of the peptides. These include; CaMKII (281–309), CaMKII (273–302), autocamtide-2-inhibitory peptide (AC3-I) and the autocamtide-2 related inhibitory peptide (AIP) which has been developed in a myristoylated form or with an antennapedia transport peptide sequence to increase its cell permeability. These peptides are believed to have cross activity with other Ca^{2+}/CaM regulated proteins (Ishida et al., 2008). Another small peptide inhibitor, CN21 (Vest et al., 2007), is based on a CaMKII inhibitory protein that was identified in the rat brain (Chang et al., 1998). The advantage of having an increased specificity to CaMKII is however limited by only partially inhibiting states of CaMKII activity.

1.2.3. Physiological Functioning in Cardiac Myocytes

In the heart, the role of the 'multifunctional' CaMKII is as wide-ranging as its upstream activator Ca^{2+}. It primarily targets the proteins that maintain the homeostasis in Ca^{2+} cycling, whether for E-C coupling, or in the promotion of growth and transcription within the nucleus. For the ventricles of the adult mouse, the ratio of the δ isoforms are split 60% for the nuclear tagged δ_B and 40% for the cytosolic δ_C (Mishra et al., 2011). Although the study also confirmed that these labels do not confine the isoforms to these specific loci, much of the research in the field has followed this trend in characterising the physiological capability of the δ-isoform. That is, the main interest of research has either been (i) CaMKIIs function as a modulator of $[Ca^{2+}]_i$ during E-C coupling or; (ii) as a mediator of gene transcription and regulation in the nucleus. This thesis will largely focus on its role within E-C coupling, with only a brief description on its regulatory role in gene transcription.

1.2.3.1. CaMKII & Excitation-Contraction Coupling

The components that enable E-C coupling in cardiac myocytes include multiple CaMKII substrates (figure 1.5). The targets located on various ion channels indicate its potential to influence the action potential, while in the CICR cascade, it is involved in each step. Immunofluorescence staining for CaMKII in cardiac myocytes depicts this strong relationship with the components of E-C coupling as it is co-localised within the T tubules and the Z bands of the cell (Wu et al., 1999). These areas are enriched with LTCC and RYR2 and signify the key role that CaMKII has on the Ca^{2+} that enters the cytosol via these two ion channels.

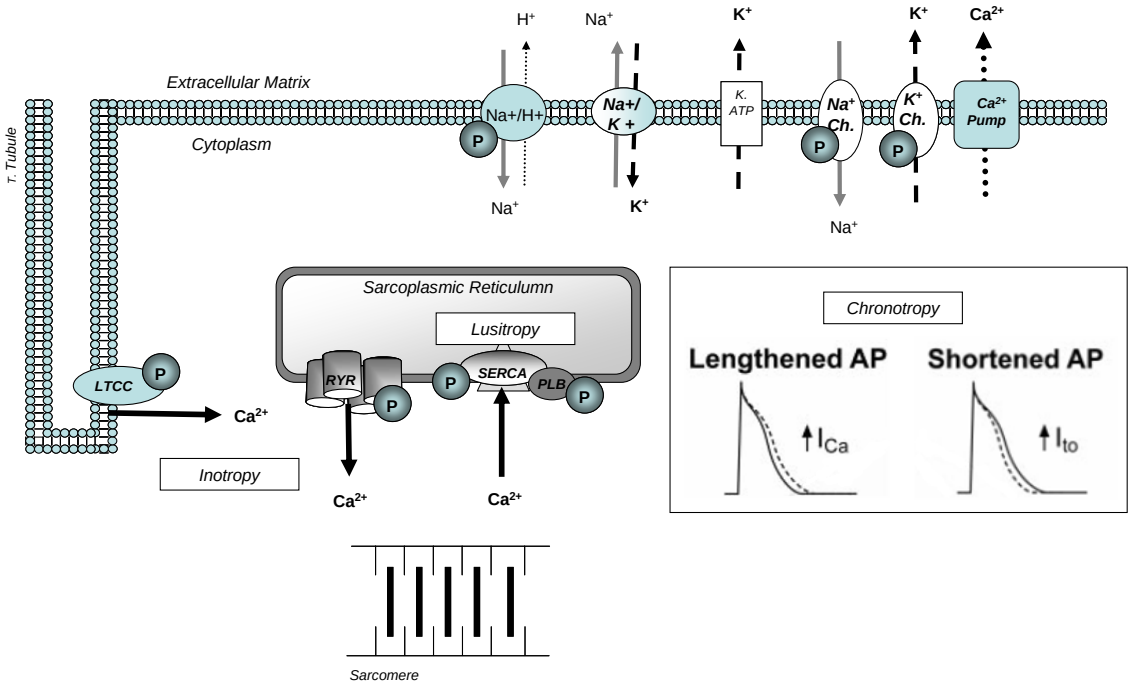

Figure 1.5: CaMKII targets within the cytosol. *Several phosphorylation sites are located on Ca^{2+} handling proteins of the SR and the ion channels located on the sarcolemmal. (1) CaMKII assists the CICR steps via phosphorylation of the LTCC, and the RYR2. (2) Lusitropy is enhanced by its activities on SERCA2a and PLB. (3) Further modifications to E-C coupling can be made by the ion channels located on the sarcolemma, which can either lengthen or shorten the duration of the action potential (highlighted by the respective dotted line) and thus the availability and timing of the contracting myocyte. LTCC, L-type Ca^{2+} channel; RYR, ryanodine receptor; PLB, phospholamban; SERCA, Sarco/Endoplasmic Reticulum Ca^{2+}-ATPase; Na^+ Ch., Na^+ Channel; K^+ Ch., K^+ Channel; NHE, Na^+/H^+ Exchange; P, phosphorylation. (Lengthened and shortened action potential figures taken from Anderson, 2009).*

1.2.3.2. Regulation of the L-type Ca^{2+} Channel

CaMKII is targeted to the sarcolemma by the binding site located on the regulatory β-subunit of the LTCC (Grueter et al., 2008). The binding sequence (486-500) parallels the sequence of the kinase regulatory domain (274-289), which interestingly includes comparable phosphorylation sites at Thr^{498} and Thr^{287}, respectively. Phosphorylation increases the ion channel open probability (Po) or facilitation, allowing a greater $I_{Ca.L}$. Hudmon et al. (2005) also demonstrated that the pore forming α-subunit of the LTCC contains various anchoring sites for CaMKII. Not only was an active CaMKII able to tether and regulate the channel's function but also its deactivated state, allowing it to possibly act as a detector of Ca^{2+} frequency of influx.

The 'positive force staircase' is seen in cells that are repeatedly depolarised, and demonstrates one of the actions of CaMKII on the LTCC (Lee, 1987; Hashambhoy et al., 2009). The progression in the amplitude of $I_{Ca.}$ demonstrates the facilitation of the ion channel as CaMKII increases the Ca^{2+} entry and a slower rate of ion channel inactivation. It may possibly compensate the Ca^{2+} dependent inactivation of the ion channel that occurs with increased activity (Maier and Bers, 2007). To confirm the involvement of the kinase, Anderson et al. (1994) used CaMKII inhibitors to block the ion channel's facilitation. It was also observed that the presence of $[Ca^{2+}]_i$ was needed for CaMKII involvement. CaMKII inhibitors also had no effect upon β-adrenergic stimulation of the ion channel, thus defining the two signalling pathways.

1.2.3.3. CaMKII and the RYR

The technical difficulties in conducting *in situ* experiments for investigating the RYR2 has made the role of CaMKII controversial. There is contradictory evidence as to whether CaMKII increases the Po of the channel (Currie et al., 2004) or decreases its

sensitivity and subsequent release of Ca^{2+} (Yang et al., 2007). CaMKII phosphorylation sites have been identified at residues $Ser^{2808/2809}$ (Witcher et al., 1991) and $Ser^{2814/2815}$ (Wehrens et al., 2004). This would imply that the ion channel is phosphorylated by CaMKII. Also, studies using isolated cardiac myocytes that overexpress CaMKII (Maier et al., 2003) or pharmacological blockade of the kinase (Li et al., 1997) support its involvement in up regulating the RYR2 and increasing the release of stored Ca^{2+} from the SR. Kushnir et al., (2010) suggest that such activity is important for the force-frequency relationship that enhances myocardial contractility. But this view is also controversial due to the incapability of such activity to suffice loading of Ca^{2+} within the SR that would be required to maintain inotropy (Eisner et al., 2009).

1.2.3.4. Ca^{2+} Uptake into SR: PLB and SERCA2a modifications

Any increase in $[Ca^{2+}]_i$ is balanced by the efficiency in its removal. CaMKII phosphorylates PLB at Thr^{17}, releasing its natural inhibition of the SERCA2a pump and admitting Ca^{2+} into the SR (Mattiazzi et al., 2005). There are possible sites of activity on Ser^{38} of SERCA2a (Narayanan and Xu, 1997) but this has not been confirmed. Although PLB activity is not essential for Ca^{2+} removal and subsequent relaxation of the cell (Li et al., 1998, DeSantiago, 2002), there is some correlation between the phosphorylation state of the Thr^{17} site and relaxation time (Hagemann et al., 2000). Some reports also suggest this might be the case with SERCA2a activity and CaMKII (Odermatt et al., 1996). During times of increased stimulation, such as increased heart rate, a frequency dependent acceleration of relaxation is a necessity for ventricular filling. Kemi et al. (2007) showed an interesting cardiac development in aerobically exercised mice. Their cells/hearts had a decrease in PLB expression relative to the

SERCA2a pump, but an increase in Thr^{17} phosphorylation due to CaMKII. This meant that the exercised mice had adapted a CaMKII dependent mechanism of Ca^{2+} uptake.

1.2.3.5. Regulation of Sarcolemmal Ion Channels

CaMKII's ability to associate with ion channels confers its prominent role in E-C coupling (Anderson, 2009). Tan et al. (2002) were the first to give a mechanistic explanation of how Ca^{2+} is able to disrupt the inactivation properties of the Na^{+} channel. They reported that interaction of the Ca^{2+} sensitive protein CaM with an IQ motif (first two amino acids: isoleucine, glutamine) at the Na^{+} channel's C terminus, was essential in reducing its inactivation gating process. CaMKII was found to work in a similar way to CaM, as it has a direct association with phosphorylation sites located on the ion channel C terminus (Wagner et al., 2006). By regulating the inactivation properties of the channel, CaMKII can increase and prolong the I_{Na} that would also augment the action potential duration. Some of the differences between the two Ca^{2+} sensitive proteins were investigated by Aiba et al. (2010), who showed that CaM does not alter the Na^{+} channel's recovery from inactivation or the magnitude of the late current as CaMKII does.

Some balance with respect to action potential duration is kept through CaMKII's regulation of K^{+} channels. Tessier et al. (1999) were the first to show that the fast outward current can be influenced by the CaMKII inhibitor KN-93 by allowing a faster I_{to} inactivation. El-Haou et al. (2009) specified this regulation to the Kv4.3 with its associated regulatory protein SAP97 being a key attachment site for CaMKII and its subsequent gating effects. Variable concentrations of Ca^{2+} also affect the gating of specific K^{+} channels subtypes. The Kv4.3 was effective during low $I_{Ca.L}$ whilst the Kv4.2 became essential during increased Ca^{2+} concentrations (Colinas et al., 2006).

Thus, CaMKII can also shorten the action potential duration by increasing I_{to}, which will then reduce $I_{Ca.L.}$ This modification can be seen as a form of self regulation as it would subsequently limit CaMKII activity.

CaMKII is reported to phosphorylate the NHE (Fliegel et al., 1992) although this has not been confirmed. During acidosis, CaMKII can still continue its activity on substrates such as the SR. This allows some contractile activity to be maintained if such cellular environment is achieved (Mattiazzi et al., 2007). Thus, the ability to phosphorylate the NHE would also be a mechanism for restoring intracellular pH.

1.2.3.6. Excitation-Transcription Coupling

CaMKII's role within the nucleus has a long term influence and underpins cellular adaptation. $CaMKII_{\delta B}$, which has the nuclear translocation sequence, is the predominant isoform in the adult heart (Mishra et al., 2011). It has gained much attention for its role in pathological cardiac hypertrophy with several genes associated with its activity including β-myosin heavy chain (Zhu et al., 2000), NCX (Mani et al., 2010), ERK1/2 (Zou et al., 2001), NFκB (Kashiwase et al., 2005). The chromatin repressor, histone deacetylase (HDAC) acts as the chief molecular mechanism for regulating transcription factors and genes. The condensation of DNA can be alleviated by HDAC phosphorylation and its subsequent translocation out of the nucleus (Zhang et al., 2007; Lu et al., 2010). Direct phosphorylation sites have been found on HDAC4 (Backs et al., 2006) whilst an indirect relationship with HDAC5 exists via the Ca^{2+} released by the nuclear IP_3R (Bossuyt et al., 2008; Wu et al., 2006). This pathway for releasing Ca^{2+} close to the nucleus by the numerous neurohormonal agents that increase the activity of the second messenger InsP3, stimulates CaMKII to relocate to the nucleus (Bare et al., 2005).

1.3. Cardiovascular Disease

1.3.1. Current Trends

Cardiovascular disease (CVD) is the generic term that encompasses the many acquired and inherited diseases of the heart and circulatory system. With 17 million deaths recorded in 2008, which accounts for 31% of all mortalities, CVD is the leading cause of death worldwide (WHO, 2011). In the U.K. this accounts for 191,000 deaths in 2008, with coronary heart disease (CHD) and stroke accounting for 88,000 (46%) and 43,000 (23%) respectively of the total cases (BHF, 2010).

The prevalence of the diseases in society has made them common terms, with coronary thrombosis (or the more expressive phrase 'heart attack') a prime example. On average acute myocardial infarction (AMI) occurs in the U.K. every two minutes and with every six minutes, 30% of these victims will die (BHF, 2010). Mortality occurs mainly from acute heart failure, as the sudden reduction in blood flow (ischaemia) to the myocardium, reduces cardiac output and forces the tissue to die (AMI). Those that do survive the acute event face further complications as the heart is remodelled to compensate for the damaged tissue. In doing so, the heart struggles to maintain cardiac output (chronic heart failure, CHF), which inevitably provides limited capability for activity and a lower quality of life.

Scientific research on risk factors, causes and prevention of CHD has had favourable results on prevalence and mortality rate within western society (BHF, 2011). Since the 1960's the U.K. mortality rate from CHD has decreased by around 50% (figure 1.6). A greater understanding of the risk factors and public awareness to these dangers is reported to have contributed to 50% of the reduction, with 40% attributed to the advancement in medical therapies, such as reperfusion therapy (Unal et al., 2004). These figures demonstrate the importance of the combined effect of primary prevention

and medical treatments in tackling such diseases. However, the estimated number of people living with heart failure is increasing rapidly (figure 1.6). One reason for this is due to an aging population as the number of people aged 85 and over has more than doubled since 1981 (ONS, 2010). The predicted annual mortality rate for those admitted to hospital with heart failure is 30% (Cleland et al., 2010). But patients discharged from cardiology wards, and who have thus gained specialist care (diagnosis and evidence based medicine to manage the condition), are more likely to survive, than those discharged from general medical wards.

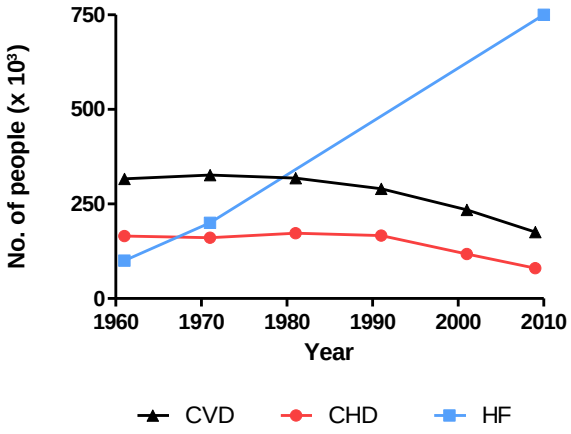

Figure 1.6: Prevalence and mortality rates of CVD in the U.K. (England, Scotland, Wales) population during the last 50 years. *Total deaths from cardiovascular disease (CVD) and in particular coronary heart disease (CHD) have gradually declined whilst the number of people living with heart failure (HF) has escalated (adapted from BHF, 2011).*

1.3.2. The Cardiovascular Disease Continuum

Dzau and Braunwald in 1991 proposed a chain of events, known as the CVD continuum (figure 1.7), to explain the pathogenic process of cardiovascular events such as AMI and CHF. Originating with a multitude of risk factors consisting of dyslipidaemia, hypertension, LVH, diabetes and smoking, it was proposed that if these factors were left untreated, a pathological progression would begin with atherosclerosis, and develop into myocardial ischaemia, heart failure and death. It was also suggested that it would be possible to intervene at any stage in the development of the disease, to prevent or delay its occurrence and thus prolong life.

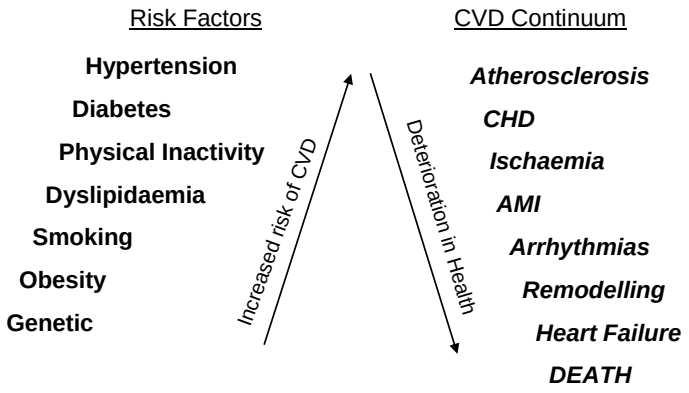

Figure 1.7: Cardiovascular Disease Continuum. *Manifestations of risk factors promote a myriad of pathological events that include atherosclerosis, myocardial ischaemia, arrhythmia and heart failure (adapted from Dzau and Braunwald, 1991).*

The risk factors contribute to atherosclerosis and vascular disease with plaque and fatty deposits that stenose (narrow) and harden the arteries. Hypertension in itself is a prominent risk factor as it adds continued stress to arterial walls which are worsened with plaque deposits. Immune cells (e.g. macrophages and T cells) and vascular smooth muscle cells amass over time and dress the injured walls with an accumulation of

cholesterol. This growth causes stenosis (narrowing of the lumen) that limits blood flow and can contribute to chronic ischaemia of the surrounding tissue.

Dependent on the location of the vascular disease, it may lead to several outcomes. In the heart it is termed CHD and if a severe stenosis is formed, will cause myocardial ischaemia. It becomes lethal when a coronary thrombosis is formed as the fibrous cap of the atherosclerotic plaque ruptures and completely blocks the arteries and impedes blood flow. The extent of MI is dependent on the timing of reperfusion therapy (see section 1.3.3.3.). This will shape the extent of injury and further CVD as remodelling of the scarred and surviving tissue has a significant effect on the development of arrhythmias and heart failure.

1.3.3. Myocardial Infarction

1.3.3.1. Myocardial Ischaemia

The heart acts as a mechanical pump to ensure blood enriched with oxygen and metabolic substrates is circulated to the tissues. It also needs to deliver blood to itself via the coronary arteries. Due to the extravascular compression, coronary flow opportunistically occurs during the diastolic phase of the contraction cycle (Klabunde, 2011). Originating at the base of the aorta are the right and left coronary arteries. They lie on the epicardial surface of the heart and divide into smaller branches and a microvascular network. These distal networks provide more vascular resistance than the coronary vessels on the epicardium and thus provide transmural pressure that influences the coronary blood flow. The coronary cycle is completed by the joining of the capillaries with cardiac veins that drain into the coronary sinus located in the right atrium.

Coronary blood flow is tightly regulated by the oxygen demand of the tissue. As the basal oxygen consumption of the tissue is very high, oxygen extraction is already near maximal at rest (70-80% of arterial oxygen content) (Duncker and Bache, 2008). Under normal conditions, a balance exists between the oxygen demand of the contracting heart (determined by heart rate, systolic pressure and LV contractility) and the supply provided by the coronary blood flow. Ischaemia will arise if this balance is disrupted (Klabunde, 2011).

Myocardial ischaemia can either occur when there is an increase in the tissue's metabolic demand, a decrease in the circulation of oxygenated blood or both. A rise in the metabolic demand occurs with increases in heart rate, inotropy, or the blood volume (preload), or the resistance that the heart has to work against in circulating blood (afterload). A reduced capacity to circulate blood arises with conditions such as; spasm

of blood vessels (vasospasm), narrowing of vessels (stenosis), or formation of blood clot (thrombus) that partly (non-occlusive) or entirely (occlusive) block a coronary artery. A decrease in the ratio of oxygen supply/demand allows myocardial hypoxia to develop. When this is sustained for a long period it gives rise to anginal chest pain. Management of chronic stable angina with β-blockers, calcium channel blockers and nitrates, reduces the oxygen demand of the tissue or improve its blood supply alleviating the angina symptoms (Chaitman and Laddu, 2012).

An acute coronary syndrome is used to describe any condition of sudden myocardial ischaemia associated with occlusive or non-occlusive thrombus formation and includes a continuum of its intensity beginning with unstable angina and non-ST segment elevation MI (NSTEMI), to the more severe ST-segment elevation MI (STEMI; Overbaugh, 2009). Unstable angina and NSTEMI usually occur from a non-occlusive thrombus, whilst a STEMI emerges from an occlusive thrombus that leads to a large risk zone. The injury usually involves a large part of the ventricular wall. When this is assessed with an electrocardiogram (ECG), the electrical conductance at systole seems to end prematurely (due to a disrupted baseline voltage in the ischaemic tissue) and elevates the ST-segment (figure 1.8A). With the QRS complex having the most characteristic change, ECG leads that overlie the infarct zone gave rise to the term Q-wave infarction. Any patients presenting to hospital with ST elevation are candidates for reperfusion therapy (see section 1.3.3.3.).

There are two main types of MI: transmural infarcts, where myocardial necrosis is incorporated through the full thickness of the ventricular wall; or nontransmural infarcts where the necrosis occurs predominantly in the subendocardium. The extent of injury not only depends on the location and the size of the occluded coronary artery

(and the amount of myocardium at risk of dying), but also the duration of ischaemia and the collateral blood flow of the surrounding tissue.

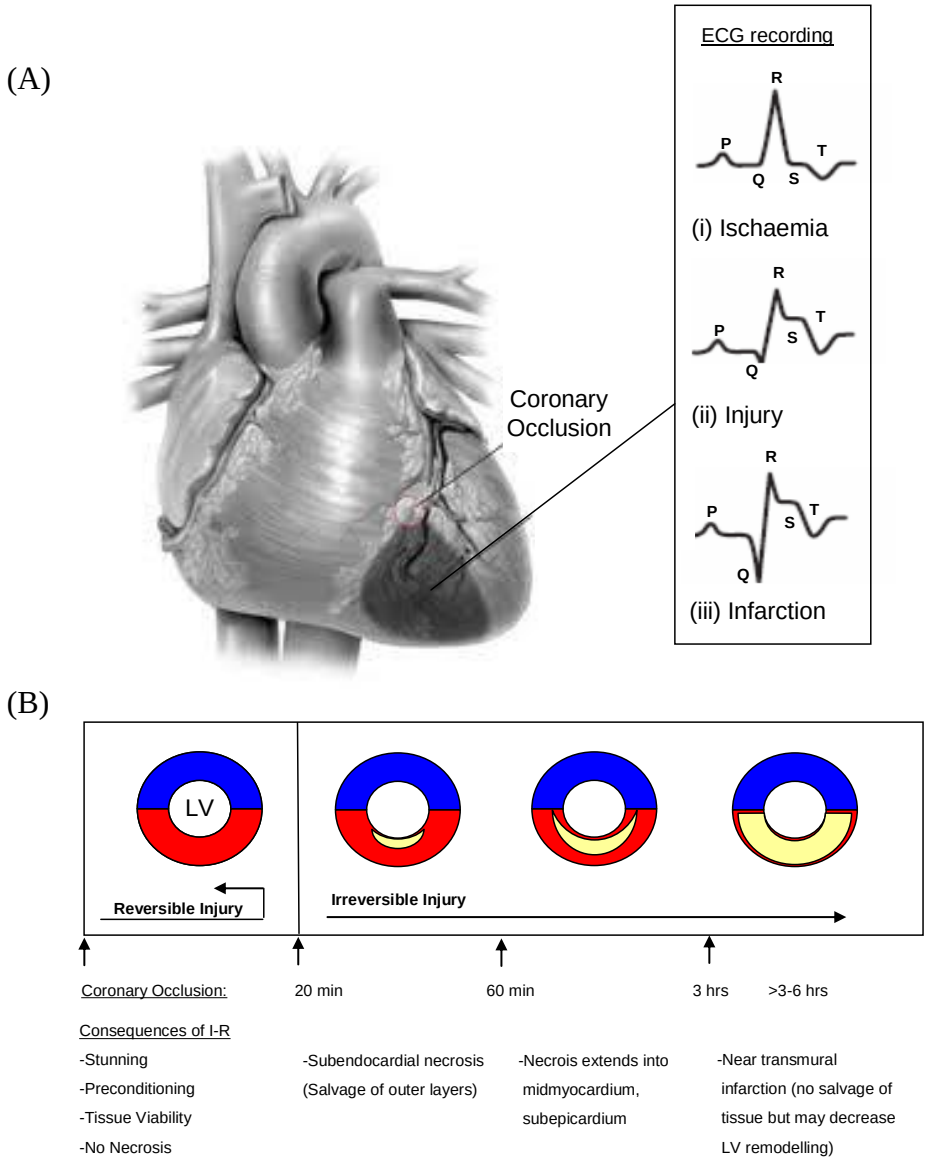

Figure 1.8: Myocardial Infarction*. (A) A coronary occlusion can disrupt the EC coupling of the myocardium. This can be measured on an ECG to indicate the extent of injury; (i) an inverted T wave is a sign of ischaemia, (ii) ST segment elevation indicates injury, (iii) abnormal Q wave shows presence of infarction (adapted from Overbaugh, 2009). (B) Reversible damage such as stunning occurs when ischaemia lasts less than 20 minutes. After this time point and in the absence of collaterals irreversible injury will extend as a wavefront from the endocardium to the epicardium: LV, left ventricle; Red, ischaemic tissue; Yellow, infarct tissue; Blue, non-ischaemic tissue (adapted from Kloner and Jennings, 2001).*

Dependent on these factors, myocardial necrosis progresses as a wavefront over time, from the subendocardium to the subepicardial layers (see figure 1.8B; Kloner and Jennings, 2001). The survival of the myocardium distal to the coronary occlusion depends primarily on the amount of collateral blood flow it receives and the timeliness of reperfusion. Collateral flow is typically minimal in this region as coronary pressure is low and distributed to the outer layers by the compression of contractions.

In the absence of significant collateral blood flow the duration of ischaemia is the main determinant of infarct size (Kloner and Jennings, 2001). Ischaemia lasting up to 20 minutes will induce changes that can be endured by the cells. Reperfusion therapy within this time frame will completely restore myocardial contractility, although the myocardium will exhibit some signs of temporary contractile dysfunction termed stunning. The mechanisms for this reversible injury are not yet fully understood but are believed to centre on the generation of reactive oxygen species (ROS) and the reversible modification of the Ca^{2+} handling proteins (Eberli, 2004). Due to these intracellular changes occurring at these later stages, stunning is seen as a form of reperfusion injury. On the contrary, a protective element exists within 'stunned' cells that have been subjected to ischaemia of no more than 10 minutes in duration. Known as preconditioning (section 1.3.4), the cells will endure a subsequent ischaemia-reperfusion insult better than cells that have not been conditioned in this way. Beyond the ischemic threshold of 20 minutes, critical factors will drive the cells to irreversible injury and death (see next section). Within 60 minutes the wavefront of tissue injury is extended from the subendocardium and there is nearly fully transmural infarction after 3 hours of coronary occlusion (Kloner and Jennings, 2001).

1.3.3.2. Cell Injury and Death

Termination of blood flow and perfusate to the working myocardial tissue will have detrimental consequences to the cellular activity of the cardiac myocytes. The decrease in perfusion pressure promptly leads to hypokinesis, signified by a marked reduction in global LV contractility and systolic pressure (Akaishi et al., 1991). The absence of oxygen drives anaerobic metabolism, a rise in catabolites and an acidic environment. Unable to supply the high energy demands of the cell, the loss of intracellular homeostasis promotes various mechanisms of injury (figure 1.9). Mitochondrial stress increases the production of ROS and oxidises membrane phospholipids, proteins and nucleic acids. All mechanisms contribute in driving cell death by oncosis, apoptosis and autophagy (Buja and Weerasinghe, 2010).

The Ischaemic Cascade

Much of the biochemical analysis of various ischaemic conditions and durations was performed prior to the 1990's, with a great deal of the research coming from the laboratory of Jennings and Reimer. It was revealed that the cessation of perfusion had immediate consequences on the cells' metabolic activity. Residual oxygen is exhausted within 10 seconds of coronary occlusion, and 90% of creatine phosphate reserve is depleted in the first minute (Jennings et al., 1990). Consequently, the tissue relies heavily on anaerobic glycolysis to maintain ATP synthesis, although this amount is only one quarter of the aerobic glycolytic production (Jennings and Reimer, 1991). A progressive reduction in ATP levels sees the values reach 35%, 9%, 7%, and 5% of control levels after 15, 30, 40 and 60 minutes of ischaemia respectively (Jennings et al., 1978). Irreversibly injured myocytes are characterised as exhibiting ATP levels below 10% of control and a cessation of anaerobic glycolysis (Jennings and Reimer, 1991).

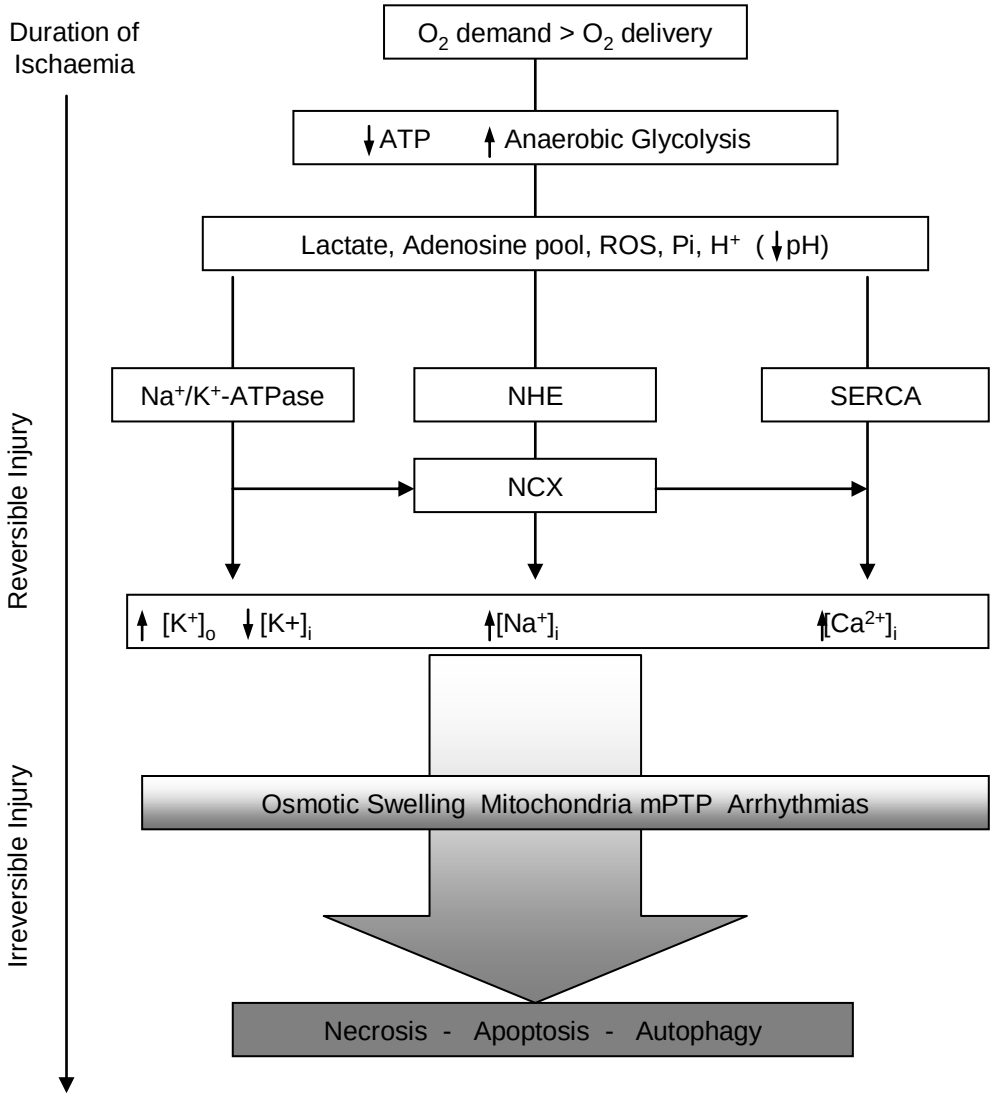

Figure 1.9: The cascade of intracellular events that is triggered by ischaemia and ends with cell death. *Anaerobic glycolysis and other components promote unfavourable changes in the cell. Ion transporters are particularly vulnerable and disrupt the intracellular and extracellular concentrations of ions. With other pro injury mechanisms, such as mitochondrial stress, injury and cell death are inevitable if ischaemic conditions continue.*

A by product of anaerobic metabolism is acidosis and lactate production. Combined with the increased catabolites from the nucleotide pools (AMP, NAD, Pi etc.) a steadily increasing osmotic load is added to the cell. These conditions favour further H_20 absorption that shrinks the extracellular space (Fiolet et al., 1993). Adenosine and other metabolites and neurotransmitters diffuse to the extracellular fluid. A concomitant stimulation of adrenergic, purinergic and muscarinic receptors stimulate intracellular signalling systems that also stretch and cause mechanical changes to the tissue (Carmeliet, 1999; Kloner and Jennings, 2001). With increased production of protons, the intracellular pH can reach 6.0 after just 10 minutes of ischaemia (Fleet et al., 1985). Acidosis disrupts glycolysis and the contractile components of the cell, which contributes to an onset of contracture (and a rising end diastolic pressure) that generally occurs after 15 minutes of ischaemia (Allen et al., 1993).

Ischaemia has a significant effect on the cells' ion concentrations and currents. The reduced capacity to generate ATP limits the functional capability of ion transporters such as the Na^+/K^+-ATPase. This prevents the transporting of K^+ into the cell and generates a net increase in $[K^+]_o$ and a loss of $[K^+]_i$. With ATP levels declining rapidly a promotion of K^+ efflux occurs by the activation of the energy sensitive I_{KATP} (Billman, 2008). Promotion of further K^+ efflux via the voltage gated K^+ channels occurs with a move towards a positive membrane potential (of around -60 mV) and away from the K^+ equilibrium, driven by the accumulation of intracellular Na^+ and Ca^{2+} (Carmeliet, 1999). Ultimately this results in a shortening of the action potential duration.

A rise in $[Na^+]_i$ is driven by two transporters: the deficiency of its extrusion by the Na^+/K^+-ATPase as a consequence of a dwindling ATP reserves; and an increased inward leak through the Na^+/H^+ exchanger as protons accumulate in the cell. Increase in Na^+ is shown to correlate with increases in Ca^{2+} due to the activity of the NCX (Tani

and Neeley, 1989). The NCX goes into a reverse mode to counteract Na^+ entry and allow more Ca^{2+} entry, although recent reports suggest that the NCX is inhibited with acidosis and thus is more pronounced during the early stages of reperfusion. There are fluctuations in the systolic and diastolic level of $[Ca^{2+}]_i$ leading to Ca^{2+} transient alternans, which produces fluctuations in the Ca^{2+} dependent membrane currents and the action potential duration (Carmeliet, 1999). The rise in diastolic $[Ca^{2+}]_i$ slightly precedes the development of contracture (Eisner et al., 1989). The peak $[Ca^{2+}]_i$ that can be generated during systole is gradually reduced due to the inability of the SR to cycle Ca^{2+}. Several factors present during ischaemia (i.e. acidosis, reduced ATP availability, oxidative stress) are thought to contribute to this deterioration (Carmeliet, 1999).

Ischaemic Arrhythmias

The dramatic changes that occur to the cell's ionic currents and constitution increase the likelihood of irregular contractions and arrhythmias. Early ischaemic arrhythmias such as ventricular premature beats or irregular ventricular tachycardia can take place within the first 10 minutes of ischaemia (phase Ia). Advancement into a life threatening ventricular fibrillation (Vfib), defined as an uncoordinated depolarisation of the tissue with no cardiac output, is rare at this stage (Carmeliet, 1999). At 20-30 minutes of ischaemia a second stage of ventricular arrhythmogenesis (phase Ib) begins. This phase has an increased likelihood of Vfib and is particularly prominent in some species such as the dog, rat and pig.

The mechanisms that trigger the arrhythmias are now better understood (Luqman et al., 2007). Disparity in the tissue's action potential duration, refractoriness and the existence of a partial or unidirectional block of conductance, will allow re-entry of some impulses to stimulate consecutive action potentials. Also, ventricular cells

have the ability to spontaneously depolarise (automaticity) under such abnormal conditions. Diastolic depolarisation, which is normally reserved for pacemaker cells, will occur in the presence of catecholamines by promoting K^+ currents similar to the pacemaker current I_f ; or in Ca^{2+} overloaded cells, a slow release of Ca^{2+} from the SR may give a current via the NCX (Carmeliet, 1999). Early afterdepolarisation (EAD) and delayed afterdepolarisation (DAD) are known as triggered arrhythmic activity as an external stimulus is needed for their occurrence. During the plateau phase of the action potential an EAD may occur when the LTCC or NCX trigger a second depolarisation current and further release of Ca^{2+} from the SR. DAD is dependent on the cell's membrane potential upon repolarisation and is triggered late in phase 3 or early in phase 4 when the repolarisation period has begun. It is thought to be manifested by a high $[Ca^{2+}]_i$ concentration during this end diastolic phase.

Cell Death

The promotion of oncosis that leads to lytic rupture is characteristic of necrosis: during ischaemia, this is the pathway that the majority of cell death appears to occur through (Dong et al., 2006). The rate of ATP reduction also determines whether there is death by apoptosis or necrosis (Sebbag et al., 1996; Buja and Weerasinghe, 2010). To what extent these pathways contribute to the final infarct has been debated over the years.

The mitochondria are central to the involvement of cellular stress and mechanisms in activating death signals (pro-apoptotic). Opening of the mitochondrial permeability transition pore (mPTP) is thought to be a pivotal contribution to death signalling (Di Lisa and Bernardi, 2006; Halestrap, 2009). Normally the inner membrane of the mitochondria is relatively impermeable but under cellular stress (increase in $[Ca^{2+}]_i$ and ROS) the mPTP opens and allows mitochondrial swelling,

cytochrome c release and a loss of ATP. The majority of evidence however suggests that opening of mPTP results in cell death by accelerated necrosis rather than apoptosis (Halestrap, 2009). Release of pro-apoptotic factors such as cytochrome c etc. into the cytosol will promote apoptosis. However, continued opening of mPTP is incompatible with generation of ATP which is essential to drive the energy-dependent apoptotic programme and as such its contribution to the full extent of this process is debated.

1.3.3.3. Reperfusion Injury

Reperfusion therapy through techniques such as thrombolysis and percutaneous coronary intervention (PCI), has helped to lower the mortality rate of patients presenting with AMI, due to its ability to return blood flow to the ischaemic region (Keeley et al., 2003). Yet, over recent years it has become clear that this restoration in perfusion can also cause injury to the remaining viable tissue (Buja, 2005). Research in animals has demonstrated that some interventions at the time of reperfusion (see section 1.3.4.2) can limit cell death and other forms of injury (Ferdinandy et al., 2007). Those that have used infarct size as a primary end point, show that as much as 50% of the damage can be attributed to reperfusion (Marzilli and Huqi, 2010). Reperfusion injury has been classified into four types:

(i) Vascular injury that disrupts the coronary flow. Even with sufficient blood flow, some areas within the myocardium will have insufficient perfusion. This is a result of several complications including, coronary embolism, vasospasm and/or inflammation (Prasad et al., 2009). Reperfusion brings endothelial disruption by the inhibition of NO synthesis and endothelial blisters and blebs (Birnbaum et al., 1997). Long ischaemic periods of over 3 hours will also allow neutrophil 'plugging' to manifest in the microvasculature, which can cause the 'no-reflow phenomenon' (Entman and Smith, 1994).

(ii) Non-lethal injury such as myocardial stunning. The stunned myocardium will delay the recovery of systolic and diastolic function in viable tissue despite the presence of coronary flow. Stunning can respond to inotropic agents and is typically seen with shorter ischaemic durations or in salvaged tissue (Kloner and Jennings, 2001).

(iii) Reperfusion arrhythmias. These occur during the early stages of reperfusion and develop into ventricular tachycardia and fibrillation. Shorter durations

of ischaemia promote their maximal occurrence; longer duration of 1-3 hours or more have a lower incidence possibly due to extensive cell death.

(iv) Lethal injury that results in cell death. Reperfusion causes death of cells that have otherwise survived the preceding ischaemic insult. The difficulty in differentiating between injuries incurred by ischaemia or subsequent reperfusion periods created much of the early scepticism and debate (Garcia-Dorado et al., 2006a). Research models of reperfusion injury can not occur without prior ischaemia. For this reason, use of agents during the early reperfusion period has been the main approach to demonstrating the existence of reperfusion injury and the potential for salvaging cells by inhibiting it (Birnbaun et al., 1997, Ferdinandy et al., 2007).

Some key intracellular mechanisms that trigger reperfusion injury are beginning to be disclosed (see figure 1.10). When the occluded artery is cleared, a rapid return of perfusate reoxygenates the cells and increases their metabolic activity. The return of ATP restores the contractile activity of the cells but with excessive activation and hypercontracture that causes sarcolemmal rupture (Piper et al., 2004). Generation of ROS from the reactivated mitochondrial electron transport chain creates a cascade (although non-selective in its reactivity) of pro injury events to which Ca^{2+} handling proteins are particularly vulnerable (Brookes et al., 2004). The restoration of the NHE to exclude H^+ for Na^+ triggers increases of activity in the NCX but in the reverse mode (Talukder et al., 2009). This contributes to a rise in $[Ca^{2+}]_i$ and the mishandling of Ca^{2+} by the SR. Ca^{2+} overload induces the opening of the mPTP and a release of further ROS, cytochrome c and pro-apoptotic factors. Other Ca^{2+}-dependent molecules such as proteases and phospholipases endorse degradation of the cell membranes (Dong et al., 2006). The osmotic load and sarcolemmal rupture contribute to cell death by necrosis

(Di Lisa et al., 2001), although apoptosis and autophagy are prominent features in later stages of the reperfusion period (Murphy and Steenbergen, 2008).

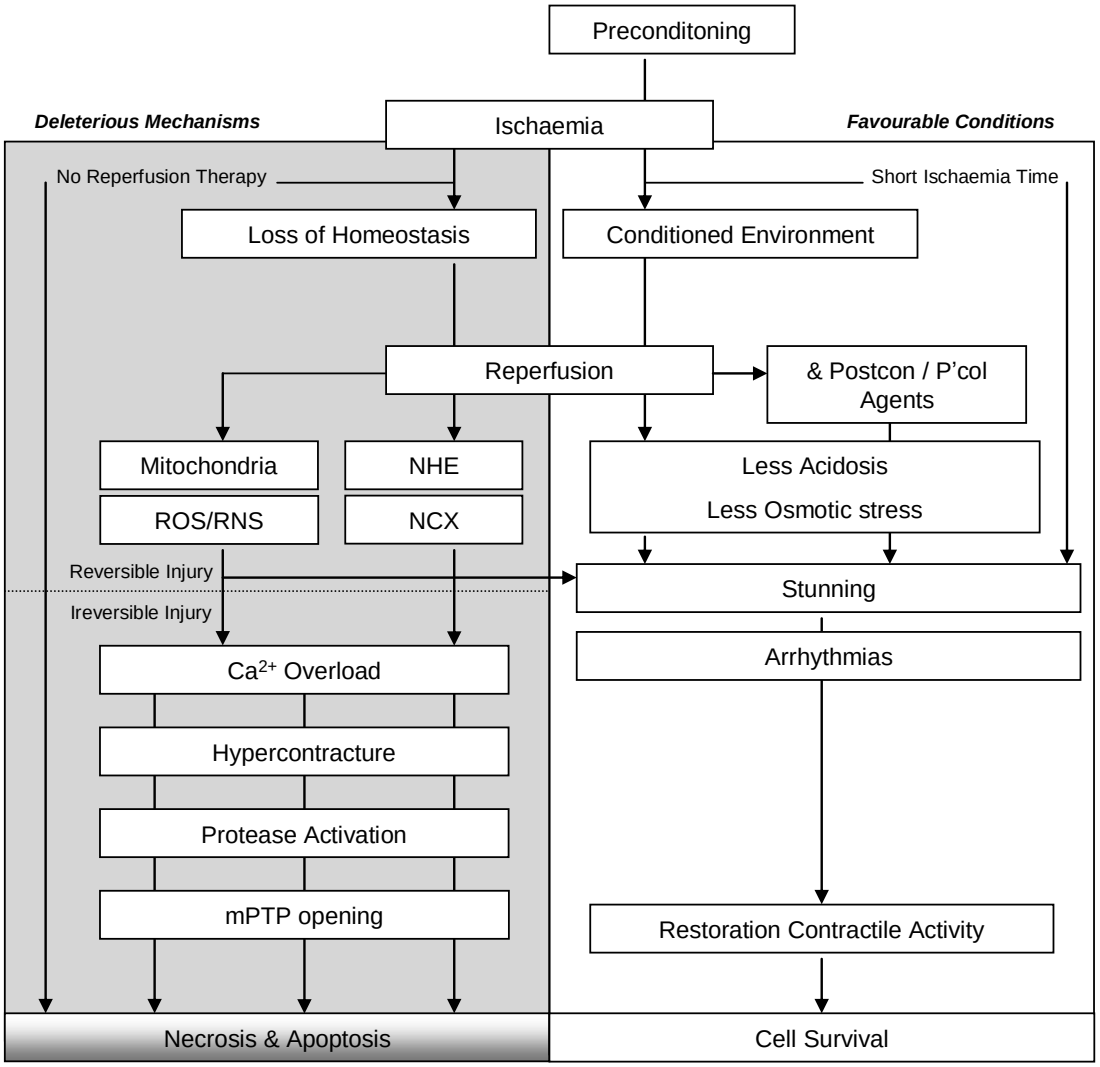

Figure 1.10: Mechanisms that trigger cell death and survival after ischaemia-reperfusion. *Prior conditioning or short ischaemia times favour shorter disruption to intracellular environment. Longer ischaemic times enforce cell death. Reperfusion is vital for cell survival but also triggers other pro-injury cascade including; ROS generation and ion transport favouring Ca^{2+} overload. mPTP opening is vital for some cellular death as closure with pharmacological aids promotes survival. Less osmotic stress and Ca^{2+} mishandling also favours restoration of normal contractile activity and cellular health. The degree of common mechanisms between the protective strategies is unknown but some elements such as mPTP closure is an end target.*

1.3.4. Cardioprotective Paradigms

Over the years, a range of cardioprotection models have been employed in various species in an attempt to prevent or lessen I-R injury (Maroko et al., 1971; Murry et al., 1986; Zhao et al., 2003). A few of the successful interventions have included: pharmacological aids such as anti-anginal drugs (Maroko et al., 1971); inert gases (Derwall et al., 2009); various synthetic receptor ligands (Ferdinandy et al., 2007); hypothermia and cardiac arrest (Tyers et al., 1977); ischaemic pre-conditioning prior to the injury (Murry et al., 1986); brief ischaemia in remote organs (Gho et al., 1996) and limbs (Schmidt et al., 2007) termed per-conditioning; or brief ischaemia immediately after the ischaemic insult, termed post-conditioning (Zhao et al., 2003). Many of the strategies show clinical potential by improving cardiac function, by reducing the cell death during ischaemia and reperfusion, or reducing contractile defects and the incidence of arrhythmias.

A lot of knowledge exists on the mechanisms that are involved in the protective effects of ischaemic or pharmacological conditioning (Ferdinandy et al., 2007; Hausenloy and Yellon, 2007; Jennings, 2011; Vinten-Johansen, 2011). The stimuli and triggers needed to activate the favourable signalling pathways (mediators) have been thoroughly explored, although the end effectors of protection remain debatable or unknown (Garcia-Dorado et al., 2006b; Buja and Weerasinghe, 2010; Yang et al., 2010; Vinten-Johansen, 2011). The end effectors have a direct role in deciding the fate of the ischaemic/reperfused cell and are of significance as potential pharmacological targets.

1.3.4.1. Ischaemic Preconditioning

Ischaemic preconditioning (IPC) is a potent endogenous cardioprotective strategy where brief cycles of ischaemia-reperfusion are instigated before a longer duration of injurious ischaemia (Murry et al., 1986). The initial exploration was to determine if the ATP utilisation and catabolic build up of several cycles of I-R had the same effect as a prolonged single duration of ischaemia (Reimer et al., 1986; Reimer, 1996). When this was then developed to investigate whether the I-R cycles prior to an extended ischaemic insult would accentuate the ATP depletion and the injury, it was surprising to discover only a quarter of the potential infarct size had been developed. The following studies suggested that IPC was capable of slowing the myocardial energy demand by reducing the rate of ATP depletion and thus reducing the extent of anaerobic glycolysis and the cellular load of catabolites (Murry et al., 1990). Although cellular arrest is the mechanism that preserves the hypothermic heart (Tyers et al., 1977), with IPC, it was later discovered that there was much more to its nature than limiting the cells metabolic activity.

The triggers of IPC protection were revealed to include the many compounds that accumulate in the ischaemic heart; including adenosine (Liu et al., 1991), bradykinin (Goto et al., 1995), noradrenaline (Banerjee et al., 1993) and opioids (Miki et al., 1998). Activation of the individual receptors with exogenous autacoids prior to I-R, induced protection comparable to IPC, whilst pharmacological blockade of the receptors during the IPC stimulus, prevented its protection (Ferdinandy et al., 2007). The release of the autacoids during the short cycles of I-R allows activation of their respective cell membrane receptors, of which many are linked to G proteins. The receptor subtypes will determine which combinatorial interactions of G-proteins and their respective signalling pathway are activated. To date, all Gαi-coupled receptors

(i.e. adenosine A_1/A_3, bradykinin B_2, opioid δ-receptors) have demonstrated the ability to trigger the IPC phenotype through protein kinase C (PKC) activation (Goto et al., 1995; Sakamoto et al., 1995; Miki et al., 1998; Downey et al., 2007; Yang et al., 2010). Typically, the Gαq-coupled receptor instigates the enzyme phospholipase C (PLC) to cleave a phospholipid into a diacylglycerol (DAG) and $InsP_3$, which can then directly or indirectly activate PKC. However, it was found with a series of investigations that although adenosine receptors (A_1/A_3) could couple to PLC and PKC activation (Parsons et al., 2000), stimulation with acetylcholine (Ach) and the other mentioned Gαi-coupled receptors, did so through a more complex pathway involving phosphatidylinositol-3 kinase/Akt (PI3K/Akt), and the generation of ROS from the mitochondria (Qin et al., 2003; Downey et al., 2007).

The cardioprotection afforded by the ligands, even after they have been washed out from heart preparations an hour earlier, is thought to be maintained via ROS activation of PKC and is still classed as the trigger phase (Baines et al., 1997; Downey et al., 2007). The IPC phenotype can be replicated by the sole exposure to small quantities of oxygen radicals (Baines et al., 1997) and H_2O_2 (Sharma and Singh et al., 2001) prior to ischaemia; and can be abolished when ROS scavengers are present with the IPC stimulus (Tanaka et al., 1994; Baines et al., 1997). Forbes et al. (2001) have suggested that a key mechanism for cardioprotection by increased generation of ROS lies with the opening of the mitochondrial ATP sensitive potassium channels (mitoK_{ATP}). But this is debated as the compound used to disclose such activity (diazoxide) can also act through the opening of the sarcolemmal K_{ATP} channels (Garlid and Halestrap, 2012). Sarcolemmal K_{ATP} channels had previously been suggested to be a key factor of IPC as the promotion of shorter action potentials would limit Ca^{2+} entry and the force of contraction, preserving valuable ATP (Gross and Fryer, 1999).

Costa et al., (2005) when using isolated mitochondria from cardiac myocytes suggested that a key link for mitoK_{ATP} opening was the cyclic guanosine monophosphate (cGMP) signalling pathway. But this would only be able to occur in the presence of PKCε, as a cGMP-dependent protein kinase (PKG) would be too large to pass the mitochondrial inner membrane. Nitric oxide and its downstream target PKG had formerly been implicated as a trigger of IPC, with PI3K/Akt pathway central to their activation (Lochner et al., 2000; Downey et al., 2007). Although PKC is also a common factor for these pathways, there are differences between species as to whether adenosine or NO is the dominant trigger of IPC.

Much of the work in the last decade has focused on IPC's ability to mediate protection during reperfusion. Hausenloy et al., (2005) were one of the first to focus on roles of the PI3K/Akt pathway and the p42/p44 mitogen activated protein kinase (MAPK) pathway (ERK1/2) during reperfusion. Earlier studies showed that their phosphorylation activity were higher at 15 minutes of reperfusion when an IPC stimulus had been used (Hausenloy et al., 2004). The IPC protection was abrogated when these inhibitors were present at reperfusion, demonstrating their key involvement in mediating protection during reintroduction of coronary flow. Evidence for the existence of reperfusion injury had already gained attention in previous years when numerous pharmacological agents had been cited as having the capability of reducing the injury if applied concomitantly (Ferdinandy et al., 2007). Many of these agents depended on PI3K/Akt and/or ERK1/2 for protection to occur, which was termed by Hausenloy and Yellon (2004) as the Reperfusion Injury Salvage Kinase (RISK)-pathway. It has since included other signalling pathways such as PKA and other members of the MAPK pathway i.e. JAK/STAT pathway (Hausenloy and Yellon, 2006). The JAK/STAT

pathway has been termed Survival Activating Factor Enhancement (SAFE) pathway by Lecour (2006).

The survival kinases carry the protective signal to the end effectors (Downey et al., 2007). But the assortment of signal transduction pathways has created numerous hypotheses for the mechanism that salvages the cells. The more established suggestions centre on stabilising the mitochondria and the closure of the mPTP during reperfusion (Javadov et al., 2003; Ferdinandy et al., 2007; Gottlieb, 2011). Juhaszova et al., (2004) suggested the protection from the PKC, ERK1/2, and PI3K/Akt signalling pathways all act to inhibit glycogen synthase kinase-3 β (GSK-3β), as it was revealed to have a direct association with the mPTP and its closure. The same study also proposed that the mitochondria's threshold for ROS is reduced after hypoxia-reoxygenation and could be reversed with pharmacological agents such as diazoxide, also implying a role for the mitoK_{ATP}. A greater tolerance to the mPTP opening by Ca^{2+} overload was also suggested after IPC by Argaud et al. (2004). However, this contradicts an earlier study by Javadov et al. (2003), where using similar methods, they showed that preconditioned cardiac myocytes that were subsequently isolated, had a greater Ca^{2+} sensitivity to mPTP opening than the controls or hearts treated with the direct mPTP inhibitor cyclosporine A. This suggested that although IPC did protect against reperfusion injury by inhibiting the mPTP *in situ*, an indirect protection must also be in place to attenuate Ca^{2+} overload and ROS overproduction. Hypercontracture and sarcolemmal rupture can also cause cell death when the mPTP is closed (Garci-Dorado et al., 2006a). Thus, physiological mechanisms that promote normal Ca^{2+} cycling and cytoskeletal integrity during reperfusion are also critical for cell survival.

IPC has a window of cardioprotection that lasts one to two hours after its induction (Yang et al., 2010). After this interval has passed, the protective phenotype is

withdrawn until a later second window of protection emerges 24-72 hours after the stimulus (Baxter et al., 1997). Referred to as late or delayed preconditioning, its protective mechanism centres on the gene expression and protein synthesis of a range of cardioprotective proteins.

Other organs have the potential for IPC (Gho et al., 1996). This has been developed further to using the peripheral tissues to condition the heart prior to the re-introduction of coronary flow (Schmidt et al., 2007). Known as per-conditioning this new phenomenon is already undergoing clinical trials (Vinten-Johansen and Shi, 2011). Bøtker et al. (2010) investigated the beneficial use of a blood pressure cuff to provide a 'conditioning' stimulus to STEMI patients being transported in an ambulance. Incidence of mortality, re-infarction and heart failure were the same in both groups but myocardial salvage was much improved in the per-conditioned group. The mechanisms of protection and the method of triggering remote preconditioning and perconditioning remain elusive, although possibly via the transfer of blood borne humoral factors, immune cells or an unknown small molecule, some common pathways leading to K_{ATP} opening and mPTP inhibition are a possibility (Vinten-Johansen and Shi, 2011).

1.3.4.2. Modified Reperfusion and Postconditioning

In the initial study on postconditioning, where repetitive bouts of ischaemia were introduced during early reperfusion, it was found to be as effective as IPC in reducing infarct size in anaesthetised open-chest dogs (Zhao et al., 2003). Cardioprotection was attributed to preserving endothelial function, reducing neutrophil accumulation and limiting ROS activity. The list of mechanisms quickly grew to include the triggering by several autacoids, the RISK signalling pathway and other components similar to IPC (Hausenloy et al., 2005). An additive protective effect of IPC and postconditioning was

reported to be possible in anaesthetised rabbit hearts (Yang et al., 2004), but this was not reproduced in isolated rat hearts (Tsang et al., 2004).

The practice of postconditioning has been described as an 'old wine in a new bottle' (Heusch, 2004) due to its similarities to a previous technique of staged reperfusion. This involves lowering the coronary flow during the initial stages of reperfusion and thus limiting post-ischaemic injury (Okamoto et al., 1986). In doing so, the heart regains activity in a progressive manner and avoids a sudden alteration in the intracellular conditions. One aspect of these techniques is that the gradual recovery from acidosis averts several mechanisms of injury. These include: the NHE from triggering a reversed NCX and Ca^{2+} overload (Inserte et al., 2009, Rodriguez-Sinovas et al., 2009); prevention of calpain activation and degradation of proteins (Inserte et al., 2009); opening of the mPTP (Cohen et al., 2007); hypercontracture and the Ca^{2+} cycling with the SR (Piper et al., 1998). The timing of the postconditioning protocol is also fundamental and must occur immediately after the ischaemic period (Yang et al., 2004).

Argaud et al. (2005) demonstrated that the threshold for mPTP opening in the presence of Ca^{2+} was higher in cells that had been postconditioned or preconditioned. However, a later study recorded a higher Ca^{2+} content in the mitochondria of postconditioned cells than IPC cells (Argaud et al., 2008). It was thus suggested that postconditioning increases the mitochondria's tolerance to $[Ca^{2+}]_i$ whilst IPC reduced the $[Ca^{2+}]_i$ and the exposure of mitochondria to Ca^{2+}. This is intriguing as much of the injury that is proposed to occur from Ca^{2+} overload occurs during the early reperfusion period and that postconditioning reduces the loss in ionic homeostasis. This was suggested by Sun et al. (2005) in an *in vitro* model of hypoxia-reoxygenation with postconditioning, as mitochondrial Ca^{2+} concentration, and ROS generation were much

lower than in controls. Apart from the differences in models used, the method of measuring total Ca^{2+} compared to free Ca^{2+} could be an explanation for these discrepancies (Ovize et al., 2010).

Postconditioning is a more complex phenomenon than IPC (Jennings, 2011). Preconditioning gives robust protection against infarction and has not been disputed within the literature (Cohen and Downey, 2011). But some investigations have been unable to reproduce the cardioprotection gained by postconditioning in pig hearts (Schwartz and Lagranha, 2006), rat hearts (Dow and Kloner, 2007) or anesthetised rabbit hearts (Hale et al., 2008). This means an optimum protocol is yet to be found (Vinten-Johansen and Shi, 2011). But its potential in clinical use has been demonstrated by Thibault et al. (2008) who recorded in STEMI patients a reduced infarct size and an improved long term functional recovery.

1.3.4.3. Pharmacological Conditioning

For technical reasons patients that are reperfused by thrombolysis (and not PCI) would not be eligible for postconditioning and would thus benefit more from pharmacological conditioning (Ovize et al., 2010). The list of successful agents in experimental models is vast with some not having a direct role in the natural phenomenon of IPC or postconditioning but able to trigger similar signalling pathways. A diverse group of naturally occurring agents tested so far includes: natriuretic peptides, adrenomedullin, erythropoietin, insulin, transforming growth factor-β (Ovize et al., 2010). A clinical example is the J-WIND trial which investigated the use of atrial natriuretic peptide in patients who had AMI (Kitakaze et al., 2007). The patients that received intravenous ANP in conjunction with reperfusion treatment had lower infarct size (measured by creatine kinase release) and reperfusion injuries than those that received a placebo.

Although the experimental design received some criticism, the modest improvement shows potential for natriuretic peptides to be used as a pharmacological treatment (Burley and Baxter, 2009; Ovize et al., 2010).

As the mishandling of Ca^{2+} is a key mechanism of cellular injury during AMI, it is crucial that there is the development of a therapeutic strategy for its management (Garcia-Dorado et al., 2012). Pharmacological agents that target the handling of intracellular Ca^{2+} have had limited success in limiting I-R injury (Talukeder et al., 2009; Garcia-Dorado et al., 2012). The most recent clinical trials have used caldaret (MCC-135) that can reduce $[Ca^{2+}]_i$ at time of reperfusion by possibly preventing the $[Na^{+}]_i$ via inhibition of the NCX (Satoh and Kitada, 2004). The drug's specific mechanism of action is unknown, but is also thought to have a positive lusitropic effect on the heart by promoting the uptake of Ca^{2+} in the SR (Satoh et al., 2001). However, its administration in STEMI patients undergoing PCI gave no limitation in infarct size or any improvement in ejection fraction (Bar et al., 2007; Tzivoni et al., 2009).

1.3.5. CaMKII and Cardiovascular Disease

Research concerning CaMKII involvement in CVD has progressed substantially since Ramirez et al. (1997) reported that in rat ventricular myocytes the δ_B subtype had the ability to increase the expression of atrial natriuretic factor (ANF), a well known marker of pathological hypertrophy. It was soon established that the failing human myocardium also had augmented levels of $CaMKII_{\delta B}$ (Hoch et al., 1999). Kirchhefer et al. (1999) reported that patients suffering from dilated cardiomyopathy had a three fold increase in CaMKII activity, when they compared them to 'healthy' hearts that were unsuccessfully used as transplants. These studies opened up the possibility that CaMKII had some role to play in CVD, although it was yet to be established if it was an epiphenomenon of hypertrophy or a key mediator. Work by Brown's laboratory substantiated the latter hypotheses by creating two transgenic mouse models: one that targeted the nuclear δ_B subtype (Zhang et al., 2002); and one that targeted the primarily cytosolic δ_C subtype (Zhang et al., 2003). Directed by a tissue specific promoter, the up regulation of either CaMKII isoforms supported the development of cardiomyopathy and abnormal functioning. Consequently, genetic models that ablated CaMKII in the heart displayed less cardiac remodelling and dysfunctional phenotypes in models of pathological hypertrophy induced by β-adrenergic stimulation (Zhang et al., 2005) and pressure-overload (Ling et al., 2009). More recently, Sossalla et al., (2010) confirmed that the failing human myocardium had increased levels of $CaMKII_{\delta B}$ and $CaMKII_{\delta C}$. They also explored the effect of the CaMKII inhibitors KN-93 and AIP on primary isolated cells from these hearts. The inhibitors reversed the pathological phenotype of the cells by improving their contractility and Ca^{2+} handling capabilities. As non-failing sheep hearts exposed to the same CaMKII inhibitors showed no adverse effects in

contractility, the authors concluded that targeting CaMKII in patients with heart failure could be a therapeutic strategy for the future.

Contractile dysfunction and arrhythmias regularly accompany maladaptation of the heart, as the tissue develops disrupted conduction properties and Ca^{2+} handling abilities (Dzau et al., 2006). Data soon emerged that CaMKII contributes to a pro-arrhythmic role (Anderson, 2007). However, the involvement of CaMKII in acute coronary syndromes is unclear. It was first suggested that CaMKII has a beneficial role in promoting the Ca^{2+} handling properties of the SR if adverse conditions of ischaemia and early reperfusion are present (Netticadan et al., 1999; Osada et al., 2000; Temsah et al., 2002). But Mattiazzi's group only found this benefit to exist under conditions of acidosis or short ischaemic durations that promote stunning (Valverde et al., 2006; Mattiazzi et al., 2007; Vila-Petroff et al., 2010). Recent research indicates that if these changes to intracellular conditions are sustained, they permit CaMKII to promote injury through Ca^{2+} overload and initiation of the intrinsic cell death pathways (Vila-Petroff et al., 2007; Zhu et al., 2007; Salas et al., 2010). These studies suggest that a pathological role for CaMKII exists but it is yet to be fully disclosed.

1.3.5.1. CaMKII as a Mediator of Cell Death

Several *in vitro* models of cell death provide evidence that CaMKII is instrumental in promoting injury. Zhu et al. (2003) created a model of apoptosis by subjecting cardiac myocytes from adult mice to sustained β-adrenergic stimulation. It was reported that the $I_{Ca.L}$ stimulates $CaMKII_{\delta C}$ to be a key mediator of cell death and not the cAMP/PKA pathway. The same laboratory also overexpressed a constitutively active $CaMKII_{\delta C}$ in rat cardiac myocytes (Zhu et al., 2007). Apoptotic cell death was instigated via the intrinsic pathway of cytochrome c release but could be reduced if pharmacological

inhibitors of CaMKII were present. In addition, adenoviral expression of a dominant negative $CaMKII_{\delta C}$ (to demonstrate isoform specificity) not only abolished apoptosis in the cells that overexpressed a constitutively active $CaMKII_{\delta C}$, but also in other standard models of cell death, e.g. oxidative stress. Other laboratories have established similar findings, with the use of angiotensin II (Palomeque et al., 2009), oubain (Sapia et al., 2010), upregulation of the LTCC (Chen et al., 2005) and simulated I-R (Vila-Petroff et al., 2007), implicating CaMKII as pro-injurious. CaMKII is not believed to directly target the mitochondria, but rather has the ability to promote Ca^{2+} overload through actions on the SR. Odagiri et al. (2009) incubated saponin-permbealized myocytes with CaM and recorded (by using fluorescence microscopy) the generation of ROS, depolarized mitochondria and opening of the mPTP, which were all reversible with CaM and CaMKII inhibitors.

An interesting study by Peng et al. (2010) revealed that $CaMKII_{\delta B}$ is not associated with the same cell death pathways as $CaMKII_{\delta C}$. In an *in vitro* model of oxidative stress or an *in vivo* model of I-R, the two isoforms had an inverse relationship to one another. That is, the expression of δ_B isoform decreased with conditions of cellular stress, whilst the δ_C isoform increased substantially and remained high for 4-24 hours after the insult had occurred. When cells that overexpressed $CaMKII_{\delta B}$ were subjected to oxidative stress the extent of their injury was also less than in the controls. Gene microarray and pharmacological manipulation suggested that the heat shock protein-70 family members were part of $CaMKII_{\delta B}$ anti-apoptotic pathway. Wu et al. (2006) had previously reported that activation of the δ_B subtype is downstream from Ca^{2+} released by the IP_3R and the nucleus and not the global Ca^{2+} oscillations incurred by E-C coupling. Knowing that PKC is a dominant target for the IP_3R and has a role

in other cardioprotection models, it would have been interesting to see whether PKC had any involvement with CaMKIIδ_B activation.

1.3.5.2. CaMKII and Ischaemia-Reperfusion Injury

The initial studies investigating CaMKII in models of I-R measured the temporal activity of the kinase and the relationship between cellular Ca^{2+} handling properties and contractile recovery. The protein expression during short ischaemic times in rat myocardium (15 minutes; Uemura et al., 2002) or gerbil cerebral tissue (5 minutes; Zalewska et al., 1996), suggested that a proportion of CaMKII translocates to the cell membrane and is restrained from autophosphorylation. Baseline samples had higher expression values of CaMKII in the cytosolic fractions than in the particulate fractions, but during ischaemia, a significantly smaller proportion was present in the cytosol and a greater proportion was expressed in the cell membrane. Ischaemic myocytes also had limited phosphorylation at the Thr^{287} site in the cytosolic fractions, while no phosphorylation was measured in the particulate fraction. After 5 and 15 minutes of reperfusion, a gradual recovery of cellular location and kinase activity had begun but not to the same extent as pre-ischaemic values. The authors commented that longer duration of ischaemia (30 minutes) resulted in irreversible damage and had prompted an even weaker expression of CaMKII (Uemura et al., 2002).

Dhalla's group investigated I-R injury in an *ex vivo* rat heart preparation, using contractile recovery as a primary end point of injury, with the analysis of isolated SR vesicles at specific periods to determine the tissue's Ca^{2+} cycling abilities. The series of investigations concluded that 30 minutes of ischaemia and up to 60 minutes reperfusion depressed the SR uptake of Ca^{2+} which contributed to the reduced contractile activity and cytosolic Ca^{2+} overload (Temsah et al., 1999; Netticadan et al., 1999; Osada et al.,

2000; Temsah et al., 2002). These studies included measurements of CaMKII activity. No changes occurred in the cytosol during ischaemia (Netticadan et al., 1999), but a significant absence was seen in the fractions that contained the SR vesicles. This reduction in CaMKII correlated with the decline in active SR proteins (SERCA2a pump and PLB phosphorylation) and the Ca^{2+} uptake by the SR (Netticadan et al., 1999). Perfusion of radical scavengers (Netticadan et al., 1999), instigating IPC (Osada et al., 2000) or altering the conditions of hypoxia and glucose deprivation (Temsah et al., 2002) prevented the decline in CaMKII activity. As these interventions limited injury to the SR and improved contractility recovery at reperfusion, it was suggested that preservation of CaMKII is associated with maintenance of the heart's normal function. Comparable data later emerged from Benter et al. (2004) who pre-treated rats with KN-93. The treated heart preparations had a significantly greater deterioration in cardiac function after 40 minutes of ischaemia and 30 minutes of reperfusion, than did the controls. These studies suggested that the molecular activity of CaMKII is influenced by ischaemia and gradually recovers at the onset of reperfusion. They also suggested that the CaMKII reduction in activity correlates with the I-R depression in Ca^{2+} handling by the SR and that this affected the contractile properties of the heart, which suffers further depression if CaMKII is inhibited.

Mattiazzi's laboratory has examined the influence of CaMKII on reversible and irreversible ischaemic injury with a particular focus on the PLB Thr^{17} site. A detailed western analysis of this CaMKII substrate disclosed that it was active during the first minutes of ischaemia before being subdued to below control levels as ischaemic duration continued (Vittone et al., 2002). But at 30 sec and 1 minute of reperfusion a significant transient increase in activity occurred and lasted up to the third minute. Hearts from PLB knockout mice in a model of stunning, had a significant deterioration

in functional recovery as a result of increased $[Ca^{2+}]_i$ (Valverde et al., 2006). Thus, PLB and its regulator CaMKII appeared to be a key mechanism to regulate $[Ca^{2+}]_i$ during reperfusion recovery after a short ischaemic time. Detailed western analysis also demonstrated that key time points in previous studies had missed a window of CaMKII activity. Uemura et al. (2002) started their analysis of CaMKII activity/expression after 5 minutes of reperfusion whereas Netticadan et al. (1999) measured it at the end of 30 minutes of reperfusion. Mattiazzi's later studies used longer durations of ischaemia to identify this transient period of CaMKII activity (Vila-Petroff et al., 2007; Salas et al., 2010). Using infarct size as a primary end point, perfusion of KN-93 (2.5 μM) for 10 minutes prior to ischaemia (45 minutes) and for 10 minutes at early reperfusion, significantly reduced the size of injury. Contractile recovery, lactate dehydrogenase release, caspase 3 activity, cytochrome C release and Bcl-2/Bax ratio were more favourable in hearts treated with a CaMKII inhibitor. The source for this CaMKII activity at reperfusion was suggested to be the NCX (and not the LTCC), as its inhibition during reperfusion limited PLB Thr^{17} phosphorylation and infarct size (Vittone et al., 2002; Salas et al., 2010). Although phosphorylation of RYR2 (Ser^{2815}) had increased significantly after 3 minutes of reperfusion, the total amount of the ion channel had decreased giving similar ratios to the pre-ischaemic samples (Salas et al., 2010).

When Erickson et al. (2008) first described the oxidative activation of CaMKII, their investigation also suggested this to promote I-R injury. The genetic model consisted of a knockout methionine sulfoxide reductase A (MSrA) that reverses Met oxidation. These mice had greater methionine oxidation at the CaMKII $Met^{280/281}$ sites, increased myocardial apoptosis and a deteriorated *in vivo* mechanical function during coronary ligation. Although infarct size was not measured, the knockout mice had a

reduced survival rate after MI. Of note is the study by Zhang et al. (2005) who used genetic inhibition of CaMKII (promotion of an inhibitory peptide) to investigate *in vivo* the effects of sustained β-adrenergic stimulation. When they subjected the mice to I-R injury, there was no reduction in infarct size, but there was a significant improvement in left ventricular contraction.

To summarise, the experimental data from Mattiazzi's laboratory suggest that pharmacological inhibition of CaMKII during long ischaemic times and at early reperfusion can prevent cell death by necrosis and apoptosis. Shorter duration of ischaemia and models of stunning the myocardium require CaMKII to maintain contractile activity. The discrepancies between the studies of long ischaemia are due to choice of analysis and the short window of CaMKII activity at early reperfusion. These can either promote recovery from reversible injury or instigate death during irreversible injury.

1.3.5.3. CaMKII in Models of Cardioprotection

Experimental models of cardioprotection have given supplementary information on how CaMKII behaves under conditions of cellular stress. The previously mentioned studies by Netticadan et al. (1999) and Osada et al. (2000) suggested that the presence of antioxidants throughout I-R or an IPC stimulus promote improved Ca^{2+} cycling ability via CaMKII. Pre-treatment with a pharmacological inhibitor of CaMKII (KN-93) can abrogate these favourable conditions (Osada et al., 2000; Benter et al., 2005). However, genetic inhibition of CaMKII in mice expressing the inhibitor peptide AIP (Zhang et al., 2005) had contradictory outcomes. Li et al. (2007) subjected these mice to IPC prior to I-R injury and demonstrated an additive protective effect to infarct limitation as a nonsignificant trend was present without IPC. There was no improvement in the

mechanical recovery with either intervention, including the control hearts subjected to IPC. But the study also focused on CaMKII's role in triggering the I_{KATP}, as their previous work (Li et al., 2006) indicated a shortening of the action potential (via K^+ channels) during its inhibition. In the absence of CaMKII, the pore forming subunit (Kir6.2) was upregulated on the sarcolemma; I_{KATP} was the same as that in control mice. When treatment with pinacidil (opener) or HMR1098 (blocker) eliminated or increased the size of MI between the control and AIP mice, it was concluded that CaMKII inhibition during IPC enhances the opening of the I_{KATP}. This study is interesting as others have suggested a role for CaMKII in promoting opening of K_{ATP}.

Yan et al. (2009) investigated the open probability of I_{KATP} in an *in vitro* model of hypoxia or oxidative stress. Using pharmacological blockade of kinases (PKC, PKG and CaMKII) channel opening was inhibited, suggesting these signalling pathways are mediators of K_{ATP} opening under cellular stress. Of interest is that KN-93 and KN-62 at concentrations above 1 µM and 5 µM respectively, significantly abrogated the I_{KATP}. Chai et al. (2011) have also recently confirmed the ability of a different pharmacological inhibitor, AIP, to reduce the open probability of I_{KATP} in rabbit ventricular cells. This study suggested that CaMKII was upstream to a PKG pathway and that generation of ROS was a key trigger. These methods of pharmacologically manipulating CaMKII contradict the suggested mechanism at work in AIP-overexpressing mice (Li et al., 2007). But they also suggest that an unseen protective element might have occurred in the studies by Osada et al. (2000) and Benter et al. (2005). Furthermore, it was reported that models of intermittent high altitude hypoxia (IHA) develop their cardioprotection properties via the K_{ATP} channel, stimulated by CaMKII activity. Six weeks of IHA treatment in rats, protected their hearts against models of Ca^{2+} paradox (Xie et al., 2004) and I-R injury (Yu et al., 2009).

Pharmacological inhibition with either KN-93 or 5-HD abolished the protective phenotype, implicating CaMKII and K_{ATP} channels as key mediators.

A favourable role for CaMKII was observed if volatile anaesthetic was used as a cardioprotective intervention. Desflurane-induced preconditioning (Lange et al., 2008) and postconditioning (Lange et al., 2009) limited infarct size in a rabbit *in vivo* model of I-R injury. If KN-93 was administered prior to these interventions it abrogated the protection, but had no significant effect on outcome per se. Desflurane protection also promoted PLB phosphorylation as described by Osada et al. (2000). However, a selective β-adrenergic inhibitor metoprolol could confer protection by down regulating the Thr^{17} and Ser^{16} sites of PLB. This would agree with Mattiazzi's hypothesis that increased PLB activity during reperfusion promotes irreversible injury.

1.4. Overview and Scope of Thesis

The thesis interrogates the role of CaMKII in the acute conditions of myocardial I-R injury. It intended to determine the consequences of using a pharmacological inhibitor of CaMKII at specific time points of ischaemia or reperfusion and during the mechanical interventions of IPC and postconditioning. In an *ex vivo* rat heart model of regional I-R injury with infarct analysis, I determined if under these conditions CaMKII was involved in irreversible injury (Chapter 2). Using a secondary cell line (H9c2 cells) as an *in vitro* model of simulated I-R and oxidative stress (Chapter 3) I tried to replicate the data in Chapter 2. The Ca^{2+} handling abilities of primary isolated cardiac myocytes (Chapter 4) were also measured and analysed under conditions of simulated I-R in order to further investigate the effects of pharmacological blockade of CaMKII.

1.4.1. Questions Addressed in this Thesis

The thesis sought to provide answers to the following questions:

i) Is CaMKII involved in promoting irreversible injury caused by acute myocardial infarction?

ii) Does the phenomenon of IPC and postconditioning involve CaMKII?

iii) Under conditions of simulated I-R, what effect does pharmacological blockade of CaMKII have on the Ca^{2+} handling properties of the cells?

1.4.2. General Hypothesis

CaMKII promotes injury in conditions of I-R injury by promoting Ca^{2+} overload. However, when these abrupt changes in intracellular conditions are subdued, CaMKII has a beneficial role in mediating the protection of IPC.

CHAPTER 2:

Involvement of CaMKII in I-R Injury and Models of Cardioprotection

2.1. Introduction

2.1.1. Mechanical Interventions for I-R Injury

Animal models of I-R injury have been essential in developing knowledge of the pathophysiology of ischemic heart disease and in allowing the exploration of possible therapeutic interventions. Within a couple of years of postconditioning's discovery in anaesthetized dogs (Zhao et al., 2003), small scale clinical trials were undertaken in patients who required revascularization by PCI (Laskey et al., 2005; Staat et al., 2005). The benefits of IPC can not apply to a patient with an acute coronary syndrome, but there would be a use if I-R is prescheduled e.g. organ transplants and CABG, (Yellon et al., 1993; Tomai et al., 1999). Also, IPC's ability to limit infarction has led to the discovery of pharmacological agents that can be used at reperfusion (Cohen and Downey, 2011).

The optimum protocol for these mechanical interventions is still unknown. Sandhu et al. (1997) reported that the rabbit heart had a 'dose-dependency' of IPC when they compared one cycle of 5 minutes I-R to three cycles. The increased number of IPC cycles reduced infarct-risk area to 4%, in comparison to 32% with the lower number. Liu and Downey (1992) had previously recorded that the rat heart needed more than one cycle of IPC (5 min I-R) for infarct limitation, although the single cycle did protect against arrhythmias. But other studies have not been able to show an additional improvement in contractile recovery if increased cycles of IPC were implemented (Baker et al., 1999). It is important, however, to achieve an acceptable balance between a preconditioned phenotype and the degree of myocardial stunning that accompanies brief periods of ischaemia. Shorter cycles lasting up to 5 minutes are the norm for instigating the IPC phenotype as periods lasting above 15 min go beyond the threshold of reversible injury (Kloner and Jennings, 2001). The animal studies that used

pharmacological antagonists to abrogate the IPC phenotype established that blocking only one of the GPCR can abolish the protection of a single IPC cycle (Goto et al., 1995; Downey et al., 2007). If multiple preconditioning cycles were used in the presence of the drug, the cardioprotected phenotype could be salvaged as further generation of the autacoids would harness protection. It became apparent with studies on postconditioning that shorter cycle durations favoured the hearts of smaller species such as the rat (Crisostomo et al., 2006). The interventions used on human myocardium have ranged between 2-6 cycles with 30-90 seconds in cycle duration (Yetgin et al., 2010), whereas the rat heart requires 3-6 cycles of 10-30 sec in duration (Crisostomo et al., 2006).

2.1.2. Involvement of CaMKII in IPC and Postconditioning

Research investigating the contribution of CaMKII to myocardial I-R injury is limited in comparison to the numerous studies that have focused on its role in pathological hypertrophy and arrhythmia. Very few studies have focused on its relationship with IPC and none have investigated whether CaMKII might have any involvement in postconditioning. What has been gathered so far is contradictory.

Some of the benefits of IPC are evident at reperfusion. These include an improved Ca^{2+} cycling ability, resistance to Ca^{2+} overload and oxidative stress, and the positive conditioning of the mitochondria by various signalling pathways (Yellon and Downey, 2003). Thus, as CaMKII is a regulator of $[Ca^{2+}]_i$, the first studies suggested that the IPC phenotype was associated with enhanced CaMKII activity (Osada et al., 2000). The improvements to the SR handling of Ca^{2+} can be removed if pharmacological inhibitors of CaMKII are present, which also deteriorate the contractile recovery usually seen during reperfusion (Osada et al., 2000; Benter et al., 2005). In

addition it was established that ischaemia has an influence on the activity of CaMKII, stimulating its translocation to the sarcolemma and reducing its autophosphorylation status (Uemura et al., 2002). How an IPC stimulus would later maintain an improvement in CaMKII activity during ischaemia or at reperfusion is unknown. But it was confirmed that shorter periods of ischaemia that cause stunning of the myocardium, favour the preservation of CaMKII activity on targets on the SR such as PLB (Vittone et al., 2002). A protective element of CaMKII might even go beyond the SR handling of Ca^{2+} and engage sarcolemmal ion channels such as K_{ATP}. *In vitro* models of oxidative stress have recently demonstrated an involvement of CaMKII with the I_{KATP} (Yan et al., 2009; Chai et al., 2011). The shortening of the action potential duration that occurs during ischaemia could serve as an intrinsic mechanism by which CaMKII activity is limited, by reducing the availability of the $I_{Ca.L}$. However, AIP transgenic hearts in which CaMKII activity is reduced offer contradictory data to this possibility. This method of CaMKII abrogation enhanced the I_{KATP} and was the suggested cause for an additive infarct limitation when an IPC stimulus was implemented (Li et al., 2007).

Two key differences in the current models investigating CaMKII are the duration of I-R and the timing of intervention. The genetic mutant models (Li et al., 2007) and Mattiazzi's studies (Vila-Petroff et al., 2007) maintain CaMKII inhibition during the early reperfusion period, whilst earlier work focused primarily on pre-ischaemia treatment. It is suggested that an increase in PLB phosphorylation of the Thr^{17} site and the SR Ca^{2+} load occurs during reperfusion and this window of activity promotes cellular injury if a long period of index ischaemia is used (Vila-Petroff et al., 2007; Salas et al., 2010). Pharmacological inhibitors or genetic manipulation of CaMKII in *in vitro* and *in vivo* studies of sustained cellular stress can limit cell injury and death (Zhang et al., 2005; Zhu et al., 2007). The key mechanisms during these

conditions have also been suggested to be the impaired handling of Ca^{2+} by the SR and the effects that this has on the mitochondria (Odagiri et al., 2009). Similar mechanisms are thought to be at work with reperfusion injury by opening of the mPTP under conditions of increased $[Ca^{2+}]_i$, and oxidative stress. The presence of a pharmacological inhibitor of CaMKII before and during reperfusion inhibited cell death by apoptosis and necrosis, as the NCX in reverse mode failed to trigger further loading of Ca^{2+} into the SR (Vila-Petroff et al., 2007; Salas et al., 2010). Other studies that suggest CaMKII as a mediator of cell death have included abrogation of CaMKII throughout the I-R period (Erickson et al., 2008). However, Lange et al. (2009) found no limitation to infarct size when rabbit hearts were subjected to 30 minutes of CAO and received a bolus of KN-93 only during the reperfusion period. This treatment did abolish desflurane induced postconditioning, suggesting that CaMKII is involved in this form of postconditioning. This window of CaMKII activity during reperfusion might also be a critical element of mechanical postconditioning. A gradual recovery from acidosis and the limitation of abrupt activation of the NHE and NCX is one of the suggested mechanisms of postconditioning protection. But how CaMKII would react to such conditions and if it is a vital component for restoration of intracellular conditions are unknown.

2.1.3. Hypothesis

The aim of these studies was to explore the role of CaMKII in I-R injury and whether it had any involvement in the phenomena of IPC and postconditioning. Using the rat isolated heart as a model the study was to determine whether a pharmacological inhibitor of CaMKII (KN-93) would have any effect on irreversible injury caused during ischaemia or at early reperfusion. The study also investigated the infarct limitation associated with various IPC or postconditioning protocols and whether there was any contribution by CaMKII.

It was hypothesised that:

i) Under control conditions, CaMK II activation beyond a certain threshold occurs at reperfusion and promotes irreversible injury.

ii) Under preconditioning and postconditioning conditions, CaMKII promotes cardioprotection.

2.1.4. Specific Objectives

(1). Develop a model of cardioprotection in an *ex vivo* model of I-R, using the mechanical interventions of IPC and postconditioning.

(2). To examine the effects of perfusing a pharmacological inhibitor of CaMKII during key stages of I-R and the cardioprotective interventions, with infarct analysis used as a primary end point of injury. This would be broken down into smaller studies investigating:

(A) CaMKII inhibition during normal I-R conditions

(B) CaMKII inhibition during IPC

(C) CaMKII inhibition during postconditioning.

2.2. Materials and Methods

The CaMKII organic inhibitor KN-93 (water soluble) and the inactive analog KN-92 were purchased from Calbiochem (Nottingham, UK). As a methoxybenzenesulfonamide compound, KN-93 competes for the CaM binding site on CaMKII with an inhibition constant of 0.37 μM (Sumi et al., 1991). KN-92 is a structural analog of KN-93 devoid of activity on CaMKII at concentration below 25 μM (Anderson et al., 1998; Singh et al., 2009). The only difference between the two compounds is that KN-93 possesses a 2-hydroxyethyl moiety. As KN-92 is not water-soluble, it was dissolved in DMSO (final DMSO concentration in the Krebs-Henseleit buffer 0.05%).

2.2.1. The Isolated Perfused Heart

The Langendorff isolated perfused heart has been a fundamental tool for investigating models of I-R injury (Verdouw et al., 1998; Skrzypiec-Spring et al., 2007). It was devised by Oscar Langendorff in 1895 to allow investigation of the mechanical activity of the isolated mammalian heart (Doring and Dehnert, 1988). The original design (figure 2.1(A)) involved an injection cannula inserted into the aorta of the heart. By connecting it to a container full of defibrinated blood, a pressurised air bottle forces the perfusate through the cannula. This closes the aortic valve (as occurs in the *in situ* heart during diastole) and directs the blood through the ostia of the right and left coronary arteries (Zimmer, 1998). Known as retrograde perfusion, only hearts perfused in this way may be termed the 'Langendorff heart' (Doring and Dehnert, 1988). A string attached to the apex of the heart and a membrane of a Marey capsule, enabled the contractions to be transferred by air pressure to a kymograph (Zimmer, 1998).

(A)

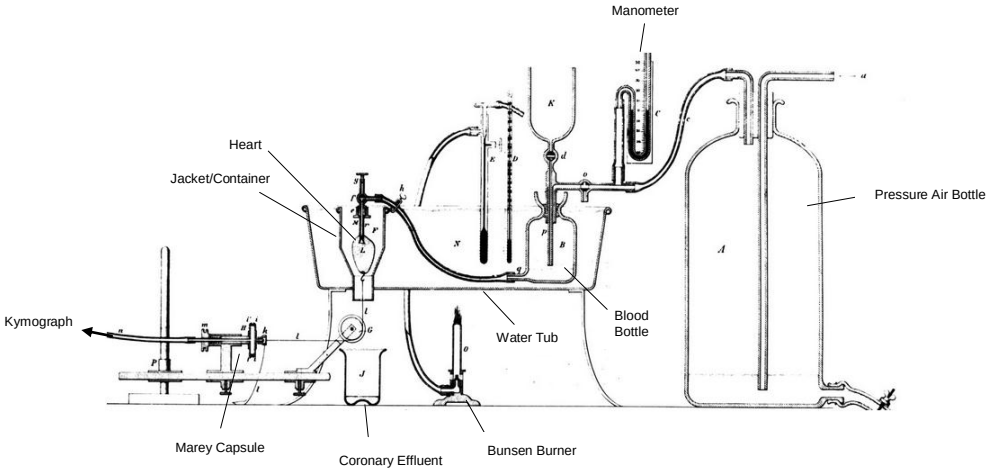

(B)

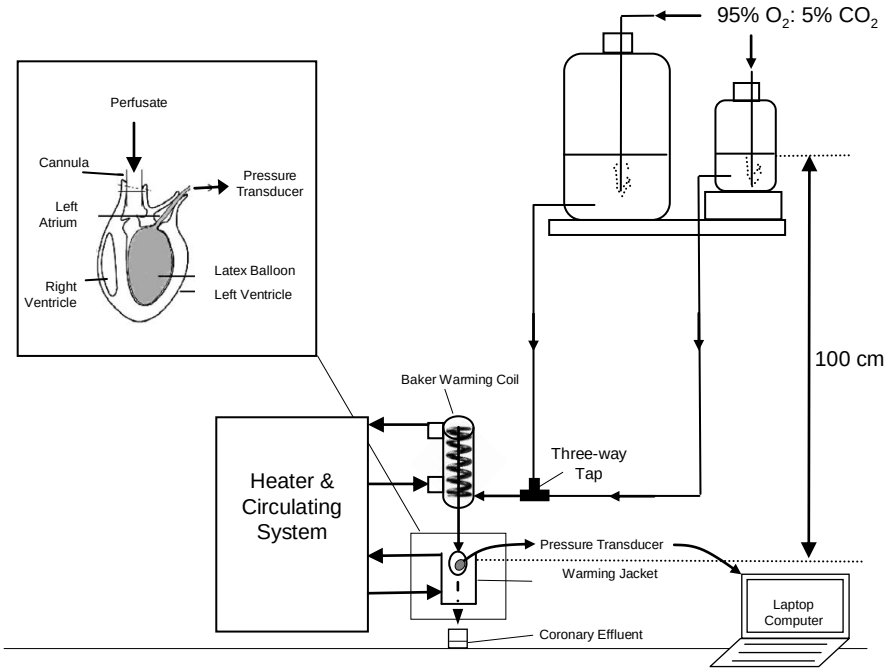

Figure 2.1: The Langendorff perfused heart. *(A) The original drawing and design of apparatus described by Oscar Langendorff in 1895. Blood flowing retrogradely into the aorta is driven by the pressure air bottle. Shortening of the heart is recorded by the attachment of string to a Marey capsule and kymograph (taken from Zimmer, 1998). (B) The constant hydrostatic pressure in this study is created by positioning reservoirs containing Krebs-Henseleit buffer 100 cm (73 mmHg) above the cannulated heart. A Baker warming coil is kept at 37^{o}C by a circulator and allows the passing perfusate to be heated. A latex balloon that is connected to a pressure transducer and computer is inserted into the left ventricle in order to measure the cardiodynamic data.*

Over the last century the Langendorff preparation has helped to develop our understanding of myocardial function, regulation of coronary blood flow and cardiac metabolism in healthy and pathological conditions. Some of Langendorff's first observations were that the heart retained its automaticity when perfused with a nutrient fluid such as blood; and that high temperature or low temperature led to patterns of tachycardia and bradycardia respectively (Zimmer, 1998). The model has since been used to test an array of cardiovascular drugs and the effects of gene alterations on heart physiology (Skrzypiec-Spring et al., 2007).

Various modifications have been made over the years to suit particular studies. Katz (1939) developed a technique of using constant flow to deliver perfusate instead of constant pressure (Skrzypiec-Spring et al., 2007). This method overrides the autoregulatory mechanisms of the coronary arteries and delivers the perfusate regardless of heart function and changes in vessel radius. The changes in the vessel radius will however be inversely proportional to the changes in the coronary perfusion pressure. As the two key measurements needed to calculate flow resistance are the perfusion pressure and the coronary flow rate (CFR), if one of these variables is made constant the other variable could be used to calculate the flow resistance. Katz realised that the readings in coronary pressure were much easier and more sensitive than those of timed collection with coronary flow. Thus Katz and colleagues used this method to evaluate the vasoactive properties of many drugs. In Chapter 4, the constant flow technique is used to isolate primary cardiac myocytes by perfusing low Ca^{2+} solutions and enzymatic digestion of the extracellular matrix. This provides a constant flow regardless of the deterioration in heart function and vasculature. Within this chapter the constant pressure is the preferred method as it is more physiologically relevant and allows the changes in vessel radius to produce the consequent changes in CFR.

The Langendorff isolated heart is limited by its lack of humoral and neuronal background. The *ex vivo* preparation continually deteriorates but can remain viable for several hours (Sutherland and Hearse, 2000) to measure biochemical, physiological and pharmacological indices. The rat heart has become a popular choice for Langendorff perfusion preparations and is the best characterised (Sutherland and Hearse, 2000). Ease of handling, animal cost, low volume of perfusion fluids and the size of hearts (in comparison to that of the mouse) are key advantages. With regard to I-R studies, the rat has minimal collateral vessels allowing the study of regional ischaemia without the need to measure and correct for collateral flow. There are key physiological differences between the rat heart and the human heart i.e. the shorter action potential duration and a dominant Ca^{2+} handling by the SR that need to be considered when evaluating the experimental data.

2.2.1.1. Perfusion Protocol for the Rat Heart

Male Sprague Dawley rats (300-450 g) obtained from Harlan UK Ltd. (Oxon, UK) or B&K Universal Ltd. (Hull, UK) were used for the studies. Animals were acclimatised in the animal house for a minimum of 7 days and subjected to 12 hour light-dark cycles. The water and feed (4% fat, 18% protein) were available ad libitum. All care and use of animals were in accordance with the UK Home Office guidelines.

The rats were anaesthetised with a mixture of sodium pentobarbital (65 mg/kg) and heparin (300 units) given concomitantly by i.p injection. Once the rat was unconscious and evoked no reflexes the thoracic cage was opened to expose the heart. The excised hearts were promptly cannulated via the aortic stump (figure 2.1) and perfused at a constant pressure of 100 cm H_20 (78 mmHg) with Krebs-Henseleit buffer (in mM: NaCl 118.5, $NaHCO_3$ 24.8, d-Glucose 11, KCl 4.7, $MgSO_4.7H_20$ 1.2, KH_2PO_4 1.2, $CaCl_2.2H_2O$ 1.25) that was pre-heated to 37^oC and aerated with 95% O_2/5% CO_2 (pH 7.3-7.5 at 37^oC). A warm jacketed chamber surrounded the heart and a temperature gauge inserted into the tissue of the right atrium was used to monitor the temperature, which was maintained in the range of 36.5-37.5^oC. A latex balloon was introduced through the left atrium after removal of the atrial appendage and positioned within the left ventricle to measure its contractile force. The balloon filled with purified water and connected to a polypropylene cannula, enabled isovolumetric pressure to be measured by a transducer that was linked to a data capture programme (Powerlab, Chart 4.0). A mercury sphygmomanometer was used to calibrate the transducer beforehand. End diastolic pressure (LVEDP) was set at 5-10 mmHg by adjusting the balloon volume.

The experiments began with a stabilisation period of 15-30 minutes in duration. Haemodynamic measurements were taken at time points that included an initial reading, after 10 minutes (designated baseline reading) and at one minute before an intervention.

The readings included; heart rate (HR; beats per minute, bpm), LVEDP, left ventricular systolic pressure (LVSP), total developed pressure (LVSP - LVEDP), rate pressure product (HR x LVSP) and coronary flow rate (CFR), measured by timed collection of the coronary effluent. This period allowed an evaluation of the heart's contractile performance ensuring it was stable (from any defects). The several decades of research on the isolated perfused rat heart, have allowed the normal physiological properties and characteristics to be highly predictable (Doring and Dehnert, 1988; Bell et al., 2011). Within this laboratory (Baxter and Yellon, 1993; Burley and Baxter, 2007) 20 years of experience of this preparation has led to the development of the following inclusion criteria:

- ✓ Normal sinus rhythm devoid of bradycardia/tachycardia, numerous ectopic beats or an episode of Vfib;
- ✓ HR between 200 and 400 bpm. The *in vivo* heart rate can reach 500 bpm but withdrawal of the autonomic influences subdues this rapid rate. A bradycardic response below 200 bpm is generally a sign of injury;
- ✓ A developed pressure of above 60 mmHg ensuring an acceptable inotropic response to the perfusate and hydrostatic pressure;
- ✓ CFR above 10 ml/min. Perfusion of hearts with saline solutions will entail greater coronary flow than blood perfusion. For the size of the adult rats used in this study an initial flow rate below 10 ml/min indicates deterioration in the vasculature.

Any hearts not meeting all of these criteria during stabilisation were excluded from further experimental manipulation.

2.2.1.2. Executing MI and Measurement of Infarct Size

Rat hearts have a consistent and prominent left anterior descending artery. This enables consistency in locating the vessel and inserting a 3-0 silk suture (Ethicon, UK) around it. A snare was formed by passing the two suture strands through a modified pipette tip. The left coronary artery was then occluded (CAO) by pulling gently on the silk threads whilst pushing with the plastic tip to compress the artery and surrounding tissue. A second plastic pipette tip locked the suture in place for the remainder of the ischaemic insult, which lasted for precisely 35 minutes. When competent with this technique, this method of instigating CAO is highly reproducible. Measuring the CFR during the initial ischaemic period will determine the extent of CAO achieved. A reduction in CFR by less than 30% indicates a poor occlusion of the artery and/or small risk zone and would not be sufficient to induce an adequate ischaemic insult to the tissue. Releasing the locked pipette tips enabled reperfusion of the ischaemic region. After 120 minutes of reperfusion the silk suture was tied tightly before Evans Blue dye (0.4%) was infused through the heart. This stained the non-ischaemic tissue as it entered the regions that were perfused by vessels other than the left anterior coronary artery. Once sufficient staining was achieved the heart was removed and stored immediately at -20^{o}C for a maximum of 72 hours.

The frozen hearts were allowed to thaw for a few minutes before being cut into transverse sections, 2 mm thick, from the apex to the base. After the cut sections had thawed for a further 2 minutes, they were then incubated at 37^{o}C in triphenyltetrazolium Chlorite (1% w/v), for 20 minutes with frequent agitation. The stained sections were then fixed in 10% formalin for 24-48 hours to enhance contrast between stained and non-stained regions before their images were scanned into the computer for planimetry analysis by the author.

By using ImageJ (v1.38; Wayne Rasband, National Institutes of Health, USA), each heart slice was characterised by three subdivisions depending on the staining obtained (figure 2.2). The areas stained with Evans Blue were regarded as non ischaemic tissue; the red areas were the ischaemic regions but with viable tissue; white/yellow areas were measured as the infarct tissue. If there was poor staining of the heart slices and not enough delineation between the regions, particularly the ischaemic and non-ischaemic areas the hearts were excluded from analysis. The definition of a red and viable tissue or a white and presence of infarction is further complicated by the regions known as peri-infarction (sometimes pink in colour) which separates the two regions. It is thus up to the analyst to decide whether to exclude or include these regions as viable tissue. The peri-infarct areas were included consistently as an infarct area within this study. If the experimental groups are known and thus predicted due to the hypothesis, subjectivity of the peri-infarct area can also determine the outcome of the analysis. As such, all analysis was done blind by coding each heart after the experiment with a sequence (date and alphabetical) that was not related to the treatment group. One method of overcoming such subjectivity is using an independent person, who is also blind to the experimental groups, to analyse the regions. This 'double-blind' method was not chosen in this study due to the workload and the consistency (i.e. same person needs to analyse all experimental groups) required for these studies over several months.

The volume of each heart section was also calculated by multiplying the areas by their thickness (~2 mm). Myocardial infarct size was expressed as the volume of infarct tissue/volume at risk x 100%. The volume of myocardium at risk was also calculated as a ratio of the whole heart volume.

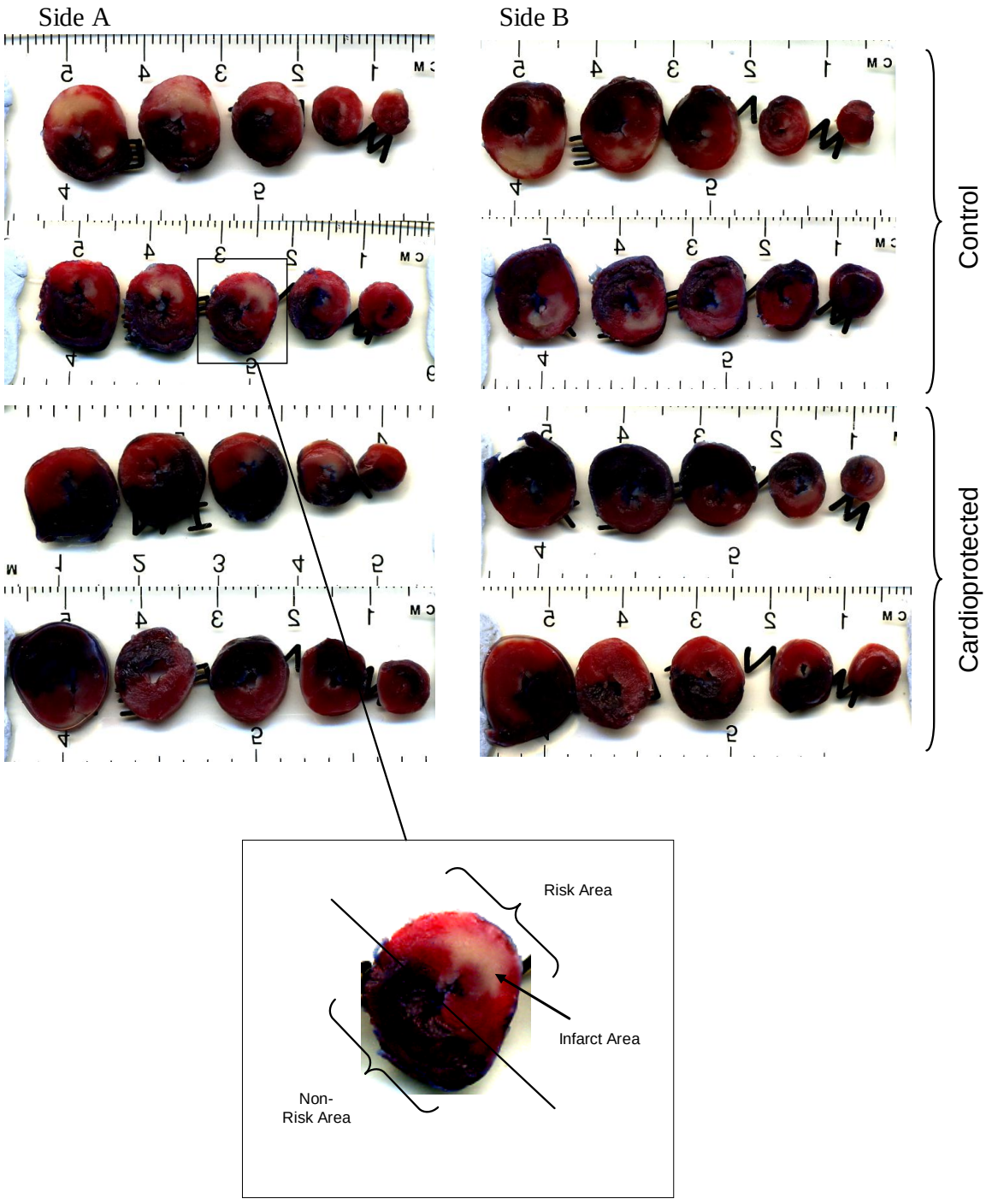

Figure 2.2: Stained transverse sections of rat hearts. *Evans Blue and tetrazolium staining was used to distinguish the non ischaemic tissue (Blue) from the ischaemic tissue (Red), with enzyme washout from the infarct tissue (White/Yellow) indicating the total extent of irreversible injury. Upper sections are from controlled experiments and demonstrate considerable infarct areas; Lower sections are hearts that have been protected by an intervention that reduces irreversible injury.*

2.2.1.3. Treatment Groups

After a period of haemodynamic stabilisation (15-30 minutes), each isolated rat heart was subjected to CAO of the left descending artery (35 minutes) followed by reperfusion (120 minutes). **Study 1** investigated the mechanical interventions of IPC and postconditioning, using infarct limitation as a primary end point. The groups varied in the duration and number of cycles that were used to trigger the cardioprotective phenotype. **Study 2(A)** investigated the effect of CaMKII inhibition on ischaemia and reperfusion injury. The two periods of injury were defined by the separation in treatment periods, pre-ischaemia or at reperfusion alone, of the pharmacological inhibitor (KN-93). The inactive analog of the organic inhibitor, KN-92, was used as a negative control. **Study 2(B)** investigated the effect of a CaMKII inhibitor on IPC. Treatment of KN-93 during the IPC cycles or at reperfusion intended to separate the two trigger phases of the intervention. **Study 2(C)** investigated the effect of CaMKII inhibition during the initiation of the postconditioning cycles. All experiments were randomised and the treatment groups are further defined below.

Study 1: Effect of mechanical interventions on I-R injury

The mechanical interruption in coronary flow to effect IPC or postconditioning was instigated by closing a tap above the cannula. This initiated global no-flow ischaemia and prevented the risk of damaging tissue around the coronary artery. The loss of heat supplied by the perfusate was counteracted by bathing the heart in pre-heated Krebs-Henseleit. As the two IPC groups differed in the intervention duration (total of 27 or 33 minutes including stabilisation period) the control group was randomised to receive a stabilisation period of either 20 or 30 minutes in duration. Figure 2.3 outlines each experimental protocol.

Study 1

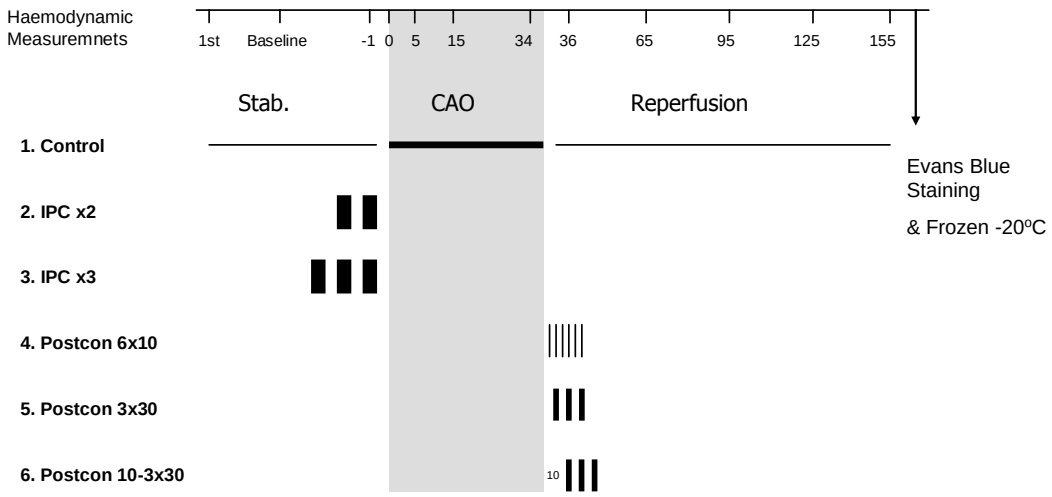

Figure 2.3: Timeline of the experimental procedures used for the groups in Study 1. *All groups received a stabilisation period, followed by 35 min of regional ischaemia and 2 hours of reperfusion (1. Control). Groups 2 and 3 included the IPC intervention of 3 minutes global ischaemia and reperfusion, for either 2 or 3 cycles respectively. Groups 4-6 received the intervention of postconditioning at reperfusion, with varying cycle duration and numbers (described in text). Haemodynamic measurements were made at specific time points throughout the experiments (time line not to scale). Stab. Stabilisation period; CAO, Coronary Artery Occlusion; IPC: Ischaemic Preconditioning; Postcon: Postconditioning.*

Group 1, Control: Perfused with Krebs-Henseleit buffer and subjected to 20-30 min stabilisation period, 35 min CAO and 120 min of reperfusion.

Group 2, IPC (**2 cycles)**: 15 min of stabilisation, 2 cycles of 3 min global ischaemia followed by 3 min reperfusion, 35 min CAO and 120 min of reperfusion.

Group 3, IPC (**3 cycles)**: 15 min of stabilisation, 3 cycles of 3 min global ischaemia followed by 3 min reperfusion, 35 min CAO and 120 min of reperfusion.

Group 4, Postconditioning (6 x 10 sec cycles): 20 min stabilisation and 35 min CAO, immediately followed by six 10 sec cycles of reperfusion and global ischaemia. The first cycle was considered the start of the reperfusion period although haemodynamic data were recorded at 1 min after the last cycle.

Group 5, Postconditioning (3 x 30 sec cycles): The postconditioning protocol was altered to three 30 sec cycles of reperfusion and global ischaemia.

Group 6, Postconditioning (10 sec reperfusion, then 3 x 30 sec cycles): An initial 10 second reperfusion period was followed by three 30 seconds of global ischaemia and reperfusion.

Study 2: The effect of using a CaMKII inhibitor on I-R injury and the mechanical interventions, IPC and postconditioning.

A drug reservoir was placed at the same height as the normal Krebs-Henseleit reservoir (figure 2.1B) and connected to the system by a three way tap. Stock concentrations of the drugs, KN-93 and KN-92, were added to a precise volume of Krebs-Henseleit buffer to attain a final concentration of 2 μM. This is the concentration used throughout the thesis and was based on concentrations reported in the literature; i.e. Dhalla's group (1 μM) and Mattiazzi's group (2.5 μM), and is 7-fold higher than the inhibition constant, Ki of 0.37 μM (Sumi et al., 1991). Perfusion times in each treatment group are depicted in figure 2.4 and defined further in the following text:

Study 2

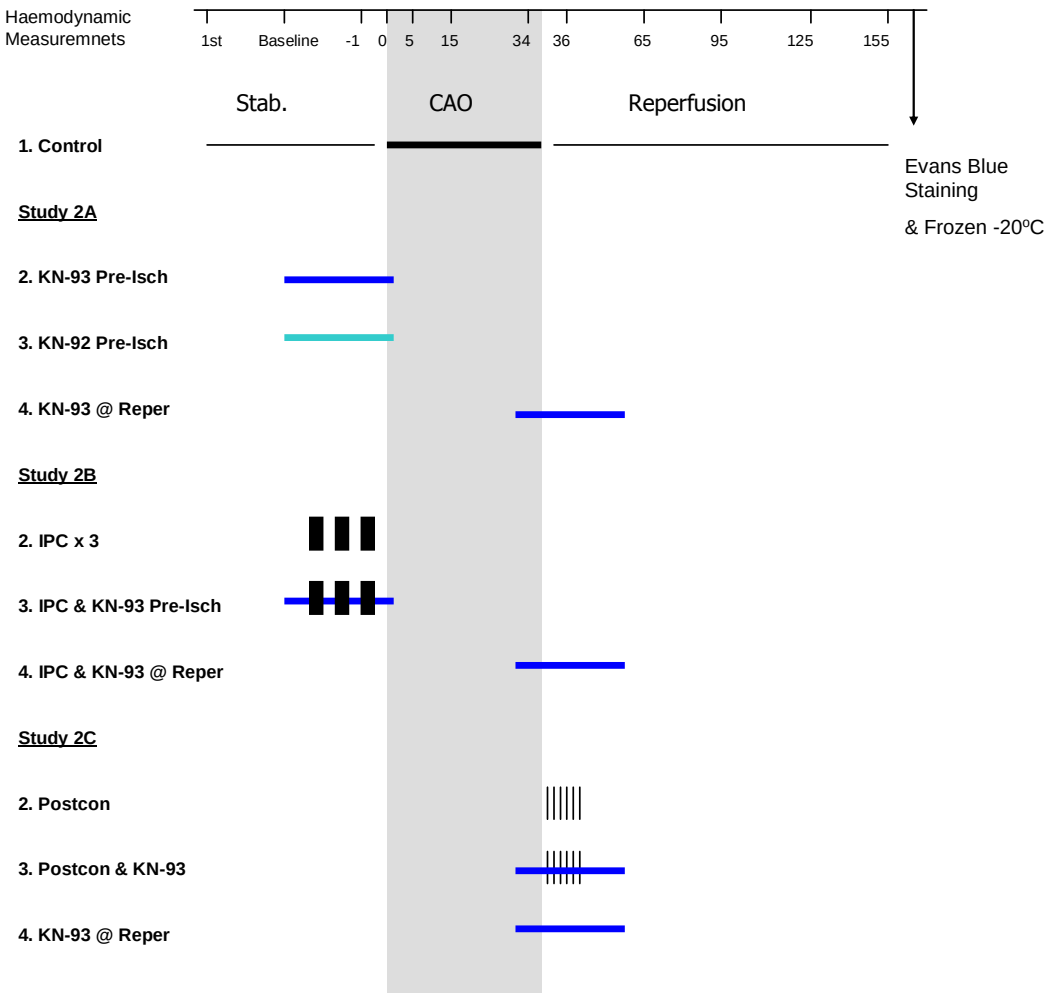

Figure 2.4: Timeline of the experimental procedures used for the groups in Study 2. *The study explored CaMKII inhibition during; (A) normal ischaemia-reperfusion protocol, (B) IPC intervention and (C) Postconditioning intervention. All groups received an initial stabilisation period (15-30 min), followed by regional ischaemia (35 min) and reperfusion (120 min). Drug perfusion prior to ischaemia was limited to a total of 12 min including the IPC intervention; and 15 min in total at reperfusion. Time line not to scale. Stab. Stabilisation period; CAO, Coronary Artery Occlusion; IPC: Ischaemic Preconditioning; Postcon: Postconditioning; Pre-Isch, Prior to Ischaemia; @ Reper, during early reperfusion.*

Study 2(A): CaMKII inhibition during ischaemia or reperfusion

Group 1, Control: Perfused with Krebs-Henseleit buffer and subjected to 20-30 min stabilisation period, 35 min CAO and 120 min of reperfusion.

Group 2, KN-93 perfusion pre-Ischaemia: After 20 min of stabilisation, KN-93 was globally perfused into the heart for 12 min before the 35 min CAO and 120 min of reperfusion.

Group 3, KN-92 perfusion pre-Ischaemia: An analog of KN-93, KN-92 (2 μM) was perfused in the same manner as group 2.

Group 4, KN-93 perfusion at reperfusion: 5 min prior to the reperfusion period, KN-93 (2 μM) was perfused globally into the heart. This ensured the drug was present at the opening of the ligated artery. Drug perfusion was continued for further 10 min into the reperfusion period.

Study 2(B): CaMKII inhibition during ischaemic preconditioning

To limit variability, study 2(A) and study 2(B) were completed side by side and in doing so incorporated the same control group.

Group 1, Control: randomly allocated as previously described.

Group 2, IPC (**3 cycles x 3 min)**: Three cycles of 3 min IPC were initiated before the CAO.

Group 3, KN-93 perfusion during IPC: 3 min prior to the IPC stimulus (3 cycles), KN-93 (2 μM) was perfused globally into the heart. Once CAO had been secured, drug-free Krebs-Henseleit perfusate was returned to the heart.

Group 4, KN-93 perfusion at reperfusion after IPC: The same IPC protocol as group 2, except that KN-93 (2 μM) was present at reperfusion as previously described.

Study 2(C): CaMKII inhibition during postconditioning

Group 1, Control: As the other described control groups.

Group 2, Postconditioning: 20 min stabilisation and 35 min CAO was immediately followed by six, 10 sec cycles of reperfusion and global ischaemia.

Group 3, KN-93 perfusion with postconditioning: 5 min prior to reperfusion and the postconditioning stimulus of 6 x 10 sec, KN-93 (2 μM) was perfused into the heart. A further 10 min of drug perfusion was added during reperfusion.

Group 4, KN-93 perfusion at reperfusion: 5 min prior to the reperfusion period, KN-93 (2 μM) was allowed to perfuse into the heart and continued for another 10 min during reperfusion.

2.2.3. Statistical Analysis

For infarct size determination in this experimental model, previous work determined that the expected difference between control and primary intervention is typically 50-60% reduction in infarct size. The standard deviation in such experiments is 10-12%. The conventional criterion of statistical significance (5%) and statistical power at 85% were adopted. With factorial design and random allocation, the minimum number required in each experimental group is 4, with randomisation to control groups increasing the number of control experiments. All numerical data are presented as mean values ± SEM. The statistical software PRISM® version 5.00 was used to analyse all data. One way-analysis of variance (ANOVA) was used to compare the mean infarct size of the groups within each study. A repeated measures ANOVA was used to analyse the haemodynamic measurements of CFR, HR, developed pressure and RPP between each group. A post hoc analysis (Newman-Keuls test) was used, and a probability level of 5% ($p < 0.05$) was defined as the level of statistical significance.

2.3. Results

2.3.1. Exclusion Criteria

Hearts were excluded from the study if during the stabilisation period any of the criteria of steady sinus rhythm, HR above 200 bpm, developed pressure above 60 mmHg or a CFR above 10 ml/min were not met. Other exclusions included; insufficient reduction in CFR during the first 15 minutes of ischaemia, or failure of the hearts to reperfuse after releasing the coronary ligature. Exclusion of hearts during the analysis included: insufficient risk zone delineation by the Evans Blue, insufficient tetrazolium staining.

In study 1 a total of 70 hearts were used, with 50 successfully completed and further reported in this chapter. Study 2A and 2B had a total of 69 hearts, with 53 experiments reported. Study 2C had a total of 41 hearts, with 21 experiments reported.

***Table 2.1**: Total No. of hearts excluded and reported in studies 1-2*

Study	Excluded:		Reported
	Experimental	Analysis	
1	12	8	50
2A & 2B	8	8	53
2C	10	10	21

2.3.2. Baseline Cardiodynamics

None of the treatment groups within the studies were significantly different in their baseline cardiodynamic data or their regions at risk of infarction (table 2.2). The hearts' initial contractile performance and CFR recorded after 10 minutes of stabilisation were consistent between all treatment groups. The control and postconditioning group of study 2(C) had the highest mean CFR (15.6 ± 1.2 ml/min and 15.4 ± 1.2 ml/min respectively) although this did not appear to be influenced by the rats' body weight. The mean risk zone volume was also greater in these two experimental groups (0.49 ± 0.03 cm^3 and 0.48 ± 0.04 cm^3 respectively) for this study. This corresponds to a larger risk-total area (64.8 ± 4.1% and 65.6 ± 5.0% respectively) indicating a higher proportion of the left ventricle was occluded, although this was not significant within the study. The risk-zone volume is consistent between the experimental groups in their respective studies and thus indicates similar magnitude of coronary ligation was implemented.

Table 2.2: Baseline cardiodynamics (Mean ± SEM) and number of hearts used for each of the studies. *Including; contractility and coronary flow data taken at 10 minutes stabilisation, the delineated risk zone volume after coronary ligation and its proportion to the total heart volume.*

Treatment Group	N	Weight (g)	CFR (ml/min)	HR (bpm)	LVDP (mmHg)	Risk Zone Volume (cm^3)	Risk-Total Area (%)
Study 1							
Control	14	350 ± 7	13.5 ± 0.7	294 ± 14	80.1 ± 4.3	0.36 ± 0.02	49.5 ± 2.6
IPC 2 x 3	7	356 ± 7	14.5 ± 0.7	288 ± 14	93.3 ± 4.6	0.36 ± 0.03	44.3 ± 3.4
IPC 3 x 3	4	406 ± 23	12.4 ± 1.0	255 ± 22	92.0 ± 5.3	0.33 ± 0.03	40.6 ± 2.0
Postcon 6 x 10	11	360 ± 6	13.2 ± 0.6	282 ± 14	71.2 ± 3.9	0.36 ± 0.02	45.1 ± 2.5
Postcon 3 x 30	4	364 ± 25	13.0 ± 1.0	269 ± 14	89.5 ± 10	0.33 ± 0.04	40.2 ± 2.2
Postcon 10-(3 x 30)	10	372 ± 11	13.5 ± 0.6	287 ± 9	80.8 ± 3.5	0.34 ± 0.02	47.1 ± 2.6
Study 2 (A) and (B)							
Control	12	385 ± 12	12.6 ± 0.5	265 ± 8	83.2 ± 6.9	0.40 ± 0.02	49.8 ± 2.4
KN-93 pre-Ischaemia	6	391 ± 12	13.4 ± 0.6	298 ± 27	84.5 ± 3.9	0.37 ± 0.03	48.0 ± 3.8
KN-92 pre-Ischaemia	7	383 ± 7	13.1 ± 0.6	281 ± 12	89.9 ± 8.6	0.42 ± 0.02	49.8 ± 2.6
KN-93 @ Reperfusion	7	417 ± 27	13.6 ± 0.6	266 ± 12	95.0 ± 10.9	0.40 ± 0.02	47.6 ± 2.0
IPC x3	10	400 ± 13	13.3 ± 0.6	261 ± 11	89.1 ± 6.1	0.38 ± 0.02	47.3 ± 1.3
IPC & KN-93	5	377 ± 17	14.3 ± 1.5	289 ± 16	82.0 ± 5.2	0.38 ± 0.03	53.0 ± 3.7
IPC & KN-93 @ Reperfusion	6	414 ± 22	14.3 ± 0.3	252 ± 10	76.8 ± 3.3	0.38 ± 0.02	47.3 ± 3.1
Study 2(C)							
Control	7	375 ± 29	15.6 ± 1.2	288 ± 12	90.6 ± 8.6	0.49 ± 0.03	64.8 ± 4.1
Postcon 6 x 10	6	374 ± 37	15.4 ± 1.2	291 ± 23	77.2 ± 6.6	0.48 ± 0.04	65.6 ± 5.0
KN-93 @ Reperfusion	4	346 ± 18	12.3 ± 2.3	300 ± 21	82.3 ± 7.5	0.44 ± 0.03	65.2 ± 4.8
KN-93 & Postcon	4	339 ± 13	12.0 ± 0.7	295 ± 25	64.8 ± 7.3	0.40 ± 0.04	55.0 ± 5.4

CFR, Coronary CFR, Coronary flow rate; HR, heart rate; LVDP, left ventricle developed pressure.

2.3.3. STUDY 1:

The use of Mechanical Interventions for Cardioprotection

Study 1 examined what effect short periods of global no-flow ischaemia and reperfusion would have, if they were instigated before (IPC) or after (postconditioning) in the rat heart. It also characterised whether the number and durations of the ischaemic cycles influenced efficacy.

Infarct size data

The primary endpoint of this study was myocardial infarct size expressed as a percentage of the risk zone volume (figure 2.5). Infarct size was 41.0 ± 3.6% in control experiments. Initiating two (IPCx2) or three cycles (IPCx3) of IPC before 35 minutes of CAO, significantly reduced the infarct size to 25.1 ± 2.0% and 18.1 ± 2.0% respectively. A 39% and 56% relative reduction suggests there is increased cardioprotection with an additional IPC cycle, but no significant difference existed between the two. None of the postconditioning groups' infarct size was significantly different to the controls. Postconditioning with six short duration cycles (Postcon-6x10) produced a lower mean infarct size (35.6 ± 4.7%) than postconditioning with three longer duration cycles (Postcon-3x30, 50.2 ± 6.0%). An initial 10 sec period of reperfusion followed by three longer cycles of global I-R (Postcon-10/3x30), had a comparable infarct size to the six short cycles (Postcon-10/3x30, 37.3 ± 4.2% vs. Postcon-6x10, 35.6 ± 4.7%). The SEM for the two IPC groups was less than the three postconditioning interventions, indicating a smaller extent of variability in infarct size when a prior intervention is used.

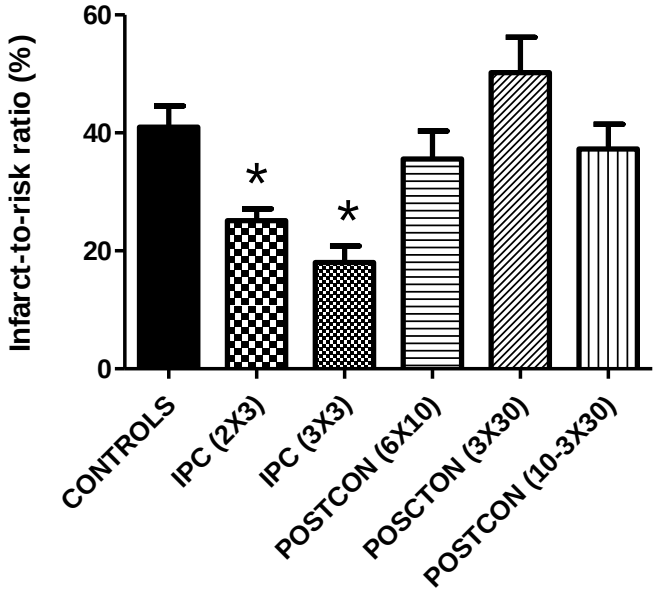

Figure 2.5: The infarct size expressed as a percentage of the risk zone volume for Study 1. *Both IPC interventions significantly reduced the infarct size when compared to control. None of the postconditioning interventions could effect a significant limitation in infarct size. N number for each experimental group is given in table 2.2. * Significantly different from Control (P<0.05, One way-ANOVA + Newman-Keuls post-hoc)*

Coronary flow and contractility data

The hearts subjected to an IPC intervention had a moderate increase in CFR prior to the CAO (data not shown). This did not affect the reduction in CFR at the onset of ischaemia, as all the groups fell below 62% of their baseline readings (figure 2.6A). The reduced CFR remained stable until the ligature was released for reperfusion. This restored the CFR to between 82-102% of the baseline readings, with Postcon-3x30 hearts having a significantly greater CFR than hearts treated to Postcon-10/3x30. All groups had a gradual run down in their CFR during the course of reperfusion. However, the IPCx3 hearts had a significantly better compensated CFR compared to some of the other groups after 30 minutes (vs. Postcon-10/3x30) and 60 minutes (vs.

Control, IPCx2, and Postcon-10/3x30) of reperfusion. At the termination of the experiment the significance in the improved CFR after IPCx3 (63.0 ± 5.0%) was lost, with the groups averaging a CFR of 48-54% of their initial capacity.

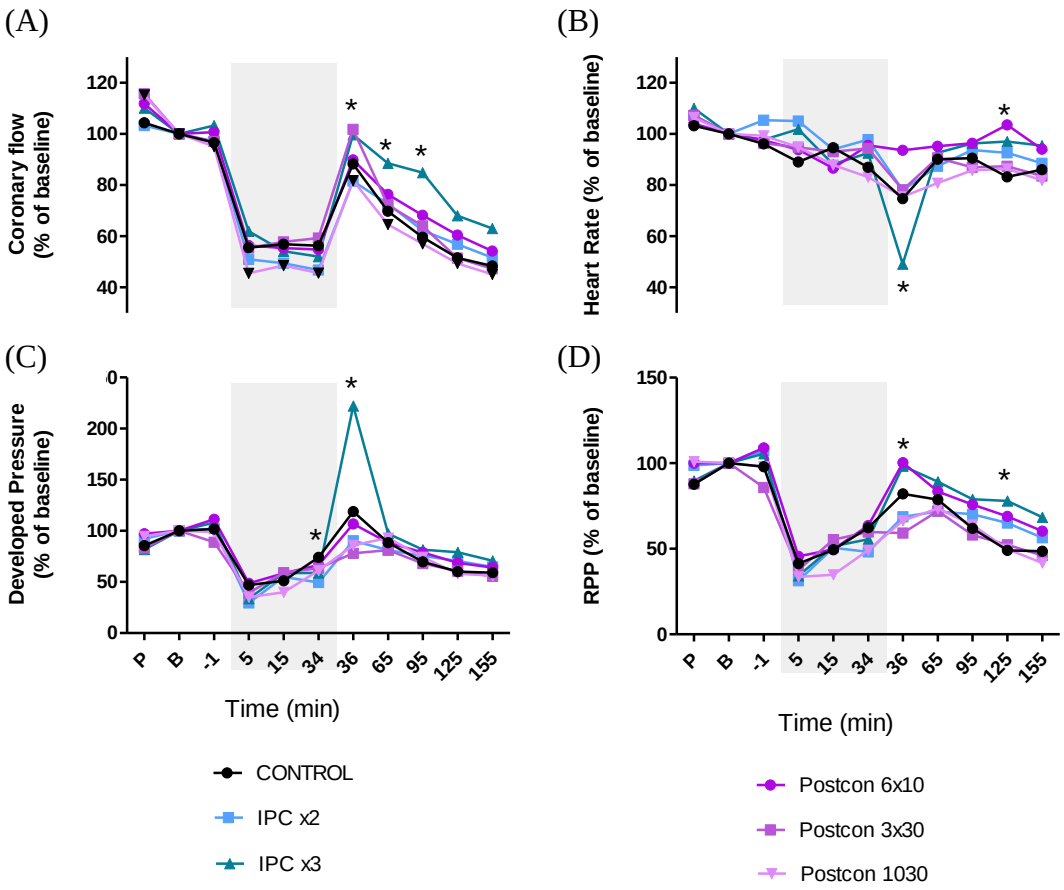

Figure 2.6: Time course of (A) Coronary Flow Rate, (B) Heart Rate (C) Developed Pressure and (D) Rate Pressure Product, expressed as a percentage of the baseline values during ischaemia and reperfusion. *Each point represents mean values for the treatment group in Study 1 taken during Stabilisation (-20 to -1 min), Ischaemia (5 to 34 min and shaded area) and Reperfusion (36 to 155 min). For clarity the SEM bars were withdrawn from the figures and is stated in the text. N number for each experimental group is given in table 2.2. * p<0.05 (repeated measures ANOVA) to a given group described in text. P, primary reading; B, baseline reading.*

When hearts received an IPC intervention, the short periods of reperfusion that followed global ischaemia, instigated a variable inotropic and chronotropic response (data not shown). That is, some hearts recovered with a contractile force beyond the preceding DP readings, whilst others were slightly depressed with each cycle that was initiated. Regional ischaemia produced no significant changes in the experimental groups' heart rate; albeit a minor rundown was evident (85-95% of baseline) after 34 minutes of ischaemia (figure 2.6B). However, the DP and subsequently the RPP of the left ventricle, in all treatment groups, were quickly depressed to at least half basal values (figure 2.6C & 2.6D). The hearts' contractile force responded positively as the ischaemic index continued; except in the IPCx2 group, which was significantly different to the control group (IPCx2, 49.4 ± 3.6% vs. Control, 74.1 ± 6.2%). This significance was not apparent when it was calculated as total myocardial work as RPP (IPCx2, 48.2 ± 3.5% vs. Control, 62.3 ± 3.6%).

The return of reperfusion induced many changes to the contractility of the ventricles. All groups except for the Postcon3x30, had incidences of uncoordinated contractile activity (Vfib) during the first minutes of reperfusion. Moderate bradycardia accompanied a positive inotropic response for most hearts, but notable in figure 2.6B and 2.6C is the hyperdynamic state (twice the DP of baseline values) and severe bradycardia of the IPCx3 group, although, when represented as RPP (figure 2.6D) it is comparable to pre-ischaemic readings. However, the small N numbers (n = 4) completed in the IPCx3 group and an incidence of Vfib in two of the hearts, skews the data and no statistical analysis was performed. After the first minute of initiating Postcon-6x10 there was one episode of Vfib and a significant preservation in heart rate (vs. Control and IPCx2). This chronotropic effect was significant for the Postcon6x10 group at 90 min of reperfusion in comparison to the Controls. Interestingly, this

significance was not conveyed to overall contractility and RPP in the Poscton6x10 group, but did so for the IPCx3 group when compared to the controls (IPCx3, 77.9 ± 12.0% vs. Control, 49.0 ± 3.5%). At termination of the experiments the IPCx3 (68.8 ± 10.6%) and Postcon6x10 (60.3 ± 6.7%) hearts had the highest mean contractility, but were not significantly different to any other of the treatment groups and the controls (56.4 ± 3.2%).

2.3.4. STUDY 2(A):

Inhibition of CaMKII During I-R Injury

Study 2(A) examined the effect of treating a rat heart to a pharmacological inhibitor of CaMKII (KN-93), before instigating I-R injury or concomitantly during the reperfusion period. An inactive analog of the inhibitor (KN-92) was also used as a negative control.

Infarct size data

The primary endpoint to this study was the measurements in myocardial infarct size expressed as a percentage of the risk zone volume (figure 2.7). Infarct size was 41.1 ± 3.9% in control experiments. Hearts pre-treated with KN-93 (2 μM) significantly reduced infarct size by 57% (17.6 ± 2.9% $p<0.05$) when compared to the controls. KN-92 (2 μM), the inactive analog of KN-93, also had a tendency to reduce the total infarct by 27% (30.0 ± 4.1%), but this was not significantly different to the controls. When KN-93 (2 μM) was perfused specifically at reperfusion there was no change to infarct size (47.7 ± 5.5%) compared to the controls.

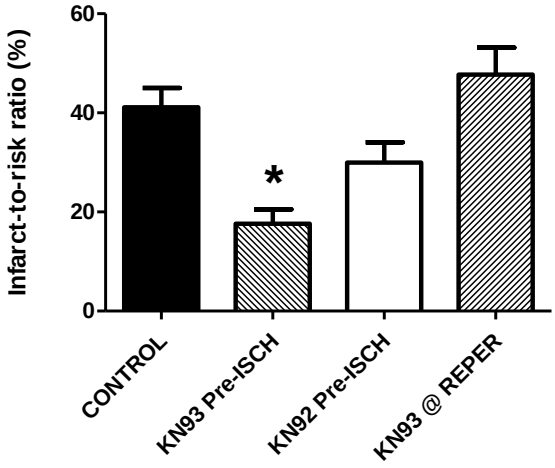

***Figure 2.7*: The infarct size expressed as a percentage of the risk zone volume for Study 2(A).** *Hearts pre-treated with the CaMKII inhibitor KN-93 (2 µM) had a significant amount of infarct limitation when compared to the controls. Perfusion of the CaMKII inhibitor during reperfusion had no effect on infarct size. KN-92 (2 µM) an analog of KN-93 that does not inhibit CaMKII had a non-significant trend of lowering the infarct size. N number for each experimental group is given in table 2.2. * Significantly different from Control (P<0.05, One way-ANOVA + Newman-Keuls post-hoc)*

Coronary flow and contractility data

Pre-treatment of either KN compound increased CFR prior to CAO. After 5 minutes of ischaemia (see figure 2.8A), hearts treated with KN-93 (PreKN-93) had a significant increase in CFR. The vasodilator effect of the compound was reversed by the 15th minute of ischaemia. This allowed all experimental groups to have a comparable CFR at this time point, which was below 60% of the baseline readings. When hearts were perfused with KN-93 5 minutes before the reperfusion period (ReperKN-93), there was a significant increase in the CFR when compared to the controls (mean difference of 15.5%). However, all groups had an equivalent CFR when the ligature was released at the start of reperfusion and at termination of the experiments.

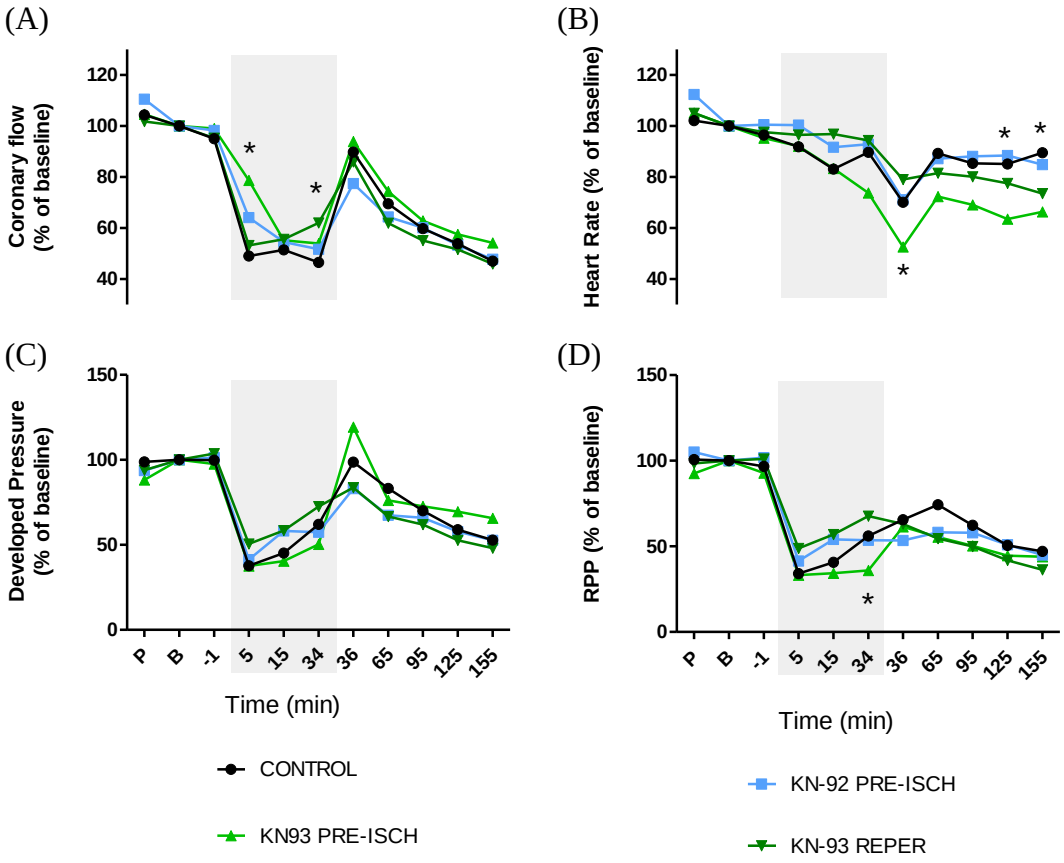

Figure 2.8: Time course of (A) Coronary Flow Rate, (B) Heart Rate (C) Developed Pressure and (D) Rate Pressure Product, expressed as a percentage of the baseline values during Study 2(A). *Each point represents mean values for the treatment groups taken during the periods of Stabilisation (-20 to -1 min), Ischaemia (5 to 34 min and shaded area) and Reperfusion (36 to 155 min). For clarity the SEM bars were withdrawn from the figures and is stated in the text. N number for each experimental group is given in table 2.2. * p<0.05 (repeated measures ANOVA) to a given group described in text. P, primary reading; B, baseline reading.*

The pre-ischaemic perfusion of KN-93 and KN-92 had a brief (3-5 minutes) effect on the hearts' basal contractility. This is demonstrated in study 2B, figure 2.10 A & C (p108) when the haemodynamic measurement was included during drug treatment.

The hearts produced a minor positive inotropic and chronotropic response before returning back to basal levels for the remainder of the treatment. Some hearts perfused with KN-93 also responded initially with negative inotropy that lasted for one or two minutes. This was a distinct behaviour of the drug when it was perfused during the last 5 minutes of ischaemia.

The depressed contractile activity (RPP, figure 2.8D) associated with ischaemia was more pronounced in PreKN-93 hearts. After 34 minutes of CAO, this was significant when the RPP of the PreKN-93 group (36.0 ± 5.2% of baseline) was compared to the ReperKN-93 group (67.7 ± 4.1%). The main component for this depression was the decreased HR (figure 2.8B) rather than the decreased LVDP (figure 2.8C), although none were significantly different as sole parameters.

Reperfusion brought a momentary period of bradycardia which was significantly greater within the PreKN-93 group than ReperKN-93 group. Some compensatory positive inotropy meant that overall myocardial work (RPP) for all groups was similar. Both KN-93 groups had one incidence of Vfib during reperfusion, whilst none were instigated with the PreKN-92 group and four incidences occurred within the Control hearts. During further reperfusion, the preKN-93 group's heart rate did not recover to the same degree as the Control heart rate (significant mean difference of 21.6% at 90 min and 23.1% at 120 min reperfusion) or the preKN-92 group (significant mean difference of 24.9% at 90 min reperfusion). However, the preKN-93 group RPP was comparable to the other groups at end of the experiments due to a non significant improvement in the contractile force.

2.3.5. STUDY 2(B):

Inhibition of CaMKII During Preconditioning

Study 2(B) examined the effect of treating heart with a pharmacological inhibitor of CaMKII (KN-93), during IPC stimulus, or at reperfusion in preconditioned hearts.

Infarct size data

The primary endpoint of this study was myocardial infarct size expressed as a percentage of the risk zone volume (figure 2.9). Infarct size was 41.1 ± 3.9% in control experiments. An IPC intervention (3 x 3) significantly reduced the infarct size to 18.8 ± 3.7%, a reduction of 54% when compared to controls. The presence of KN-93 (2 μM) during the IPC intervention (preKN-93&IPC) produced a reduction in infarct size to 10.5 ± 2.5%, a relative reduction of 74% when compared to controls. IPC maintained a low infarct size of 22.1 ± 4.2% (a 46% reduction) when KN-93 (2 μM) was present during the reperfusion period (IPC&reperKN-93). An added protection was suggested when the hearts were pre-treated with KN-93 and IPC, but this was not significantly different to IPC alone.

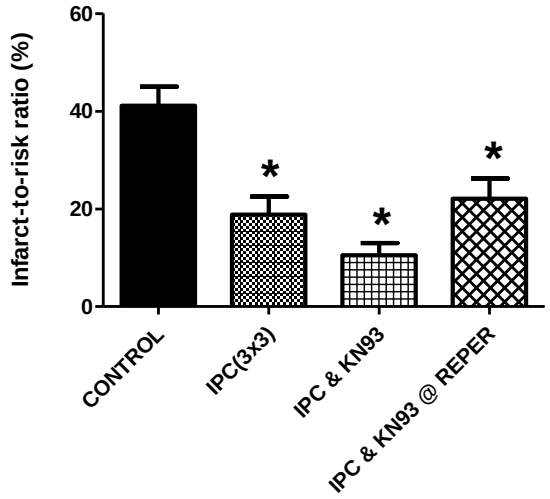

Figure 2.9: The infarct size expressed as a percentage of the risk zone volume for Study 2(B). *Hearts subjected to an IPC intervention in the presence of KN-93 (2 µM) maintained their cardioprotective phenotype. Perfusion of KN-93 (2 µM) at reperfusion, after an IPC protocol had been initiated also maintained significant infarct limitation. N number for each experimental group is given in table 2.2.* * *Significantly different from Control (P<0.05, One way-ANOVA + Newman-Keuls post-hoc)*

Coronary flow and contractility data

In the preKN-93&IPC group, a final haemodynamic measurement was made during the stabilisation period (at 14 minutes), in the presence of KN-93 (2 µM). This pre-treatment prior to an IPC intervention significantly increased the CFR (129.2 ± 12.2%) above baseline values and the other treatment groups (figure 2.10A). This significance was maintained after 5 minutes of ischaemia but was reversed by the 15th minute as CFR fell to 55.1 ± 3.5% of baseline readings. A non-significant increase in CFR was measured when KN-93 was perfused 5 minutes before reperfusion (mean difference 17.8% with Controls). All groups had an equivalent CFR when the ligature was released and at termination of the experiments.

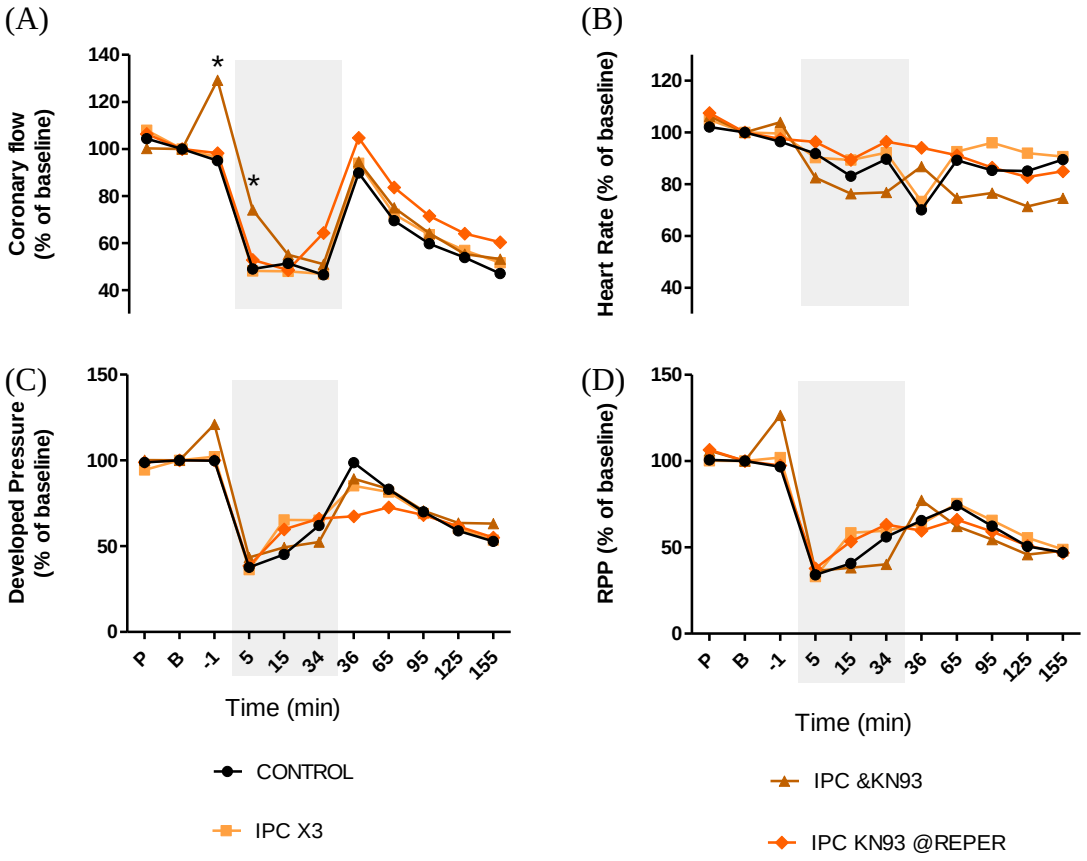

Figure 2.10: Time course of (A) Coronary Flow Rate, (B) Heart Rate (C) Developed Pressure and (D) Rate Pressure Product, expressed as a percentage of the baseline values during Study 2(B). *Each point represents mean values for the treatment groups taken during the periods of Stabilisation (-20 to -1 min), Ischaemia (5 to 34 min and shaded area) and Reperfusion (36 to 155 min). For clarity the SEM bars were withdrawn from the figures and is stated in the text. N number for each experimental group is given in table 2.2. * $p<0.05$ (repeated measures ANOVA) to a given group described in text. P, primary reading; B, baseline reading.*

The final stabilisation measurement within the preKN-93&IPC group (figure 2.10) demonstrates the enhancement in contractile function when there is an increase in coronary flow (Gregg effect). The magnitude of increased myocardial workload (RPP, figure 2.10D) was variable amongst these treated hearts. As such, the groups' contractile parameters were not significantly different to one another (RPP of preKN-93&IPC, 126.6 ± 10.6 vs. RPP of Control, 96.6 ± 5.2%).

No further significance was found between the hearts of IPCx3 or the hearts subjected to IPC and KN-93 treatment prior or after the CAO. The perfusion of KN-93 at end of ischaemia had a negligible rise in contractile activity, whilst the pre-ischaemic treatment of KN-93 kept the overall RPP to 40.2 ± 2.9% of baseline values. The incidences of Vfib during the first minute of reperfusion were more frequent within this study with: Controls 4/12; IPCx3 4/10; preKN-93&IPC 2/5; IPC&KN-93reper 3/6. All parameters at the end of the experiments were comparable to one another.

2.3.6. STUDY 2(C):

Inhibition of CaMKII During Postconditioning

Study 2(C) examined the effect of treating the heart with a pharmacological inhibitor of CaMKII (KN-93), in parallel with a postconditioning intervention (6 x10 cycles).

Infarct size data

The primary endpoint of this study was myocardial infarct size expressed as a percentage of the risk zone volume (figure 2.11). Infarct size was 30.1 ± 2.6% in control experiments. There was no significant difference in the infarct size of hearts that underwent a postconditioning intervention of 6 x10 cycles (24.8 ± 2.7%). Inhibition of CaMKII with KN-93 during reperfusion also resulted in infarct size (25.5 ± 5.4%) comparable with the controls and postconditioning group. Postconditioning in the presence of KN-93 had no significant effect on infarct size (39.5 ± 6.2%). In fact, a trend towards an increase in infarct size (additional 55-60%) was seen when these two interventions were combined although some variability existed in the group.

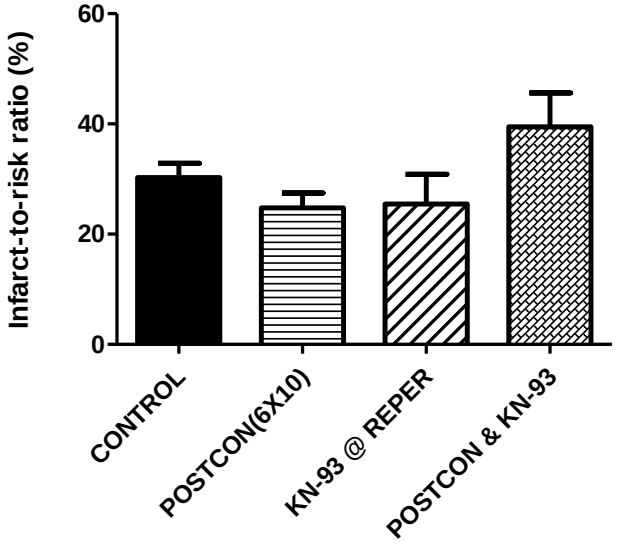

Figure 2.11: The infarct size expressed as a percentage of the risk zone volume for Study 2(C). *Postconditioning or the treatment of KN-93 at reperfusion has comparable infarct size to controlled experiments. Combining postconditioning and KN-93 treatment had a non significant increase in infarct size. N number for each experimental group is given in table 2.2.*

Coronary flow and contractility data

The CFR for all groups was comparable during stabilisation and CAO (figure 2.12A). An non-significant rise occurred with KN-93 treatment prior to reperfusion. When this was combined with postconditioning a significant but variable rise to 123.8 ± 13.3% of baseline levels occurred. This was reversed by 30 minutes of reperfusion, with all groups having comparable CFR at termination of experiment.

The primary RPP reading (figure 2.12D) of the hearts subjected to postconditioning and KN-93 treatment (postconKN-93) was significantly less than the hearts subjected to postconditioning alone. KN-93 treatment at the end of ischaemia brought a significant increase in overall contractility to hearts in the postconKN-93

group, but only a non significant rise in the heart rate of those treated only to KN-93 (KN-93reper).

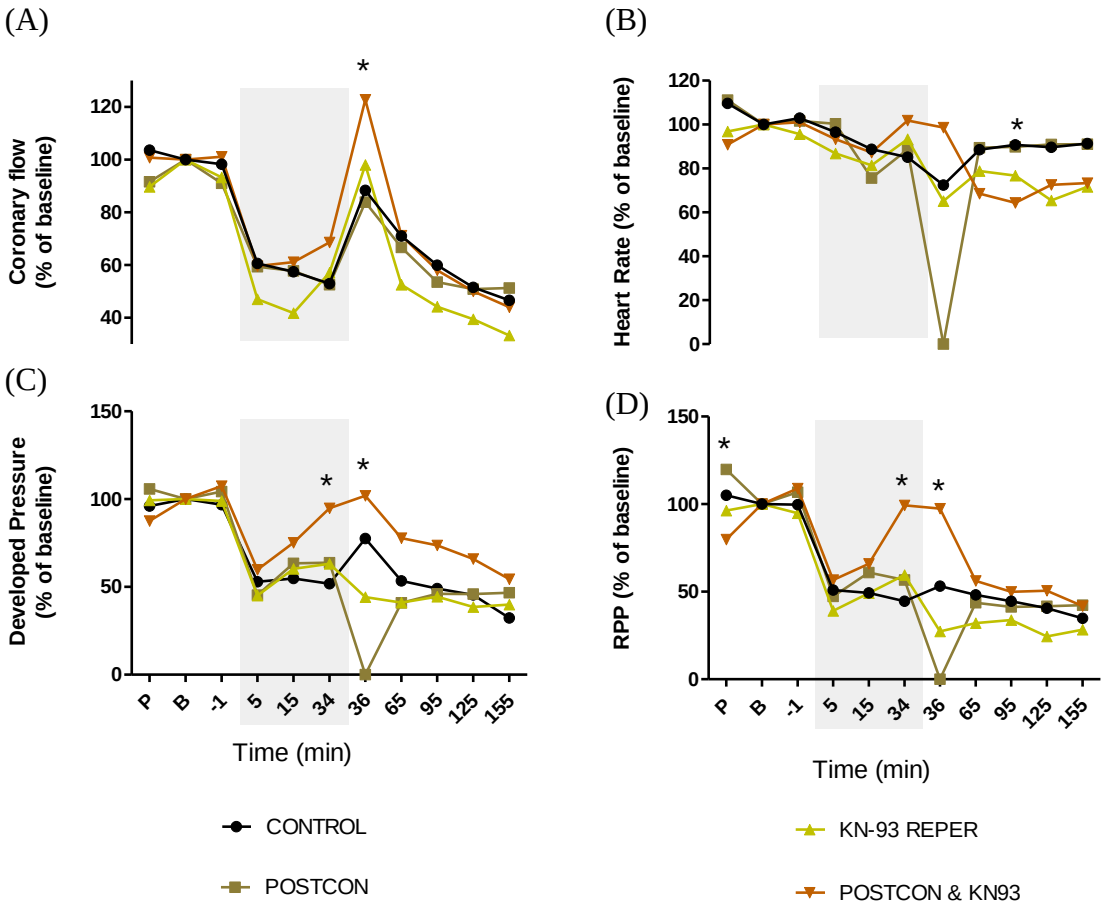

Figure 2.12: Time course of (A) Coronary Flow Rate, (B) Heart Rate (C) Developed Pressure and (D) Rate Pressure Product, expressed as a percentage of the baseline values during Study 2(C). *Each point represents mean values for the treatment groups taken during the periods of Stabilisation (-20 to -1 min), Ischaemia (5 to 34 min and shaded area) and Reperfusion (36 to 155 min). For clarity the SEM bars were withdrawn from the figures and is stated in the text. N number for each experimental group is given in table 2.2. * p<0.05 (repeated measures ANOVA) to a given group described in text. P, primary reading; B, baseline reading.*

Return of reperfusion instigated Vfib in all groups and was more prevalent in this study, with every heart in the postconditioning group (6/6) and majority of the control group (4/7) developing Vfib. Although sample numbers were low, KN-93 limited the Vfib occurrence to one out of four hearts. Thus, no contractile data was available for the postconditioning group at 1 min of reperfusion and is marked as zero on figures 2.12(B-D). Overall myocardial work for postconKN-93 was high during the early stages of reperfusion. Interestingly, whilst significant improvement was maintained during the first 30 minutes of reperfusion, the HR continued to drop to significant levels at 60 minutes. The KN-93reper and postconKN-93 had similar HR at termination of experiment, 20% lower than the controls and postconditioning group. Overall contractility (RPP) for the groups was the same.

2.4. Discussion

The studies' major findings are summarised as follows:

- The CaMKII inhibitor KN-93 is protective against ischaemia-reperfusion injury, if administered before ischaemia but not during reperfusion. This suggests that CaMKII at some stage in ischaemia promotes cellular injury. On these grounds, the first hypothesis that *CaMKII activation at reperfusion promotes irreversible injury can be rejected.* However, the KN compounds could have non-specific activity and this warrants further investigation as the inactive analog, KN-92, demonstrated some degree of protection when perfused prior to ischaemia.

- Postconditioning is not as robust as IPC in limiting infarct size in a rat isolated heart model of acute myocardial infarction. The inhibition of CaMKII with KN-93 does not abrogate the protective effect of IPC when administered at the time of the IPC stimulus or at reperfusion, although an additive protective effect of IPC and CaMKII inhibition is possible. These data suggest that cardioprotection by IPC does not require a functional CaMKII, and thus leads to rejection of the second hypothesis that *under IPC conditions, CaMKII promotes cardioprotection*. No significant protection was conferred with a postconditioning intervention, although, the addition of a CaMKII inhibitor during the intervention seemed to promote further injury. Further studies are needed to investigate the activity of CaMKII during postconditioning.

2.4.1. CaMKII Promotes Cellular Injury During Ischaemia

The basis of the first hypothesis lies in previous research demonstrating that I-R and other pathological diseases involve CaMKII activity to promote cellular injury (Zhu et al., 2003; Li et al., 2007; Vila-Petroff et al., 2007). Study 2A, confirms this general perception of CaMKII since the presence of KN-93 during ischaemia significantly reduced infarct size. This is in agreement with research that used genetically modified CaMKII (Li et al., 2007; Yang et al., 2006) or pharmacological inhibition of the kinase (Vila-Petroff et al., 2007; Salas et al., 2010) to prevent I-R injury. However, a disparity exists with the conclusion of Mattiazzi's studies (Vila-Petroff et al., 2007; Salas et al., 2010) that pharmacological inhibition of CaMKII, with KN-93 (2.5 μM), prevents reperfusion injury. In study 2A, the treatment of the same inhibitor at a similar concentration did not prevent irreversible injury if it was only administered at reperfusion. This confirms the findings of Lange et al. (2009) which used a bolus of KN-93 when reperfusion was initiated. A slightly different model of 45 min global ischaemia was used by Vila-Petroff et al. (2007) and Salas et al. (2010), but their protocol also involved a 10 minute pre and post-ischaemic treatment with the inhibitor. This suggests that KN-93 must be present during early ischaemia for any protection to occur.

Mattiazzi's detailed western blot analysis suggested the window of CaMKII activity (measured by phosphorylation of the PLB Thr^{17} site) during the first minutes of reperfusion was the cause of irreversible injury. Uemura et al. (2002) also reported that there was a restrained autophosphorylation state of CaMKII under ischaemic conditions and at reperfusion. But, Mattiazzi's studies were not conclusive on whether treatment with KN-93 specifically conferred protection during reperfusion. A NCX inhibitor, KBR7943 administered in a similar protocol to KN-93, limited PLB Thr^{17}

phosphorylation at reperfusion, but no evidence for the actions of KN-93 treatment was given. Thus either KN-93 is ineffective in competing with CaMKII during the short window of its activation at reperfusion; or CaMKII augments injury that has already been sustained during the ischaemic period. The latter concept would have to consider the lack of phosphorylation reported on the Thr^{287} site during ischaemia. Another CaMKII status (i.e. oxidation at $Met^{280/281}$) could be responsible for the injury.

The significant amount of salvaged tissue with pre-ischaemic treatment of KN-93 did not improve the hearts' overall contractility or CFR at the end of experimentation. The hearts showed signs of bradycardia with KN-93 treatment but not with KN-92 treatment, indicating that this reduced rate was a product of CaMKII inhibition. If cardiac function had been used as the end point of injury, as measured in the studies by Dhalla's group (Osada et al., 2000) and Benter et al. (2004), then the studies on CaMKII inhibition during ischaemia would not have shown any beneficial effect. Yet, CaMKII is a vital component of E-C coupling and this outcome would be expected. One interesting observation was that the RPP at the end of ischaemia was lower after pre-treatment of KN-93, than in all other groups in study 2A and study 2B. A limitation in ATP utilisation during ischaemia with CaMKII inhibition can not be ruled out as a possible mechanism of its cardioprotection. However, it needs to be emphasised that functional measurements in the present model are subsidiary to infarct size. Regional ischaemia models do not have sufficient sensitivity to reliably determine changes in global LV contractility.

2.4.2. The Non-specific Activity of the KN Compounds

The negative control, KN-92, demonstrated some degree of cardioprotection (27% lower infarct than controls) when perfused prior to an ischemic insult (study 2A). It matched the KN-93 increase in CFR during the stabilisation period and incurred no incidences of Vfib during the first minute of reperfusion. KN-93 and KN-92 are structurally similar, but differ in that KN-93 can compete with CaM for the binding site of CaMKII regulatory domain. Studies have revealed that the KN compounds can specifically inhibit the activity of the LTCC (Gao et al., 2006) and the Kv channels (Rezazadeh et al., 2006). This could be one explanation for the anti-arrhythmic activities of KN-92 during reperfusion. The vasodilator effect of the KN compounds could also be due to effects on the LTCC, as demonstrated by the active hyperaemia associated with LTCC blockers. However, KN-92 did not match the bradycardia initiated by KN-93. This suggests that the concentration used in this study was not sufficient to prolong action potential duration (via the inhibition of the Kv channels) and that it was specifically an inhibitory role of CaMKII.

The potency and permeability of KN-93 has made it a favoured pharmacological inhibitor of CaMKII in this study and several other published studies. Other research has not revealed the same degree of activity for KN-92. Contradicting the anti-arrhythmic activities in study 2A, it failed to emulate KN-93 in reducing atrial fibrillation (Chelu et al., 2009) and post-acidosis arrhythmias (Said et al., 2008). Research specifically looking at cell death has also reported no significant effect of KN-92 in models of liver I-R injury (Tsung et al., 2007), neuronal cell death (Takano et al., 2003) or oxidative stress (Palomeque et al., 2009).

2.4.3. Postconditioning is Not as Robust as IPC in Limiting Infarct Size

Although the widespread notion is that postconditioning of the heart can limit I-R injury (Zhao et al., 2003; Hausenloy and Yellon, 2006), the data presented here are in agreement with other recent research (Dow and Kloner, 2007; Manintveld et al., 2007) that has failed to emulate the current trend. IPC successfully reduced infarct size by up to 56% when compared to controls confirming that a mechanical intervention prior to an ischaemic insult is robustly cardioprotective in rat hearts *ex vivo*. A 39% reduction in infarct size was obtained in the 2 x 3 min IPC group and an additional IPC cycle (3 x 3 min) limited infarct by up to 56% in comparison to the controls. While the two IPC groups were not significantly different to one another a 'dose-dependency' of preconditioning has been described previously (Sandhu et al., 1997). The IPC stimulus increased the CFR prior to the CAO (data not shown) which is reported to be an effect of adenosine release and K_{ATP} channel opening (Akatsuka et al., 1994). Only the 3 cycle stimulus caused a significant improvement in CFR after 30 min and 60 min of reperfusion, which was then lost at the end of the protocol.

Postconditioning with the 6 x 10 sec intervention showed a minor trend towards protection (13-26% reduction in infarct size), but this was not significant. Several studies, reviewed by Crisotomo et al. (2006) demonstrated that the cardioprotective effect of postconditioning is less than that of IPC, but the degree of protection reported was a minimum of 36% relative to the controls. A large variance (infarct size range 6-50%) within the groups could indicate that either a variable amount of irreversible damage was caused during ischaemia or that postconditioning only salvages tissue under meticulous conditions that have yet to be established.

The optimum duration of the occlusion and subsequent reperfusion during postconditioning is unknown, but data here and in the literature do indicate that shorter

cycle durations favour the hearts of smaller species such as the rat (Crisotomo et al., 2006). The infarct size was 44% less when postconditioning with 6 x 10 sec was used, than when the longer occlusion duration of 3 x 30 sec was used. But due to the variance within each of these groups, this difference did not reach statistical significance. The brief increase in CFR after postconditioning with 6 x 10 sec also suggest the release of autacoids such as adenosine were in effect, but did not mediate further protection.

2.4.4. Inhibition of CaMKII Does Not Abrogate the Protective Effect of IPC

IPC successfully protected the heart from subsequent I-R injury. However, the original hypothesis that IPC is mediated by CaMKII can be rejected, as perfusion of the CaMKII inhibitor KN-93 either during the trigger phase of IPC (10.5 ± 2.5%) or during the early reperfusion period after an IPC stimulus (22.1 ± 4.2%) did not abolish this protection. Instead, an added protection occurred when the drug was perfused in conjunction with an IPC stimulus. Li et al. (2007) have also reported additive cardioprotection with IPC and CaMKII inhibition during I-R, although their model used mutant mice. This contradicts Osada et al. (2000) and Benter et al. (2004) who used KN-93 to abrogate the protection afforded with IPC. The treatment protocols varied slightly to the ones used in study 2B, in that treatment of KN-93 was given prior to the IPC rather than during the IPC cycles or at reperfusion. This pre-treatment eradicated the improved contractile recovery of IPC in both studies, which also correlated well with the SR Ca^{2+} uptake reported by Osada et al. (2000). As seen with the data in study 2A, KN-93 can influence the cardiodynamics of the heart, but when using infarct as a final end point of injury, this modification is cardioprotective. The cardiodynamic data for the IPC groups did not improve in study 2B, but did so at occasions during reperfusion in study 1 further demonstrating that these surrogate measures of injury are unreliable. Also,

IPC did not reduce the incidence of Vfib even with KN-93 treatment, indicating that an unknown pro-arrhythmic mechanism was in place at the return of reperfusion.

IPC is known to protect with a range of triggers and mediators such as activation of the K_{ATP} channel and the RISK pathway. As CaMKII inhibition during ischaemia limits irreversible injury, it could be speculated that IPC might also protect against I-R injury by limiting CaMKII activity. The added protection with IPC and KN-93 treatment could also indicate that a dose dependent limitation in CaMKII activity occurred. However if KN-93 at 2 μM concentration completely abolishes CaMKII activity, then it might suggest that there are separate mechanisms of protection at work. Further research is needed to determine if these stimuli work together or are different to one another in achieving protection from I-R.

Inhibiting CaMKII during postconditioning, although not significantly different to the other groups, had a moderate adverse effect on the intervention. The infarct size after postconditioning in study 2C ranged between 15-32% whereas the presence of KN-93 increased this to between 28-56%. One documented mechanism of postconditioning protection is its effect on the Ca^{2+} handling of the SR. Whether CaMKII inhibition by KN-93 would limit this beneficial activity remains to be seen in models that show significant protection by a postconditioning intervention. In the absence of a successful postconditioning protocol in these studies, further investigations were not implemented.

2.5. Conclusion

The data reported here suggest that CaMKII has a pro-injury role during ischaemia but is not a potential pharmacological target during the early reperfusion period. However, caution is needed when using KN-93 as non specific activity of the drug could contribute to the outcomes. This makes its analog KN-92 an essential tool as a negative control. IPC could mediate some of its protection by regulating CaMKII rather than supplementing its activity. It is possible that the two interventions are mechanistically distinct as the combination of the two is additive. Postconditioning is not as robust as IPC in limiting infarct size. In my hands, postconditioning was ineffective and it remains to be seen if CaMKII plays any role in this phenomenon.

CHAPTER 3:

In Vitro Model of I-R with H9c2 cells

3.1. Introduction

3.1.1. *In Vitro* Models of Ischaemia-Reperfusion Injury

In vitro models of I-R have been developed to simulate the pathological state of cellular injury. In doing so, several advantages are gained over whole heart models (Marber et al., 2000). These include: the manipulation of the extracelluar environment; isolation of cells from the influence of vascular, hormonal and neuronal components; prevention of interaction with other cells of a different type; description of pharmacological actions at a single cell level; genetic manipulation; and increased specificity in targeting the signalling pathways. The disadvantages with the *in vitro* studies are that they lack all the components of *in situ* conditions of I-R insult; and the cell phenotype may not match those of the whole heart level.

The current models that mimic I-R injury are based on depriving the cells of substrates. This has been done by limiting glucose in the medium (Matsui et al., 2007; Lynn et al., 2008); arresting glycolis with the substitution of compounds such as 2-deoxyglucose (2-DG, Agnetti et al., 2005); or lowering the oxygen levels to conditions of hypoxia/anoxia (Hwang et al., 2008; Lynn et al., 2008). Matching the composition of extracelluar ischaemic conditions with high sodium and lactate concentrations, or a decreased pH level can also add to the models' authenticity (Esumi et al., 1991; Lee et al., 2007). A large amount of oxidative stress is generated during I-R injury, and thus studies have replicated this by treating cells with H_2O_2, which is a direct product of superoxide from the mitochondria (Brookes et al., 2004).

The phenomena of IPC and postconditioning have also been simulated at the cellular level (Budas et al., 2004; Sun et al., 2005). This has confirmed that the protection afforded by such strategies is inherent to cardiac myocytes (Diaz and Wilson,

2006). Many methods have been developed to determine the cells' viability after these cardioprotective strategies. The advantage of using a cell based model is that it can differentiate between cell death by necrosis or apoptosis. The latter process will require a longer duration for it to become apparent in order to allow such hallmarks as DNA fragmentation to occur (Diaz and Wilson, 2006). In doing so, the ends of the nucleic acids can then be labelled by terminal deoxynucleotidyl transferase dUTP nick end labeling (TUNEL). However, more rapid determination of cells that are permeable to staining dyes, such as trypan blue or propidium iodide can be done if the sarcolemma is damaged. The uptake of dyes allows the damaged cells to be quantified by microscopic examination. A colorimetric assay can also be used to determine the quantity of enzymes such as creatine kinase or lactate dehydrogenase (LDH) that have been released into the extracellular medium as a result of cell death. Alternatively, a reducible reagent (MTS, see section 3.2.4.2) can be specific for intracellular dehydrogenase enzymes that will determine if the cells are still viable or not. All in all, *in vitro* models and measurements of cellular injury and viability have become common methods in assessing various cardioprotective strategies. Combined with other molecular, genetic, biochemical and pharmacological techniques they can help to elucidate key mechanisms and signalling components that are at work in limiting or stimulating cellular injury.

3.1.2. *In Vitro* Models of Cellular Injury by CaMKII Activity

A variety of *in vitro* models have investigated the possible role of CaMKII activity in promoting cellular injury. Chronic exposure of cardiac myocytes to angiotensin-II, oubain, β-adrenergic stimulation and H_2O_2 are all reported to have caused cell death by the uncontrolled activity of CaMKII (Zhu et al., 2003; Palmoeque et al., 2009; Sapia et

al., 2010). These studies have suggested that pathological conditions that continually subject cells to an enhanced Ca^{2+} entry (via LTCC or the reverse mode NCX) or its mishandling by the SR lead to various cell death pathways. Yet, if CaMKII inhibitors are present in these models, a significant amount of damage can be prevented. Accordingly it has been proposed that CaMKII is a key mechanism for these pathological pathways. However, an interesting exception has been suggested by Palmoeque et al. (2009). That is, the generation of oxidative stress by continued angiotensin-II stimulation can lead to CaMKII activity and apoptosis at subdiastolic $[Ca^{2+}]_i$. Twenty four hours of angiotensin-II stimulation in quiescent rat cardiac myocytes led to cell death in the absence of changes to the $[Ca^{2+}]_i$. Various conditions were altered to demonstrate that CaMKII was the key mechanism of apoptosis and not $[Ca^{2+}]_i$, including compartmentalised Ca^{2+} (via activation of the IP_3R), phosphatases or ROS. Further analysis suggested that the downstream trigger for apoptotic cell death was CaMKII regulation of p38MAPK and its disruption of the Bax/Bcl-2 proteins. Other studies have confirmed that the activation of CaMKII is promoted with prolonged H_2O_2 treatment (Zhu et al., 2007; Peng et al., 2010). Peng et al. (2010) have recently suggested that it is isoform specific as overexpression of $CaMKII_{\delta B}$ promoted cell viability during H_2O_2 treatment whilst overexpression of $CaMKII_{\delta C}$ exacerbated cell injury.

Few *in vitro* models have investigated CaMKII with regard to simulated I-R injury. Vila-Petroff et al. (2007) subjected isolated cardiac myocytes to an acute period (45 minutes) of simulated ischaemia solution (high sodium-lactate, high K^+, acidosis, no glucose). When the cells returned to normal physiological solution, cell death was accompanied by hypercontracture and Ca^{2+} overload, which CaMKII inhibitors, KN-93 and AIP, were successful in preventing. Zhu et al. (2007) used a variety of extracellular

conditions to challenge cardiac myocytes expressing a dominant negative $CaMKII_{\delta C}$. Twenty four hours of chronic stimulation with H_2O_2, acidosis or hyperkalaemia promoted apoptosis. But when CaMKII was suppressed, a significant reduction in TUNEL-positive cells was measured.

Due to the reported non-specific activity of the KN compounds, corroboration of another inhibitor is usually used to confirm a CaMKII role. Peptides are inefficient in passing the cell membrane when perfused in the Langendorff heart. However, in a cell culture model there is sufficient time for the peptides to penetrate the cell membrane due to uptake through lipophilicity. Also, higher concentrations can be more effectively and economically achieved. A more specific inhibitor of CaMKII, AIP (Ishida et al., 1995) can thus be adopted. CaMKII is also involved with multiple targets within the cell and several key hypotheses can be raised and tested within an *in vitro* model. Thus the aim of this chapter was to replicate the conditions of chapter 2 within an *in vitro* model and test the effects of two separate pharmacological inhibitors of CaMKII.

3.1.3. Hypothesis

The aim of these studies was to develop an *in vitro* model of I-R injury and to investigate whether the pharmacological inhibitors of CaMKII afforded protection at this cellular level. Using the H9c2 cell line, two models of cell death was used. The first involved the simulation of the ischaemic extracelluar conditions (high lactate, high K^+, acidosis) and reperfusion. The second study involved prolonged exposure to oxidative stress and glucose deprivation. Two pharmacological inhibitors of CaMKII, KN-93 and AIP, were used in order to determine the involvement of CaMKII activity. The inactive analog of KN-93, KN-92 was also used as a control for the unspecific activity of these compounds.

It was hypothesised that:

CaMKII inhibitors will promote cell viability in a model of cellular injury by simulated I-R or by oxidative stress.

3.1.4. Specific Objectives

(A) Develop an *in vitro* model of cell death and injury that simulated the conditions of ischaemia.

(B) Test whether CaMKII inhibition with KN-93 or a more specific inhibitor, AIP, protected against cell death within the model and use KN-92 as a negative control.

(C) Further investigate possible downstream mechanisms of protection with CaMKII inhibition.

3.2. Materials and Methods

The organic CaMKII inhibitor KN-93 (water soluble), the inactive analog KN-92 and the cell permeable autocamtide-2 related inhibitory peptide II (AIP) were purchased from Calbiochem (Nottingham, UK). KN-92 and AIP were dissolved in DMSO (final DMSO concentration in the solution was 0.07% and <0.03% respectively).

3.2.1. The H9c2 Cell Line

H9c2 cells are derived from embryonic rat heart. They can proliferate into myoblasts or differentiate into non-proliferating myotubes if the serum, that contains natural differentiating inhibitors, is withdrawn from the medium (Kimes and Brandt, 1976). The cells have been thoroughly characterised since their first isolation by Kimes and Brandt (1976) and have maintained many of the functional properties found in adult cardiac myocytes (Hescheler et al., 1991; Sipido and Marban, 1991; Lax et al., 2005). They can simultaneously contract and produce action potentials (Kimes and Brandt, 1976), which are characteristic of the cardiac action potential (Hescheler et al., 1991; Sipido and Marban, 1991). The mitochondria are sensitive to the intracellular Ca^{2+} pools and respond to agents that release Ca^{2+} from the SR (Lax et al., 2005). A skeletal muscle isoform of the α_{1S} subunit of the LTCC is adopted upon differentiation into myotubes, although this is reversible with retinoic acid stimulation (Menard et al., 1999). Some other characteristics of skeletal muscle cells have also been compared to the H9c2 cells. These include a smaller t-tubule system and an acetylcholine response that is characteristic of skeletal myocytes rather than cardiac myocytes (Kimes and Brandt, 1976). The authors concluded that muscle cell lines that are in long term

culture will tend to have similar characteristics as they are all derived from the embryonic mesoderm.

The cell line has been used in several studies that have investigated I-R injury at the cellular level. When introduced to models of hypoxia-reoxygenation and serum withdrawal, loss of mitochondrial function and the up-regulation of pro-apoptotic factors such as caspases and Bax accumulation induced cell death by apoptosis (Bonavita et al., 2003). In a similar model, Hou and Hsu (2005) used GFP to monitor the translocation of the Bax protein to the mitochondria, allowing further analysis of this apoptotic pathway. When the cells were introduced to the metabolic inhibitor rotenone (5 μM), they quickly adopted features of necrosis (rupture of cytoplasmic membrane) that was independent of caspase activation (Yaglom et al., 2003). This mode of cell death that occurred within a 4 hour time frame was preceded by the generation of ROS and the depolarisation of mitochondrial membranes. Sardao et al. (2007) have also reported that oxidative stress (by tert-butylhydroperoxide treatment) alone generated sufficient ROS to cause cell death that had characteristics of membrane blebbing and Bax accumulation around the mitochondria. The cells also possess endogenous capabilities of protection. Preconditioning with cycles of hypoxia-reoxygenation (Sakamoto et al., 1998; Jiao et al., 2008) or metabolic stress (Kabakov et al., 2002) have all been reported to limit cell injury and promote cell viability. Also, postconditioning models that include short cycles of hypoxia-reoxygenation at the end of the ischaemic insult have recently been described (Mykytenko et al., 2008; Zhu et al., 2011).

Hoch et al. (1998) reported that various isoforms of CaMKII (δ_C, δ_B, δ_D, δ_I) are expressed in H9c2 cells. The isoforms were revealed to be dependent on the differentiation state of the cell line, with the exception of the δ_C isoform which always

preserved a dominant expression. The sub-cellular localization of CaMKII was identified to such structures as the plasma membrane, SR and the perinuclear region. These loci are similar in adult cardiac myocytes, although the translocation of $CaMKII_{\delta B}$ to the nucleus was weak. However, when hypertrophy was stimulated in the cells by IGF-II treatment, the increase in cell size could be reversed with a CaMKII inhibitor cocktail (Chu et al., 2008). Up regulation of genes after vasopressin (Woischwill et al., 2005) or digoxin (Chen et al., 2011) treatment has also been reported to be CaMKII sensitive. Whether CaMKII is involved in simulated I-R injury in H9c2 cells has not been investigated.

3.2.2. Cell Maintenance

H9c2 cells were purchased from the European Collection of Cell Cultures and grown in 75cc vented flasks, with high glucose Dulbecco's modified Eagle's medium (DMEM, Invitrogen, components listed in appendix 1.1) that was supplemented with 10% fetal calf serum (HyClone, Peribo) at $37^{o}C$, 5% CO_2. To maintain the myoblast phenotype the cells were split when they reached a confluence of 60-70%. This was done by: washing the cells briefly with phosphate buffered saline (PBS; Invitrogen, components listed in appendix 1.2), trypsinizing the adherent cells by adding 3 ml of TrypLE Express (Invitrogen) and incubating the cells for 2 minutes to dissociate the cells from the flasks, re-suspending the cells in DMEM and then transferring appropriate aliquots to new culture flasks. Each passage was recorded numerically with the addition of 1 point to every splitting procedure. All experiments involved cells with passage numbers up to 20, with 0 considered as the original purchased passage number.

3.2.2.1 Cell Preparation/Subculture

Several culture flasks were used to harvest cells for each experiment. After the addition of trypsin, the cells were centrifuged (at 110 x g for 5 min) and re-suspended into a smaller volume of medium. Counting the cells with a haemocytometer allowed seeding densities to be approximated prior to each experimental investigation. All cells were seeded at a density of $3x\ 10^4$ (unless stated), in a 24 well plate. Each treatment group contained three wells and the plates were left overnight in growth medium before the investigation.

3.2.3. Characterisation of the Cells

3.2.3.1. Dual Labelled Imaging

Cells were seeded ($1x\ 10^5$) overnight in a 35 mm glass bottom culture dish (MatTek Corporation). After washing with PBS, cells were fixed in 2% paraformaldehyde (in PBS) for 15 min. Cells were then washed with PBS prior to 10 min incubation with Triton X-100 (0.1%). PBS containing Rhodamin-Phalloidin (1 µg/ml) and Hoechst 33342 (0.5 µg/ml) were used for the staining (15 min room temperature) of the myofilaments and nucleus respectively. The fluorescent imaging was done with a widescope microscope (Leica, DMIRB) at x63 magnification.

3.2.4. *In Vitro* Models of Cell Injury

3.2.4.1. Experimental Design and Treatment Groups

Two methods were used to induce cell death and injury. The first study used the metabolic inhibitor 2-deoxyglucose (2-DG) and an ionic composition similar to that of extracelluar ischaemic conditions (Esumi et al., 1991). This was composed of (in mM), NaCl 137, KCl 12, MgCl2 0.49, CaCl2 0.9, HEPES 4, 2-DG 10, sodium lactate 20, adjusted to a pH of 6.5 (with NaOH). The removal of glucose and its replacement with its analogue 2-DG was intended to arrest metabolism by inhibiting hexokinase (Horton et al., 1973). The addition of sodium lactate, lowering of the pH and the high K^+ content (hyperkalemia) imitates the extracelluar conditions in the heart exposed to ischaemia (Brar et al., 2000). Lack of blood and oxygen are needed for the term 'ischaemia' to be used, strictly speaking, but this solution was designated as 'ischaemia-mimicking' within this study. A modified Krebs-Henseleit solution (in mM, NaCl 137, KCl 3.8 mM, $MgCl_2$ 0.49, $CaCl_2$ 0.9 mM, HEPES 4, D-Glucose 10) adjusted to pH 7.4 (with NaOH), was used as the physiological buffer. This was given to the control group as a time-matched control, as the pre-treatment solution and for the 'reperfusion' period where metabolism was restored for 2 hours (designated restoration period). Both solutions were prepared prior to each experiment, sterilised with 0.2 µm syringe filter (Corning) and pre-heated to 37^{o}C. Preliminary studies without replication over a period of 2 to 24 hours (data not shown) had determined that a minimum of 14 hours of the ischaemic solution and 2 hours of restoration were needed to reduce the cell viability (assessed with an MTS assay) to below 50%.

The second study involved mimicking the oxidative stress that occurs during an I-R insult. Large generation of oxidative stress can lead to necrotic and apoptotic cell death (Brookes et al., 2004). A longer period of 24 hours was used to mimic other

investigations with no restoration period (Zhu et al., 2007). A manufactured DMEM medium that had the exclusion of glucose, pyruvate and serum with the addition of H_2O_2 was used to induce cell injury. The control group for this study was the no glucose/serum DMEM that excluded the H_2O_2, as preliminary investigation revealed a 50% reduction in cell viability by substrate withdrawal alone. The addition of H_2O_2 further reduced cell viability. The H_2O_2 concentration reported within the literature that inflicts cell damage ranges between 20 µM to 200 µM or even higher (Zhu et al., 2007; Peng et al., 2010). A concentration gradient within the ranges used by Zhang et al. (2007) of 20-50 µM was initially investigated and it was determined that 40 µM was sufficient to reduce cell viability by another 50%. Further details of the treatment groups and the concentration used for each of the drugs are given below. All solutions were prepared in sterile tubes and pre-heated to 37^{o}C.

Study 1: Metabolic inhibition and ischaemia-mimicking solution

All cells including the controls were washed once with PBS prior to an hour of pre-treatment with a physiological buffer and the respected agents. The physiological solution was replaced with the ischaemia-mimicking solution for 14 hours. Restoration of metabolism was initiated by the replacement of a physiological buffer and included changes for the control. The drug treatments included (figure 3.1): two concentrations of the CaMKII inhibitor KN-93 (1 and 5 µM), its inactive analog KN-92 (5 µM), two concentrations of AIP (40 and 200 nM), and a DMSO control equivalent to the highest dissolved concentration (0.07%). Cell viability was assessed by a colorimetric assay and involved an MTS reagent added to all wells for 2 hours, before being analysed by a multiplate reader (see section 3.2.4.2).

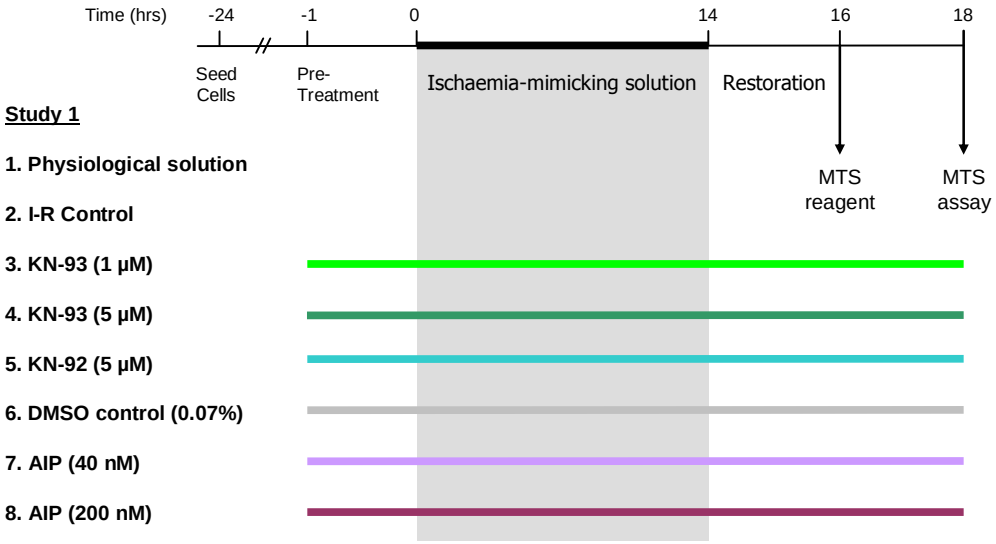

Figure 3.1: Timeline of the experimental procedures for study 1. *Cells were seeded in three wells (all treatment groups were on one 24 well plate) for each treatment group the day before the experiments. All groups were washed and subjected to their respective 1 hour pre-treatment in physiological solution. The ischaemia-mimicking solution including the respective treatment drugs or controls were applied to the cells for 14 hours. Restoration of metabolism was instigated for 2 hours prior to the addition of the MTS reagent for a further 2 hours. This enabled the measurements of activity of dehydrogenase enzymes to determine cell viability. The experiment was performed on three separate occasions.*

Study 2: Oxidative Stress and Glucose Deprivation

A 10 mM H_2O_2 solution was freshly made with the no glucose DMEM, from a 30% w/v H_2O_2 stock solution (Fisher Scientific). Stock concentrations of the drugs and the 10 mM H_2O_2 solution were then added to the no glucose DMEM to make a final 40 µM H_2O_2 solution with the treatment groups (figure 3.2) respective drug concentrations. After one wash with PBS the cells were incubated for 24 hours with the oxidative stress solution. The MTS assay was then performed as described below.

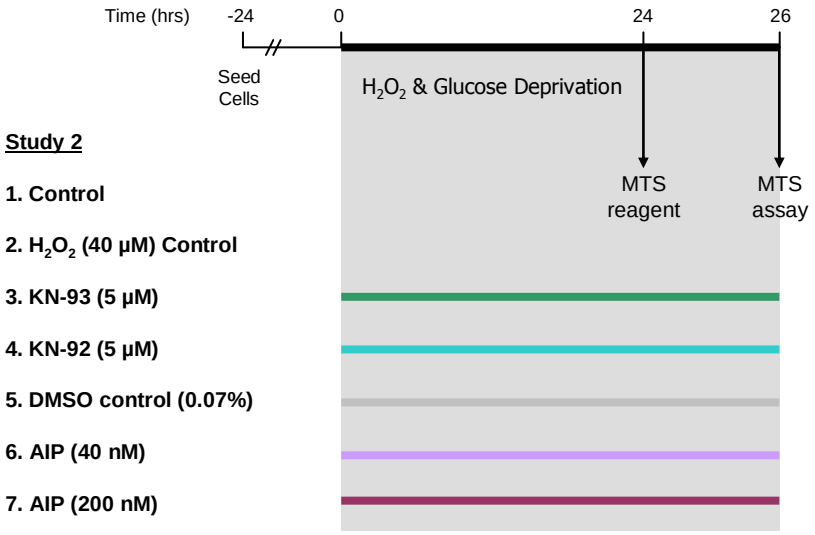

Figure 3.2: Timeline of the experimental procedures for study 2. *Cells were seeded in three wells of a 24 well plate the day before the experiments. After washing the cells, the respective drug treatments and the H_2O_2 solutions (40 µM) in no Glucose DMEM were added to the cells for 24 hours. The MTS reagent was then added for a further 2 hours before being assayed. The drug concentrations mimicked those for study 1 except that only the highest concentration of KN-93 (5 µM) was tested. The experiment was performed on three separate occasions.*

3.2.4.2. Assessment of Cell Viability (MTS assay)

To measure cell viability a tetrazolium compound [3-(4,5-dimethylthiazol-2-yl)-5-(3-carboxymethoxyphenyl)-2-(4-sulfophenyl)-2H-tetrazolium, inner salt; or MTS] was added to the cells using the commercially available CellTiter 96® AQueous Non-Radioactive Cell Proliferation Assay (Promega). For each 100 µl of solution in the wells, 20 µl of reagent was added and incubated for 2 hours at 37^{o}C. The principle of the assay is that MTS is reduced into formazan in the presence of dehydrogenase enzymes, which are only present if the cells are metabolically active. The quantity of the formazan is then measured according to its 490 nm absorbance (optical density, OD)

by a plate reader (Dynex Technologies, UK). A blank well that contains no cells and thus no dehydrogenase, is created to measure the background absorbance of the culture medium or the solution that the cells are present in. The equation below was then used to calculate the cell viability for each of the treatment groups by comparing them to the time-matched controls.

$$\frac{\text{Mean OD of treated cells} - \text{Mean OD of blank}}{\text{Mean OD of control cells} - \text{Mean OD of blank}} \times 100 = \text{Cell Viability (as a \% of control)}$$

To determine the efficacy of the MTS assay in measuring cell viability and death, a supplementary study was performed. This involved a comprehensive analysis of cell death and viability during three similar time periods (14, 15 and 16 hours) of simulated ischaemia used in study 1. These time periods identify a threshold of injury for the H9c2 cell line, as extending the 'ischaemic' period by one or two hours substantially increased the injury sustained by the cells. Figure 3.3 shows a timeline of the cells subjected to 14, 15 or 16 hours of the ischemia-mimicking solution and then two hours of restoration. Three measurements were then undertaken for these cells. The MTS assay as previously described was initiated in three wells with a sample from each of these wells also being used for the LDH assay (see next section). Three more wells undergoing the same treatments were kept for measurements of the cells by Trypan blue exclusion (described below).

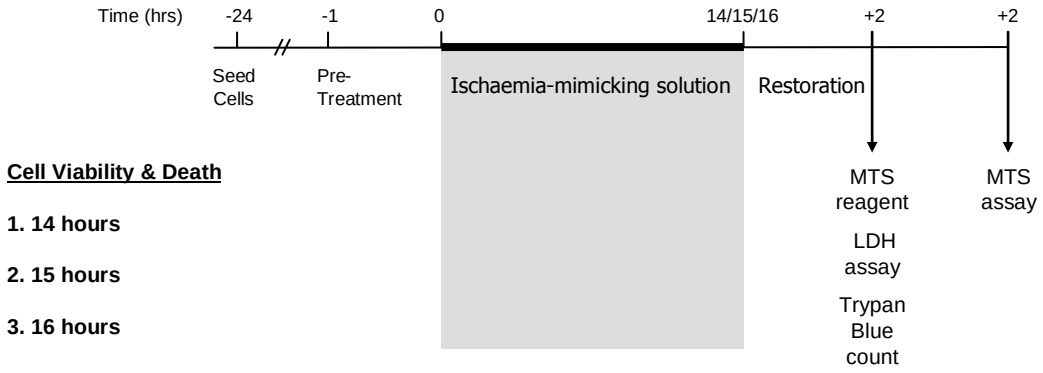

Figure 3.3: Timeline for the cell viability and death comparison. *Cells were treated to same ischaemic solution as study 1 for 14-16 hours and then 2 hours of restoration. Three measurements were used to determine the extent of cellular injury inflicted by the different indexes. The MTS and LDH assay were performed from the same wells whilst additional wells were plated for the trypan blue count.*

3.2.4.3. Trypan Blue Exclusion

A viable cell will hold an intact cell membrane and thus will exclude dyes such as trypan blue. Although it is an indirect measurement of cell viability, as the cell may have lost its capacity to function even though the membrane is intact, it is a popular method to count the number of viable cells within a population. Three wells were designated for this measurement. The medium and cells for each individual well was collected (by adding 250 µl TrypLE Express) and centrifuged at 18000 x g for 5 min. The supernatant was discarded and the cell pellet was re-suspended in 50 µl medium without serum. 50 µl of trypan blue (0.4%, Sigma-Aldrich) was then mixed with the cell suspension and left for precisely 3 minutes. A cell count was then initiated on a microscope using a haemocytometer. The unstained (viable) and stained (nonviable) cells were then counted and calculated as a percentage of viable cells. After centrifugation and resuspension, the total number of cells counted within the wells treated to the ischaemic-mimicking solution was approximately 15% lower than the wells treated with the physiological solution. This indicates that a portion of the cells

had been completely degraded or were otherwise non-collectable and were not accounted for within this analysis. This is an inherent limitation of the technique since the cells that are counted are always still intact.

3.2.4.4. LDH Assay

When the sarcolemma is ruptured during necrotic cell death a stable cytosolic enzyme lactate dehydrogenase (LDH) is released into the solution. The CytoTox 96® Non-Radioactive Cytotoxicity Assay (Promega) measures the released LDH by reduction of a tetrazolium salt into a red formazan product. As a positive control, lysis buffer (to stimulate 100% cell death, 9% v/v Triton X-100) is added to one group of time-matched controls. After the 2 hour restoration period, 50 µl was taken from each well and added to a 96 well plate. A further 50 µl of the LDH assay was added to each well for 30 minutes before the reaction was terminated by another 50 µl of stop solution (1M acetic acid). The absorbance (490 nm) of each well was then recorded on a plate reader and expressed as a percentage of the positive control (or complete cell death).

3.2.5. Statistical Analysis

All numerical data are presented as mean values ±SEM. The statistical software PRISM® version 5.00 (Graphpad) was used to analyse all statistical data; with the spreadsheet Excel (Microsoft) used for some of the data handling. Linear regression analysis was performed to determine the relationship between the MTS assay and the LDH assay or trypan blue counted cells. A one-way ANOVA compared the mean scores of all treatment groups within each study, followed by a post hoc analysis (Newman-Keuls test). A probability level of 5% ($p<0.05$) was defined as the level of significance.

3.3. Results

3.3.1. Characterisation of Cells

Imaging of H9c2 cells

Bright field and dual labelled images (nucleus and myofilaments) of the H9c2 cells were captured on a widescope microscope (figure 3.4). The bright field images depict the mononucleated myoblast as a flat two dimensional cell with an outer membrane. Figure 3.4A also shows that they link to each other by cytoplasmic bridges when grouped close to one another. As originally described by Kimes and Brandt (1976), the nucleus contain two to four prominent nucleoli. Staining for the actin filaments with rhodamine-phalloidin enhances the structural dimensions of the cell. It makes obvious the spindle-shaped structure of the cells which also organise in linear parallel array when grouped together. Nuclear staining brings out the single nuclei in each myoblast. Figure 3.4C is an example of the myoblasts immediately after cell division. These cells have lost their spindle shaped structure and appear more like embryonic cardiac myocytes.

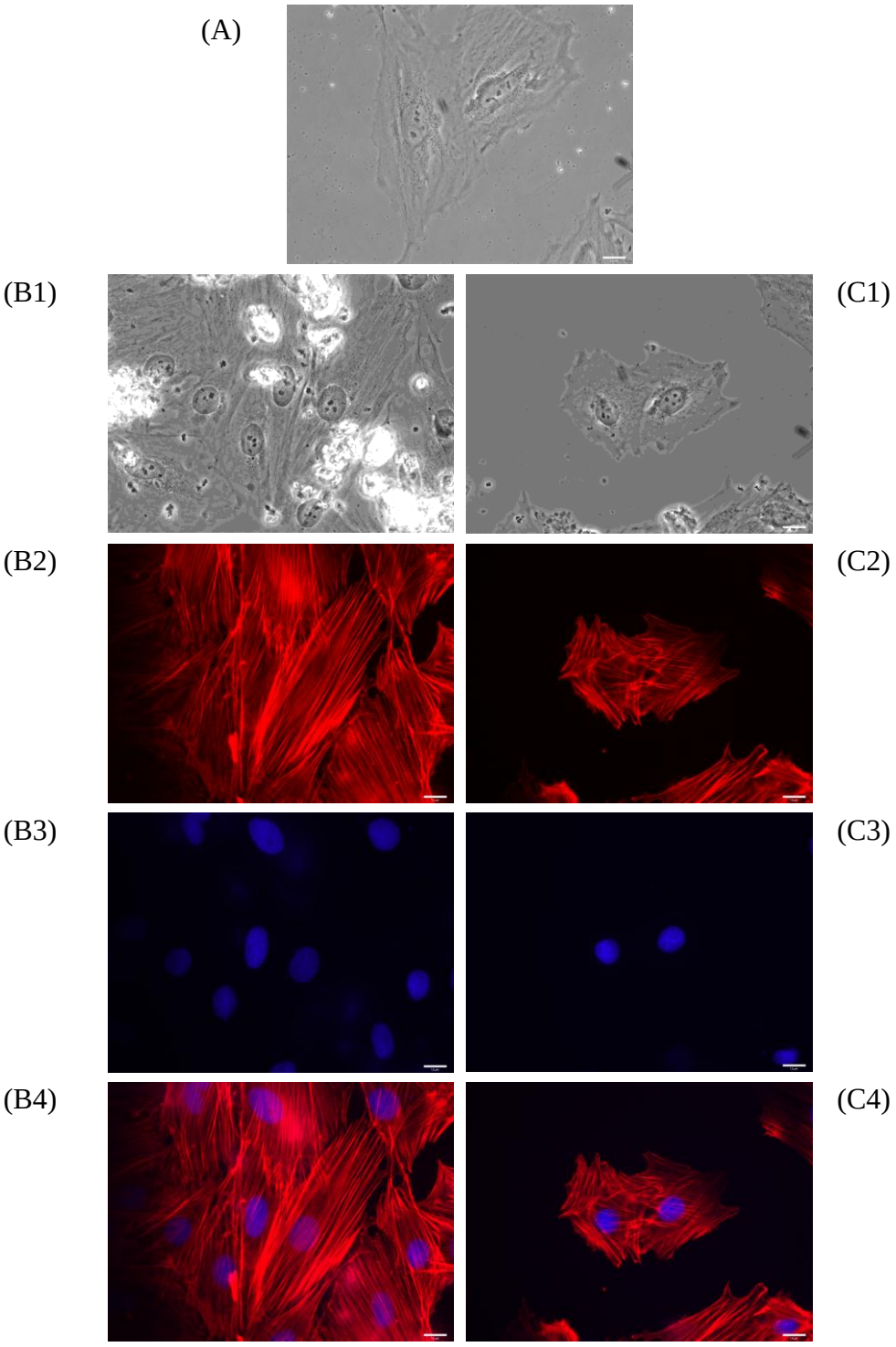

Figure 3.4: H9c2 cells fixed and dual labelled with Rhodamin-Phalloidin and Hoechst 33342. *(A) Brightfield image of two H9c2 myoblasts. (B) H9c2 cells grouped together or (C) after proliferating, captured by (1) brightfield image, (2) Rhodmain-Phalloidin stained for actin filaments, (3) Hoechst 33342 staining for the nucleus, (4) merged fluorescence images. All captured on a widescope microscope (Leica, DMIRB) x63 magnification. White bar measures 15 µm.*

3.3.2. Extent of Cell Injury After Periods of Simulated I-R Injury

Three different techniques were used to determine the viability of the cells after being subjected to a period of simulated I-R. Preliminary investigations indicated that the cells had a critical threshold for cellular injury when introduced to the ischaemic solution (high sodium lactate, high K^+, acidosis and 2-DG). As shown in figure 3.5A, this threshold time was 14 hours of simulated ischaemia. When the mean data for the four separate experiments were analysed, the viability of the cells as determined by the MTS assay revealed that 14 hours (24.7 ± 13.5%) and 16 hours (24.5 ± 14.7%) of simulated ischaemia were comparable in effect. When the cells were subjected to trypan blue staining, which discloses the cells that do not have an intact cell membrane, there was also only a small rise in cellular injury after the additional 2 hour period (62.7 ± 16.4% vs. 73.8 ± 17.0%, not significant). The LDH assay, which measures the extent of cells that have released their intracellular content, had a considerable increase during the additional couple of hours (28.5 ± 6.7% vs. 63.0 ± 16.0%, $p = 0.0943$).

What is also evident from these data sets is the extent of variability that was present within the cell preperations. A high MTS assay score of 64-67% was recorded for one out of the four experiments in each of the time periods. This corresponded to a lower amount of released LDH (10-17%) or the trypan blue counted cells (14-46%). Thus, linear regression analysis was performed to compare the viability of cells measured by an MTS assay with the two measurements of cell membrane integrity (figure 3.5B). The LDH assay ($r^2 = 0.6203$, $p<0.0024$) and the trypan blue count ($r^2 = 0.8630$, $p<0.0001$) had a significant correlation with the MTS assay. The negative relationship indicates that when the MTS assay was reported to be low, it corresponded with a high proportion of released LDH and an even higher proportion of trypan blue staining.

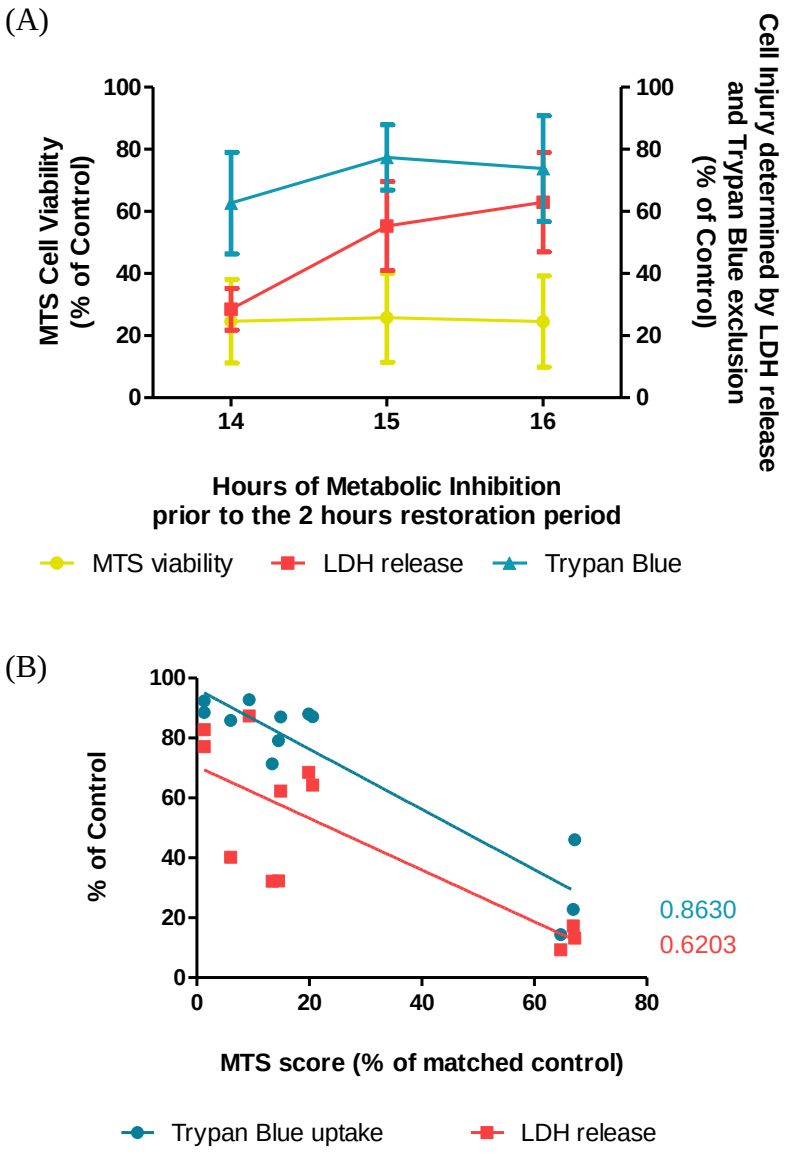

Figure 3.5: The viability of H9c2 cells was determined after 14-16 hours of simulated ischaemia and 2 hours restoration by MTS assay, LDH release and trypan blue exclusion. *Cells were seeded in 24 well plates and subjected to the I-R protocol the day after. Three wells were used for each analysis that was performed on four separate occasions. (A) Mean ± SEM data from four experiments for each of the ischaemic time periods. (B) Linear regression of the cell viability determined by an MTS assay and the trypan blue uptake (r^2 = 0.8630) or LDH release (r^2=0.6203) in each individual experiment.*

When the cells maintained considerable viability, the cell membrane also maintained its integrity. Stages of cell injury are also apparent within the data. When the metabolic activity of the cell is low, the first sign of further injury is the uptake of trypan blue staining. This is then followed by the complete rupture of the membrane that would have allowed the release of intracellular contents such as LDH. The critical time point for this complete rupture was at 14-15 hours of simulated ischaemia. The extent of injury after 16 hours was considered too lethal for the cells with 15 hours also containing much variability. As such, 14 hours ischaemia was considered as a suitable index insult to reduce cell viability and produce a significant amount of sarcolemmal injury, but with little variability in the LDH release.

3.3.3. Inhibition of CaMKII During Simulated I-R Injury

The H9c2 cells were subjected to 14 hours of simulated ischaemia with 2 hours of restoration, in the presence or absence of CaMKII inhibitors/KN-92 (figure 3.6). The I-R control (38.67 ± 13.8%), KN-92 treated cells (40.27 ± 13.6%) and the control for DMSO (38.73 ± 14.7%) showed similar cell viability. There was some variability within these groups as demonstrated by the high SEM. A one-way ANOVA did not detect any significant difference between these controls and of those cells treated with the CaMKII inhibitors KN-93 or AIP. The two concentrations of KN-93 at 1 µM (42.60 ± 6.3%) and 5 µM (45.77 ± 5.4%) did not result in any difference to the controls but were associated with less variability. The presence of AIP (40 nM) had the lowest variability of all the treatment groups (54.17 ± 2.3%) and had a mean difference of 15.5% in its cells viability when compared to the I-R controls, but this was not significant. Treatment with the higher concentration of AIP (200 nM), also resulted in

increased cell viability (51.10 ± 14.3%) after the I-R insult, but was associated with the same high variability as the controls.

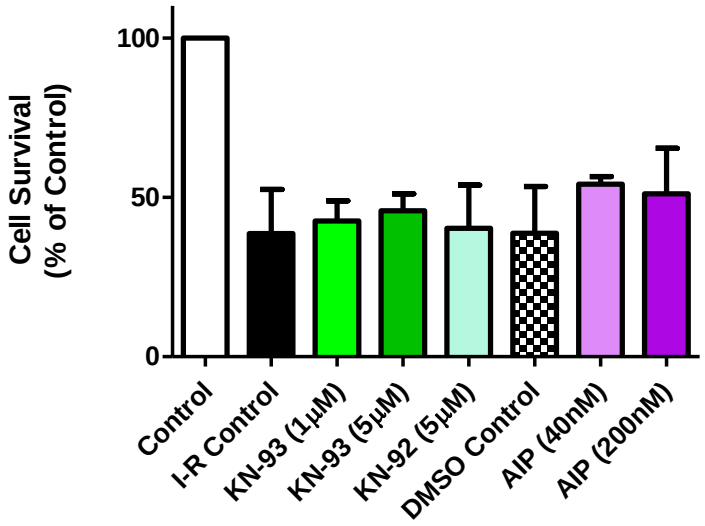

Figure 3.6: Viability of H9c2 cells after 14 hours of ischaemic mimicking solution and 2 hours restoration with/without the presence of CaMKII inhibitors. *H9c2 cells were seeded in 24 well plates overnight. After pre-treatment for 1 hour with physiological buffer and their respective treatment drugs, the cells were introduced to 14 hours of ischaemic solution and 2 hours restoration also in the presence of the CaMKII related agents. Cell viability was then determined by an MTS assay. A one-way ANOVA detected no significant difference between the I-R control and the drug treatments. The data are for three separate experiments (N = 3).*

3.3.4. Inhibition of CaMKII During Oxidative Stress

A preliminary investigation determined that H9c2 cells treated with a medium containing no serum and glucose (XG DMEM) for 24 hours reduced the viability (determined by an MTS assay) of the cells to 46.9% (figure 3.7A). Injury was augmented by the addition of H_2O_2 (40 µM). This is presented in figure 3.7B as a percentage of the cells treated with only XG DMEM. As such, the viability of these cells within the new injury control group was halved (48.7 ± 5.4% of XG DMEM) by the additional treatment with oxidative stress.

The presence of the CaMKII inhibitors did not prevent any significant amount (determined by one-way ANOVA) of cellular injury, as a high concentration of KN-93 (5 µM) had a similar survival rate (47.8 ± 6.3%) to the injury control, whereas the AIP treated cells were also not different. However, when all the groups means were compared to one another (one-way ANOVA), the cells treated with both concentrations of AIP were significantly less injured than the KN-92 (5 µM) treated cells. AIP at 40 nM also had the highest mean score (62.0 ± 4.7%) of all treatment groups, whilst a 5-fold increase in AIP concentration (200 nM) produced a similar cell viability, but with lower variability (59.3 ± 1.3%). However, although AIP-treated cells had higher viability than the Injury Control cells, the differences were not statistically significant. The DMSO control was not significantly different to any of the treatment groups (53.6 ± 2.7%).

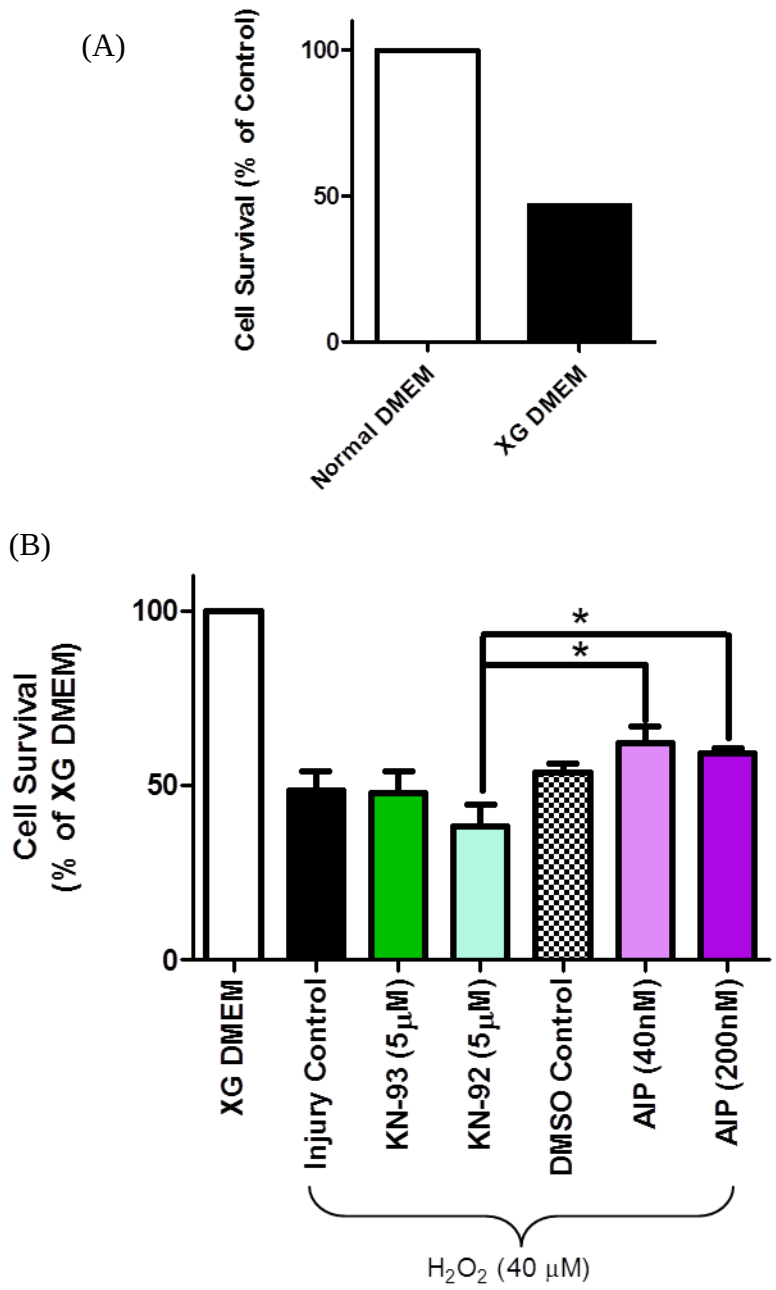

Figure 3.7: The viability of H9c2 cells determined by MTS assay after 24 hours of H_2O_2, glucose/serum deprivation and CaMKII related agents. *Cells were seeded in 24 well plates (3 wells per group) and subjected to oxidative stress and glucose/serum deprivation (XG DMEM) for 24 hours. (A) Cell viability with the XG DMEM (n=2 seperate experiments). (B) Cell viability, expressed as a percentage of viability in the XG DMEM group, is further reduced with the addition of 40 μM H_2O_2 (injury control). CaMKII inhibitors KN-93 and AIP did not limit injury when compared to the injury control. But both AIP concentrations were significantly different to the KN-92 treated cells (n = 3 seperate experiments). XG DMEM, no glucose DMEM. (*P<0.05 one-way ANOVA followed by Newman-Keuls post test).*

3.4. Discussion

The study's major findings can be summarised as follows:

- The small molecule CaMKII inhibitor, KN-93, or the more specific peptide inhibitor, AIP, did not promote H9c2 cell viability after periods of simulated I-R or oxidative stress. Thus, the original hypothesis that *CaMKII inhibition would promote cell viability in an in vitro model of cellular injury* can be rejected.

- The cells treated with 40 nM AIP attained a higher mean viability score than all the other treatment groups in both models of cellular injury, but this was deemed statistically non-significant. This could indicate that some of the cellular stress might have involved CaMKII activity, but as a high concentration of KN-93 did not match such readings, further investigations and different methods of analysis would be needed.

- There was more variability (demonstrated by an increase in SEM) when the H9c2 cells were treated to simulated I-R than when they were treated with oxidative stress. This was not due to the methods used to analyse cell viability as three separate techniques demonstrated similar amount of variability. As some of the treatment groups that included CaMKII inhibitors reduced the variability, it is possible that an intracellular signalling component contributed to these differences.

3.4.1. CaMKII Inhibition Does Not Promote H9c2 Cell Viability

The two models of cellular injury used in this study were designed to mimic the conditions that occur in the *in situ* heart during ischaemia and subsequent reperfusion. In doing so it was hypothesised that CaMKII activity and cellular injury would be promoted and that they were both related. The conditions used in the studies have previously been documented to promote cell injury and death (Esumi et al., 1991; Zhu et al., 2007). This was replicated within these studies as less than 50% of the cells were viable at the end of the experiments. However, the same pathological conditions have been reported to exacerbate cellular injury through the activity of CaMKII (Vila-Petroff et al., 2007; Zhu et al., 2007). This was not repeated in these models as the presence of two different CaMKII inhibitors throughout the periods of cellular injury did not promote a significant increase in cell viability. Thus, it can be concluded that when H9c2 cells are exposed to simulated I-R or the combination of oxidative stress and substrate deprivation, there is no involvement of CaMKII activity in the cellular injury.

The previous studies that have suggested a pro-injurious role of CaMKII during cellular stress have not used the H9c2 cell line. Cells are either derived from the adult (Zhu et al., 2007; Sapia et al., 2010) or neonatal hearts (Peng et al., 2010). The detailed study by Hoch et al. (1998) demonstrated that $CaMKII_{\delta C}$ is the prominent isoform in the H9c2 myoblasts. $CaMKII_{\delta C}$ targets the Ca^{2+} handling proteins in the cytosol and has been made accountable for instigating cell death (Zhu et al., 2007; Peng et al., 2010). Thus, as H9c2 cells maintain their ability to contract (Kimes and Brandt, 1976) and respond to different Ca^{2+} agents that can stimulate apoptosis (Lax et al., 2005; Lax et al., 2006) an active $CaMKII_{\delta C}$ could have been expected in these cells. Nevertheless, as the cells were unstimulated during the study, the lack of E-C coupling and Ca^{2+} cycling

activities might have made this isoform less active in comparison to cells that are isolated from the whole heart.

If the cells did possess sufficient protein levels of CaMKII, the cellular stress instigated within these studies would be expected to activate the kinase. Acidosis, hyperkalemia and oxidative stress are known activators of CaMKII (Zhu et al., 2007). When compared to the injury controls there was an insignificant increase in mean cell viability when cells were treated with AIP (40 nM) after I-R (mean difference of 15.5%) and oxidative stress (mean difference of 13.33%). These differences were above the protective ranges demonstrated by the CaMKII inhibitors of Zhu et al. (2007). They reported that KN-93 (2 μM) and AIP (5 μM) prevented apoptosis (<10 % of TUNEL positive cells) in cardiac myocytes isolated from 2-3 months old rat hearts that were subjected to 24 hours of acidosis (pH 5.5), hyperkalemia (K^+ 60 mM) or oxidative stress (H_2O_2 20 μM). Except for the concentration of H_2O_2, the individual components chosen by Zhu et al. (2007) were more extreme than the conditions chosen in this study and were more reliable in producing cellular injury. On the other hand, the H9c2 cells had acquired sufficient cell injury within the models used in this study. But the variation between experiments deemed the results not statistically significant. The only exception was with the KN-92 treated cells which had a significant decrease in cell viability after treatment with H_2O_2 if compared to the AIP treated cells. As the cells were also treated with a high concentration of KN-93 (5 μM) and showed no clear relationship between or within the pharmacological modulators of CaMKII, it would support the fact that CaMKII could not have been a major factor for cellular injury within the H9c2 cells.

3.4.2. The H9c2 Cells as a Model of I-R Injury

After 14 hours of simulated I-R injury the viability of the H9c2 cells had been reduced to 38.67 ± 13.8% when measured by MTS assay. Measuring viability by trypan blue exclusion or by LDH assay had determined that although some cell membrane integrity had been lost, the majority of the cells had not undergone complete rupture that is characteristic of cell death by necrosis. The MTS assay had a strong correlation with the trypan blue measurements and would have been sufficient to demonstrate if the cells had irreversible damage. Thus if the kinase had any significant involvement with the resulting cell injury, this should have been detected in the measurements of cell viability used in the study. Whether these measurements were also sensitive enough to determine if the CaMKII inhibitors were protective against apoptotic signalling pathways would require further investigations.

Secondary cell lines and immature cardiac myocytes are more resistant to cellular stress than adult cardiac myocytes (Marber, 2000). It has also been suggested that programmed cell death in embryonic cells is caspase dependent and that as they develop to terminally differentiated cardiac myocytes they move to a caspase-independent death pathway (Bahi et al., 2006). Although this theory challenges many studies that have shown at the cellular (Uchiyama et al., 2004; Stephanou et al., 2001) and the whole heart level (Mocanu et al., 2000; Holly et al., 2002) that adult cardiac myocytes can instigate significant cell death through caspases, it could be suggested that cell injury in this study was different to those that have previously investigated the involvement of CaMKII through a caspase dependent pathway. The H9c2 cells have shown to have both a caspase-dependent and a caspase-independent pathway to cell death (Bahi et al., 2006). As the models used in this study included several factors that could have determined cell viability it can not be certain which mechanisms were

relevant to cell injury. There is some inconsistency reported in the literature as Uetani et al. (2009) prevented H9c2 cells from apoptosis during hypoxia treatment with a caspase-3 inhibitor, but Aki et al. (2001) who used similar conditions saw no effect with a pan-caspase inhibitor. When Yaglom et al. (2003) subjected H9c2 cells to a metabolic inhibitor rotenone, rapid ATP depletion and cell death (within 4 hours) could also not be prevented by caspase inhibitor and were characteristic of necrosis. But the inhibition of the JNK pathway was capable of reducing rapid cell death by limiting the extent of mitochondrial depolarisation. Jung et al. (2007) also used 2-DG and hypoxia to report that JNK and p53 are the main effectors of H9c2 viability. CaMKII has been associated with the p38MAPK pathway during conditions of oxidative stress in adult cardiac myocytes (Palmoeque et al., 2009), but it has not been determined if it has any involvement with the JNK pathway. Yet, when H9c2 cells were treated with H_2O_2 it was reported to stimulate cell death through a caspase-dependent pathway (Youn et al., 2005). Although this model of cellular injury showed the strongest trend of protection by the CaMKII inhibitor AIP, in this study, it was surprising to see how little influence the CaMKII inhibitors had over the fate of the H9c2 cells.

3.5. Conclusion

The presence of the CaMKII pharmacological inhibitors KN-93 or AIP did not promote the viability of the H9c2 cells when they were subjected to simulated I-R or oxidative stress. This would suggest that the patterns of injury sustained by the cells in both these models were not promoted by CaMKII activity. Similar models of cell injury have found the same pharmacological inhibitors of CaMKII to promote cell viability. But these studies used primary cell lines and not a secondary cell line that lacks contractile activity. Further studies determining the levels of CaMKII activity are needed to determine whether the H9c2 cell line would be a suitable model in investigating the role of CaMKII and cellular injury.

CHAPTER 4:

The Measurement of Ca^{2+} Transients in Adult Rat Ventricular Cells During Simulated I-R and CaMKII Inhibition

4.1. Introduction

4.1.1. Ca^{2+} handling During Ischaemia-Reperfusion

A key feature of I-R injury is the failure to maintain intracellular Ca^{2+} homeostasis that can trigger arrhythmic activity and cell death (Piper et al., 1999; Dong et al., 2006; Luqman et al., 2007). During ischaemia, Ca^{2+} overload will occur just prior to the onset of contracture (Barry et al., 1987; Eisner et al., 1989). Imbalances in ion transport through the Na^+/K^+-ATPase, NHE and NCX are thought to be central to the accumulation of Ca^{2+} (Talukder et al., 2009) that is always preceded by a rise in $[Na^+]_i$. The conditions at reperfusion also favour mishandling of Ca^{2+} which increases the likelihood of arrhythmic activity (Murphy and Steenbergen, 2008; Talukder et al., 2009). In both circumstances, the relationship between the SR and the mitochondria is critical to how the cells will handle $[Ca^{2+}]_i$ (Dorn and Scorrano, 2010; Ruiz-Meana et al., 2010). Both organelles act as buffering sinks to the rising $[Ca^{2+}]_i$, but if the mitochondria are compromised too much, opening of the mPTP and cell death is inevitable (Halestrap, 2009).

It has been established over many years that Ca^{2+} uptake by the SR is impaired during I-R (Lee et al., 1967; Toba et al., 1978; Osada et al., 2000). Models that have genetically modified SERCA2a (either through abrogation or gain-of-function) demonstrate that if uptake of Ca^{2+} into the SR is promoted, a reduced $[Ca^{2+}]_i$, better contractile recovery and infarct limitation are possible (Talukder et al., 2009; Shintani-Ishida and Yoshida, 2011). However, it has also been noted that this sequestered Ca^{2+} may encourage cell death and hypercontracture, as it is released by the SR during the next oscillation (Piper et al., 2006). A recent study by Valverde et al. (2010) has shed new light on the changes that occur to the SR Ca^{2+} handling ability during I-R. By

using pulsed local field fluorescence, intracellular Ca^{2+} measurements were recorded in the *in situ* mouse heart during global ischaemia (12 min in duration) and reperfusion. It was revealed that the Ca^{2+} content of the SR gradually increases during ischaemia. Then at reperfusion, the overloaded SR releases its Ca^{2+} content contributing to Ca^{2+} overload in the cytosol.

Many cell based models have suggested that the SR has a physiological threshold for sequestration of Ca^{2+} (Lakatta, 1992; Jiang et al., 2004; Eisner et al., 2009). When this upper limit of Ca^{2+} content is surpassed, diastolic events of spontaneous Ca^{2+} release will occur from the RYR2 in the form of Ca^{2+} 'sparks' and propagating Ca^{2+} waves (Eisner et al., 2009). The generation of Ca^{2+} 'sparks' from the SR are believed to be caused by a small group of RYR2 or IP_3R. These local Ca^{2+} events can raise the cytosolic $[Ca^{2+}]_i$ to ~200 nM (Cheng and Lederer, 2008). Numerous sparks can propagate an event of CICR through the cell that emerges as a Ca^{2+} wave (Bootman et al., 2001). If the Ca^{2+} activity is enough to generate an inward current through the NCX it can lead to a pro-arrhythmic event such as an afterdepolarisation (Eisner et al., 2009).

There has been much debate with respect to the interrelationship between the SR Ca^{2+} load, its sequestered threshold and the activity of the RYR2 open probability (P_o) that is needed to stimulate a diastolic event. Many factors present during ischaemia, such as oxidative stress and acidosis, have also been shown to limit the release rate of Ca^{2+} through the RYR2 (Xu et al., 1996; Choi et al., 2000). An interesting study by Yang and Steele (2001) measured the Ca^{2+} spark activity of rat ventricular myocytes in an environment of reduced ATP content. They measured a reduction in the Ca^{2+} spark frequency that subsequently caused an increase in the SR Ca^{2+} content. Thus, although Ca^{2+} load in the SR was increased, ATP was a strong determinant of the spontaneous

Ca^{2+} release through the RYR2. Similar findings have been reported in a model using metabolic inhibitors (Overend et al., 2001). These studies could explain why the abnormal loading of Ca^{2+} into the SR was measured in a model of global ischaemia by Valverde et al. (2010). However, what was also suggested by Yang and Steel (2001) was that although the frequency of Ca^{2+} sparks was decreased, the magnitude of the diastolic event to trigger arrhythmic activity (i.e. ischaemic arrhythmias) would be greater. Accordingly, the various facets of ischaemia influence the activities of the SR and its Ca^{2+} handling ability but it is still to be determined whether promoting or discouraging these activities is beneficial under such conditions.

4.1.2. Ca^{2+} Handling by CaMKII During I-R

CaMKII could be foreseen to influence several factors during I-R injury, but its activity on the cell's Ca^{2+} handling ability is currently the best described (Hudmon and Schulman, 2002; Maier and Bers, 2007). Yet, there is a lack of research on how CaMKII influences the Ca^{2+} handling properties of cells during I-R. Dhalla's studies suggested that deterioration in CaMKII activity during I-R matched the same decline in the Ca^{2+} handling ability of the isolated SR vesicles (Netticadan et al., 1999; Osada et al., 2000). However, the significant reduction in infarct size with KN-93 pre-treatment in Chapter 2 and the work of others (Vila-Petroff et al., 2007; Erickson et al., 2008) suggest that CaMKII activity during I-R promotes irreversible injury. Mattiazzi's studies suggested that CaMKII activity through the reverse mode of the NCX causes cellular injury during the first minutes of reperfusion. The study by Vila-Petroff et al. (2007) used the fluorophore Indo-1 to record the Ca^{2+} activity of quiescent cardiac myocytes subjected to simulated I-R protocol. Treatment with the CaMKII inhibitors KN-93 (1 μM) or AIP (1 μM) prevented reperfusion injury by limiting the occurrence

of large and spontaneous Ca^{2+} oscillations that would have otherwise caused membrane rupture and cell death. The key mechanism of protection with CaMKII inhibition was suggested to be prevention of the phosphorylation of the Thr^{17} site on PLB. Phosphorylaton would increase SERCA2a activity and promote SR Ca^{2+} overload. There was no reference to the Ca^{2+} handling properties during ischaemia and whether Ca^{2+} overload prior to reperfusion was also prevented. Yang et al. (2006) reported similar findings to Mattiazzi's studies with their genetically modified AC3-I mice. This method of targeting CaMKII activity reduced the SR Ca^{2+} content making them less susceptible to MI induced apoptosis. As PLB ablation (and increased SERCA2a activity) removed the protection, it was strongly suggested that this was CaMKIIs' primary target. Other *in vitro* models of sustained CaMKII activation have also supported the hypothesis that promoting SR Ca^{2+} uptake and overload is a key mechanism of cellular death (Zhu et al., 2003).

Whether uncontrolled activity on the RYR2 can contribute to cytosolic Ca^{2+} overload during the ischaemic period is questionable, but studies have focused on the RYR2 as a pro-arrhythmic target for continued CaMKII activity. In conditions of systolic dysfunction such as heart failure, increased RYR2 activity would promote unregulated Ca^{2+} release. An interesting observation is that by preventing CaMKII activity, either pharmacologically or by genetic manipulation, a reduced Ca^{2+} spark frequency (and subsequently the occurrence of arrhythmias) have resulted in an increased SR Ca^{2+} load (Ai et al., 2005; Sag et al., 2009). However, an earlier investigation reported that under controlled conditions CaMKII inhibition with KN-93 reduced the SR Ca^{2+} load (Li et al., 1997).

An important element to these studies is the proportion or the fractional release of Ca^{2+} into the cytosol to any given SR Ca^{2+} load (Trafford et al., 2001). In conditions

such as heart failure the sustained CaMKII activity may reduce the total Ca^{2+} content of the SR, but it will (at least initially) also allow an augmented release of Ca^{2+} to maintain the transients' amplitude (Kohlhaa et al., 2006; Toischer et al., 2010). This can be achieved via CaMKII facilitation on the LTCC and the RYR2. With subsequent CaMKII inhibition, the SR fractional release of Ca^{2+} can be normalised due to limited activities of these CaMKII targets. This is also the case when there is an increase in the SR Ca^{2+} load. Although Ai et al. (2005) demonstrated the ability of KN-93 to significantly increase the SR Ca^{2+} load, only minor inotropic effects and Ca^{2+} release were measured as CaMKII targets on ion channels were also subdued. Thus, during ischaemia the many factors (such as the NCX, LTCC and the SR) that force the disproportionate cycling of Ca^{2+} and a rise in $[Ca^{2+}]_i$ will only have minor influence in cells where CaMKII is inhibited. Whether CaMKII inhibition limits the initial rise in $[Ca^{2+}]_i$ during ischaemia or whether it allows the cell to better handle this incursion remains to be seen.

4.1.3. Hypothesis

The aim of these studies is to elucidate the protective role of CaMKII inhibition during I-R injury and further characterise the pharmacological tools used in the thesis. By field stimulating freshly isolated adult rat ventricular myocytes, their Ca^{2+} transients were to be recorded under the influence of CaMKII inhibition, either during normoxic conditions or in a model of simulated I-R injury. A new multi-parametric analytical tool would analyse the activity of the baseline $[Ca^{2+}]_i$ and the Ca^{2+} transient's morphology, amplitude and kinetics in order to discriminate the cells Ca^{2+} cycling ability under these conditions.

The main hypothesis:

Simulated ischaemia will have an adverse effect on intracellular Ca^{2+} homeostasis, which will lead to a rise in the diastolic Ca^{2+} concentration.

It was also hypothesised that:

(i) The CaMKII inhibitor KN-93 and the peptide inhibitor AIP will have comparable effects on the cells Ca^{2+} handling ability.

(ii) The non-specific activity of the KN compounds will have a comparable limitation on the cells Ca^{2+} handling ability.

(iii) CaMKII inhibition during simulated ischaemia will promote cell viability and limit the rise in diastolic Ca^{2+} concentration.

4.1.4. Specific Objectives

(A) Freshly isolate adult rat cardiac myocytes and determine suitable conditions that would allow field stimulation to regulate their contractile activity.

(B) Load the cells with a suitable fluorophore in order to measure the cardiac myocytes' Ca^{2+} transients.

(C) Find a suitable model that would allow the characterisation of the cells' Ca^{2+} transients during a prolonged period of time.

(D) Develop a cell model of simulated I-R injury that would assess the interventions of pharmacological CaMKII inhibition under such conditions.

(E) Use a new multi parametric analytical tool to analyse and characterise the cells' Ca^{2+} transients.

4.2. Materials and Methods

The CaMKII organic inhibitor KN-93 (water soluble), the inactive analog KN-92 and the cell permeable Autocamtide-2 related inhibitory peptide II (AIP) were purchased from Calbiochem (Nottingham, UK). KN-92 and AIP were dissolved in DMSO (final DMSO concentration in the solution was 0.05% and <0.006% respectively).

4.2.1. Isolation of Adult Rat Cardiac Myocytes

The isolation and culture of viable adult rat ventricular myocytes were radically advanced in the late 1970's. By using crude collagenase it became possible to dissociate, with a greater viability of the cells, the strong and physically connected intercalated discs and extracellular matrix (Powell and Twist, 1976). Prior to this, trypsinisation that has no selectivity towards extracellular proteins and mincing of younger hearts, including embryonic cardiac myocytes, was the method for harvesting the cells (Harary and Farley, 1960). Embryonic and neonatal cells had an advantage in allowing longer term culture but a key drawback was that they were physiologically immature. This differentiation in their physiology and response to conditions such as ischaemia were soon identified (Marber, 2000). The standard technique used in this chapter was developed within the laboratory using the protocol from Sian Harding's laboratory (Jones et al., 1990).

Cell Isolation Procedure

All procedures leading to the excision of hearts from male Sprague Dawley rats (300-400g) and their immediate cannulation on the Langendorff perfusion apparatus are described in Chapter 2. The rig was modified with a peristaltic pump (Watson-Marlow,

Falmouth) that provided a constant volume of perfusate (10 ml/min), primarily to regulate the flow rate during the enzymatic digestion of the connective tissue. The raised reservoirs that supplied the constant pressure of perfusate in Chapter 2 were replaced with 50 ml centrifuge tubes bathed in a 37^{o}C water bath. The protocol then followed similar methods described by Jones et al. (1990):

- **5 minutes perfusion with Krebs-Henseleit buffer** (see Chapter 2); to resume normal contractile activity and stabilise the heart.
- **5 min of a low Ca^{2+} perfusate** (in mM: NaCl 120, D-glucose 20, KCl 5.4, $MgSO_4$ 5, pyruvate 5, taurine 20, HEPES 10, nitrilotriacetic acid 5, $CaCl_2$ 0.014); bubbled with 95% O_2 and 5% CO_2. The combination of the Ca^{2+} chelator, nitrilotriacetic acid and the lowered $CaCl_2$ concentration (predicted free Ca^{2+} concentration of 0.9059 µM when calculated using a program for determining free metal concentration http://maxchelator.stanford.edu) stops the heart from contracting and lowers the intracellular Ca^{2+} concentration.
- **Minimum 10 min enzymatic digestion with recycled low dispase Liberase** (0.13 mg/ml, Roche Applied Science); contained in a similar perfusate to the 'low Ca^{2+}' solution with the exception of a higher Ca^{2+} concentration (200 µM) and the absence of nitrilotriacetic acid, (in mM: NaCl 120, D-glucose 20, KCl 5.4, $MgSO_4$ 5, pyruvate 5, taurine 20, HEPES 10, $CaCl_2$ 0.2).

As soon as the heart was transferred to a petri dish inside a ventilated hood, all conditions and materials were kept sterile. The right ventricle was removed and the remaining left ventricular tissue was dissected into smaller pieces. Fresh enzyme solution was passed through a 0.22 µm micro filter (Corning, USA) and added to the sliced tissue before a magnetic stirrer separated the remaining suspension of cells at 200

rpm. As the supernatant from the first 5 min of stirring presented a large proportion of rounded cells, it was discarded. The remaining tissue was then dissociated with a further 15-30 minutes of stirring in new enzyme solution. Filtered through a wire sieve, the second harvest contained the highest percentage of rod shape cells. This was centrifuged for 1 minute, 1000 rpm at room temperature to form a pellet of dissociated ventricular cells. The cells were then re-suspended in 3 ml of (1X) M199 media (components listed in appendix 1.3; Sigma-Aldrich) containing additional metabolites and antibiotics (in mM; pyruvate 2.5, creatine 5, taurine 5, insulin 10^{-7} M, penicillin 50 I.U.). As the Ca^{2+} concentration within the medium is 1.85 mM, this method rapidly re-introduces Ca^{2+} to the cells. This eliminates the non-healthy and marginally Ca^{2+} tolerant cells. With this protocol a 40-50% population of rod shaped cardiac myocytes was counted on a haemocytometer (from a total that included rounded cardiac myocytes), which allowed the estimation of further seeding densities.

4.2.2. Confocal Laser Scanning Microscopy

The Leica TCS-SP5 RS Confocal Laser Scanning Microscope, based on a Leica DMI 6000 inverted microscope system, provided the platform to acquire detailed images of a contracting myocyte and its Ca^{2+} oscillation. As shown in figure 4.1 the exciting laser light will pass an acousto-optical tuneable filter (AOTF) and an acousto-optical beam splitter (AOBS). This 'tuneable' device provides greater selectivity of the excitation light (or wavelength) and enhances the resolution of the sample to be imaged. The objective lens determines the field of view, magnification and resolution by focusing the light transmission on the sample. The emitted light is then passed through a pinhole that is conjugated to the determined focal point. This allows only the focused light to reach the photodetection system, limiting the amount of blurring that is generated by the

out of focus light. A resonant scanner can oscillate mirrors that reflect the light at high speed in order to scan or change the light direction. This enables fluorescent live cell images to be captured at a rapid acquisition rate.

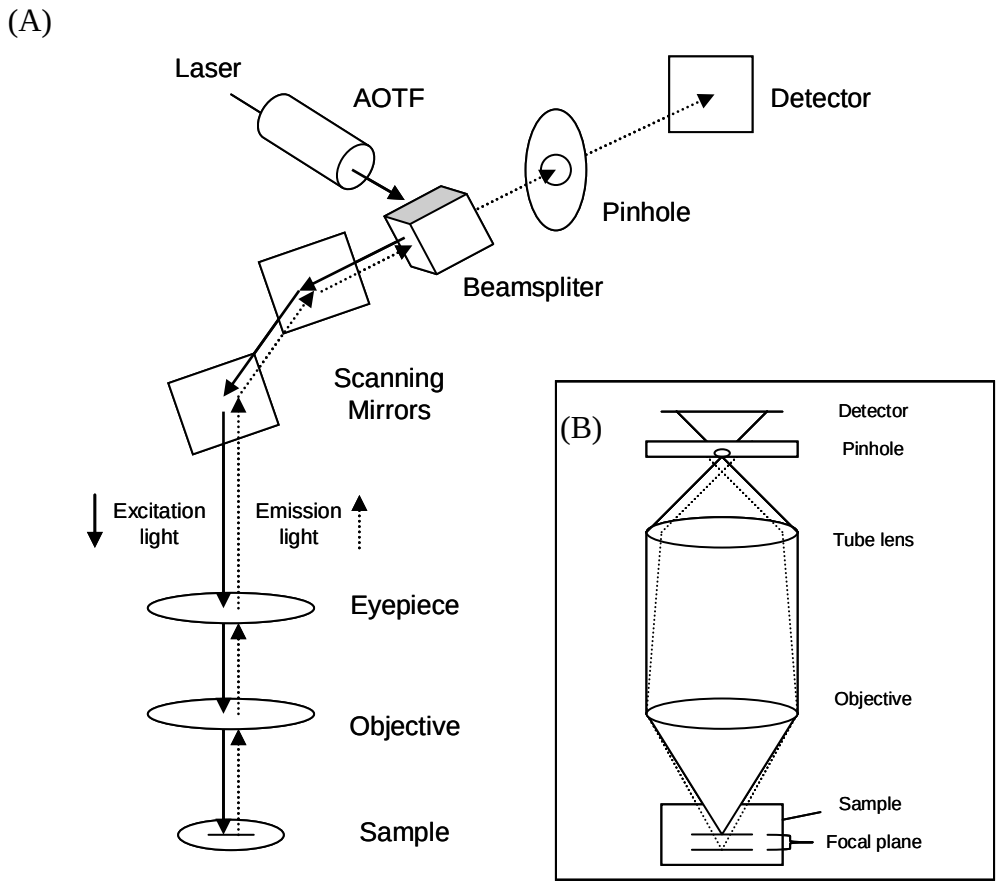

Figure 4.1: Schematic diagram of Leica TCS-SP5 and the principal of confocal imaging. *(A) The Leica TCS-SP5 has acousto-optical components that can channel (AOTF) and split the laser beams. The mirror arrangements can change the line scan direction. With a resonant scanner this can be done at high-speeds that is suitable for live cell imaging. The objective focuses the laser onto the sample and the emitted light is captured on a photodetection system. (B) The key principal of a confocal microscope is the ability to match the light excited by the objective with a pinhole. This limits the amount of unfocused light emitted by the sample to be captured by the detector allowing an enhanced resolution of the image (adapted from Demchenko, 2009).*

Set-Up of the instrument

All experiments were recorded using: 40x oil-immersion objective (numerical aperture = 1.4) in two dimensions (x,y) with time, 1280 x 256 pixels (pixel size: 189.39 nm x 189.95 nm), at a sample rate of 1 image per 49 ms. A large pinhole of 249.82 µm compromises the 'confocality' of the microscope, but gives a deeper Z-slice and provides the absorbance of Ca^{2+} to be conducted at a greater depth of field throughout the cell. The 488 nm laser line from a class IIIb Argon laser running at 30% power was selected to excite Fluo4 (Invitrogen) and the AOTF attenuated to 8% of the laser power was selected whilst the photomultiplier tube (PMT) gain remained within the range of 820-860 V.

Choice of fluorophore

Fluo4 is a Ca^{2+} selective fluorescent probe favoured for its rapid imaging capabilities (i.e. kinetics of Ca^{2+} binding/unbinding, high signal to noise range) and its excitation at a single wavelength (488 nm) which is matched to the argon laser line. It was chosen as the Ca^{2+} indicator, as it is an enhanced version of its predecessor Fluo-3. This includes a brighter emission at equivalent concentration and a faster loading time. The K_d (Ca^{2+}) is 345 nM and is ideal in quantifying cytosolic Ca^{2+} in the 100 nM to 1 µM range (Gee et al., 2000). The high affinity for Ca^{2+} is based on the compound's possession of a calcium-specific polyaminocarboxylic acid, (1,2-bis(o-aminophenoxy)ethane-N,N,N',N'-tetraacetic acid; BAPTA). However, one disadvantage of using such a fluorophore is that the fluorophore can be saturated at low [Ca^{2+}] that would then give errors in Ca^{2+} estimation (Takahashi et al., 1999). Calibration to known quantities of [Ca^{2+}] was not implemented in these studies as they were designed as proof of concept although semi-quantitative analysis could still be predicted, as the values are based on the dissociation constant (K_d). A nonratiometric indicator will also not be able to

correct for artefacts due to bleaching, laser intensity or probe loading. However, Fluo4's properties permit rapid acquisition of images (including Ca^{2+} sparks) making it superior over other fluorophores.

4.2.3. Experimental Protocol

The experiments involved pacing cardiac myocytes with an electric field stimulator whilst superfusing Tyrode's solution or an ischaemic mimicking solution (see section 4.2.3.3) containing modulators to CaMKII. To replicate the experimental conditions in each culture dish a removable 'pod' (figure 4.2) was devised to: a) embrace carbon electrodes in the centre of the dish; b) provide delivery and removal of the desired perfusate; c) present an enclosed environment that could be flushed with nitrogen.

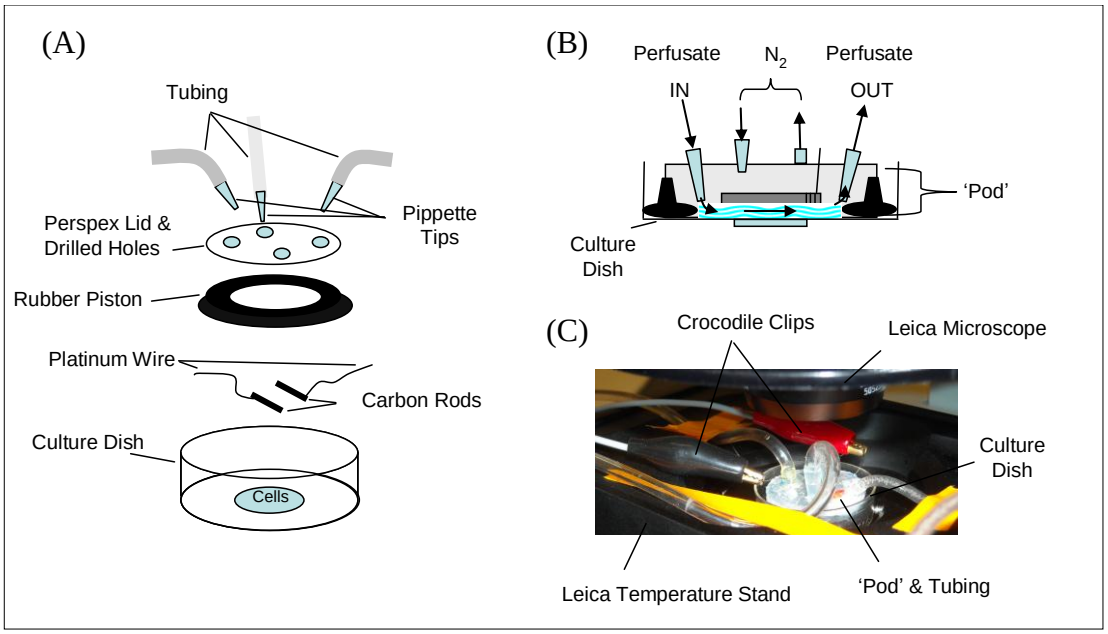

Figure 4.2: Assembly and structure of the experimental 'pod'. *(A) The main components included; a modified rubber piston from a 50 ml syringe, with a roof made from clear Perspex fixed in place with nontoxic silicon filler (Geocel, Plymouth), two carbon electrodes parallel to one another and attached to platinum wires, tubing and pipette tips for delivery and removal of perfusate and Nitrogen gas. (B) Cross section schematic of the experimental pod. (C) Digital photograph of the pod used in an experiment.*

4.2.3.1. Preparation of Cells

A manufactured 35 mm petri dish (MatTek Corporation) containing an 11 mm glass cover slip in the centre of the base was used to culture the cells. After pre-coating with murine extracellular matrix (0.42 µg/µl; Sigma-Aldrich), 2 x 10^3 rod shape cells were seeded with 2 ml of the supplemented M199 medium. Before commencing the first experiment, cells were settled for 30 min in a 37^{o}C, 5% CO_2 incubator with all other experiments completed within the same day of isolation. The cells were washed twice with Tyrode's solution (in mM; NaCl 135, KCl 5, HEPES 5, glucose 10, $MgCl_2$ 1.2, $CaCl_2$ 1.25, pH 7.4) prior to loading with the fluorophore at room temperature. To enhance membrane penetration, an acetoxymethyl (AM) ester derivative of Fluo4 was used. Once inside the cell, esterases cleave the ester creating an indicator that is membrane impermeant. However, AM has a low affinity to aqueous solutions and needs to be solubilised in DMSO. An initial concentration and loading time of 5 µM for 10 minutes was used to load the cells in some of the initial time control experiments of study 1 and 2. This was then modified to 2.5 µM for 15 minutes in all other experiments to conserve the fluorophore and reduce the final concentration of the solvent, DMSO, from 0.5% to 0.25%. Cells were washed three times with the Tyrode's solution and allowed 15 min at room temperature for the de-esterification of the fluorescent probe.

4.2.3.2. Field Stimulation and Criteria for Cell Selection

The studies that have investigated electric field stimulation of cardiac myocytes have noted the promotion of electrolysis at the site of the electrodes, particularly when high stimulus voltage (above 50 V) is applied (Heller et al., 2003). The accumulation of oxidation products can influence cell viability and as such would be a critical artefact of the experimental protocol in a model of simulated I-R injury (Maddaford et al., 1999; Heller et al., 2003). To avoid this, choice of material and configuration of the electrodes were of utmost importance to limit any confounding injury to the cells. Tandon et al. (2009) describe methods for stimulating cardiac myocytes with minimum generation of electrolysis by using carbon rods and platinum wire. This set up was replicated in these experiments with two 10 mm carbon rods (Goodfellow Cambridge Ltd, Huntingdon) placed parallel to one another at a distance of 10 mm. For stimulation efficiency, electrodes must be placed at the bottom of the dish and at the diameter of the dish, with adequate medium to cover the electrodes in order to constrain the field lines between them (Tandon et al., 2009). Holes (0.5 mm diameter) drilled at opposite ends not only allowed the attachment of platinum wire (Goodfellow Cambridge Ltd, Huntingdon) but also assisted in balancing the opposing polarity of the electric fields. Steel rods with crocodile clips allowed easy attachment between the field stimulator and the platinum wire. Square-wave pulses were delivered to the cells at a frequency of ~1Hz, 5ms in duration at 25 volts. The stimulation frequency and the pulse duration of Ca^{2+} transients are the best understood regulators of CaMKII activation (Couchonnal and Anderson, 2008). De Koninck et al. (1998) reported that pacing frequencies above 1Hz would stimulate the autophosphorylation site of Thr^{287} site. Thus, to prevent this artificial activity, a low pacing frequency was selected. A slower pacing rate also enables a period of resting diastolic phase between each Ca^{2+} transient. This allows any

'inter-transient activity' such as Ca^{2+} sparks to also be recorded (see section 4.2.4.3). Before the first recording was initiated, a 15 min stimulation period was used to exclude any of the rod shape cells that showed any irregular contractile activity. Other selection criteria included visible striation patterns and absence of membrane blebbing or other signs of injury.

4.2.3.3. Simulation of Ischaemia and Reperfusion

When compared to quiescent cells, electriclly stimulated cells exhibit a more frequent and severe dysfunction when they are exposed to the same hypoxia protocol (Maddaford et al., 1999). This is due to the contractile activity increasing metabolic demand of the cell, which increases the demand for oxygen. Ischaemic conditions can be mimicked by manipulating the Tyrode's solution to exclude glucose and oxygen, an acidic pH and an increased K^+ concentration. A solution with a high K^+ concentration was not employed owing to the effects on the specific signalling mechanisms that CaMKII is involved with. The simulated ischaemia solution contained (in mM: NaCl 125, KCl 5, $MgCl_2$ 1.2, HEPES 10.4, $CaCl_2$ 1.25), pH 6.0. In contrast to the ischaemic solution used in Chapter 3, the removal of glucose was not replaced by the metabolic inhibitor 2-DG or sodium lactate. The latter has been shown to quickly enforce severe irreversible injury and allowing the cells to generate their own intracellular lactate is a better simulation of ischaemic conditions (Maddaford et al., 1999). With the removal of glucose a replacement was needed to maintain osmolarity. This was done by adding a higher HEPES content (Tyrode's solution, 288 mOsm vs. Ischaemic mimicking solution, 276 mOsm). The pH was lowered to 6.0 (with NaOH) to simulate the extracellular pH conditions and has been shown to induce a [pH]i of ~6.7 (Zheng et al., 2005).

Hypoxic solutions were prepared by vigorous bubbling (4 L/min) of the ischaemic mimetic solutions with nitrogen gas (oxygen free, BOCs) for a minimum of 60 min. By introducing this gaseous environment to the perfusate a passive diffusion of oxygen down its partial pressure gradient will make the solutions hypoxic. The partial pressure of oxygen (pO_2) was not measured during the experiments as a microelectrode could not be used in conjunction with the gas pod. However, using a similar preparation in another setting, the changes in pO_2 were recorded as proof of concept. By assuming that the oxygen tension of a normoxic solution is 150 mmHg (21% of normal atmospheric pressure), a ProCFE 5 µm low noise polarised carbon fibre microelectrode (Dagan corporation, Minneapolis, USA), recorded an 85-91% reduction in the oxidised electrical current (using a VA-10 npi voltammetric/amperometric amplifier; Scientifica, Sussex, U.K.). This converted the oxygen tension within the solution to a pO_2 of 14-23 mmHg. Equilibrating the solutions with nitrogen reduced their temperature to 16^{o}C, in comparison to the normal Tyrode's solution of 21^{o}C. This was corrected by placing the glass container in a pre-heated tub at 25^{o}C. Tubes running from the glass container to the water tub acted as a pressure vent to allow the nitrogen gas to escape and prevent an increase in ambient pressure. Peristaltic pumps (Watson-Marlow, Falmouth) controlled the delivery and removal of the perfusate to 5 ml/min. To prevent diffusion of atmospheric oxygen to the hypoxic solutions during superfusing, the 'Gas Pod' received a jet of Nitrogen (1 L/min) throughout the simulated ischaemia period.

4.2.3.4. Treatment Groups

Study 1: The effect of a short pacing period and CaMKII inhibitors

This study intended to monitor the cells' baseline Ca^{2+} transients under normoxic conditions. It was to determine how the Ca^{2+} transients would be affected after a short period of pacing (10-15 min), with or without the CaMKII related agents. To capture a full description of the cells' Ca^{2+} cycling ability, the images were recorded for 1 min at a rate of 49 ms per image. Two time points (figure 4.3) were selected and labelled as 'pre-treatment', for the first recordings and an 'after-treatment', following the 10-15 min of pacing and drug perfusion. To gain a greater representation of the population of cells in every culture dish, each experiment consisted of selecting and recording 3 cells within close proximity of each other. This meant that a total of 5 min was given to complete three cell recordings. The specified treatment time commenced after the last cell recording and included (see figure 4.3):

(1) Only Tyrode's solution

(2) CaMKII inhibitor, KN-93 (2 μM)

(3) Inactive analog of KN-93, KN-92 (2 μM)

(4) CaMKII inhibitory peptide, AIP (10 nM)

(5) CaMKII inhibitory peptide, AIP (40 nM)

After 10 minute treatment, the same recording process was repeated (after-treatment) but in the presence of the respective intervention. This method forfeited the cell recordings at precise time intervals of pacing and drug intervention, for a better representation of the cell population.

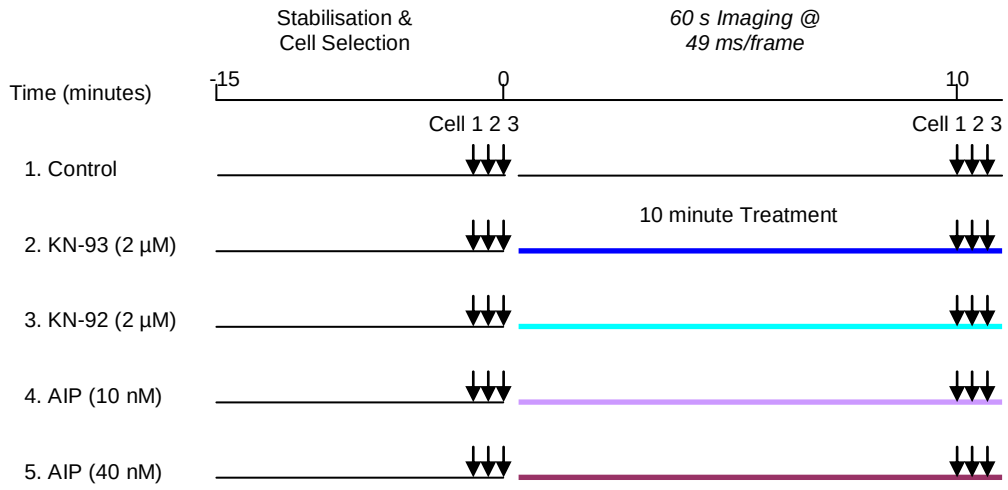

Figure 4.3: Timeline of the experimental procedures used for the groups in Study 1. *Each cell received 15 minute of electrical field stimulation prior to their 1 minute pre-treatment recording. After the last cell recording the groups had a minimum of 10 minute treatment. Then another 1 minute after-treatment recording was taken for each of the cells.*

Study 2: The effect of simulated I-R with or without the CaMKII inhibitors

One cell was selected during the 15 minutes normalisation period on the same criteria as study 1. Challenging the cells to simulated I-R required a total of 50 minute period and thus involved subjecting the cells to a longer exposure of the laser treatment. The imaging time was reduced to 10 seconds, for every minute of the experiment in order to minimise phototoxicity. The first group of experiments included a time control lasting 50 minutes under normal conditions to evaluate the degree of cellular damage. The second group were subjected to the standard I-R protocol that included; (1) 10 minutes of a stabilisation period with Tyrode's solution (5 ml/min) to characterise the Ca^{2+} oscillations under stable conditions. (2) A 30 minute 'simulated ischaemia' challenge with a hypoxic and modified Tyrode's solution. (3) 10 minutes of restoring the metabolism with normal Tyrode's solution. The treatment groups included the addition

of pharmacological agents 5 minutes prior to the ischaemic challenge, throughout the ischaemic challenge, and during the first 5 minute period of restoration. Figure 4.4 depicts the timeline for the experimental groups and included:

1) Time controls- 50 minute of imaging the cells with normoxic Tyrode's solution.
2) Ischaemic controls – 10 minute stabilisation, 30 minute of simulated ischaemia, 10 minute restoration of metabolism.
3) Ischaemia and drug perfusion - 5 minute of stabilisation, 5 minute of drug perfusion under normoxic conditions, 30 minute of simulated ischaemia including presence of drug, 5 minute reoxygenation including the drug, 5 minute of normoxic conditions without the drug.

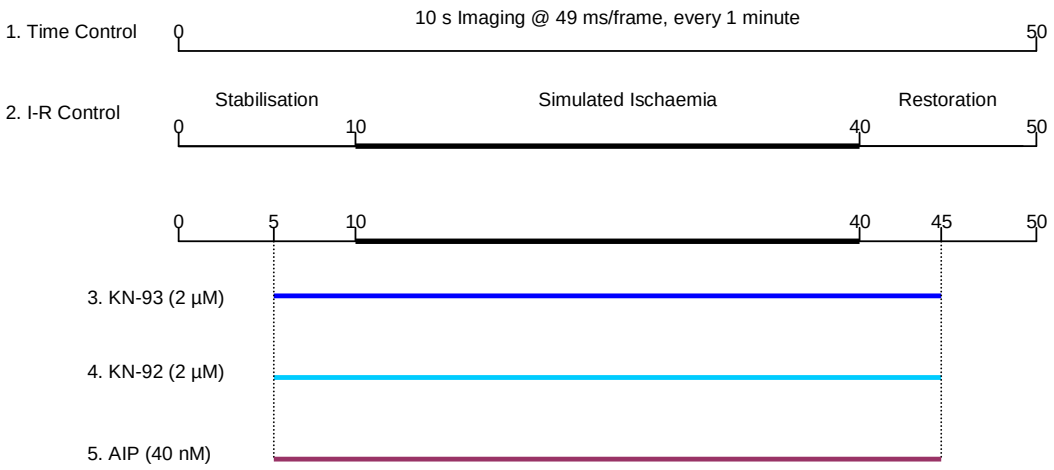

Figure 4.4: Timeline of the experimental procedures used for the groups in Study 2. *After 15 minutes of field stimulation one cell was selected for either; (1) 50 minute time control experiment, (2) simulated ischaemia and restoration of metabolism, (3) simulated ischaemia and restoration of metabolism in the presence of CaMKII inhibitors. Every minute* Ca^{2+} *transients were recorded by 10 seconds of imaging at 49 ms/frame.*

4.2.4. Analysis of the Ca^{2+} Oscillations

4.2.4.1. Converting the Images to Raw Data in an Excel Spreadsheet

The LAS AF Lite software (Leica, version 2.3.5) was used to convert the recorded images of specific regions of interest (ROI) to raw numerical data in Excel (Microsoft). Each ROI measures the mean intensity of the gray-scale values and to avoid X/Y dimensional bias, square ROI with the dimensions 7.5 x 7.5 µm were selected to capture the sufficient numbers of pixels. Avoiding any nuclear regions or the fringes subjected to cell shortening, each image was mapped with five ROI (figure 4.5A). Although one ROI would have been sufficient to measure the cell's Ca^{2+} transient, additional boxes allowed more scrutiny and the synchronicity of the intracellular events. For each ROI a 10 sec or 1 min experimental recording would produce 205 or 1225 consecutive data points respectively. This enabled a comparable timeline in the changes in fluorescence (ΔF) to represent the cell's Ca^{2+} oscillations (figure 4.5B). The cell length (um) during cell shortening and its subsequent non-stimulated resting period were also recorded at given time points by using the ruler supplied by the software. This represents the cell's contractile capability and is calculated by the change in cell length relative to the non-stimulated length (%).

4.2.4.2. Analysis of the Ca^{2+} Oscillations by SALVO Software

Synchrony – Amplitude – Length – Variability of Oscillation (SALVO) is a new multi-parametric analytical tool that has been developed by Dr. Chris George and Dr. Nicole Sylvester (Welsh Heart Institute, Cardiff University). Using Python programming, the software is designed to use algorithms to analyse a Ca^{2+} transient's morphology, amplitude and kinetics. As shown in figure 4.5C, the data entered into SALVO is

fashioned with transient ‘peaks’ and ‘valleys’ that have been automatically detected by the software.

(A)

(B)

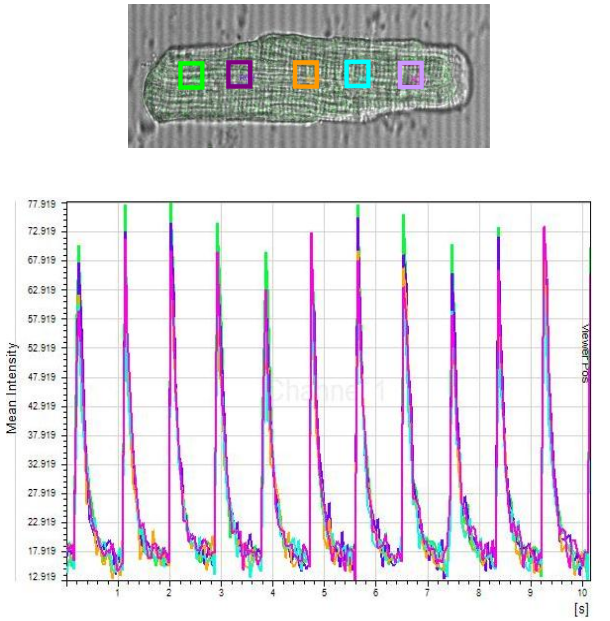

(C)

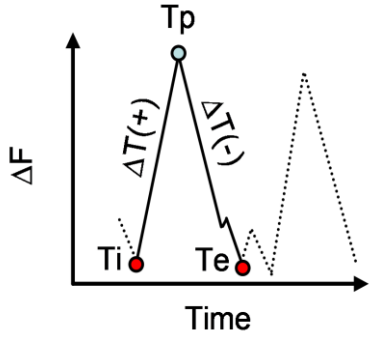

Figure 4.5: An isolated adult rat cardiac myocyte and a recording of its mean fluorescence intensity against time, which was then measured for Ca^{2+} transients’ peaks and valleys by the SALVO software. *(A) Image of a cardiac myocyte and its real time Ca^{2+} fluorescence (green pixels), that were measured by five square region of interest (coloured boxes). (B) The mean intensity of each ROI were converted to data points plotted against time to depict the oscillations of Ca^{2+}. (C) Using specific algorithms the SALVO software measures each characteristic data point to allow analysis of specific parameters. Ti, transient initiation point; Tp, transient peak; Te, transient end.*

A transient initiation point (Ti) will be detected at a 'valley', when a negative gradient (i.e. reduction in Ca^{2+}-dependent fluorescence) is followed by a positive gradient (i.e. increase in Ca^{2+}-dependent fluorescence over a designated threshold). Peak transient (Tp) will be determined when the positive rise of an oscillation returns to a negative gradient. The end of a transient (Te) is detected upon another distinguished positive change in gradient. Triangulation between these points allows the calculation and determination of a myriad of parameters, which characterise an oscillation and the Ca^{2+} handling properties of the cell. Such an auto detection method has limitations as it is prone to error when the fluorescence signal to noise ratio is low, and thus needed to be proof read and modified to limit any anomalies that might distort the data output. Modifications and corrections were needed for: (i) the start and end of a trace, to ensure they were matched to baseline values and not during a transient; (ii) any multiple Te points that were detected on a transient (due to noise) but did not signify the end of the transient was deleted; (iii) only one Tp was allowed per transient, and included the deletion of a second Tp during Ca^{2+} dysfunction such as an EAD.

4.2.4.3. SALVO Parameters

The SALVO parameters dissect the transient's recordings and their recurring phases into specific data sets that can then describe the cellular Ca^{2+} profile. This includes; a systolic phase which considers the magnitude of the Ca^{2+} oscillation and the kinetics at which this fluctuation occurs; a diastolic phase, where the cells 'inter-transient activity' would be inspected for its fluorescent intensity and non stimulated Ca^{2+} events such as Ca^{2+} sparks; and other parameters such as synchrony and the regularity of Ca^{2+} transients height that describe the organisation and robustness of each oscillation. The definitions of the SALVO parameters that are used to scrutinise each Ca^{2+} transient are

listed below. Black arrows and lines are examples of the measurements undertaken to calculate each parameter; ΔF, change in Fluorescence; Fo, baseline Fluorescence.

Morphology of Transient

Height (units = ΔF/Fo):

The average height or peak amplitude of all the transients in a trace. Reflects the SR Ca^{2+} load, the aptitude of the RYR2 and the cells Ca^{2+} buffering capability.

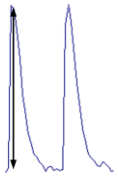

Length (sec):

The average length of a Ca^{2+} transient in a trace. Represents the duration of the released Ca^{2+} and its subsequent removal from the cytosol.

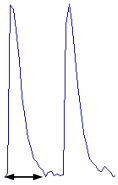

Standardised Area (arbitrary units, a.u.):

Calculates the area within a Ca^{2+} transient and standardises to the baseline value. It demonstrates the magnitude and the duration of a global Ca^{2+} event.

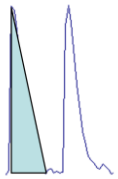

Mean Intensity (a.u.):

The mean fluorescence intensity of the ROI throughout the recording period. It accounts for the cell's basal Ca^{2+} fluorescence and the global Ca^{2+} transients' intensity.

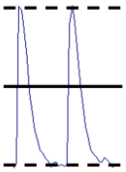

Transient Kinetics

Rate Up (ΔF/s):

The rate of the Ca^{2+} transient to reach its peak. Represents the open probability and the conductance of the releasing channels.

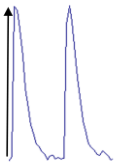

Rate Decay (ΔF/s):

The rate of the Ca^{2+} transient to reach its end point. Represents the removal of Ca^{2+} from the cytosol, both into the SR and through the sarcolemmal ion transporters.

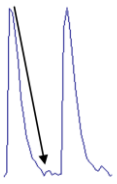

Inter-Transient Noise (ITN)

The ITN is the basal parameter that measures the activity of the point-to-point difference in the fluorescence intensity between each Ca^{2+} transient. ITN is associated with localised low-amplitude Ca^{2+} events that occur during the resting period. The ITN parameters include:

Average Magnitude; ITNAvMag (a.u.):

The average magnitude of the signal variability that occurs in-between each Ca^{2+} transient. Represent the small diastolic Ca^{2+} release events or Ca^{2+} sparks and other Ca^{2+} quanta.

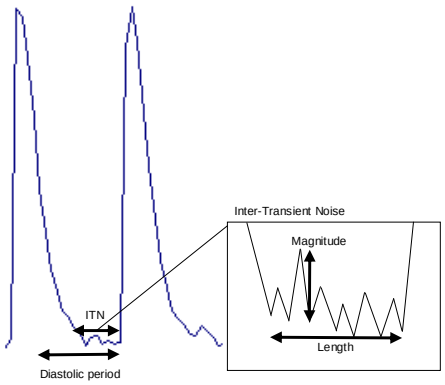

Average of the mean base value, ITNamb (a.u.):

The ITNAvMag normalised to the baseline fluorescence.

Length; ITNlength (a.u.):

The total length of time for the ITN. The length of time that ITN activity is continued within a transient.

Total; ITNTotal (a.u.):

The total sum of ITN within a recording. Includes the magnitude and the length of time that ITN continues for in a trace.

Synchrony and Conformity

Synchrony (%, where 100% is perfect synchronisation):

Calculates the juxtaposition of the transients' peak amplitude from all the ROI. Demonstrates synchronisation of Ca^{2+} release across the cell.

Height Regularity:

The cumulative standard deviation of each transient's peak amplitude. Reflects Ca^{2+} transient control. As height regularity tends to 0, the height of the transients becomes perfectly consistent.

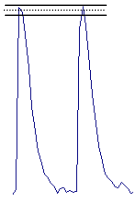

4.2.4.4. Incidences of Ca^{2+} Dysfunction and Stunning

Each recording was checked for incidences of Ca^{2+} dysfunction, such as Ca^{2+} waves, an afterdepolarisation or stunning as these occurrences are not accounted for as a specific parameter in the SALVO software. A cell generating a Ca^{2+} wave was characterised as a non-synchronised release of Ca^{2+} that spread throughout the cell moving concurrently from one ROI to another. Other Ca^{2+} dysfunction events were characterised as an uncoordinated release of Ca^{2+}. Stunning is defined within this chapter as an event where no Ca^{2+} transients were generated by the cells. Examples of these occurrences are given in figure 4.12.

4.2.5. Statistical Analysis

All numerical data are presented as mean values ± SEM, unless otherwise stated. The statistical software PRISM® version 5.00 (Graphpad) was used to analyse all statistical data, with the spreadsheet Excel (Microsoft) used for the initial handling of the SALVO data output. A one-way ANOVA followed by post hoc Newman-Keuls test) was used to compare baseline (pretreatment) values between the treatment groups for study 1 and study 2. A two way repeated measures ANOVA followed by the Bonferroni post hoc test was used to analyse the cells' baseline recordings (pre-treatment) with the post treatment recordings in study 1. A two-way ANOVA followed by Bonferroni post hoc test was used for all other statistical analysis. $P<0.05$ was considered statistically different.

4.3. Results

4.3.1. Exclusion Criteria

The cardiac myocytes were selected for experimentation based on their structural integrity and response to electric field stimulation. Further exclusion was put in place during supplementary analysis to eliminate the cells that had unobserved defects in their Ca^{2+} handling abilities. This scrutiny involved analysis during the first 10 minutes of the stabilisation period and consisted of: a) any rise in the diastolic baseline fluorescence; b) signs of arrhythmia; c) poor fluorophore measurements; d) any considerable cell movement out of the original focal plane.

Using these criteria, there was a completion of 22 experiments in study 1 and 26 experiments for study 2, of which there were four exclusions in each of the studies during further analysis. Thus, data for the normoxic study is represented by 8-15 different cells per experimental group that have come from 3-5 rat hearts. The data for the simulated ischaemia-restoration study is represented by 5-6 cells per experimental group, which have come from 4-5 rat hearts.

4.3.2. Characteristics of the Adult Rat Ventricular Myocytes

To determine whether there was homogeneity amongst the cells prior to experimentation, the first recordings for all groups in study 1 and 2 were analysed with an ANOVA test. The cells descriptive data, such as resting length, field-stimulated length and their respective baseline and mean intensity fluorescence readings are described in table 4.1. Statistical analysis determined no significant difference between the mean values of these parameters, suggesting that each group had similar baseline values prior to experimentation. The cells had a baseline fluorescence score of 22.5 ± 2.5 a.u. allowing a resting cell length of 100 ± 5.0 µm. Upon electrical stimulation the cells contracted and shortened by 5.0 ± 0.5%. The cellular response to this electrical impulse created the greatest variability between the groups as the mean intensity for each Ca^{2+} transient varied between 35.2 and 53.3 a.u. Analysis of additional parameters that describe the Ca^{2+} transient and inter-transient activity is given in figure 4.6. A statistical difference was identified between the duration of a Ca^{2+} transient in the time controls (0.67 ± 0.01 s) of study 2 and the AIP group (0.79 ± 0.02 s) of study 2 (figure 4.6). The pacing rate on the field stimulator could have caused this as it was set with a changeable dial and not a definitive setting of 1 Hz. However, the pacing rates described in table 4.1 (measured by the frequency in peak transients) were not significantly different. The most likely cause for this discrepancy is that the higher Fluo4 concentration (5 µM) originally loaded in some of the cells within the time control group, created a larger signal-to-noise fluorescence. This was automatically detected by the SALVO programme as an earlier formation of a 'valley' and thus an earlier endpoint to the Ca^{2+} transient. A non-significant trend can be detected in the transients length of time controls in study 1 (0.69 ± 0.01 s), which also included cells subjected to a higher fluorophore concentration.

Table 4.1 – Descriptive data (Mean ±SEM) of the cells first recordings prior to the normoxic (study 1) or simulated ischaemia (study 2) experiments.

Experimental Groups	n (cells/hearts)	Cell Length (µm)	Rate (Hz)	Cell Shortening (%)	Baseline (a.u)	Mean Intensity (a.u)
Study 1						
Control	14/5	98.8 ± 4.4	1.10 ± 0.02	6.4 ± 0.3	26.6 ± 3.9	53.3 ± 8.1
KN93 (2 µM)	12/4	103.2 ± 3.1	1.03 ± 0.04	7.8 ± 0.7	22.8 ± 3.2	51.4 ± 8.3
KN92 (2 µM)	8/3	105.6 ± 5.6	1.04 ± 0.04	6.7 ± 0.8	17.0 ± 1.0	35.2 ± 1.8
AIP (10 nM)	8/3	103.0 ± 5.8	1.03 ± 0.05	6.6 ± 0.6	19.3 ± 1.6	35.2 ± 2.2
AIP (40 nM)	7/3	94.1 ± 2.2	1.02 ± 0.02	4.5 ± 0.6	24.3 ± 1.6	45.3 ± 5.9
Study 2						
Time Control	6/4	102.3 ± 3.1	1.04 ± 0.05	6.1 ± 0.9	26.7 ± 2.3	47.3 ± 3.8
Ischaemic Control	6/5	96.0 ± 3.4	1.06 ± 0.03	6.8 ± 1.2	23.1 ± 3.0	45.3 ± 6.0
KN93 (2 µM)	5/5	105.6 ± 3.9	1.03 ± 0.03	6.3 ± 0.8	19.8 ± 3.5	38.0 ± 6.3
KN92 (2 µM)	5/5	100.2 ± 4.8	1.03 ± 0.04	6.2 ± 0.9	22.8 ± 2.1	44.0 ± 2.5
AIP (40 nM)	5/5	100.2 ± 6.9	1.00 ± 0.03	5.0 ± 0.5	23.6 ± 2.5	41.7 ± 4.6

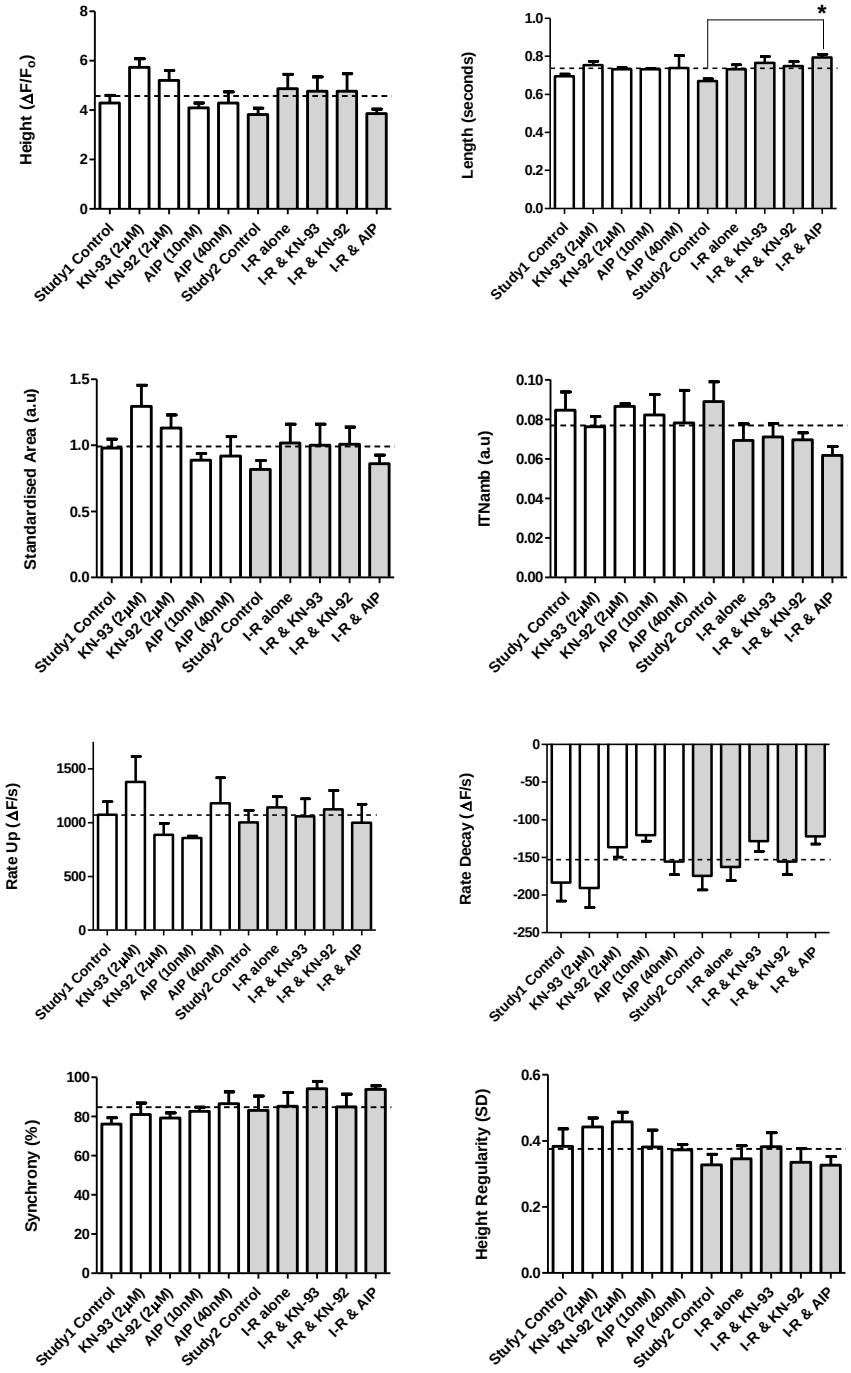

Figure 4.6: Mean data (±SEM) from all the cells first recordings of the Ca^{2+} transients' parameters identified by SALVO. *White bars indicate the one minute recordings from the normoxic experiments in study 1. Shaded bars indicate the first 10 s recordings from the simulated ischaemia-reoxygenation protocol in study 2. Dashed lines specify mean score between the groups. (*p<0.05 by One-way ANOVA). N number for each experimental group is given in table 4.1.*

The SALVO measurements in the inter-transient noise activity (ITNamb) also suggest a higher amount of signal-to-noise fluorescence was recorded within the time controls of study 2. Other parameters of the Ca^{2+} transients, such as height, standardised area and the rate of Ca^{2+} release, follow a similar outline of intensity between the groups. A quicker rate of Ca^{2+} release is in concert with the height of the Ca^{2+} transient and its standardised area. The KN-93 group in study 1 for example, has a Ca^{2+} transient with a peak height (5.7 ± 0.35 a.u.), rate up (1377 ± 238 ΔF) and standardised area (1.3 ± 0.16 a.u.) greater than any other group. Interestingly, the rates of Ca^{2+} transients decay (or Ca^{2+} removal) are ~10-20% slower than the Ca^{2+} rate up (or Ca^{2+} release); demonstrating the difference between the passive transport of Ca^{2+} through ion channels to its uptake against a concentration gradient with ion transporters such as SERCA2a. Synchronicity between the Ca^{2+} transients' recorded in five ROI, average 84.8 ± 4.6% homology. The shorter 10 second recordings in study 2 have a trend in maintaining a lower deviation in height regularity than the longer recordings.

To summarise, the first recordings in all experimental groups are not significantly different to one another, indicating that the experiments to start with are using functionally similar cells. The cells that underwent the longer period of laser scanning were not different to the shorter period indicating the shorter 10 second period was sufficient to capture enough data. Data for some of the parameters in further analysis is normalised to these first recordings in order to standardise the effects of treatments.

4.3.3. Effect of the CaMKII Inhibitors Under Normoxic Conditions

Study 1 investigated the response of the field stimulated ventricular myocytes to short term normoxic drug perfusion or an equivalent time period in the controls. Thus, each experimental group had their pre-treatment recordings (first recordings) compared to their respective post-treatment recordings. A two-way ANOVA also tested whether there was any interaction between the treatment groups and time course.

Cell size measurements

The cell length measurements during the resting diastolic phase (figure 4.7A) and during cell shortening (figure 4.7B) showed no significant interaction effects (i.e. where one of the variables is affected by the other) between the treatment groups and the two time recordings. A post-hoc test of the mean myocyte length and their subsequent shortening capability before and after the respected drug treatment, also detected no significant difference had occurred to these cell dimensions. Of note was that the cells treated with KN-93 or KN-92 had a minor reduction in their cell shortening as they were measured at 88.5 ± 6.4% and 91.0 ± 11.9% respectively, of their basal recordings. This was not demonstrated in the time-matched controls. The cells treated with AIP (40 nM) had also reduced to 87.0 ± 2.8 μm (or 92.4 ± 2.9% of its basal length) and had a non significant weaker reduction of 3.3 ± 0.3% of its cell length. When the cells were subjected to a lower concentration of AIP (10 nM), the post-treatment cell length was similar to basal measurements (101.0 ± 6.1 μm or 98.1 ± 5.9% of basal) and the contractile activity had also been maintained to 6.8 ± 1.1% of the resting cell length.

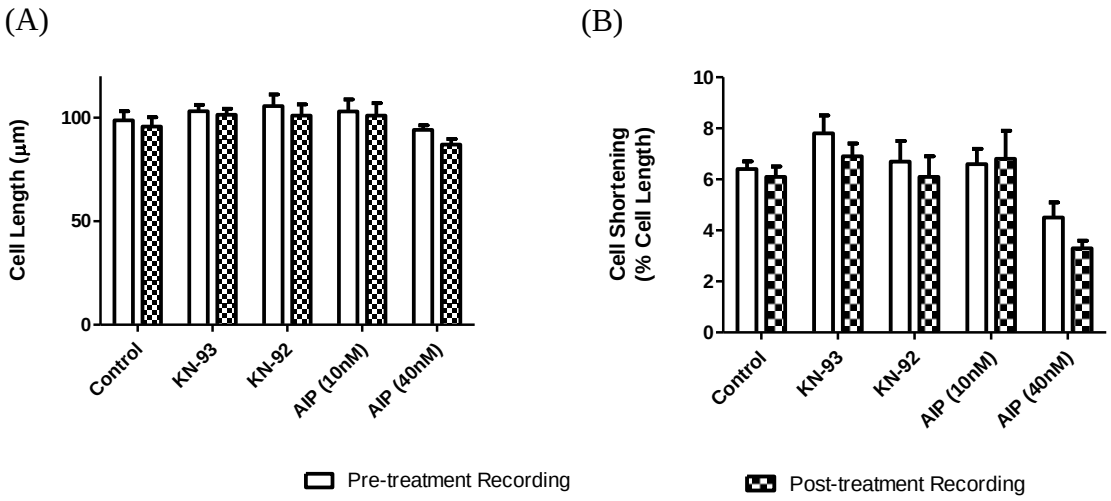

Figure 4.7: Cardiac myocytes length measurements at rest (A) and after electrical stimulation (B), before and after the treatments of study 1. *Two-way repeated measures ANOVA detected no significant interaction between the treatment groups and the time periods. Further comparisons of the treatment groups' individual mean measurements detected no significance in the cells post-treatment measurements. n = 7-14 cells from 3-5 hearts.*

Incidences of Ca^{2+} dysfunction

Most of the Ca^{2+} transients responded to the post-treatment recording without any observable changes. However, there were incidences of Ca^{2+} dysfunction. There was a noticeable increase in the frequency of contractile defects when the CaMKII inhibitor peptide AIP (40 nM) was present. After 45 s of imaging, 4 out of 7 cells developed irregular fibrillatory beating that had not recovered by the end of the 1 minute recording. This was visible on the transient recordings as a chaotic event of diastolic Ca^{2+} release (figure 4.8E) in three of the traces and an occasional aberrant beating in the other.

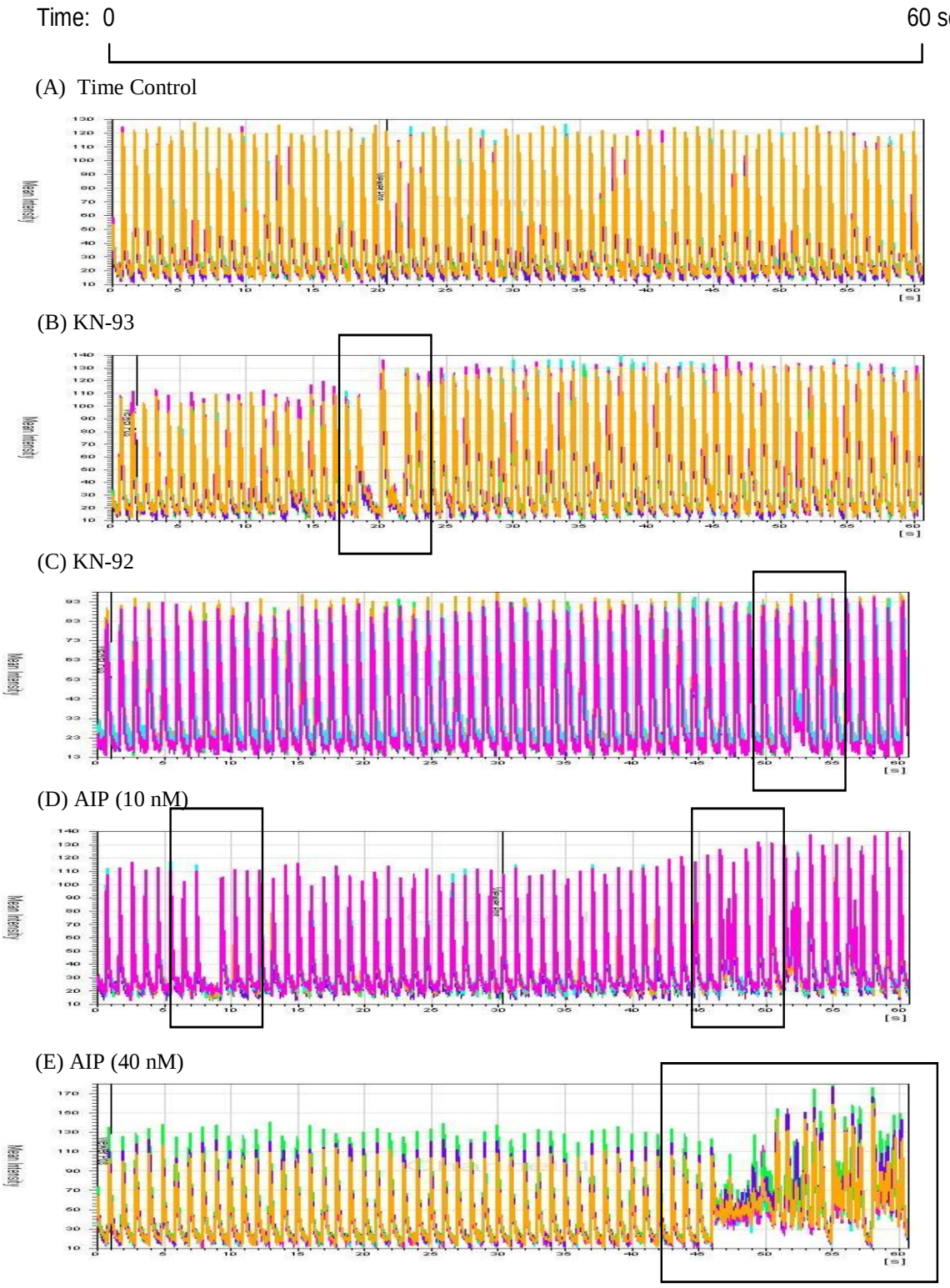

Figure 4.8: Examples of the incidences of Ca^{2+} dysfunction during the one minute post-treatment recordings. *The mean intensity of each ROI is plotted against time and overlaid on top of each other. Different colours signify each ROI although only one colour is prominent due to the synchronicity between regions. (A) Time control (B) KN-93 treatment (C) KN-92 treatment (D) AIP 10 nM treatment (E) AIP 40 nM treatment. Highlighted in the rectangular boxes are the incidents of Ca^{2+} dysfunction.*

A lower concentration of AIP at 10 nM was not as arrhythmogenic, yet there was one similar event of non recoverable diastolic Ca^{2+} release (t = 38 s) and one event of ectopic beating that responded with positive inotropy (figure 4.8D). Treatment with the organic CaMKII inhibitor KN-93 had one incidence of Ca^{2+} dysfunction (figure 4.8B). The cell had a prolonged period of removing Ca^{2+} that resulted in a missed contraction before responding with a positive inotropic effect. The 14 cell recordings in the time control and the 8 cells in the KN-92 group remained in synchrony with the field stimulator.

Parameters selected by SALVO

Two-way repeated measures ANOVA revealed that none of the Ca^{2+} handling parameters measured by the SALVO software showed any significant interaction between time and treatment. When comparing only between the two time periods (first recordings vs. post recordings) rate up, rate decay and height regularity were revealed to be significant during the post treatment recording (see 4.10). This indicates that some cells experienced alterations in their Ca^{2+} transients' morphology during treatment but there was no consistent pattern of difference between treatment groups. This is further illustrated in figure 4.9A (height of Ca^{2+} transient) where a small decrease in ΔF was observed within all post-treatment recordings (chequered bars). Although ANOVA suggested a significant effect ($F(1,18) = 8.78$, $p = 0.0083$), post hoc testing did not reveal where the statistical difference lay. When the means of other parameters were further analysed within the individual treatments by post hoc analysis, some differences were significant within groups. KN-93 and KN-92 treatment significantly limited the rate of Ca^{2+} released (rate up) into the cell by 11.2% and 19.5% respectively. The rate of Ca^{2+} removal (rate decay) was only significantly restricted (by 10.4%) after KN-93 treatment. The steady state of the Ca^{2+} transients were all affected after drug treatment,

but more so with AIP (40 nM) treatment. There was a 44% increase in the height regularity of this group that reflects the significant amount of Ca^{2+} dysfunction that occurred during the post-treatment recording. Similar distortion was observed with the lower concentration of the drug but was less consistent and not significant. Despite the amount of dysfunction that occurred after AIP treatment, there was no disruption to the synchrony of these occurrences in the ROI, indicating they were a global cellular event.

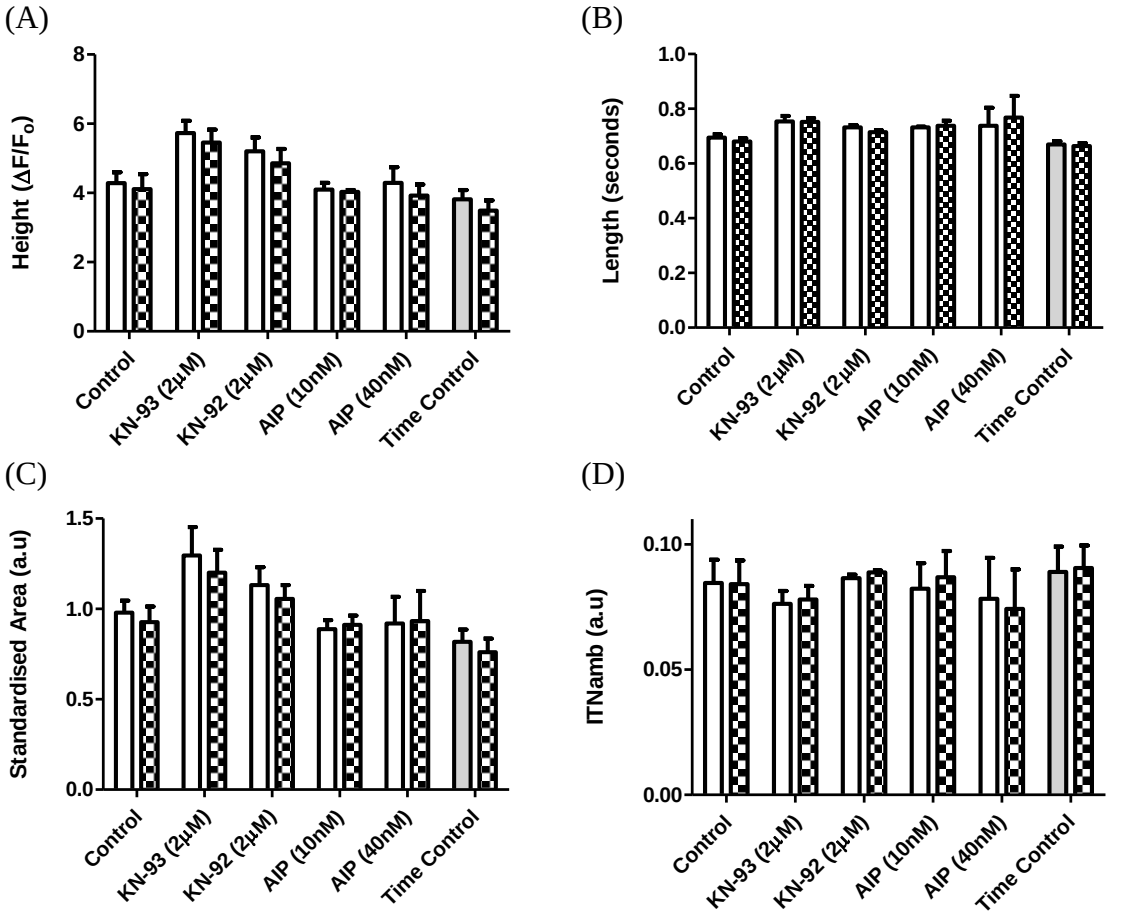

Figure 4.9: Comparison of the cells Ca^{2+} transient recordings before and after treatment in study 1. *(A) Height (B) Length (C) Standardised Area (D) Inter-transient activity. Two-way repeated measures ANOVA revealed no significant interaction between the treatment groups and time periods. Although Height (A) of the Ca^{2+} transient was lower in all treatment groups at the end of the post-treatment period, post hoc testing revealed no significant differences for any parameter. White bars are first recordings, chequered bars are post-treatment recordings, and shaded bars are time control recordings from study 2 (taken at 0 and 10 min). n = 7-14 cells from 3-5 hearts.*

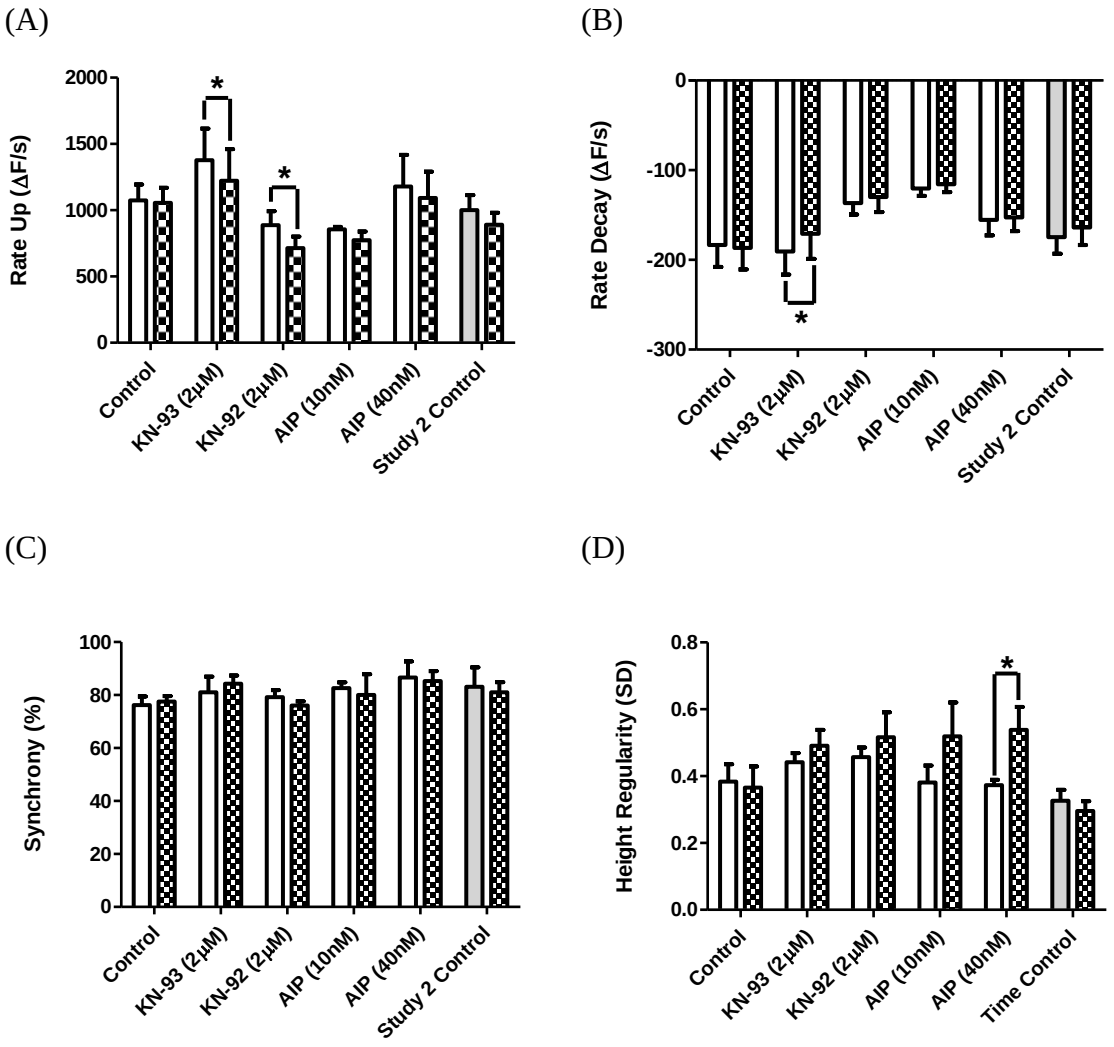

Figure 4.10: Comparison of the cells Ca^{2+} transient recordings before and after treatment in study 1. *(A) Rate Up (B) Rate Decay (C) Synchrony (D) Height Regularity. Two-way repeated measures ANOVA revealed no significant interaction between the treatment groups and time periods. There was significance when comparing the two time periods with respect to Rate Up (A) Rate Decay (B) and height regularity (D). A post test of the first recordings and the post-treatment means within each group revealed significant changes had occurred in some parameters after KN-93 (Rate Up and Rate Decay), KN-92 (Rate Up) and AIP 40 nM (Height regularity) treatment. White bars are first recordings, chequered bars are after treatment recordings, and shaded bars are time control recordings from study 2 (taken at 0 and 10 min).* ***** *$p<0.05$ when comparing within treatment groups. n = 7-14 cells from 3-5 hearts.*

4.3.4. Response to Simulated Ischaemia and Reperfusion

Study 2 investigated the myocytes' response to an environment that simulated acute ischaemia (low pH, glucose deficit and hypoxia) followed by a sudden return of normal superfusate to promote reperfusion injury. A shorter 10 s recording, for each minute of the experiment, was designed to capture sufficient information to summarise the cells' Ca^{2+} handling ability, whilst limiting their cells exposure to phototoxicity. Any rise in $[Ca^{2+}]_i$ during simulated ischaemia and loss in Ca^{2+} handling ability was used as markers of cell injury.

4.3.4.1. Changes in Cell Dimensions

All cells that underwent the simulated I-R protocol survived. At termination of the experiment they had maintained their cellular structure and had some degree of rhythmicity. In spite of this, marked changes in cell length, contraction and Ca^{2+} handling ability occurred during both the simulated ischaemia and the restoration period.

The minor reduction in cell length measured in study 1 was consistent with the first 10 min of stabilisation in study 2 (figure 4.11A). Although the osmolarity of ischaemic buffer was matched to the Tyrode's solution, this gradual decline in resting length was reversed in the new environment. A two-way ANOVA revealed no significant interaction between the time course and treatment groups. A post hoc analysis of the means determined that the swelling in the I-R controls was significant to the time controls at 30 and 40 min of experimentation (mean difference, 7.3% and 10.3% respectively). When the normoxic Tyrode's buffer was restored, the cells had returned to a length comparable to the time controls by the end of experimentation.

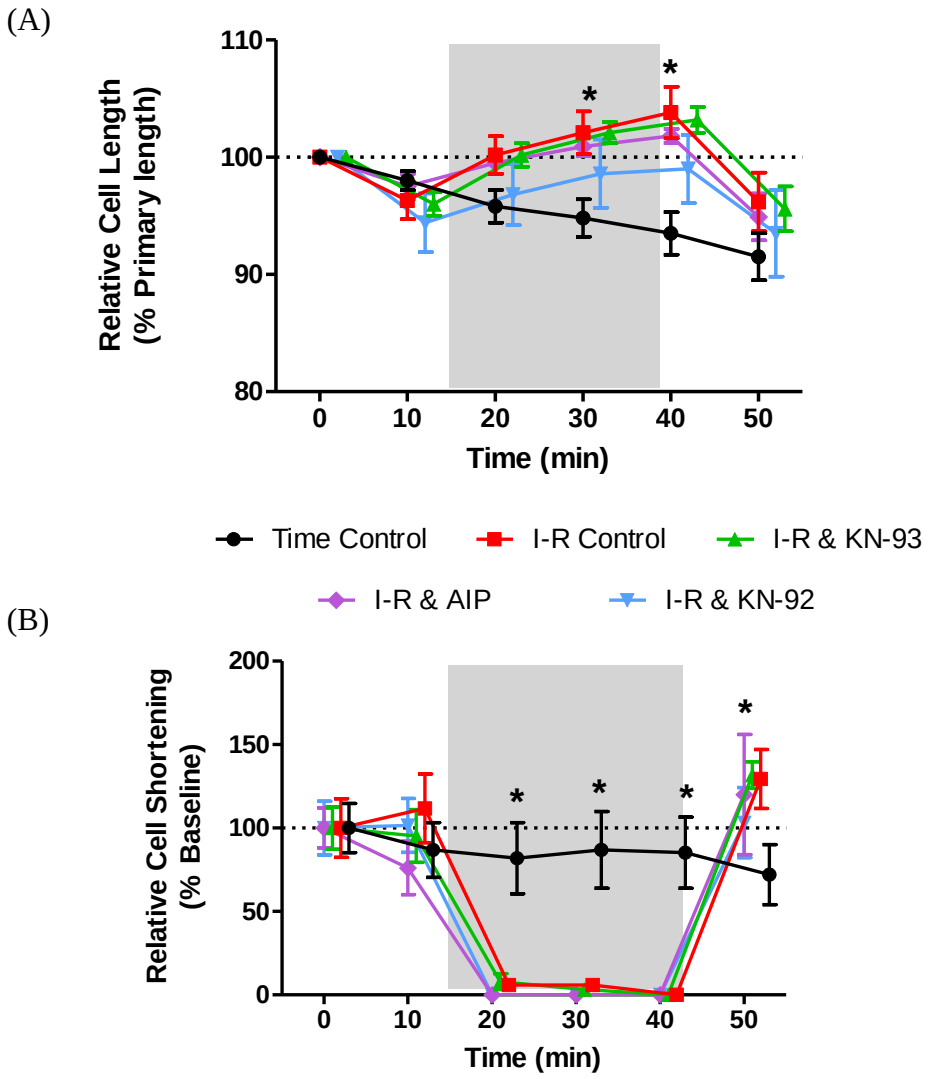

Figure 4.11: Time course of the effects of simulated I-R on resting cell length (A) and cell shortening (B) in the presence and absence of CaMKII inhibitors. *A two-way ANOVA compared each treatment groups mean scores at specific time periods of the experiment. A significant interaction was found in the variables of the cell shortening data. Whilst both cell length and cell shortening data had a significant difference when all treatment groups were compared during the two time periods. This was due to the deviation of the cell size measurements under ischaemic conditions to the time controls. None of the treatment drugs changed the course of the cells morphology or contractile activity when compared to I-R controls. The data sets (±SEM) have been separated at the x axis for clarity. Shaded area denotes period of 'ischaemia'.* ***** *$p<0.05$ when comparing time controls with the I-R controls. n = 5-6 cells from 4-5 hearts.*

None of the drug treatments significantly altered the fluctuation in cellular dimensions that was instigated by the ischaemic solution, although the cells treated with KN-92 incurred the greatest variability and were not deemed to be significant to the time controls at any time point. Dimensions of the AIP treated cells were only significant to the time-matched controls at 40 minutes of experimentation.

Cell contraction (figure 4.11B) was abolished throughout the ischaemic period in all treatment groups and an instant recovery of mechanical function emerged in conjunction with the return of normal superfusate. Two-way ANOVA deemed these changes as having a significant interaction, which was also of significance when only the treatment groups or time periods were compared. At the termination of the experiment, recovery in contractile activity within the I-R control group (129 ± 17.6%) and those treated with KN-93 (131 ± 7.9%) was at a significantly enhanced capacity to the timed controls (72 ± 18%). The KN-92 (103 ± 20.9%) and AIP (120 ± 36.0%) groups, although not statistically different to the I-R groups or time controls, were more variable (large SEM) in their return to mechanical function.

4.3.4.2. The Effects of Simulated I-R on Cellular Ca^{2+} Handling

Cellular Ca^{2+} transients were evoked during the ischaemic period even though there was an absence of contractile activity (see next section for SALVO analysis). Only when the cells were 'stunned', which occurred in some cells at later stages of ischaemia was there a lack of Ca^{2+} cycling activity. In the presence of normoxic Tyrode's solution, the combination of 50 min electrical stimulation and intermittent laser scanning admitted a minor and progressive depression of the amplitude of the Ca^{2+} transients (figure 4.12A). Each oscillation was characterised by a sharp release of Ca^{2+}, followed by a characteristic decay phase prior to the subsequent oscillation. At the onset of the simulated ischaemia, a significant transformation occurred to the Ca^{2+} handling ability (figure 4.12B). This included an abrupt decline in transient amplitude, and a moderate rise in diastolic $[Ca^{2+}]_i$ within some cells. The return of normoxic superfusate to the cells, reinstated the magnitude of each Ca^{2+} transient and returned the diastolic $[Ca^{2+}]_i$ towards the baseline levels.

As noted in figure 4.12 C-D and quantified in figure 4.13 the cells had episodes of mishandling Ca^{2+}. These were either aberrant Ca^{2+} dysfunction amongst the Ca^{2+} transients, large propagation of Ca^{2+} waves, or no Ca^{2+} activity at all ('stunning'). To summarise the figures:

- In the time controls two cells had an episode of Ca^{2+} dysfunction after 35, 40 or 45 minutes of experimentation. There were no incidents of Ca^{2+} waves or stunning.
- Subjecting cells to 30 minutes of an ischaemic mimetic solution did not incur much Ca^{2+} dysfunction in any of the treatment groups. Such contractile defects were generated with the return of the normoxic superfusate.

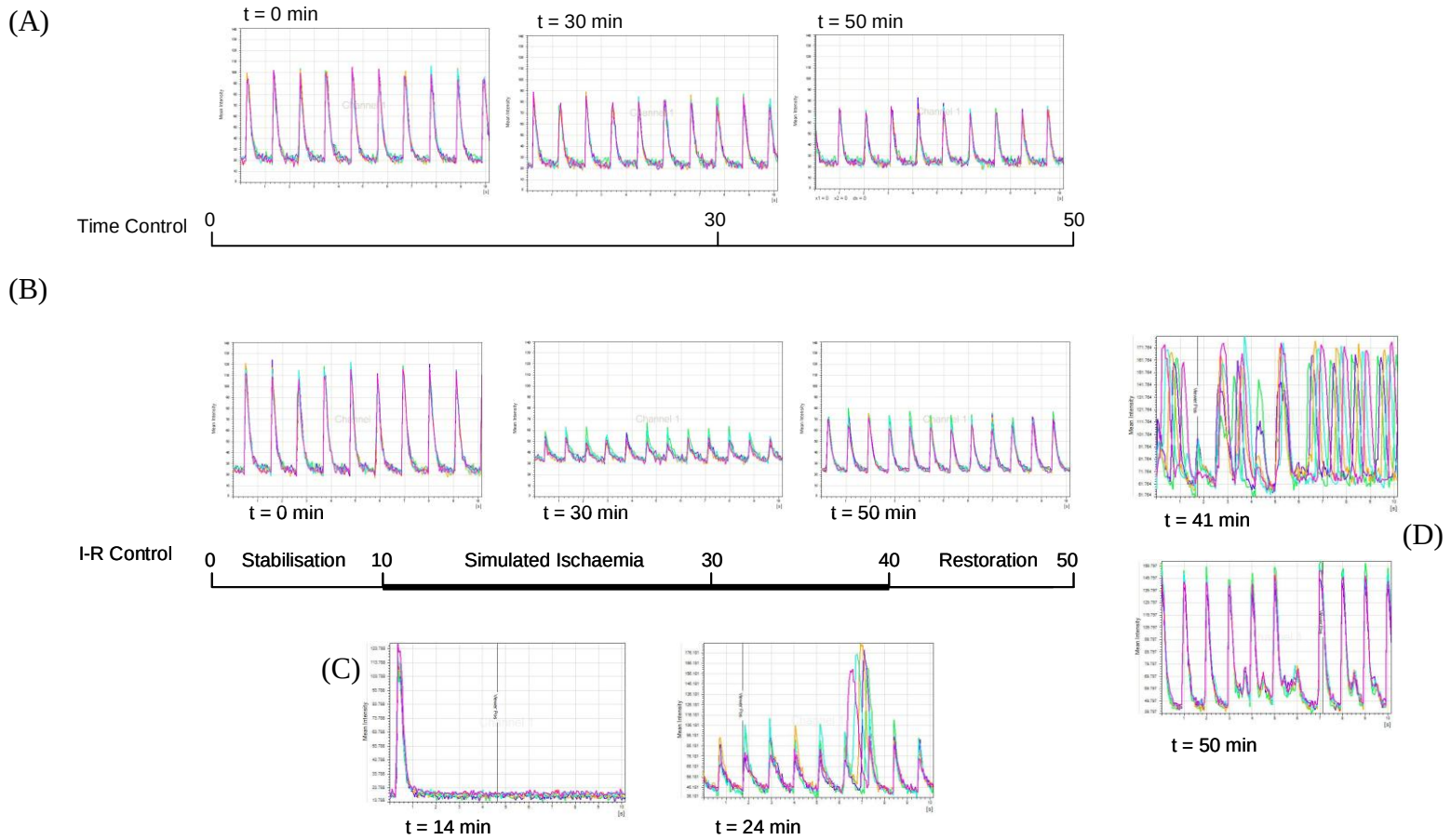

Figure 4.12: Example of Ca^{2+} transient recordings (mean intensity vs. time) at selected time points during study 2. *(A) Time control recordings at 0, 30 and 50 min of experimentation. (B) I-R control experiment at 0, 30 and 50 min of experimentation. (C) Examples of a stunned cell responding with an episode of hypercontracture (left); and a Ca^{2+} wave being generated whilst maintaining Ca^{2+} transient activity (right). (D) Ca^{2+} waves occurring during the first minute of reoxygenation (top) and arrhythmic activity at the end of the experimentation (bottom). Each recording shows the overlaid traces of five ROI from one cell. 't' denotes the time point when the recording was taken.*

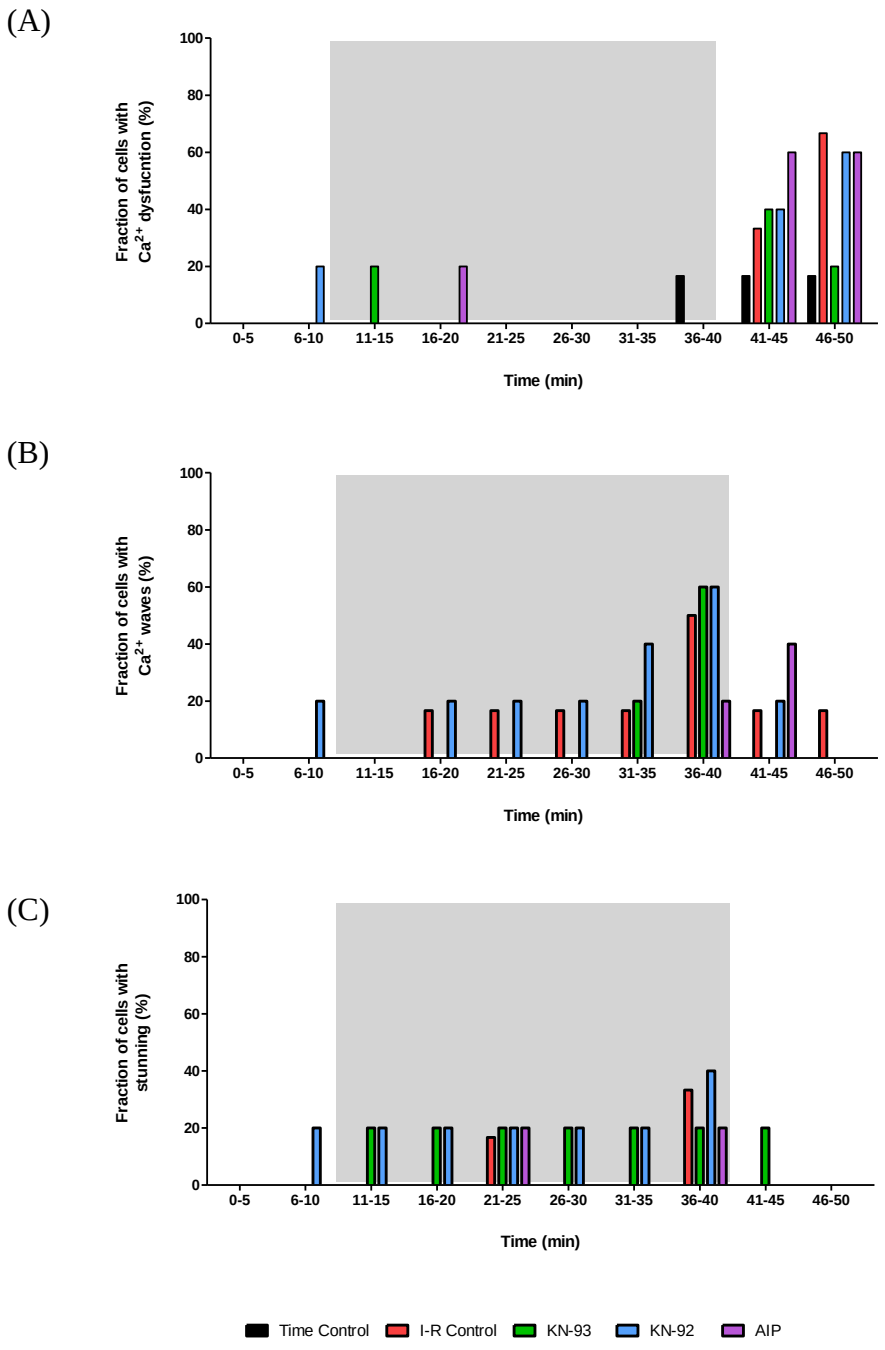

Figure 4.13: A tally of the episodes of Ca^{2+} dysfunction (A), Ca^{2+} waves (B) or stunning (C), that occurred in the cells subjected to simulated I-R at specific time periods of the experiment. *None of the drug treatments abolished any Ca^{2+} dysfunction. AIP had the lowest number of cells that generated Ca^{2+} waves during simulated ischaemia although this phenomenon also occurred during the restoration period. The KN-93 treated cells had the lowest incidences of Ca^{2+} dysfunction at end of experimentation.*

- None of the treatments protected the cells against episodes of Ca^{2+} dysfunction at the restoration stages, but the cells treated with KN-93 incurred the fewest (one cell) during the last 5 minutes of experimentation.
- The generation of Ca^{2+} waves was more apparent in the latter stages of the ischaemic period, although treatment with KN-92 and the I-R control had one cell propagating waves within 10 minutes of simulated ischaemia and continued to do so until the restoration of normoxia. Over half the cells in the I-R control, KN-93, and KN-92 treated cells generated Ca^{2+} waves at the end of the ischaemic period. AIP treatment incurred the fewest incidences during the ischaemic period, but two cells responded in this way during the restoration period.
- One cell from each of the KN treatment groups reacted instantly to the ischaemic buffer and failed to generate Ca^{2+} transients. This was combined with the generation of many Ca^{2+} waves in the KN-92 group. Stunning in other groups occurred at the end of the ischaemic period but was not a universal behaviour. During restoration one cell from the AIP treatment failed to generate any Ca^{2+} transients but this did recover.

4.3.4.3. SALVO Analysis of the Cellular Ca^{2+} Handling

As many aspects of the Ca^{2+} transients were changed in study 2, the parameters analysed by the SALVO software are further categorised into four groups that best describe features of the cells' intracellular Ca^{2+} handling ability: (1) the shape of each Ca^{2+} transient; (2) the rate at which the Ca^{2+} is cycled; (3) the inter-transient and diastolic activity; (4) the synchrony and conformity of each ROI to portray the intracellular harmony throughout the cell.

1. Transient morphology and volume of Ca^{2+} cycled in the cytosol

As shown in figure 4.14, when ischaemia is initiated the morphology of the Ca^{2+} transients changes. Error bars have been removed for clarity (and are included in the appendices), and key time points have been selected to describe some of the parameters. A two-way ANOVA detected significance within the drug treatments and in the time period. These differences between the time control and the I-R control can be summarised as follows:

- The first minute of ischaemia confines the cell's standardised area measurements to around half of its Ca^{2+} cycling proficiency (48.2 ± 9.3% of the first recording).
- This is due to the reduction in the height of each Ca^{2+} transient (figure 4.14C) as the length (figure 4.14B) remains relatively constant throughout the experiment.
- The height and standardised area of the transients continue to fall (to below 25% first recording) until normal superfusate is restored.
- Reoxygenation rapidly restores 53.0 ± 11.7% of the Ca^{2+} transients' standardised area, which by the end of experimentation reaches comparable levels to the matched time controls (time control, 66.2 ± 12.4% vs. I-R control, 69.9 ± 11.1%).

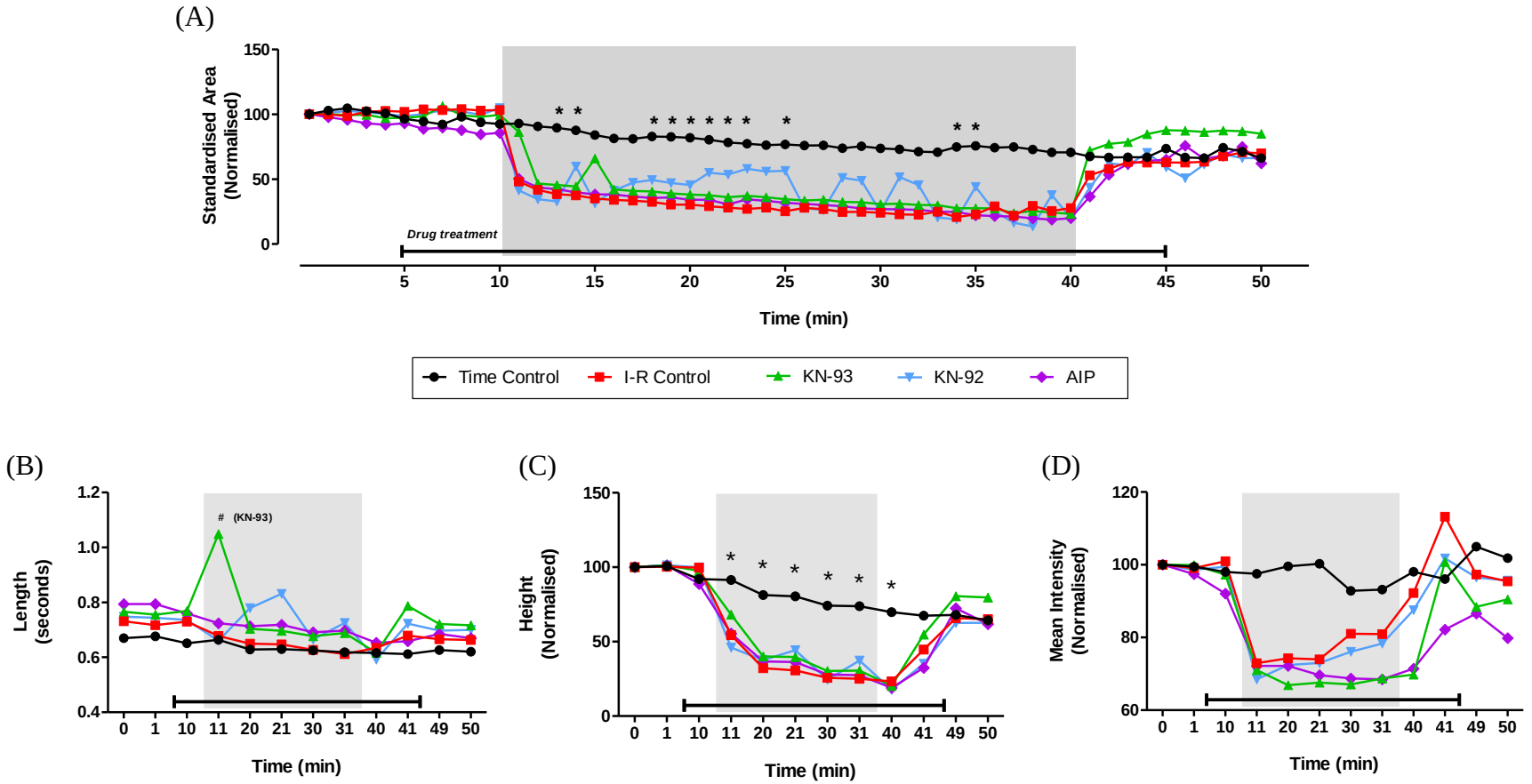

Figure 4.14: Time course of the SALVO parameters (Mean only) that describe the cells Ca^{2+} transients' morphology, when subjected to simulated I-R. *(A) Standardised Area (B) Length of Ca^{2+} transient (C) Height of Ca^{2+} transient (D) Mean intensity of $[Ca^{2+}]_i$. All data, except for length, is normalised (%) to the first recording. (B-D) are selected time points through the time course. In all parameters, two-way ANOVA detected no significant interaction between the treatment groups and time. The significance between the treatment groups is described in text. Shaded area indicates period of ischaemia. * $p<0.05$ when comparing I-R Control vs. Time Control, # $p<0.05$ I-R Control vs. the labelled drug treatment. n = 5-6 cells from 4-5 hearts.*

- The mean intensity (figure 4.14D) for each recording includes the cell's diastolic fluorescence (see next section). This gradually rises after the onset of ischaemia to reach peak intensity at the first minute of reoxygenation, before returning to comparable levels as the time control by the end of experimentation.

None of the drug treatments, when statistically compared to the I-R control, significantly altered the course of the Ca^{2+} transients' morphology, standardised area or mean intensity. However, some aspects were distorted with drug treatment and are summarised as follows:

- The incidences of Ca^{2+} waves and the large discharge of Ca^{2+} within the cytosol are reflected in the standardised area measurements by the divergence of the mean data for the treatment groups KN-93 and KN-92 during ischaemia. One cell in particular from the KN-92 group continuously propagated Ca^{2+} waves and forced the large error bars within the data set (see appendices 1).

- The measurements in the Ca^{2+} transient length also reflect these arrhythmic occurrences. One cell from each of the KN treated groups exhibited an episode of hypercontracture and a large release of Ca^{2+} (lasting 2.5 sec in KN-93 group).

- AIP prevented any of these large releases of Ca^{2+} during ischaemia.

- During reoxygenation KN-93 treated cells responded with the largest measurements in the Ca^{2+} transients' standardised area (KN-93, 85.0 ±8% vs I-R control, 69.9 ±11.1%), although this was not significant.

- The length of the Ca^{2+} transients peaked during the first minute of reoxygenation possibly signifying the occurrences of arrhythmic activity.

- An interesting observation with the KN-92 group was a dip in the standardised area measurements at 46 min when the drug was removed.

- AIP was more variable with its standardised area during the later stages of restoration due to some occurrence of Ca^{2+} dysfunction.

- The mean intensity for the KN-92 group matched the I-R control whilst KN-93 and AIP remained low until reoxygenation.

2. Rate of intracellular Ca^{2+} cycling

As the onset of ischaemia inflicted changes to the magnitude of Ca^{2+} cycled in the cytosol, it also affected the rate at which this occurred (figure 4.15). A two-way ANOVA revealed a significant interaction only in the rate of Ca^{2+} removal, but both treatment and time had significant effects on the kinetics of these Ca^{2+} transients. These changes are summarised as follows:

- In the I-R controls the first minute of ischaemia reduced the Ca^{2+} release and removal rate to 50.8 ± 5.3% and 55.3 ± 6.0% respectively of their first ability. Both rate up and rate decay were significantly reduced (compared to time controls) throughout the 30 min ischaemia reaching levels as low as 21.1 ± 3.5% and 40.7 ± 9.8% respectively. Reoxygenation immediately reversed the transients' kinetics although at 41 min the rate of release (33.9 ± 3.4%) was slower to recover than the rate of decay (66.3 ± 11.1%). At the end of experimentation the rate of Ca^{2+} release did not return to levels comparable to those of the time control (48.7 ± 5.8% vs. time controls 70.0 ± 9.7%) although this was not significant.

- None of the treatment groups significantly altered the Ca^{2+} transients' kinetics during the time course of I-R.

- The first 5 minutes of drug treatment during normoxic conditions did not replicate the significant changes seen in study 1. This could either mean that the pre-treatment time was too short, the recording time was not sufficient or that one of the analyses was anomalous.

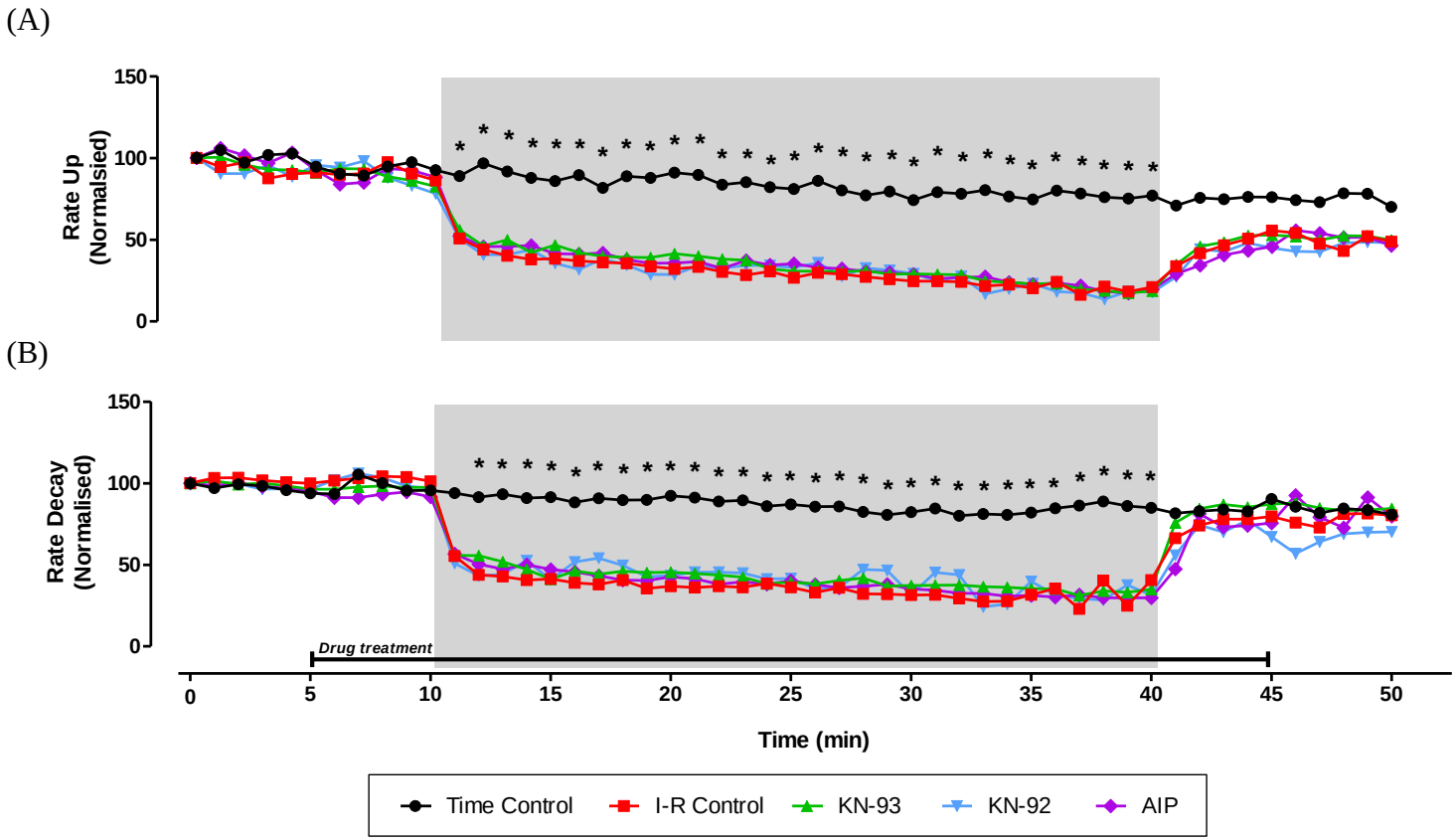

Figure 4.15: Time course of the SALVO parameters (Mean only) that describe the Ca^{2+} transients' kinetics, when subjected to simulated I-R. *(A) Rate of Ca^{2+} released into the cell. (B) Rate of Ca^{2+} removed from the cytosol. Data are normalised (%) to the first recording. A two-way ANOVA detected no significant interaction between the treatment groups and treatment time during Ca^{2+} release but it was of significance during Ca^{2+} removal. Further significance between the treatment groups is described in text. Shaded area indicates period of ischaemia. (* $p<0.05$ when comparing within the treatment groups). n = 5-6 cells from 4-5 hearts.*

- The KN-93 treated cells recovered the highest rate of removal (75.7 ± 17.0%) after the first minute of reoxygenation although this was variable. KN-93 recovery of height and standardised area for each Ca^{2+} transients corresponds to this removal rate - The dip in KN-92 standardised area at 46 min is also matched with its removal rate.

- AIP and KN-92 were slower to recover their rate of release and were significantly different to the time controls at 41 min and 42 min.

3. Inter-transient and diastolic activity

Mean baseline fluorescence and inter-transient activity were categorised and quantified into four key parameters by the SALVO software (figure 4.16): a) the average baseline intensity of the inter-transient fluorescence readings; b) the average magnitude of the Ca^{2+} released (including Ca^{2+} sparks) in-between the transients (ITN Av.Mag); c) the total duration of inter-transient activity (ITN Length); d) the total sum of the absolute difference in magnitude for the inter-transient Ca^{2+} activity (ITN Total). None of the parameters when analysed by two-way ANOVA, displayed any significant interaction between the treatment groups and time period. All treatment groups subjected to simulated I-R expressed large SEM bars (appendices 3) and as such the data exhibited little statistical difference when the treatment groups' means were compared at individual time points. This demonstrates that there was a heterogeneous response to these I-R conditions. Generally, half the cells were vulnerable to a rise in $[Ca^{2+}]_i$ and ITN activity (I-R control 3/6 cells, KN-93 3/5 cells, KN-92 3/5 cells, AIP 2/5 cells).

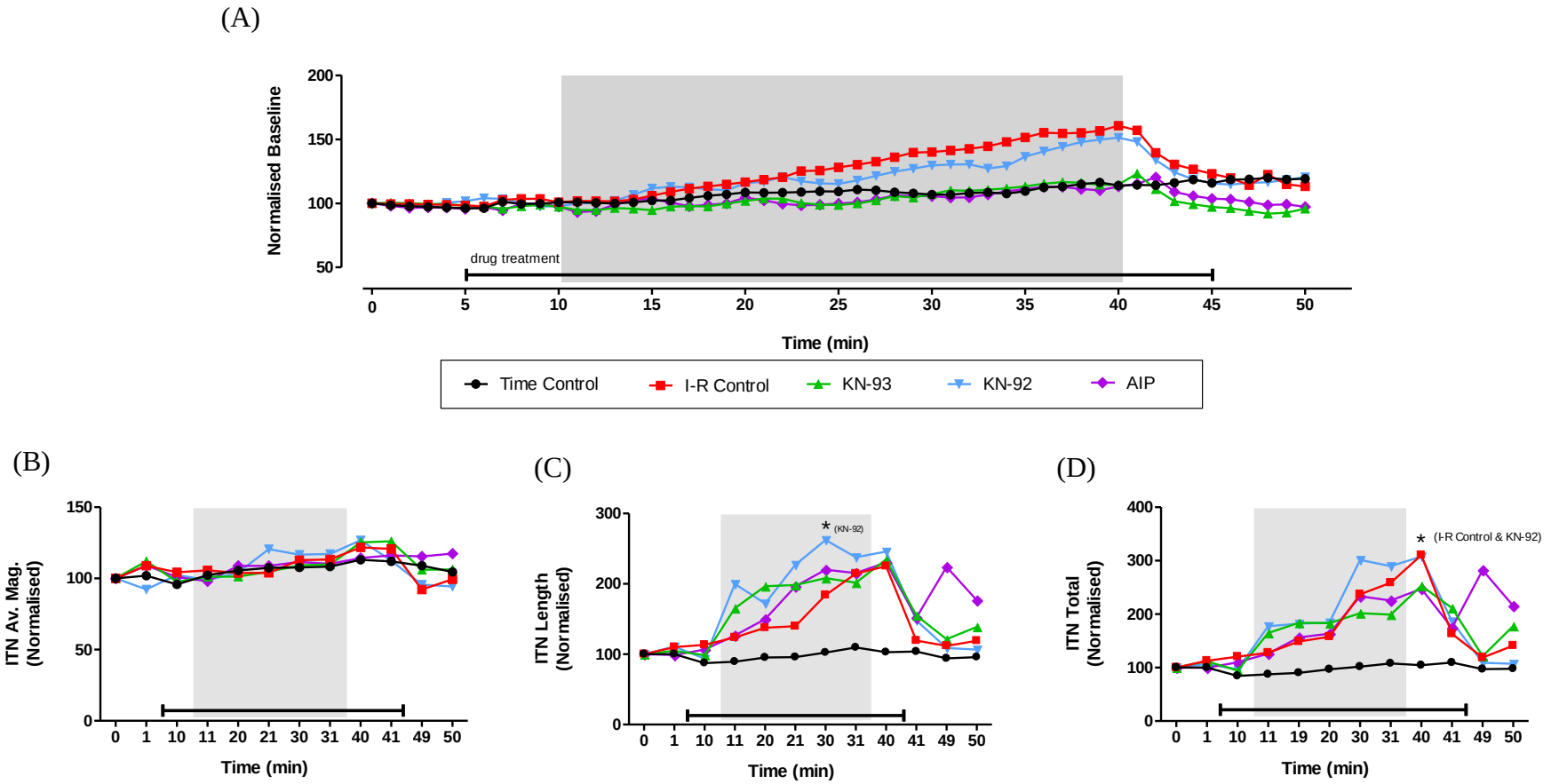

Figure 4.16: Time course of the SALVO parameters (Mean only) that describe the baseline and inter-transient activity of the cells when subjected to simulated I-R. *(A) Baseline fluorescence (B) Average magnitude of ITN (C) Length of ITN (D) Total amount of ITN. Data are normalised (%) to the first recording. None of the parameters had any significant interaction between the treatments and time periods. Baseline, ITN Length and ITN Total had significant effects within the treatment and time periods, but average magnitude of ITN did not. Further comparison between the treatment groups means at specific time periods are described in text. Shaded area indicates period of ischaemia. (***** $p<0.05$ when comparing within the time controls). n = 5-6 cells from 4-5 hearts.*

The data in figure 4.16 can be summarised as follows:

(a) Baseline Intensity

- The rise in baseline $[Ca^{2+}]_i$ was more prominent in the I-R controls and the KN-92 treated cells, peaking at 160.6 ± 22.8% and 151.4 ± 25.8% respectively at 40 min. KN-93 and AIP groups showed a moderate rise in $[Ca^{2+}]_i$ (114.6 ± 30.3% and 113.1 ± 11.5% respectively), with their mean values matching the time controls at this time point (114.0 ± 13.3%). Reoxygenation returned the $[Ca^{2+}]_i$ towards the baseline readings, with some cells treated with the CaMKII inhibitors displaying intensities below the time control group and their baseline readings. This removal rate corresponds with the Ca^{2+} transients' kinetics as there is an imbalance between the rate of Ca^{2+} removal and its release.

(b) ITN Average Magnitude

- The mean data for the ITN Av.Mag suggests that there was no significant difference between the magnitudes of the localised Ca^{2+} events (i.e. Ca^{2+} sparks and other Ca^{2+} quanta) generated with the time controls and the I-R protocol. At 40 min, a small consistent rise under normoxic conditions (113.1 ± 2.7%) was comparable to the ischaemic groups; I-R controls (121.8 ± 15.0), KN-93 (125.3 ± 17.3%), KN-92 (126.8 ± 18.7%), AIP (114.4 ± 9.4%).

- At the end of reoxygenation the magnitude of the Ca^{2+} sparks had gradually reduced towards baseline values, although the AIP group maintained some of this activity.

(c) ITN Length

- The total length of time for the ITN activity increased and peaked in all I-R groups at 40 minutes of experimentation; I-R controls (225.0 ± 57.0%), KN-93 (234.7 ± 61.9%),

KN-92 (245.9 ± 51.4%), AIP (230.4 ± 66.9%). The large variability came with the cells that were stunned or generated little Ca^{2+} transients. When compared with the time control, only KN-92 was deemed significant at 30 minutes of experimentation.

- The return of Ca^{2+} transients (at 41 min) reduced the time available for ITN activity and thus the length of ITN. The Ca^{2+} dysfunction generated within the AIP group during the last minutes of experimentation forced a high measurement in ITN length.

(d) ITN Total

- The total amount of ITN was predominantly shaped by the length of time for each ITN activity. Only the cells treated with KN-92 and I-R control had a total ITN activity significantly different to the time controls (time control, 104.4 ± 7.0% vs. KN-92, 307.8 ± 102.0% and I-R control, 310.3 ± 105.8%). The KN-93 (253.3 ± 48.0%) and AIP (247.6 ± 78.9%) contained large amount of variability and were not significantly different to the I-R controls. Return of normoxic perfusate and Ca^{2+} transients reduced the total amount of ITN, except for the AIP group.

4. Synchrony and conformity within the cells

The five ROI selected within each cell were analysed for the intracellular synchrony of Ca^{2+} release. This harmony is critical for E-C coupling. There was no significant interaction between the measured variables (two-way ANOVA). However, there was significance amongst the treatment groups and between the time periods. There was a gradual deterioration between the ROI synchronicity as time progresses through normoxic and ischaemic conditions (figure 4.17A). The initial ischaemic decline in Ca^{2+} transients shape and kinetics did not disrupt the cells global release of Ca^{2+}. Nevertheless, during the latter stages of ischaemia (last 5 minutes) and at early stages of reoxygenation there was a modest disruption when compared to the time controls. Although all groups deviated from the time controls during the 40^{th} minute only the I-R controls were significantly different (time control, 75.1 ±5.8% vs. I-R control, 42.3 ±14.1%). A slow recovery in each ROI harmony was restored in all treatment groups by the end of experimentation.

The deviation between each of the Ca^{2+} transients' height was used as a measurement of regularity and steady state. It would also signify whether there was any mechanical alternans as any score away from 0 would indicate less regularity. A two-way ANOVA did not detect any interaction between these variables, but there was significance amongst the treatment groups and between the various time periods. The Ca^{2+} transients did not lose their steady state during ischaemia, but the smaller height of each transient did moderately reduce the overall deviation. The only significant deviation (compared to all groups) was with KN-93 treated cells. The first was during the early ischaemic period, triggered by a sole episode of hypercontracture, and the other was during the first minute of reoxygenation. The restoration period manifested the highest degree of mechanical alternans with all treatment groups except for KN-92

generating more than the time controls. At the end of experimentation KN-92 maintained this lower degree of deviation although this was not deemed significant to the other treatment groups.

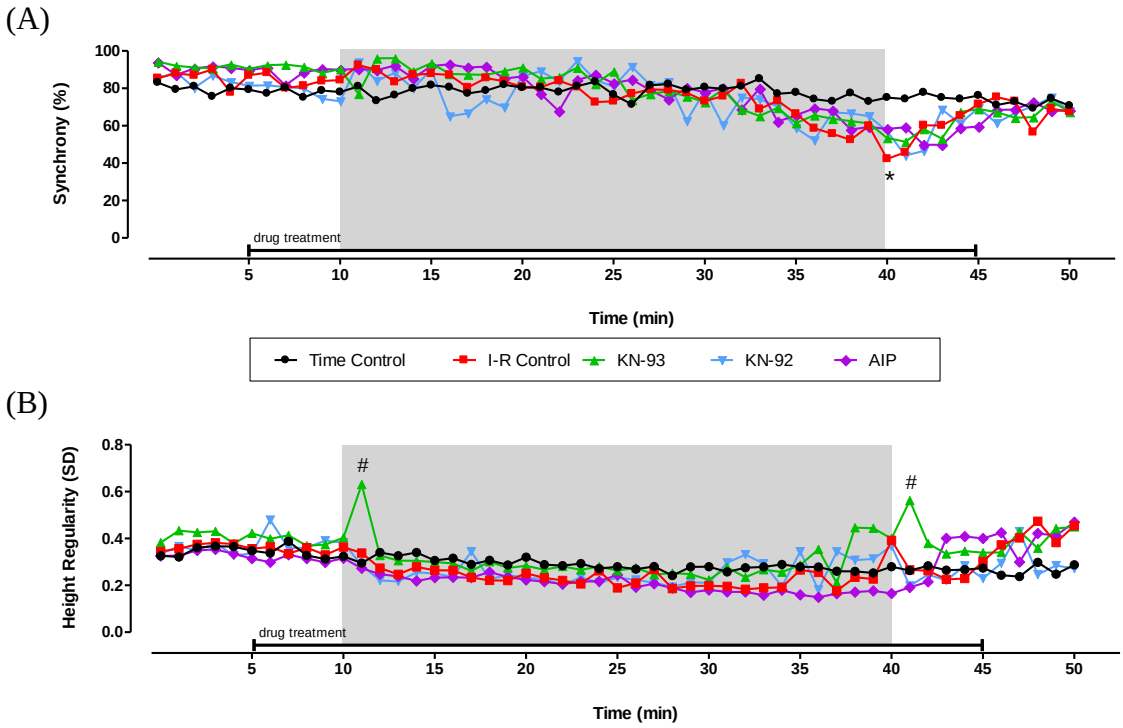

Figure 4.17: Time course of the SALVO parameters that describe the synchronicity amongst the cells ROI and regularity of the Ca^{2+} transients. *(A) Synchrony of ROI (B) Regularity of Ca^{2+} transient height. A two-way ANOVA determined none of the parameters had any significant interaction between the treatments and time periods. Both synchrony and height regularity had significant effects within the treatment and time periods. Further comparison between the treatment groups means at specific time periods are described in text. Shaded area indicates period of ischaemia. (***** $p<0.05$ when comparing the time controls with I-R controls, # $p<0.05$ when comparing KN-93 treated cells with all other treatment groups). n = 5-6 cells from 4-5 hearts.*

4.4. Discussion

The studies' major findings are summarised as follows:

- Under normoxic conditions the CaMKII inhibitor KN-93 limited the rates of Ca^{2+} release and removal from adult rat ventricular cells when field stimulated at 1 Hz. The rate of Ca^{2+} release might be due to the non-specific activity of the KN compounds as KN-92 also demonstrated these effects. On these grounds, the sub-hypothesis that *the non-specific activity of the KN compounds will have a comparable limitation on the cells Ca^{2+} handling ability* can be accepted.

- It was also hypothesised that *the CaMKII inhibitor KN-93 and the peptide inhibitor AIP will have comparable effects on the cells Ca^{2+} handling ability*. This was not verified during the short exposure times of study 1, or parameters selected by SALVO measured in study 2. Only by limiting the rise in $[Ca^{2+}]_i$ during ischaemia, were there any comparable effects, but these were not significantly different to the controls. On these grounds, this sub-hypothesis can be rejected.

- Simulated I-R had a substantive effect on the cells' Ca^{2+} handling, contractile performance and cell dimensions. This *adverse effect on intracellular Ca^{2+} homeostasis* was hypothesised. The parameters measured by the SALVO software disclosed no significant changes between the cells treated with the CaMKII inhibitors and the controls. This indicates that CaMKII had no significant activity on these functional characteristics.

- It was hypothesised that simulated ischaemia would *lead to a rise in the diastolic Ca^{2+} concentration*. Despite the marked intracellular changes in Ca^{2+} handling, only 50% of the I-R controls had a substantial rise in $[Ca^{2+}]_i$. There was only a minor rise in $[Ca^{2+}]_i$ in the presence of the CaMKII inhibitors KN-93 and AIP, but with the inconsistent rise

in the control group and the KN-92 treated cells this meant that there were no significant difference between the treatment groups.

- The presence of the CaMKII inhibitors did not abolish the occurrence of Ca^{2+} dysfunction during simulated I-R. The inhibitory peptide AIP had the lowest occurrence of Ca^{2+} waves during simulated ischaemia, whereas during the last 5 minutes of experimentation KN-93 treated cells had the lowest occurrence of Ca^{2+} dysfunction.

4.4.1. The Similar Effects of the KN Compounds on Ca^{2+} Handling

Under normoxic conditions, study 1 revealed that the cells treated with KN-93 or KN-92 had a significant reduction in their ability to release Ca^{2+} (figure 4.10). Gao et al. (2006) demonstrated that both KN-93 and KN-92 can limit the $I_{Ca.L}$ without affecting CaMKII activity. As the $[Ca^{2+}]$ outside the SR (provided by the $I_{Ca.L,}$) is one element that can influence the Po of the RYR2 (Fabiato, 1983), the non-specific activity of the KN compounds could be suggested to have been demonstrated in this study. However, the rate of Ca^{2+} release from the RYR2 is also proportional to the total rise in $[Ca^{2+}]_i$ (Eisner et al., 2009). There was no significant reduction in the height of the Ca^{2+} transient after any of the KN treatments. Comparative measurements with known inhibitors of LTCC and K^+ channels would further disclose if these occurrences are due to the drug treatments or artefacts of the experimental design and analysis.

The significant reduction in the Ca^{2+} transients rate of decay after KN-93 treatment (figure 4.10) was not matched by any of the other groups in study 1 and in particular, in the presence of KN-92. This replicates the findings of others but in particular those of DeSantiago et al. (2002). Using rat ventricular myocytes that were stimulated at 1 Hz (23^oC), they demonstrated that 10 minutes treatment of KN-93 (1

μM) could significantly limit the rate at which the Ca^{2+} transients decline. They also used the CaMKII inhibitory peptide AIP (20 μM) to replicate this limited uptake of Ca^{2+} and other measurements, such as the Ca^{2+} transient height to signify a CaMKII specific role. The much lower concentration of AIP used in this study did not replicate these findings, but another component to their experiments was the cessation of field stimulation during drug treatment in order to de-phosphorylate CaMKII. To match physiological conditions and those of chapter 2, this was not replicated in these studies.

The rate of contraction used in this study is arguably not physiologically relevant for the rat cardiac myocyte, but it was intended to prevent the artificial stimulation of CaMKII and allow the measurements in ITN activity. Any rates above 1 Hz would activate Ca^{2+} transients that lead to autophosphorylation CaMKII (De-Koninck and Schulman, 1999). This limitation was avoided to ensure that the I-R experiments were initially void of autonomic CaMKII activity. This could also explain why only minor reductions were seen in study 1 in the presence of the CaMKII inhibitors. Studies by Vila-Petroff et al. (2007) have also demonstrated no change in Ca^{2+} transient activity when the cells were stimulated at 0.5 Hz in the presence of KN-93 (1 μM) and AIP (1 μM). At this rate of field stimulation this was also the case with DeSantiago et al. (2002), as 1 Hz was the minimum rate at which any detectable changes could be seen in Ca^{2+} transient activity when CaMKII was inhibited. As no other aspects of the Ca^{2+} transients and inter-transient activity were significantly altered, future studies would benefit from a higher pacing frequency.

4.4.2. The Arrhythmic Activity of the CaMKII Inhibitory Peptide

The 40 nM concentration used for AIP was determined by its inhibitory potency (IC_{50} = 4 nM). At this concentration, AIP under normoxic conditions of study 1, promoted an uncontrolled arrhythmic activity in 4/7 cells. The SALVO parameters signified these occurrences within the regularity of the height of the Ca^{2+} transient (figure 4.10). The chaotic release of Ca^{2+} demonstrated in figure 4.8 was absent from all other treatment groups during study 1, with only one incidence generated at the lower AIP concentration of 10 nM. The cells lost their Ca^{2+} handling ability after 45 seconds of imaging and the observations of the surrounding cells revealed that this was a specific event to the cells being recorded. The viability of cells can be compromised with fluorescence imaging. Knight et al. (2003) exposed isolated chondrocytes that had been loaded with Fluo-4 (5 μM) to 1 hour of confocal imaging (0.8 sec of exposure time every 10 sec). The reduced viability of the cells 24 hours later was reported to be due to the generation of ROS when the light interacted with the fluorophore. Why only the AIP treatment stimulated such activity in study 1 is unknown, but the combination of the peptide, field stimulation and confocal imaging forced the cells to react in a way that has not been previously reported. When the imaging was limited to shorter durations in study 2 (10 seconds every 1 minute), although the total duration stimulated by the confocal laser was greater, it incurred little Ca^{2+} transient abnormalities in the time control cells until later stages of the experiment. The short 10 second period was also sufficient to capture enough data about the Ca^{2+} handling properties of the cells (figure 4.6) and would thus also be a suitable approach for future studies under normoxic conditions.

4.4.3. Simulation of I-R conditions

The main focus of the study was to analyse the Ca^{2+} handling ability of field stimulated cardiac myocytes during simulated I-R in the presence of two different CaMKII inhibitors. The analysis of the Ca^{2+} transients with a multi-parametric tool was to thoroughly define the involvement of CaMKII under such cellular conditions. To simulate ischaemic conditions there were three key changes to the extracellular environment. Removal of glucose and lowering the O_2 content of the perfusate was designed to challenge the metabolic activity of the cells, whilst acidification was intended to rapidly mimick anaerobic conditions. The cells reacted instantly to the new environment with the loss of physical contraction (figure 4.11B), a 50% reduction in the Ca^{2+} transients' morphology (figure 4.14) and an increase in length indicative of swelling (figure 4.11A). Generation of Ca^{2+} waves, a rise in $[Ca^{2+}]_i$ and Ca^{2+} dysfunction were all indicative of cellular stress. With complete cessation in contractile activity, it can be suggested that the ischaemic factors had managed to dissociate E-C coupling. As reported by Maddaford et al. (1999), with changes in cell morphology, Ca^{2+} transient morphology and cessation of contraction, it can be assumed that the cells were enduring an ischaemic environment.

Such actions can be explained by the known inhibitory effect of acute hypoxia on the LTCC (Hool, 2000) and the fact that acidosis can decrease the sensitivity of the contractile apparatus to Ca^{2+} (Crampin et al., 2006). The latter constituent combined with a restricted $I_{Ca.L.}$ has also been described to lower the systolic Ca^{2+} transient, restrict the opening probability of the RYR2 and thus the rate at which Ca^{2+} was released globally in the cell. When acidosis alone inhibits the opening of the RYR2 it allows further loading of Ca^{2+} into the SR that is subsequently released (Choi et al., 2000). But under the conditions used in study 2, there was no noticeable recovery in the

peak Ca^{2+} transients during the ischaemic conditions. This suggests that either the loading of Ca^{2+} into the SR was not sufficient to install a recovery in peak systolic Ca^{2+} or, the mechanisms that induce CICR were continuously subdued. Only the generation of Ca^{2+} waves at later stages were indicative of an overloaded SR. The $[pH]_i$ was not measured during the study but the onset of cell swelling and the limited contractile activity would suggest that intracellular acidosis was attained.

It was hypothesised that the cells not exposed to the CaMKII inhibitors would significantly increase their $[Ca^{2+}]_i$. Using only hypoxic Tyrode's solution, Budas et al. (2004) recorded cell death with Ca^{2+} overload in paced (0.5 Hz) guinea-pig ventricular cells, within 16.8 ± 2.8 minutes of experimentation. Subjecting cardiac myocytes isolated from the rat heart to a hypoxic and ischaemic mimicking solution (high K^+, low pH and high sodium-lactate), can also compel the cells to Ca^{2+} overload (defined as 135% of baseline values) within a 20 minutes time frame (Chen et al., 2005). The 30 minutes ischaemic period was chosen for study 2 to emulate the index of ischaemia in chapter 2 and to limit the exposure time of the cells to the confocal imaging. Why there was discrepancy within these data sets is unidentified. All experimental conditions were designed to be controllable (i.e. constituents of the solution, the perfusion flow rate, nitrogen flow rate and temperature) and thus reproducible. Acidosis alone is known to stimulate a rise in $[Ca^{2+}]_i$ (Orchard et al., 1987). This was a controllable element of the solutions and thus had to include another condition. The only unknown extracellular component was the pO_2 of the ischaemic solution. Measuring the pO_2 during the ischaemic period would have eliminated the possibility of it being a variable condition, but this was not technically feasible. Several steps are taken to prepare the isolated cardiac myocytes for Ca^{2+} imaging. Dissociating cells from the tissue, re-introducing Ca^{2+}, their short term culture and loading with the fluorophore all contain

agents that can be predicted to enhance or deteriorate the integrity of the cells (taurine, DMSO, penicillin etc.). But as all cells underwent similar conditions, this should not have been a significant factor. It is known that at a cellular level there is more of a non-deterministic nature (stochasticity) to the cells, where as tissue and organ preparations have more of a deterministic nature (Perc et al., 2008). One possibility is that individual cells could have reacted differently to the combination of simulated ischaemia and the artefacts of the confocal laser such as the generation of ROS. Whilst some cells could have an adverse effect, others might even have been preconditioned by the consistent short laser treatments.

4.4.4. Involvement of CaMKII During Simulated Ischaemia

At the end of simulated ischaemia there is a non-significant separation in the mean values of the baseline fluorescence between some of the treatment groups (figure 4.16). The time controls (113.9 ± 13.3%) and the treatment by both CaMKII inhibitors (KN-93, 114.6 ± 30.3% & AIP, 113.1 ± 11.5%) are lower than the I-R control (160.6 ± 22.8%) and the KN-92 treated cells (151.4 ± 25.8%). Despite the variability it could be suggested that CaMKII inhibition does confine the rise in $[Ca^{2+}]_i$ when cells are subjected to electrical stimulation and an ischaemic mimicking solution. However, there is nothing in the Ca^{2+} transients' morphology, kinetics or their conformity to suggest that CaMKII inhibition had improved these aspects of the cells' Ca^{2+} handling ability.

Pedersen et al. (2009) measured a greater reduction in peak Ca^{2+} transients with KN-93 when cells were stimulated at 0.5 Hz and subjected to 5 minutes of acidification. It was also suggested that further loading of the Ca^{2+} into the SR and the incidence of Ca^{2+} waves were CaMKII dependent. But the Ca^{2+} waves that were generated in study

2 were frequent after 25 minutes of simulated ischaemia and were not prevented with KN-93 treatment. Only the inhibitory peptide AIP showed signs of reducing such uncoordinated release of Ca^{2+}. Under ischaemic conditions the accumulation of Ca^{2+} in the SR would have also been determined by other factors that prevent the release of Ca^{2+} from the RYR2 (Yang and Steele, 2001; Valverde et al., 2010). These conditions would have been suited to propagate further Ca^{2+} waves. However, as these occurrences were subdued until the latter stages it can only be suggested that the same conditions would have limited the activity of CaMKII. Whether this was associated with the continued suppression of the Ca^{2+} transients or the change in metabolic conditions is unknown, but further studies looking at each individual component are needed. As the CaMKII inhibitors did not prevent the increase in cell size that occurred in the presence of the ischaemic solutions, it can be suggested that the prevention of intracellular acidosis and a rising $[Na^+]_i$ that would have triggered oncotic swelling, are not within the capacity of the CaMKII inhibitors. Whether or not the reverse mode of the NCX was triggered is unknown, and would have been dependent on other factors including the extent of the diminishing ATP pool in maintaining a functional Na^+/K^+-ATPase. It could be that these variables would have been a better predictor of cellular stress than the rising $[Ca^{2+}]_i$ and possibly have further explained the discrepancies that occurred between the treatment groups.

4.4.5. Involvement of CaMKII During Restoration of Metabolism

The return of the normoxic Tyrode's solution reversed the increase in cell length and restored many components of the E-C coupling that were comparable with the time controls. These included: contractile activity; the height of Ca^{2+} transients; the rate of Ca^{2+} removal; their synchronisation amongst ROI and the lowering of $[Ca^{2+}]_i$ to pre-

ischaemic values. There were signs of cell injury in the parameters that did not match the time controls (i.e. rate of Ca^{2+} release, height regularity) and the occurrence of Ca^{2+} dysfunction. There were no signs of hypercontracture (defined by Dworschank et al., 2005, as a cell contraction beyond 55% of the resting cell length) and no cell membrane rupture that would have resulted in cell death. Reperfusion injury is also characterised by Ca^{2+} overload (Vila-Petroff et al., 2007), but this was not present in this model.

The mean baseline fluorescence for all treatment groups was maintained for one minute post reperfusion (figure 4.16), before returning to an equivalent value to the time controls by the 45^{th} minute of experimentation. All cells had a similar rate in reducing their baseline fluorescence allowing the cells treated with CaMKII inhibitors to have an overall mean value lower than the time control. This suggests that the exchanges in extracellular environment had stimulated the cells to an enhanced capacity for removal of Ca^{2+} from the cells. Other investigations have shown a rapid decline in Ca^{2+} after short duration of ischaemia (Marban et al., 1990). But when ischaemic duration lasts for more than 20 minutes in the *ex vivo* heart (Miklos et al., 2003) or 45 minutes in a cellular model (Vila-Petroff et al., 2007) cellular injury is associated with a high $[Ca^{2+}]_i$.

The rate of Ca^{2+} removal in all treatment groups was matched to the time controls within two minutes of reperfusion (figure 4.15). This is interesting as CaMKII activity was not needed for such recovery. Rat derived cardiac myocytes cycle 92% of the $[Ca^{2+}]_i$ through the SR (Bers, 2000). As such these cells would have been an ideal model to disclose if CaMKII inhibition had any ability in reducing the cells capacity to remove Ca^{2+}. Surprisingly, KN-93 treated cells had a much improved rate of Ca^{2+} decay compared to the other treatment groups at 1 minute of reperfusion. Whether this was due to an increased rate constant as they were also the first to react with greater peak of Ca^{2+} transients is unknown.

The rate of Ca^{2+} release was not maintained to the same degree as the time controls or the pre-ischemic values (figure 4.15). This was in conjunction with a normal return of the peak Ca^{2+} transients, indicating that the amount of Ca^{2+} released had been maintained. This is a sign of cellular injury and has been noted in *ex vivo* models of I-R injury (Miklos et al., 2003). The ROS generated during the restoration of metabolism may target the large number of sulfhydryls groups on the RYR2 (Eu et al., 1999). How the RYR2 react to the ROS is thought to depend on their concentration as small amounts have been shown to increase Po of the RYR2, whilst larger quantities could produce irreversible damage to the ion channel (Zima and Blatter, 2006). However, such cellular injury was not reduced by the CaMKII inhibitors.

The cells treated with KN-93 produced the highest recovery in height of each Ca^{2+} transient (figure 4.14). This was also evident in the standardised area of the Ca^{2+} transient. This had occurred by the first minute of restoration and was maintained at a higher mean value than all groups including the time controls throughout the reperfusion period. The height of a Ca^{2+} transient is indicative of a greater load of Ca^{2+} within the SR (Eisner et al., 2009). This could lead to KN-93 increasing the SR Ca^{2+} load and explain why there were incidences of Ca^{2+} waves during the later stages of ischaemia. But the KN-93 treated cells that had recorded incidences of Ca^{2+} waves during ischaemia had no arrhythmic activity during the restoration period. Possibly in these cells the release of Ca^{2+} from the SR had succeeded in relieving some of the demands that were placed on the cells.

If signs of Ca^{2+} dysfunction during the latter stages of the experiment were to be used as a marker of injury, the KN-93 treated cells showed better signs of recovery than any other treatment group (figure 4.13). However, the height regularity and thus the steady state of the Ca^{2+} transients were more variable with the CaMKII inhibitors

(figure 4.17). KN-93 in particular had incidences in the first minute of reperfusion, whilst treatment with AIP triggered such activity after three minutes of reperfusion. An interesting observation is that the KN-92 treated cells had matched the time controls variability in height of the Ca^{2+} transients. Thus, although some aspects of Ca^{2+} handling were improved by CaMKII inhibition not all were beneficial.

4.5. Conclusion

The study was to determine whether CaMKII inhibition would improve the cells' Ca^{2+} handling ability during an episode of simulated ischaemia. As Ca^{2+} overload is a known marker of cell injury and both CaMKII inhibitors limited the rise in $[Ca^{2+}]_i$, it can be suggested that CaMKII inhibition during simulated ischaemia had improved some aspects of the cells' Ca^{2+} handling ability. However, the evidence presented is not conclusive, due to the variability that occurred with $[Ca^{2+}]_i$ in a number of cells that were not treated with a CaMKII inhibitor. Also, other global Ca^{2+} events and parameters were shown not to have a significant amount of CaMKII activity. Thus, how two different CaMKII inhibitors can limit a rise in $[Ca^{2+}]_i$ during simulated ischaemia, without interfering with the cells' global Ca^{2+} events warrants further investigation. It could be that measuring other artefacts of ischaemia, such as $[Na^{+}]_i$ or ROS, would associate better with the effects of the CaMKII inhibitors. Other aspects of the cells' Ca^{2+} handling ability, such as Ca^{2+} dysfunction in the presence of KN-93, were improved with CaMKII inhibition. But which parameter is chosen as a marker of cellular health can also determine the outcome. KN-92 also showed an ability to improve the steady state of Ca^{2+} transients that were better than the CaMKII inhibitors.

4.6. Study Limitations

There are some limitations that need to be considered with this study. The first is the constraints placed on the isolated cells due to the nature of the experiments. The temperature and the rate of stimulation were much lower than those expected for a cardiac myocyte from a rat heart. The limited activity of CaMKII at 1 Hz has previously been mentioned, but the lower temperature could also have been a key factor and can be seen in two ways. Either it would have promoted a quicker rate of CaMKII autoinactivation (Jama et al., 2009), thus limiting CaMKII activity, or it could have restricted the phosphatase activity (Valverede et al., 2005), thus promoting the activity of the CaMKII substrates. The simulation of ischaemic conditions could also not have truly emulated the pathological condition. Hyperkalemia was intentionally left out of the ischaemic solution, whilst the build up of the metabolites that is common to ischaemia, could not have been reproduced within a model that uses a high flow rate.

Although minimal photobleaching is predicted with the use of Fluo4 (Knight et al., 2003) there are other limitations in using an ion sensitive fluorophore. These include compartmentalisation, phototoxicity and sensitivity to acidosis. All of these factors could have distorted aspects of the cells' Ca^{2+} handling ability. The 2D confocal imaging could not have captured the true spatial distribution of Ca^{2+}, whilst the data acquisition was only set to record $1/6^{th}$ of the whole experiment time. Despite such limitations, with time permitting the model would be a useful tool to answer further questions about the ability of pharmacological inhibitors to offset the injury instigated by simulated ischaemia and reperfusion.

CHAPTER 5:
General Discussion

5.1. Principal Findings

The principal findings of the thesis are:

(1) In an *ex vivo* model of regional I-R injury, CaMKII promotes irreversible injury. Chapter 2 demonstrated that a pharmacological inhibitor of CaMKII, KN-93, can limit infarct size if it is used prior to index ischaemia. Treatment of the drug only during reperfusion had no effect on limiting irreversible injury. This would indicate that CaMKII activity at reperfusion does not promote irreversible injury. However, it cannot be ruled out that activity of CaMKII at reperfusion may still promote irreversible injury and that the KN-93 inhibitor is ineffective within this short time frame.

(2) The mechanical intervention of IPC does not require functional CaMKII for cardioprotection. In chapter 2 the presence of a CaMKII inhibitor KN-93, either during the trigger phase of IPC or during the mediator phase of reperfusion did not abrogate the protection of the intervention. The combined treatments of IPC and KN-93 had an additive protective effect against myocardial infarction. This could indicate that two distinct cardioprotective signalling pathways were instigated or that there was an accumulative regulation of CaMKII activity.

(3) Models of cellular injury in the H9c2 cells do not involve CaMKII activity. In chapter 3, the two models of cellular injury, simulated I-R and oxidative stress, subjected to the embryonic cell line H9c2 did not involve CaMKII. The inhibition of CaMKII by two different pharmacological inhibitors was used to confirm this. Although there were some minor differences between the cells treated with the CaMKII inhibitory peptide AIP, it would suggest that the pathway to cell injury in H9c2 cells was independent of CaMKII activity.

(4) Cardiac myocytes paced at 1Hz and subjected to simulated I-R do not involve a significant amount of CaMKII activity in relation to Ca^{2+} handling. Chapter 4 disclosed that there was no significant involvement of CaMKII in the cellular Ca^{2+} signals analysed by the SALVO software, when the cells had been subjected to 30 minutes of simulated ischaemia and 10 minutes of restoration. Under normoxic conditions KN-93 treatment had some capacity to limit the cells' rate of Ca^{2+} release and Ca^{2+} removal. This was not replicated by either of the two CaMKII inhibitors, during conditions of simulated ischaemia when a substantial decline in Ca^{2+} regulation had been instigated in the cells, or after the Ca^{2+} transients were restored to the cells. There was a trend in the cells treated with the two CaMKII inhibitors not to raise their diastolic Ca^{2+}, as occurred within some of the control cells and the KN-92 treated cells. For the non-SALVO analysis of Ca^{2+} abnormalities, treatment of cells with the inhibitor AIP had the lower incidence of Ca^{2+} waves by the end of simulated ischaemia, whilst the KN-93 treated cells had a lower incidence of Ca^{2+} dysfunction at the end of restoration period. The rate of Ca^{2+} release was also altered in cells treated with an inactive analog of KN-93, KN-92, during the normoxic studies and indicates some unspecific characteristics of these compounds.

5.2. The Work in Context

The multifunctional CaMKII is widely thought of as a key mediator of several cardiovascular diseases as it has been shown to be pro-hypertrophic and pro-arrhythmic. However, its involvement in AMI is less clear. Previous experimental data, primarily from the laboratory of Mattiazzi, suggest that pharmacological inhibition of CaMKII during long ischaemic periods and at early reperfusion can prevent cell death by necrosis and apoptosis. Several more studies using *in vitro* models of chronic cellular stress support this notion, as cell death can be limited if the mishandling of Ca^{2+} by CaMKII is abrogated. Yet, shorter durations of ischaemia and models of myocardial stunning are believed to require CaMKII to maintain contractile activity. With interventions such as IHA and volatile anaesthetics also reported to require an active CaMKII to instigate cardioprotection from I-R injury, the role of CaMKII remained to be determined.

The data presented in chapter 2 support the concept that CaMKII has a pro-injury role during I-R. When a pharmacological inhibitor of CaMKII was present during index ischaemia the extent of myocardial infarction was limited. This replicates the findings of Vila-Petroff et al. (2007) and Salas et al. (2010). Chapter 2 dissociates from these two studies however, as it also questions the timing of the intervention. This disclosed that CaMKII inhibition is only effective against irreversible injury when it is used as a pre-ischaemic treatment. Consequently, as AMI is in the majority of cases an unpredictable occurrence, it seems that CaMKII inhibition may not be an appropriate strategy during reperfusion therapy. But operations such as organ transplant and CABG do have a scheduled period of I-R and could thus benefit from pharmacological inhibition of CaMKII. The data in chapter 2 also support a strategy where a prior intervention such as IPC can be further enhanced if it is combined with a CaMKII

inhibitor. This confirms what was seen with the hearts of mice by Li et al. (2007) in their model of a GM CaMKII. The previous studies in the rat heart suggested that CaMKII is a mediator for the IPC improvements in contractile activity (Osada et al., 2000; Benter et al., 2005). Chapter 2 is the first to propose that within these species CaMKII activity is not a pre-requisite for cardioprotection by IPC, if infarct is used as a final end point of injury. Thus it can be concluded that CaMKII is a mechanism that supports irreversible injury.

Interventions that target early reperfusion are used to disclose the signalling pathways that mediate their effects during this critical period. Although the model used by Vila-Petroff et al. (2007) and Salas et al. (2010) had pre-treated hearts with KN-93, it is believed that CaMKII activity during reperfusion (via the NCX and the SR) promotes necrosis and apoptosis. The data from chapter 2 questions this assumption. Chapter 3 and 4 were designed to recreate the findings of chapter 2 in cell model in order to interrogate these hypotheses further by using methods that are unavailable in the Langendorff model. Chapter 3 revealed that the H9c2 cell line subjected to injury by simulated ischaemia or oxidative stress does not involve CaMKII activity. This study was the first to interrogate CaMKII within this cell line using such models, as previous studies have tended to use primary cells. Whether the lack of reversible injury was due to different mechanism of injury or a deficient CaMKII expression was not further pursued.

Consequently, chapter 4 used field stimulated primary ventricular myocytes from the rat heart in order to analyse their Ca^{2+} handling properties with and without the CaMKII inhibitors. Although the model followed similar conditions used in previous studies, this study was distinctive in its characterisation of Ca^{2+} activity during the simulated ischaemic period. A detailed analysis of these variables by the SALVO

software revealed no significant involvement of CaMKII. Under normoxic conditions, the CaMKII inhibitors had minimal influence on the Ca^{2+} transients suggesting that there was negligible CaMKII activity when the cells were paced at 1Hz. This confirms the findings by DeSantiago et al. (2002) and Vila-Petroff et al. (2007). The decision to analyse inter-transient activity for low-amplitude Ca^{2+} events constrained the use of a higher pacing rate. With a significant depression also occurring to the cells Ca^{2+} handling properties during simulated ischaemia, it could be speculated that within this model CaMKII activity would have been continually suppressed. This would imply that ischaemia does not promote the kinase's activity. Such conclusions were made by Netticadan et al. (1999) and Osada et al. (2000) who measured alterations in CaMKII activity contained within the SR vesicles during I-R.

With these findings in mind, why do the studies in chapter 2 and those within the literature need pre-treatment of a pharmacological inhibitor of CaMKII (or a GM CaMKII) for cardioprotection? In chapter 4 there was no rise in $[Ca^{2+}]_i$ when cells were treated with the CaMKII inhibitors. Was this a favourable condition instigated by the CaMKII inhibitors? As not all cells within the two control groups responded with a rising $[Ca^{2+}]_i$ it can not be concluded that this was a CaMKII-mediated event. Also, CaMKII is regulated by ATP, Ca^{2+}/CaM, and oxidative stress; these are all present during the reperfusion period. Thus the only conclusion that can be drawn is that the inhibitors are ineffective within the short time period of early reperfusion, to effect the favourable changes needed to salvage reperfused myocardium.

There was also a trend for some protection in chapter 2 when the inactive analog KN-92 was used as a pre-treatment. This indicated that the non-specific activity of the compound could be at work with KN-93. Chapter 4 indicated that this could be the rate that Ca^{2+} is released in the cell, which would correlate with what is already known about

their activity on specific ion channels. Where the two KN compounds differed, was that KN-92 showed similar signs to the I-R control group in subjecting some cells to a rise in intracellular Ca^{2+} during ischaemia.

CaMKII is up-regulated during pathological hypertrophy and has recently been described as having therapeutic potential (Sossalla et al., 2010). It is plausible that in the future patients will be treated chronically to suppress CaMKII activity. On the basis of the data in this thesis such pre-treatment could also be beneficial to conditions of acute coronary syndromes and justify further research in the field.

5.3. Limitations of the Thesis and Future Outlook

Whether pre-ischaemic treatment of KN-93 abrogates the activity of CaMKII at reperfusion, would have answered some key questions in this thesis and in the literature. A detailed western analysis on CaMKII activity during such conditions was attempted, but the inability to find suitable conditions for the antibodies limited the data that was able to be presented.

With time permitting the data from chapter 4 could be expanded with some modifications of the model. The rate at which the cardiac myocytes were paced, physiological temperature and prolonging the duration of simulated ischaemia could all be further investigated. The aim was to have additional treatment groups of pharmacological inhibitors during simulated ischaemia and at the beginning of the restoration period. Such interventions can not be performed within whole hearts and this justifies the use of *in vitro* analysis to interrogate CaMKII activity during ischaemia. With hindsight, a detailed analysis of the Ca^{2+} handling parameters with the SALVO software should be implemented once a successful strategy is determined. This would also enable several methods (such as other ion fluorescent indicators) to be

instigated at a key time point rather than throughout the protocol. As CaMKII is a multifunctional kinase, understanding its role holds great potential within an environment such as I-R. The use of healthy hearts within these studies also fails to capture the progression of CaMKII that occurs with CVD, which would add further complexity (or even normality) to such future investigations. Indeed, the absence of common comorbidities, such as hypertension in most I-R models is now recognised as a major general limitation (Ferdinandy et al., 2007).

And a major limitation is the reliance on pharmacological inhibitors. Ideally, a fuller approach would complement the pharmacology with molecular genetic approaches e.g. siRNA, knock out, dominant negative mutants etc.

5.4. Concluding Remarks

The research in this thesis confirms the notion that pharmacological inhibition of CaMKII during AMI can prevent irreversible injury. It also confirms that an early intervention such as IPC does not require a functional CaMKII to mediate its cardioprotection. Thus, the potential for salvageable tissue during AMI will be enhanced in the absence of CaMKII activity. It raises questions on whether an intervention targeting CaMKII during reperfusion therapy can be successful; and the nature of the cells or the conditions required for CaMKII to mediate cellular injury. As stated in chapter one the thesis sought to provide answers to the following questions:

i) Is CaMKII involved in promoting irreversible injury caused by acute myocardial infarction?

ii) Does the phenomenon of IPC and postconditioning involve CaMKII?

iii) Under conditions of simulated I-R, what effect does pharmacological blockade of CaMKII have on the Ca^{2+} handling properties of the cells?

The net result of the thesis is that it establishes CaMKII as having deleterious consequences during I-R and that a natural phenomenon such as IPC does not recruit CaMKII activity. Thus it answers the first two proposed questions of the thesis. Only some conclusions can be drawn about the effects of the pharmacological inhibitors on Ca^{2+} handling, but the information provided gives further details about the characteristics of the kinase within the current *in vitro* and *ex vivo* models of I-R. I conclude that CaMKII is an intricate regulator of cellular signalling, that promotes injury under conditions of I-R injury. As such, understanding its role in I-R may underpin the development of future therapeutic strategies for the management of AMI.

Appendices

Appendix 1.1: Components of High Glucose DMEM, Invitrogen

Components	Molecular Weight	Concentration (mg/L)	mM
Amino Acids			
Glycine	75	30	0.4
L-Arginine hydrochloride	211	84	0.398
L-Cystine 2HCl	313	63	0.201
L-Glutamine	146	580	3.97
L-Histidine hydrochloride-H2O	210	42	0.2
L-Isoleucine	131	105	0.802
L-Leucine	131	105	0.802
L-Lysine hydrochloride	183	146	0.798
L-Methionine	149	30	0.201
L-Phenylalanine	165	66	0.4
L-Serine	105	42	0.4
L-Threonine	119	95	0.798
L-Tryptophan	204	16	0.0784
L-Tyrosine	181	72	0.398
L-Valine	117	94	0.803
Vitamins			
Choline chloride	140	4	0.0286
D-Calcium pantothenate	477	4	0.00839
Folic Acid	441	4	0.00907
Niacinamide	122	4	0.0328
Pyridoxine hydrochloride	204	4	0.0196
Riboflavin	376	0.4	0.00106
Thiamine hydrochloride	337	4	0.0119
i-Inositol	180	7.2	0.04
Inorganic Salts			
Calcium Chloride (CaCl2-2H2O)	147	264	1.8
Ferric Nitrate (Fe(NO3)3"9H2O)	404	0.1	0.000248
Magnesium Sulfate (MgSO4-7H2O)	246	200	0.813
Potassium Chloride (KCl)	75	400	5.33
Sodium Bicarbonate (NaHCO3)	84	3700	44.05
Sodium Chloride (NaCl)	58	6400	110.34
Sodium Phosphate monobasic (NaH2PO4-2H2O)	154	141	0.916
Other Components			
D-Glucose (Dextrose)	180	4500	25
Phenol Red	376.4	15	0.0399

Appendix 1.2: Components of PBS, Invitrogen

Components	Molecular Weight	Concentration (mg/L)	mM
Inorganic Salts			
Potassium Phosphate monobasic (KH2PO4)	136	144	1.06
Sodium Chloride (NaCl)	58	9000	155.17
Sodium Phosphate dibasic (Na2HPO4-7H2O)	268	795	2.97

Appendix 1.3: Components of M199 medium, Sigma-Aldrich

	M0393	M0650	M2154	M2520	M3769
	[powder]	[10×]	[1×]	[powder]	[powder]
COMPONENT	g/L	g/L	g/L	g/L	g/L
Inorganic Salts					
$CaCl_2 \cdot 2H_2O$	0.1396	2	0.2	0.2	0.2
$Fe(NO_3)_3 \cdot 9H_2O$	0.00072	0.0072	0.00072	0.00072	0.00072
$MgSO_4$ (anhydrous)	0.09767	0.9767	0.09767	0.09767	0.0967
KCl	0.4	4.0	0.4	0.4	0.4
KH_2PO_4	0.06	—	—	—	—
Na • Acetate (anhydrous)	0.05	0.5	0.05	0.05	0.05
$NaHCO_3$	—	—	2.2	—	—
NaCl	8.0	68.0	6.8	6.0	6.8
Na_2HPO_4 (anhydrous)	0.04788	—	—	—	—
NaH_2PO_4 (anhydrous)	—	1.22	0.122	0.122	0.122
Amino Acids					
L-Alanine	0.025	0.25	0.025	0.025	0.025
L-Arginine • HCl	0.07	0.7	0.07	0.07	0.07
L-Aspartic Acid	0.03	0.3	0.03	0.03	0.03
L-Cystine • HCl • H_2O	0.00011	0.0011	0.00011	0.00011	0.00011
L-Cysteine • 2HCl	0.026	0.26	0.026	0.026	0.026
L-Glutamic Acid	0.0668	0.668	0.0668	0.0668	0.0668
L-Glutamine	0.1	—	—	0.1	—
Glycine	0.05	0.5	0.05	0.05	0.05
L-Histidine • HCl • H_2O	0.02188	0.2188	0.02188	0.02188	0.02188
Hydroxy-L-Proline	0.01	0.1	0.01	0.01	0.01
L-Isoleucine	0.02	0.2	0.02	0.02	0.02
L-Leucine	0.06	0.6	0.06	0.06	0.06
L-Lysine • HCl	0.07	0.7	0.07	0.07	0.07
L-Methionine	0.015	0.15	0.015	0.015	0.015
L-Phenylalanine	0.025	0.25	0.025	0.025	0.025
L-Proline	0.04	0.4	0.04	0.04	0.04
L-Serine	0.025	0.25	0.025	0.025	0.025
L-Threonine	0.03	0.3	0.03	0.03	0.03
L-Tryptophan	0.01	0.1	0.01	0.01	0.01
L-Tyrosine • 2Na • $2H_2O$	0.05766	0.5766	0.05766	0.05766	0.05766
L-Valine	0.025	0.25	0.025	0.025	0.025
Vitamins					
Ascorbic Acid • Na	0.0000566	0.0005625	0.0000566	0.0000566	0.0000566
D-Biotin	0.00001	0.0001	0.00001	0.00001	0.00001
Calciferol	0.0001	0.001	0.0001	0.0001	0.0001
Choline Chloride	0.0005	0.005	0.0005	0.0005	0.0005
Folic Acid	0.00001	0.0001	0.00001	0.00001	0.00001
Menadione (sodium bisulfite)	0.000016	0.00016	0.000016	0.000016	0.000016
myo-Inositol	0.00005	0.0005	0.00005	0.00005	0.00005
Niacinamide	0.000025	0.00025	0.000025	0.000025	0.000025
Nicotinic Acid	0.000025	0.00025	0.000025	0.000025	0.000025
p-Amino Benzoic Acid	0.00005	0.0005	0.00005	0.00005	0.00005
D-Pantothenic Acid • ½Ca	0.00001	0.0001	0.00001	0.00001	0.00001

Pyridoxal • HCl	0.000025	0.00025	0.000025	0.000025	0.000025
Pyridoxine • HCl	0.000025	0.00025	0.000025	0.000025	0.000025
Retinol Acetate	0.00014	0.0014	0.00014	0.00014	0.00014
Riboflavin	0.00001	0.0001	0.00001	0.00001	0.00001
DL-α-Tocopherol Phosphate • Na	0.00001	0.0001	0.00001	0.00001	0.00001
Thiamine • HCl	0.00001	0.0001	0.00001	0.00001	0.00001
Other					
Adenine Sulfate	0.01	0.1	0.01	0.01	0.01
Adenosine Triphosphate • 2Na	0.001	0.01	0.001	0.001	0.001
Adenosine Monophosphate • Na	0.0002385	0.002385	0.0002385	0.0002385	0.0002385
Cholesterol	0.0002	0.002	0.0002	0.0002	0.0002
Deoxyribose	0.0005	0.005	0.0005	0.0005	0.0005
Glucose	1.0	10.0	1.0	1.0	1.0
Glutathione (reduced)	0.00005	0.0005	0.00005	0.00005	0.00005
Guanine • HCl	0.0003	0.003	0.0003	0.0003	0.0003
HEPES	—	—	—	5.958	—
Hypoxanthine	0.0003	0.003	0.0003	0.0003	0.0003
Phenol Red • Na	0.0213	0.213	0.0213	0.0213	—
TWEEN® 80	0.02	0.2	0.02	0.02	0.02
Ribose	0.0005	0.005	0.0005	0.0005	0.0005
Thymine	0.0003	0.003	0.0003	0.0003	0.0003
Uracil	0.0003	0.003	0.0003	0.0003	0.0003
Xanthine • Na	0.000344	0.00344	0.000344	0.000344	0.000344
ADD					
L-Glutamine	—	0.1 at 1×	0.1	—	0.1
Sodium Bicarbonate	0.35	2.2 at 1×	—	2.2	2.2

	M4530	**M5017**	**M7528**	**M7653**	**M9163**
	[1×]	[powder]	[1×]	[1×]	[10×]
COMPONENT	g/L	g/L	g/L	g/L	g/L
Inorganic Salts					
$CaCl_2 \cdot 2H_2O$	0.2	0.2	0.2	0.1396	1.396
$Fe(NO_3)_3 \cdot 9H_2O$	0.00072	0.00072	0.00072	0.00072	0.0072
$MgSO_4$ (anhydrous)	0.09767	0.09767	0.09767	0.09767	0.9767
KCl	0.4	0.4	0.4	0.4	4.0
KH_2PO_4	—	—	—	0.06	0.6
Na • Acetate (anhydrous)	0.05	0.05	0.05	0.05	0.5
$NaHCO_3$	2.2	—	2.2	0.35	—
NaCl	6.8	6.8	6.0	8.0	80.0
Na_2HPO_4 (anhydrous)	—	—	—	0.04788	0.4788
NaH_2PO_4 (anhydrous)	0.122	0.122	0.122	—	—
Amino Acids					
L-Alanine	0.025	0.025	0.025	0.025	0.25
L-Arginine • HCl	0.07	0.07	0.07	0.07	0.7
L-Aspartic Acid	0.03	0.03	0.03	0.03	0.3
L-Cystine • HCl • H_2O	0.00011	0.00011	0.00011	0.00011	0.0011
L-Cysteine • 2HCl	0.026	0.026	0.026	0.026	0.26
L-Glutamic Acid	0.0668	0.0668	0.0668	0.0668	0.668
L-Glutamine	0.1	0.1	—	—	—
Glycine	0.05	0.05	0.05	0.05	0.5
L-Histidine • HCl • H_2O	0.02188	0.02188	0.02188	0.02188	0.2188
Hydroxy-L-Proline	0.01	0.01	0.01	0.01	0.1
L-Isoleucine	0.02	0.02	0.02	0.02	0.2
L-Leucine	0.06	0.06	0.06	0.06	0.6
L-Lysine • HCl	0.07	0.07	0.07	0.07	0.7
L-Methionine	0.015	0.015	0.015	0.015	0.15
L-Phenylalanine	0.025	0.025	0.025	0.025	0.25
L-Proline	0.04	0.04	0.04	0.04	0.4
L-Serine	0.025	0.025	0.025	0.025	0.25
L-Threonine	0.03	0.03	0.03	0.03	0.3
L-Tryptophan	0.01	0.01	0.01	0.01	0.1
L-Tyrosine • 2Na • $2H_2O$	0.05766	0.05766	0.05766	0.05766	0.5766
L-Valine	0.025	0.025	0.025	0.025	0.25

Vitamins					
Ascorbic Acid • Na	0.0000566	0.0000566	0.0000566	0.0000566	0.000566
D-Biotin	0.00001	0.00001	0.00001	0.00001	0.0001
Calciferol	0.0001	0.0001	0.0001	0.0001	0.001
Choline Chloride	0.0005	0.0005	0.0005	0.0005	0.005
Folic Acid	0.00001	0.00001	0.00001	0.00001	0.0001
Menadione (sodium bisulfite)	0.000016	0.000016	0.000016	0.000016	0.00016
myo-Inositol	0.00005	0.00005	0.00005	0.00005	0.0005
Niacinamide	0.000025	0.000025	0.000025	0.000025	0.00025
Nicotinic Acid	0.000025	0.000025	0.000025	0.000025	0.00025
p-Amino Benzoic Acid	0.00005	0.00005	0.00005	0.00005	0.0005
D-Pantothenic Acid • ½Ca	0.00001	0.00001	0.00001	0.00001	0.0001
Pyridoxal • HCl	0.000025	0.000025	0.000025	0.000025	0.00025
Pyridoxine • HCl	0.000025	0.000025	0.000025	0.000025	0.00025
Retinol Acetate	0.00014	0.00014	0.00014	0.00014	0.0014
Riboflavin	0.00001	0.00001	0.00001	0.00001	0.0001
DL-α-Tocopherol Phosphate • Na	0.00001	0.00001	0.00001	0.00001	0.0001
Thiamine • HCl	0.00001	0.00001	0.00001	0.00001	0.0001
Other					
Adenine Sulfate	0.01	0.01	0.01	0.01	0.1
Adenosine Triphosphate • 2Na	0.001	0.001	0.001	0.001	0.01
Adenosine Monophosphate • Na	0.0002385	0.0002385	0.0002385	0.0002385	0.002385
Cholesterol	0.0002	0.0002	0.0002	0.0002	0.002
Deoxyribose	0.0005	0.0005	0.0005	0.0005	0.005
Glucose	1.0	1.0	1.0	1.0	10.0
Glutathione (reduced)	0.00005	0.00005	0.00005	0.00005	0.0005
Guanine • HCl	0.0003	0.0003	0.0003	0.0003	0.003
HEPES	—	—	5.958	—	—
Hypoxanthine	0.0003	0.0003	0.0003	0.0003	0.003
Phenol Red • Na	0.0213	0.0213	0.0213	0.0213	0.0213
TWEEN 80	0.02	0.02	0.02	0.02	0.2
Ribose	0.0005	0.0005	0.0005	0.0005	0.005
Thymine	0.0003	0.0003	0.0003	0.0003	0.003
Uracil	0.0003	0.0003	0.0003	0.0003	—
Xanthine • Na	0.000344	0.000344	0.000344	0.000344	—
ADD					
L-Glutamine	—	—	0.1	0.1	0.1 at 1×
Sodium Bicarbonate	—	2.2	—	—	0.35 at 1×

Appendix 2.1

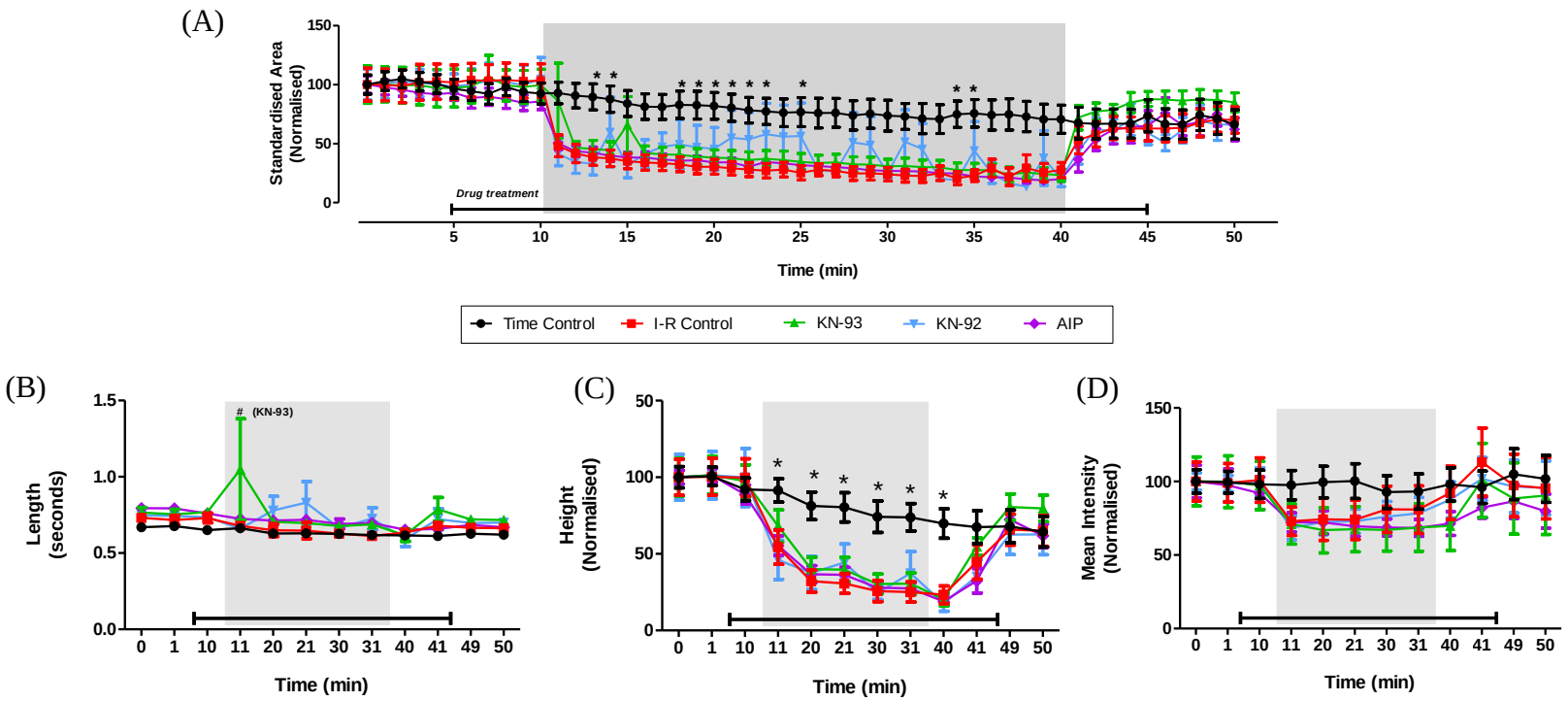

Replica of Figure 4.14: Time course of the SALVO parameters (Mean ± SEM) that describe the cells Ca^{2+} transients' morphology, when subjected to simulated I-R. *(A) Standardised Area (B) Length of Ca^{2+} transient (C) Height of Ca^{2+} transient (D) Mean intensity of $[Ca^{2+}]_i$. All data, except for length, is normalised (%) to the first recording. (B-D) are selected time points through the time course. In all parameters, two-way ANOVA detected no significant interaction between the treatment groups and time. There was a significance detected with treatment and with time. The significance between the groups is described in text. Shaded area indicates period of ischaemia.* ****** *$p<0.05$ when comparing I-R Control vs. Time Control,* $^{\#}$ *$p<0.05$ I-R Control vs. the labelled drug treatment. n = 5-6 cells from 4-5 hearts.*

Appendix 2.2

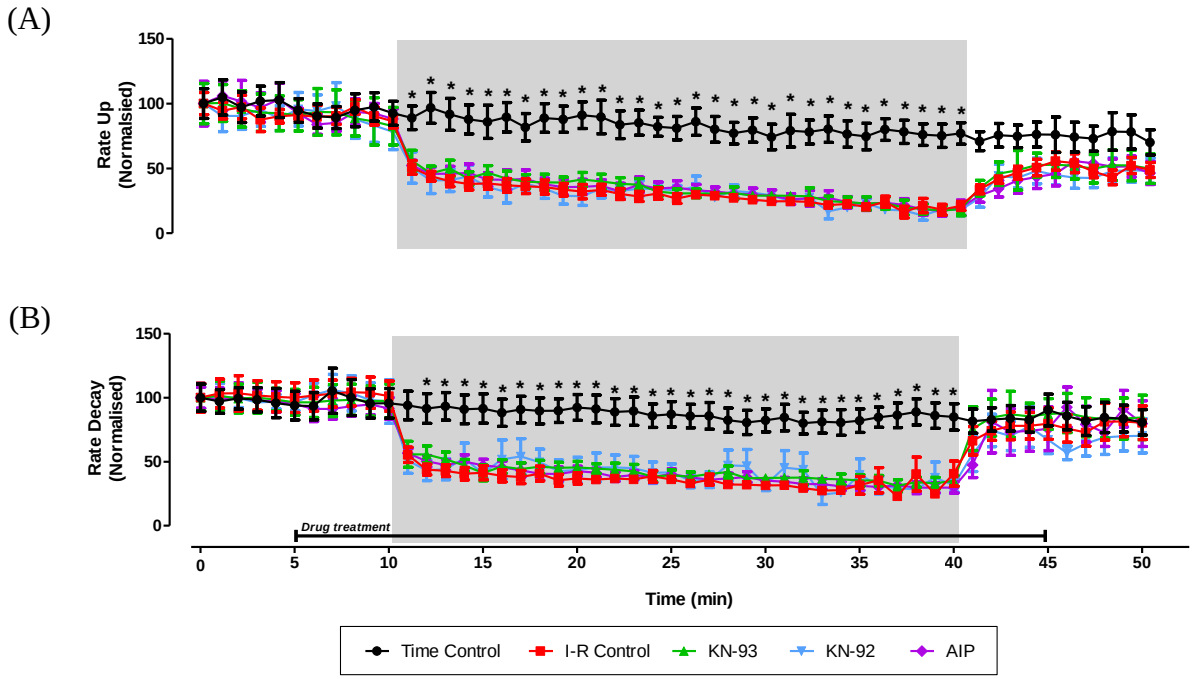

Replica of Figure 4.15: Time course of the SALVO parameters (Mean ± SEM) that describe the Ca^{2+} transients' kinetics, when subjected to simulated I-R. *(A) Rate of Ca^{2+} released into the cell. (B) Rate of Ca^{2+} removed from the cytosol. Data are normalised (%) to the first recording. A two-way ANOVA detected no significant interaction between the treatment groups and time during Ca^{2+} release but it was of significance during Ca^{2+} removal. Further significance between the treatment groups is described in text. Shaded area indicates period of ischaemia. (***** $p<0.05$ when comparing within the treatment groups).*

Appendix 2.3

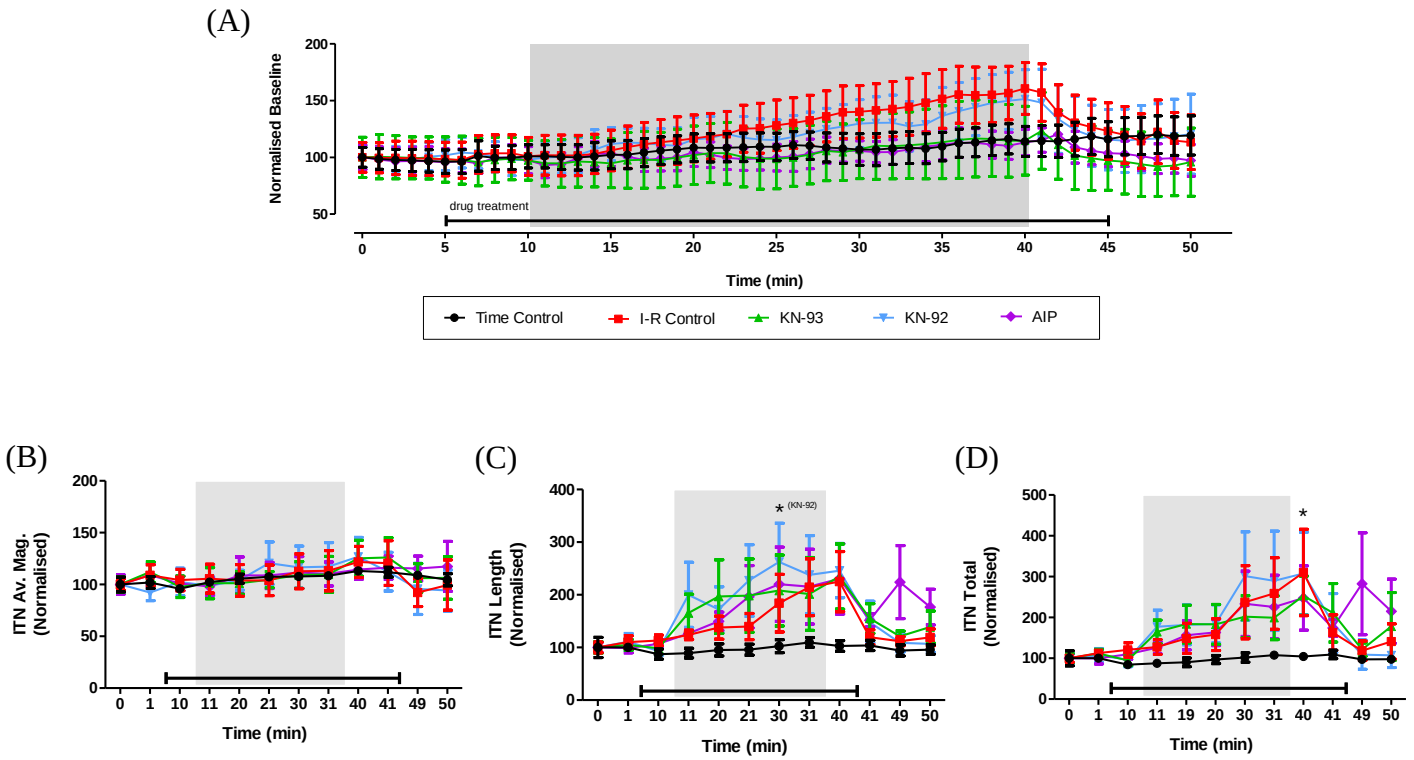

Replica of Figure 4.16: Time course of the SALVO parameters (Mean ± SEM) that describe the baseline and inter-transient activity of the cells when subjected to simulated I-R. *(A) Baseline fluorescence (B) Average magnitude of ITN (C) Length of ITN (D) Total amount of ITN. Data are normalised (%) to the first recording. None of the parameters had any significant interaction between the treatments and time periods. Baseline, ITN Length and ITN Total had significant effects within the treatment and time periods, but average magnitude of ITN did not. Further comparison between the treatment groups means at specific time periods are described in text. Shaded area indicates period of ischaemia. (* $p<0.05$ when comparing within the time controls).*

Appendix 2.4

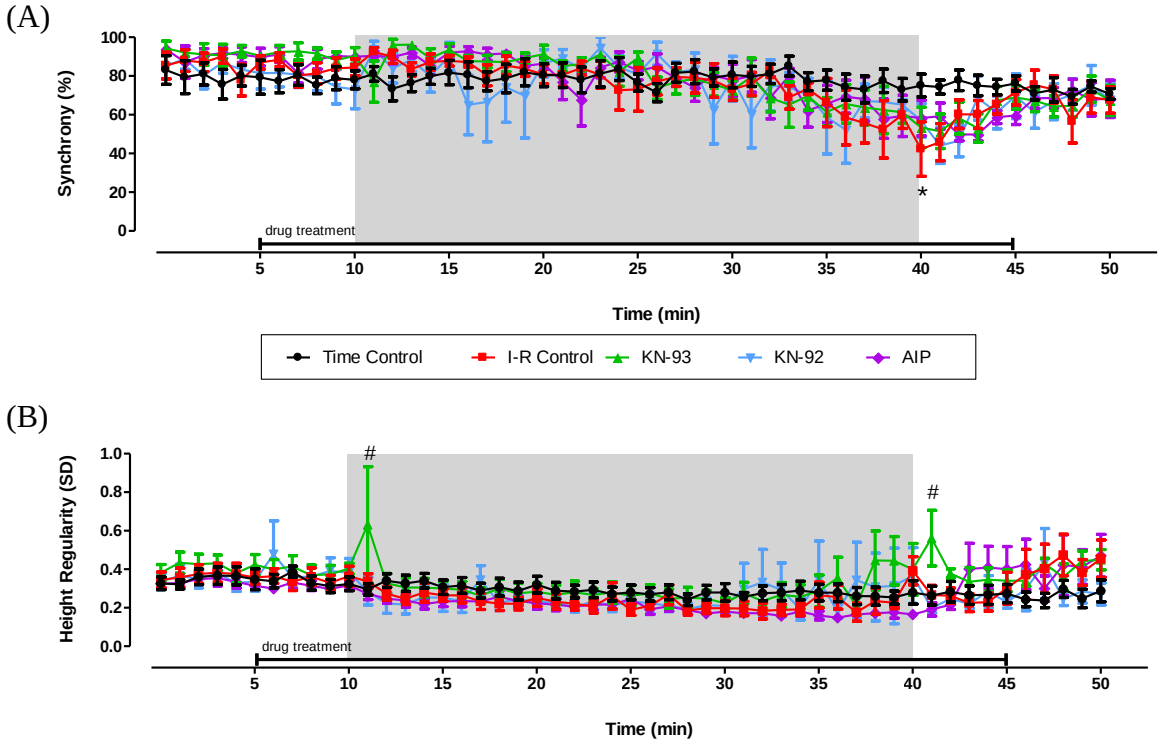

Replica of Figure 4.17: Time course of the SALVO parameters (Mean ± SEM) that describe the synchronicity amongst the cells ROI and regularity of the Ca^{2+} transients. *(A) Synchrony of ROI (B) Regularity of Ca^{2+} transient height. A two-way ANOVA determined none of the parameters had any significant interaction between the treatments and time periods. Both synchrony and height regularity had significant effects within the treatment and time periods. Further comparison between the treatment groups means at specific time periods are described in text. Shaded area indicates period of ischaemia. (* $p<0.05$ when comparing the time controls with I-R controls, # $p<0.05$ when comparing KN-93 treated cells with all other treatment groups).*

References

Abraham ST, Benscoter HA, Schworer CM, Singer HA. (1997). A role for Ca^{2+}/calmodulin-dependent protein kinase II in the mitogen-activated protein kinase signaling cascade of cultured rat aortic vascular smooth muscle cells. *Circ Res*.;81(4):575-84.

Agnetti G, Maraldi T, Fiorentini D, Giordano E, Prata C, Hakim G, Muscari C, Guarnieri C, Caldarera CM. (2005). Activation of glucose transport during simulated ischemia in H9c2 cardiac myoblasts is mediated by protein kinase C isoforms. *Life Sci*. 5; 78(3):264-70.

Ai X, Curran JW, Shannon TR, Bers DM, Pogwizd SM. (2005). Ca^{2+}/calmodulin-dependent protein kinase modulates cardiac ryanodine receptor phosphorylation and sarcoplasmic reticulum Ca^{2+} leak in heart failure. *Circ Res*.; 97(12):1314-22.

Aiba T, Hesketh GG, Liu T, Carlisle R, Villa-Abrille MC, O'Rourke B, Akar FG, Tomaselli GF. (2010). Na^{+} channel regulation by Ca^{2+}/calmodulin and Ca^{2+}/calmodulin-dependent protein kinase II in guinea-pig ventricular myocytes. Cardiovasc Res.; 85(3):454-63.

Akaishi M, Ikegawa T, Nishikawa Y, Yokozuka H, Handa S, Nakamura Y. (1991).Variations in myocardial contraction sequence under various hypoxic cond itions. *Basic Res Cardiol*.; 86(4):363-77.

Akatsuka Y, Egashira K, Katsuda Y, Narishige T, Ueno H, Shimokawa H, Takeshita A. (1994). ATP sensitive potassium channels are involved in adenosine A2 receptor mediated coronary vasodilatation in the dog. *Cardiovasc Res*.; 28(6):906-11.

Aki T, Mizukami Y, Oka Y, Yamaguchi K, Uemura K, Fujimiya T, Yoshida K. (2001). Phosphoinositide 3-kinase accelerates necrotic cell death during hypoxia. *Biochem J*.; 358(Pt 2):481-7.

Allen DG, Cairns SP, Turvey SE, Lee JA. (1993). Intracellular calcium and myocardial function during ischemia. *Adv Exp Med Biol*. ; 346:19-.29.

Anderson ME, Braun AP, Schulman H, Premack BA. (1994). Multifunctional Ca^{2+}/calmodulin-dependent protein kinase mediates Ca^{2+}-induced enhancement of the L-type Ca^{2+} current in rabbit ventricular myocytes. *Circ Res.*; 75(5):854-61.

Anderson ME. (2007). Multiple downstream proarrhythmic targets for calmodulin kinase II: moving beyond an ion channel-centric focus. *Cardiovasc Res.*; 73(4):657-66.

Anderson ME. (2009). Sticky fingers: CaMKII finds a home on another ion channel. *Annu Rev Med*.; 42:225-46.

Argaud L, Gateau-Roesch O, Augeul L, Couture-Lepetit E, Loufouat J, Gomez L, Robert D, Ovize M. (2008). Increased mitochondrial calcium coexists with decreased reperfusion injury in postconditioned (but not preconditioned) hearts. *Am J Physiol Heart Circ Physiol*.; 294(1):H386-91.

Argaud L, Gateau-Roesch O, Chalabreysse L, Gomez L, Loufouat J, Thivolet-Béjui F, Robert D, Ovize M. (2004). Preconditioning delays Ca^{2+}-induced mitochondrial permeability transition. *Cardiovasc Res*.; 61(1):115-22.

Argaud L, Gateau-Roesch O, Raisky O, Loufouat J, Robert D, Ovize M. (2005). Postconditioning inhibits mitochondrial permeability transition. *Circulation*; 111(2):194-7.

Backs J, Song K, Bezprozvannaya S, Chang S, Olson EN. (2006). CaM kinase II selectively signals to histone deacetylase 4 during cardiomyocyte hypertrophy. *J Clin Invest*.; 116(7):1853-64.

Bahi N, Zhang J, Llovera M, Ballester M, Comella JX, Sanchis D. (2006). Switch from caspase-dependent to caspase-independent death during heart development: essential role of endonuclease G in ischemia-induced DNA processing of differentiated cardiomyocytes. *J Biol Chem*.; 281(32):22943-52.

Baines CP, Goto M, Downey JM. (1997). Oxygen radicals released during ischemic preconditioning contribute to cardioprotection in the rabbit myocardium. *J Mol Cell Cardiol*.; 29(1):207-16.

Baker JE, Holman P, Gross GJ. (1999). Preconditioning in immature rabbit hearts: role of K_{ATP} channels. *Circulation*.; 99(9):1249-54.

Banerjee A, Locke-Winter C, Rogers KB, Mitchell MB, Brew EC, Cairns CB, Bensard DD, Harken AH. (1993). Preconditioning against myocardial dysfunction after ischemia and reperfusion by an alpha 1-adrenergic mechanism. *Circ Res*.; 73(4):656-70.

Bär FW, Tzivoni D, Dirksen MT, Fernández-Ortiz A, Heyndrickx GR, Brachmann J, Reiber JH, Avasthy N, Tatsuno J, Davies M, Hibberd MG, Krucoff MW; CASTEMI Study Group. (2007). Results of the first clinical study of adjunctive CAldaret (MCC-135) in patients undergoing primary percutaneous coronary intervention for ST-Elevation Myocardial Infarction: the randomized multicentre CASTEMI study. *Eur Heart J*.; 27(21):2516-23.

Bare DJ, Kettlun CS, Liang M, Bers DM, Mignery GA. (2005). Cardiac type 2 inositol 1,4,5-trisphosphate receptor: interaction and modulation by calcium/calmodulin-dependent protein kinase II. *J Biol Chem*.; 280(16):15912-20.

Barry DM, Nerbonne JM. (1996). Myocardial potassium channels: electrophysiological and molecular diversity. *Annu Rev Physiol*. ;58:363-94.

Barry WH, Peeters GA, Rasmussen CA Jr, Cunningham MJ. (1987). Role of changes in [Ca^{2+}]i in energy deprivation contracture. *Circ Res*; 61(5):726-34.

Baxter GF, Mocanu MM, Yellon DM. (1997). Attenuation of myocardial ischaemic injury 24 h after diacylglycerol treatment in vivo. *J Mol Cell Cardiol*.; 29(7):1967-75.

Baxter GF, Yellon DM. (1993). Attenuation of reperfusion-induced ventricular fibrillation in the rat isolated hypertrophied heart by preischemic diltiazem treatment. *Cardiovasc Drugs Ther*.;7(2):225-31.

Beard NA, Laver DR, Dulhunty AF. (2004). Calsequestrin and the calcium release channel of skeletal and cardiac muscle. *Prog Biophys Mol Biol*.; 85(1):33-69.

Bell RM, Mocanu MM, Yellon DM. (2011). Retrograde heart perfusion: the Langendorff technique of isolated heart perfusion. *J Mol Cell Cardiol*.;50(6):940-50.

Benter IF, Juggi JS, Khan I, Akhtar S. (2004). Inhibition of Ras-GTPase, but not tyrosine kinases or Ca^{2+}/calmodulin-dependent protein kinase II, improves recovery of cardiac function in the globally ischemic heart. *Mol Cell Biochem*.; 259(1-2):35-42.

Benter IF, Juggi JS, Khan I, Yousif MH, Canatan H, Akhtar S. (2005). Signal transduction mechanisms involved in cardiac preconditioning: role of Ras-GTPase, Ca^{2+}/calmodulin-dependent protein kinase II and epidermal growth factor receptor. *Mol Cell Biochem*.; 268(1-2):175-83.

Berridge MJ. (2009). Inositol trisphosphate and calcium signalling mechanisms. *Biochim Biophys Acta*.; 1793(6):933-40.

Bers DM. (2000). Calcium fluxes involved in control of cardiac myocyte contraction. *Circ Res*.; 87(4):275-81.

Bers DM. (2002). Cardiac excitation-contraction coupling. *Nature*. 10; 415(6868):198-205.

Billman GE. (2008). The cardiac sarcolemmal ATP-sensitive potassium channel as a novel target for anti-arrhythmic therapy. *Pharmacol Ther*.; 120(1):54-70.

Birnbaum Y, Leor J, Kloner RA. (1997). Pathobiology and Clinical Impact of Reperfusion Injury. *J Thromb Thrombolysis*.; 4(2):185-195.

Bonavita F, Stefanelli C, Giordano E, Columbaro M, Facchini A, Bonafè F, Caldarera CM, Guarnieri C. (2003). H9c2 cardiac myoblasts undergo apoptosis in a model of ischemia consisting of serum deprivation and hypoxia: inhibition by PMA. *FEBS Lett*.;536(1-3):85-91.

Bootman MD, Fearnley C, Smyrnias I, MacDonald F, Roderick HL. (2009). An update on nuclear calcium signalling. *J Cell Sci*.; 122(Pt 14):2337-50.

Bootman MD, Lipp P, Berridge MJ. (2001). The organisation and functions of local Ca^{2+} signals. *J Cell Sci*.; 114(Pt 12):2213-22.

Bossuyt J, Helmstadter K, Wu X, Clements-Jewery H, Haworth RS, Avkiran M, Martin JL, Pogwizd SM, Bers DM. (2008). Ca^{2+}/calmodulin-dependent protein kinase IIdelta and protein kinase D overexpression reinforce the histone deacetylase 5 redistribution in heart failure. *Circ Res*.; 102(6):695-702.

Bøtker HE, Kharbanda R, Schmidt MR, Bøttcher M, Kaltoft AK, Terkelsen CJ, Munk K, Andersen NH, Hansen TM, Trautner S, Lassen JF, Christiansen EH, Krusell LR, Kristensen SD, Thuesen L, Nielsen SS, Rehling M, Sørensen HT, Redington AN, Nielsen TT. (2010). Remote ischaemic conditioning before hospital admission, as a complement to angioplasty, and effect on myocardial salvage in patients with acute myocardial infarction: a randomised trial. *Lancet*.; 375(9716):727-34.

Brar BK, Jonassen AK, Stephanou A, Santilli G, Railson J, Knight RA, Yellon DM, Latchman DS. (2000). Urocortin protects against ischemic and reperfusion injury via a MAPK-dependent pathway. *J Biol Chem*. 24; 275(12):8508-14.

Braun AP, Schulman H. (1995). The multifunctional calcium/calmodulin-dependent protein kinase: from form to function. *Annu Rev Physiol*.;57:417-45.

Bridge JH, Ershler PR, Cannell MB. (1999). Properties of Ca^{2+} sparks evoked by action potentials in mouse ventricular myocytes. *Journal of Physiology*; 518:469–478.

Bridge JH, Smolley JR, Spitzer KW. (1990). The relationship between charge movements associated with I_{Ca} and I_{Na-Ca} in cardiac myocytes. *Science*; 248(4953):376-8.

British Heart Foundation (2010) Coronary heart Disease Statistics, 7th Edition. Peter Scarborough, Prachi Bhatnagar, Kremlin Wickramasinghe, Kate Smolina, Colin Mitchell and Mike Raymer. Department of Public health, University of Oxford.

British Heart Foundation (2011) Trends in coronary heart disease, 1961-2011. Peter Scarborough , Prachi Bhatnagar, Kremlin Wickramasinghe, Mike Raymer. Department of Public health, University of Oxford.

Brookes PS, Yoon Y, Robotham JL, Anders MW, Sheu SS. (2004). Calcium, ATP, and ROS: a mitochondrial love-hate triangle. *Am J Physiol Cell Physiol*.; 287(4):C817-33.

Buck J, Sinclair ML, Schapal L, Cann MJ, Levin LR. (1999). Cytosolic adenylyl cyclase defines a unique signaling molecule in mammals. *Proc Natl Acad Sci U S A*.; 96(1):79-84.

Budas GR, Jovanovic S, Crawford RM, Jovanovic A. (2004). Hypoxia-induced preconditioning in adult stimulated cardiomyocytes is mediated by the opening and trafficking of sarcolemmal KATP channels. *FASEB J*.; 18(9):1046-8.

Buja LM. (2005). Myocardial ischemia and reperfusion injury. *Cardiovasc Pathol*.;14(4):170-5.

Buja LM, Weerasinghe P. (2010). Unresolved issues in myocardial reperfusion injury. *Cardiovasc Pathol*.; 19(1):29-35.

Burley DS, Baxter GF. (2007). B-type natriuretic peptide at early reperfusion limits infarct size in the rat isolated heart. *Basic Res Cardiol*. 2007 Nov;102(6):529-41.

Burley DS, Baxter GF. (2009). Pharmacological targets revealed by myocardial postconditioning. *Curr Opin Pharmacol*.; 9(2):177-88.

Carmeliet E. (1999). Cardiac ionic currents and acute ischemia: from channels to arrhythmias. *Physiol Rev*.; 79(3):917-1017.

Cartwright EJ, Schuh K, Neyses L. (2005). Calcium transport in cardiovascular health and disease--the sarcolemmal calcium pump enters the stage. *J Mol Cell Cardiol*.; 39(3):403-6.

Chai Y, Zhang DM, Lin YF. (2011). Activation of cGMP-dependent protein kinase stimulates cardiac ATP-sensitive potassium channels via a ROS/calmodulin/CaMKII signaling cascade. *PLoS One*. 29; 6(3):e18191.

Chaitman BR, Laddu AA. (2011). Stable angina pectoris: antianginal therapies and future directions. *Nat Rev Cardiol*.; 9(1):40-52.

Chang BH, Mukherji S, Soderling TR. (1998). Characterization of a calmodulin kinase II inhibitor protein in brain. *Proc Natl Acad Sci U S A* ; 95(18):10890-5.

Chao LH, Stratton MM, Lee IH, Rosenberg OS, Levitz J, Mandell DJ, Kortemme T, Groves JT, Schulman H, Kuriyan J. (2011). A mechanism for tunable autoinhibition in the structure of a human Ca^{2+}/calmodulin- dependent kinase II holoenzyme. *Cell.;* 146(5):732-45.

Chelu MG, Sarma S, Sood S, Wang S, van Oort RJ, Skapura DG, Li N, Santonastasi M, Müller FU, Schmitz W, Schotten U, Anderson ME, Valderrábano M, Dobrev D, Wehrens XH. (2009). Calmodulin kinase II-mediated sarcoplasmic reticulum Ca^{2+} leak promotes atrial fibrillation in mice. *J Clin Invest*.; 119(7):1940-51.

Chen X, Zhang X, Kubo H, Harris DM, Mills GD, Moyer J, Berretta R, Potts ST, Marsh JD, Houser SR. (2005). Ca^{2+} influx-induced sarcoplasmic reticulum Ca^{2+} overload causes mitochondrial-dependent apoptosis in ventricular myocytes. *Circ Res.* ; 97(10):1009-17.

Chen ZC, Yu BC, Chen LJ, Cheng KC, Lin HJ, Cheng JT. (2011). Characterization of the mechanisms of the increase in PPARδ expression induced by digoxin in the heart using the H9c2 cell line. *Br J Pharmacol.;* 163(2):390-8.

Cheng H, Lederer WJ. (2008). Calcium sparks. *Physiol Rev*.; 88(4):1491-545.

Choi HS, Trafford AW, Orchard CH, Eisner DA. (2000). The effect of acidosis on systolic Ca^{2+} and sarcoplasmic reticulum calcium content in isolated rat ventricular myocytes. *J Physiol*.; 529 Pt 3:661-8.

Chu CH, Tzang BS, Chen LM, Kuo CH, Cheng YC, Chen LY, Tsai FJ, Tsai CH, Kuo WW, Huang CY. (2008). IGF-II/mannose-6-phosphate receptor signaling induced cell hypertrophy and atrial natriuretic peptide/BNP expression via Galphaq interaction and protein kinase C-alpha/CaMKII activation in H9c2 cardiomyoblast cells. *J Endocrinol*.; 197(2):381-90.

Cleland J.G., McDonagh T., Rigby A.S., Yassin A., Whittaker T., Dargie H.J. (2010) The national heart failure audit for England and Wales 2008-2009. *Heart* 97(11):876-86.

Cohen MV, Downey JM. (2011). Is it time to translate ischemic preconditioning's mechanism of cardioprotection into clinical practice? *J Cardiovasc Pharmacol Ther*.; 16(3-4):273-80.

Cohen MV, Yang XM, Downey JM. (2007). The pH hypothesis of postconditioning: staccato reperfusion reintroduces oxygen and perpetuates myocardial acidosis. *Circulation*.; 115(14):1895-903.

Colbran RJ. (1993). Inactivation of Ca^{2+}/calmodulin-dependent protein kinase II by basal autophosphorylation. *J Biol Chem*.; 268(10):7163-70.

Colinas O, Gallego M, Setién R, López-López JR, Pérez-García MT, Casis O. (2006). Differential modulation of Kv4.2 and Kv4.3 channels by calmodulin-dependent protein kinase II in rat cardiac myocytes. *Am J Physiol Heart Circ Physiol*.; 291(4):H1978-87.

Colomer JM, Mao L, Rockman HA, Means AR. (2003). Pressure overload selectively up-regulates Ca^{2+}/calmodulin-dependent protein kinase II in vivo. *Mol Endocrinol*.; 17(2):183-92.

Costa AD, Garlid KD, West IC, Lincoln TM, Downey JM, Cohen MV, Critz SD. (2005). Protein kinase G transmits the cardioprotective signal from cytosol to mitochondria. *Circ Res*.; 97(4):329-36.

Crampin EJ, Smith NP, Langham AE, Clayton RH, Orchard CH. (2006). Acidosis in models of cardiac ventricular myocytes. *Philos Transact A Math Phys Eng Sci*.; 364(1842):1171-86.

Crisostomo PR, Wairiuko GM, Wang M, Tsai BM, Morrell ED, Meldrum DR. (2006). Preconditioning versus postconditioning: mechanisms and therapeutic potentials. *J Am Coll Surg*.; 202(5):797-812.

Currie S, Loughrey CM, Craig MA, Smith GL. (2004). Calcium/calmodulin-dependent protein kinase IIdelta associates with the ryanodine receptor complex and regulates channel function in rabbit heart. *Biochem J*.; 377(Pt 2):357-66.

De-Koninck P, Schulman H. (1998) Sensitivity of CaM kinase II to the frequency of Ca2+ oscillations. *Science*. 279: 227-30.

Demaurex N, Distelhorst C. (2003). Cell biology. Apoptosis--the calcium connection. *Science*.; 300(5616):65-7.

Demchenko, Alexander P. (2009). Introduction to Fluorescence Sensing. *Springer Science+Business Media B.V.*

Derwall M, Coburn M, Rex S, Hein M, Rossaint R, Fries M. (2009). Xenon: recent developments and future perspectives. *Minerva Anestesiol*.; 75(1-2):37-45.

DeSantiago J, Maier LS, Bers DM. (2002). Frequency-dependent acceleration of relaxation in the heart depends on CaMKII, but not phospholamban. *J Mol Cell Cardiol*.; 34(8):975-84.

Di Lisa F, Bernardi P. (2006). Mitochondria and ischemia-reperfusion injury of the heart: fixing a hole. *Cardiovasc Res*.; 70(2):191-9.

Di Lisa F, Menabò R, Canton M, Barile M, Bernardi P. (2001). Opening of the mitochondrial permeability transition pore causes depletion of mitochondrial and cytosolic NAD^+ and is a causative event in the death of myocytes in postischemic reperfusion of the heart. *J Biol Chem*.; 26;276(4):2571-5.

Diaz RJ, Wilson GJ. (2006). Studying ischemic preconditioning in isolated cardiomyocyte models. *Cardiovasc Res*.; 70(2):286-96.

Dong Z, Saikumar P, Weinberg JM, Venkatachalam MA. (2006). Calcium in cell injury and death. *Annu Rev Pathol*.; 1:405-34.

Doring HJ, Dehnert H. (1987). The isolated perfused heart according to Langendorff. *BVM-Biomesstechnic Verlag*.

Dorn GW, Scorrano L. (2010). Two close, too close: sarcoplasmic reticulum-mitochondrial crosstalk and cardiomyocyte fate. *Circ Res*.; 107(6):689-99.

Dow J, Kloner RA. (2007). Postconditioning does not reduce myocardial infarct size in an in vivo regional ischemia rodent model. *J Cardiovasc Pharmacol Ther*.; 12(2):153-63.

Downey JM, Davis AM, Cohen MV. (2007). Signaling pathways in ischemic preconditioning. *Heart Fail Rev*.; 12(3-4):181-8..

Duncker DJ, Bache RJ. (2008). Regulation of coronary blood flow during exercise. *Physiol Rev*.; 88(3):1009-86.

Dworschak M, d'Uscio LV, Breukelmann D, Hannon JD. (2005). Increased tolerance to hypoxic metabolic inhibition and reoxygenation of cardiomyocytes from apolipoprotein E-deficient mice. *Am J Physiol Heart Circ Physiol*.; 289(1):H160-7.

Dzau V, Braunwald E. (1991). Resolved and unresolved issues in the prevention and treatment of coronary artery disease: a workshop consensus statement. *Am Heart J*. 121(4 Pt 1):1244-63.

Dzau VJ, Antman EM, Black HR, Hayes DL, Manson JE, Plutzky J, Popma JJ, Stevenson W. (2006). The cardiovascular disease continuum validated: clinical evidence of improved patient outcomes: part II: Clinical trial evidence (acute coronary syndromes through renal disease) and future directions. *Circulation*.; 114(25):2871-91.

Eberli FR. (2004). Stunned myocardium--an unfinished puzzle. *Cardiovasc Res*. 63(2):189-91.

Eisner DA, Kashimura T, O'Neill SC, Venetucci LA, Trafford AW. (2009). What role does modulation of the ryanodine receptor play in cardiac inotropy and arrhythmogenesis? *J Mol Cell Cardiol*.; 46(4):474-81.

Eisner DA, Nichols CG, O'Neill SC, Smith GL, Valdeolmillos M. (1989). The effects of metabolic inhibition on intracellular calcium and pH in isolated rat ventricular cells. *J Physiol*; 411:393-418.

El-Haou S, Balse E, Neyroud N, Dilanian G, Gavillet B, Abriel H, Coulombe A, Jeromin A, Hatem SN. (2009). Kv4 potassium channels form a tripartite complex with the anchoring protein SAP97 and CaMKII in cardiac myocytes. *Circ Res*. 27; 104(6):758-69.

Entman ML, Smith CW. (1994). Postreperfusion inflammation: a model for reaction to injury in cardiovascular disease. *Cardiovasc Res*.; 28(9):1301-11.

Erickson JR, Joiner ML, Guan X, Kutschke W, Yang J, Oddis CV, Bartlett RK, Lowe JS, O'Donnell SE, Aykin-Burns N, Zimmerman MC, Zimmerman K, Ham AJ, Weiss RM, Spitz DR, Shea MA, Colbran RJ, Mohler PJ, Anderson ME. (2008). A dynamic pathway for calcium-independent activation of CaMKII by methionine oxidation. *Cell*. 2; 133(3):462-74.

Esumi K, Nishida M, Shaw D, Smith TW, Marsh JD. (1991). NADH measurements in adult rat myocytes during simulated ischemia. *Am J Physiol*.; 260:H1743-52.

Eu JP, Xu L, Stamler JS, Meissner G. (1999). Regulation of ryanodine receptors by reactive nitrogen species. *Biochem Pharmacol*.; 57(10):1079-84.

Fabiato A. (1983). Calcium-induced release of calcium from the cardiac sarcoplasmic reticulum. *Am J Physiol*.; 245(1):C1-14.

Fearnley CJ, Roderick HL, Bootman MD. (2011). Calcium signaling in cardiac myocytes. *Cold Spring Harb Perspect Biol*.; 1; 3(11)

Ferdinandy P, Schulz R, Baxter GF. (2007). Interaction of cardiovascular risk factors with myocardial ischemia/reperfusion injury, preconditioning, and postconditioning. *Pharmacol Rev*.; 59(4):418-58.

Fiolet JW, Schumacher CA, Baartscheer A, Coronel R. (1993). Osmotic changes and transsarcolemmal ion transport during total ischaemia of isolated rat ventricular myocytes. *Basic Res Cardiol*.; 88(5):396-410.

Fleet WF, Johnson TA, Graebner CA, Gettes LS. (1985). Effect of serial brief ischemic episodes on extracellular K^+, pH, and activation in the pig. *Circulation*.; 72(4):922-32.

Fliegel L, Walsh MP, Singh D, Wong C, Barr A. (1992). Phosphorylation of the C-terminal domain of the Na^+/H^+ exchanger by Ca^{2+}/calmodulin-dependent protein kinase II. *Biochem J*. 15; 282 :139-45.

Forbes RA, Steenbergen C, Murphy E. (2001). Diazoxide-induced cardioprotection requires signalling through a redox-sensitive mechanism. *Circ Res*.; 88(8):802-9.

Gao L, Blair LA, Marshall J. (2006). CaMKII-independent effects of KN93 and its inactive analog KN92: reversible inhibition of L-type calcium channels. *Biochem Biophys Res Commun*. 14; 345(4):1606-10.

Garcia-Dorado D, Ruiz-Meana M, Inserte J, Rodriguez-Sinovas A, Piper HM. (2012). Calcium-mediated cell death during myocardial reperfusion. *Cardiovasc Res.* 1;94(2):168-80.

Garcia-Dorado D, Rodriguez-Sinovas A, Ruiz-Meana M, Inserte J, Agulló L, Cabestrero A. (2006a). The end-effectors of preconditioning protection against myocardial cell death secondary to ischemia-reperfusion. *Cardiovasc Res*.; 70(2):274-85.

Garcia-Dorado D, Vinten-Johansen J, Piper HM. (2006b). Bringing preconditioning and postconditioning into focus. *Cardiovasc Res*.; 70(2):167-9.

Genka C, Ishida H, Ichimori K, Hirota Y, Tanaami T, Nakazawa H. (1999). Visualization of biphasic Ca2+ diffusion from cytosol to nucleus in contracting adult rat cardiac myocytes with an ultra-fast confocal imaging system. *Cell Calcium.*; 25(3):199-208.

Gho BCG, Schoemaker RV, van den Doel MA, Duncker DJ, Verdouw PD. (1996). Myocardial protection by brief ischemia in non-cardiac tissue. *Circulation.*; 94: 2193–2200.

Goto M, Liu Y, Yang XM, Ardell JL, Cohen MV, Downey JM. (1995). Role of bradykinin in protection of ischemic preconditioning in rabbit hearts. *Circ Res*.; 77(3):611-21.

Gottlieb RA. (2011). Cell death pathways in acute ischemia/reperfusion injury. *J Cardiovascular Pharmacol Ther*. 16(3-4):233-8.

Griffiths EJ, Rutter GA. (2009). Mitochondrial calcium as a key regulator of mitochondrial ATP production in mammalian cells. *Biochim Biophys Acta*.; 1787(11):1324-33.

Grimm M, Brown JH. (2010). Beta-adrenergic receptor signaling in the heart: role of CaMKII. *J Mol Cell Cardiol*.; 48(2):322-30.

Gross GJ, Fryer RM. (1999). Sarcolemmal versus mitochondrial ATP-sensitive K^+ channels and myocardial preconditioning. *Circ. Res*. 14; 84(9):973-9.

Grueter CE, Abiria SA, Wu Y, Anderson ME, Colbran RJ. (2008). Differential regulated interactions of calcium/calmodulin-dependent protein kinase II with isoforms of voltage-gated calcium channel beta subunits. *Biochemistry*. 12; 47(6):1760-7.

Hagemann D, Kuschel M, Kuramochi T, Zhu W, Cheng H, Xiao RP. (2000). Frequency-encoding Thr^{17} phospholamban phosphorylation is independent of Ser16 phosphorylation in cardiac myocytes. *J Biol Chem*.; 275(29):22532-6.

Hale SL, Mehra A, Leeka J, Kloner RA. (2008). Postconditioning fails to improve no reflow or alter infarct size in an open-chest rabbit model of myocardial ischemia-reperfusion. Am J Physiol Heart Circ Physiol; 294(1):H421-5.

Halestrap AP. (2009). Mitochondrial calcium in health and disease. *Biochim Biophys Acta*.; 1787(11):1289-90.

Halestrap AP, Clarke SJ, Javadov SA. (2004). Mitochondrial permeability transition pore opening during myocardial reperfusion--a target for cardioprotection. *Cardiovasc Res*.; 61(3):372-85.

Harary I. and Farley B. (1960). In vitro studies of single isolated beating heart cells. *Science*.; 131(3414):1674-5.

Harr MW, Distelhorst CW. (2010). Apoptosis and autophagy: decoding calcium signals that mediate life or death. *Cold Spring Harb Perspect Biol*.; 2(10):a005579.

Hashambhoy YL, Winslow RL, Greenstein JL. (2009). CaMKII-induced shift in modal gating explains L-type Ca^{2+} current facilitation: a modeling study. *Biophys J*.; 96(5):1770-85.

Hausenloy DJ, Mocanu MM, Yellon DM. (2004). Cross-talk between the survival kinases during early reperfusion: its contribution to ischemic preconditioning. *Cardiovasc Res*.; 63(2):305-12.

Hausenloy DJ, Yellon DM. (2004). New directions for protecting the heart against ischaemia-reperfusion injury: targeting the Reperfusion Injury Salvage Kinase (RISK)-pathway. *Cardiovasc Res*.15; 61(3):448-60.

Hausenloy DJ, Tsang A, Mocanu MM, Yellon DM. (2005). Ischemic preconditioning protects by activating prosurvival kinases at reperfusion. *Am J Physiol Heart Circ Physiol*.; 288(2):H971-6.

Hausenloy DJ, Yellon DM. (2006). Survival kinases in ischemic preconditioning and postconditioning. *Cardiovasc Res*.; 70(2):240-53.

Hausenloy DJ, Yellon DM. (2007). Preconditioning and postconditioning: united at reperfusion. *Pharmacol Ther*.; 116(2):173-91.

Heller LJ, Mohrman DE, Smith JA, Wallace KB. (2003). Multitrack system for superfusing isolated cardiac myocytes. *Am J Physiol Heart Circ Physiol*.; 284(5):H1872-8.

Hescheler J, Meyer R, Plant S, Krautwurst D, Rosenthal W, Schultz G. (1991). Morphological, biochemical, and electrophysiological characterization of a clonal cell (H9c2) line from rat heart. *Circ Res*.; 69(6):1476-86.

Heusch G. (2004). Postconditioning: old wine in a new bottle? *J Am Coll Cardiol*.; 44(5):1111-2.

Hilgemann DW, Yaradanakul A, Wang Y, Fuster D. (2006). Molecular control of cardiac sodium homeostasis in health and disease. *J Cardiovasc Electrophysiol*.; 17 Suppl 1:S47-S56.

Hoch B, Haase H, Schulze W, Hagemann D, Morano I, Krause EG, Karczewski P. (1998). Differentiation-dependent expression of cardiac delta-CaMKII isoforms. *J Cell Biochem*.; 68(2):259-68.

Hoch B, Meyer R, Hetzer R, Krause EG, Karczewski P. (1999). Identification and expression of delta-isoforms of the multifunctional Ca^{2+}/calmodulin-dependent protein kinase in failing and nonfailing human myocardium. *Circ Res*.; 84(6):713-21.

Hoch B, Wobus AM, Krause EG, Karczewski P. (2000). delta-Ca^{2+}/calmodulin-dependent protein kinase II expression pattern in adult mouse heart and cardiogenic differentiation of embryonic stem cells. *J Cell Biochem*.; 79(2):293-300.

Hoffman L, Stein RA, Colbran RJ, Mchaourab HS. (2011). Conformational changes underlying calcium/calmodulin-dependent protein kinase II activation. *EMBO J*.; 30(7):1251-62.

Holly TA, Drincic A, Byun Y, Nakamura S, Harris K, Klocke FJ, Cryns VL. (1999). Caspase inhibition reduces myocyte cell death induced by myocardial ischemia and reperfusion in vivo. *J Mol Cell Cardiol*.; 31(9):1709-15.

Hool LC. (2000). Hypoxia increases the sensitivity of the L-type Ca^{2+} current to beta-adrenergic receptor stimulation via a C2 region-containing protein kinase C isoform. *Circ Res*.; 87(12):1164-71.

Horton RW, Meldrum BS, Bachelard HS. (1973). Enzymic and cerebral metabolic effects of 2-deoxy-D-glucose. *J Neurochem*.; 21(3):507-20

Hou Q, Hsu YT. (2005). Bax translocates from cytosol to mitochondria in cardiac cells during apoptosis: development of a GFP-Bax-stable H9c2 cell line for apoptosis analysis. *Am J Physiol Heart Circ Physiol*.; 289(1):H477-87.

House SJ, Singer HA. (2008). CaMKII-delta isoform regulation of neointima formation after vascular injury. *Arterioscler Thromb Vasc Biol*.; 28(3):441-7.

Høyer-Hansen M, Jäättelä M. (2007). Connecting endoplasmic reticulum stress to autophagy by unfolded protein response and calcium. *Cell Death Differ*. 14(9):1576-82.

Hudmon A, Schulman H. (2002). Structure-function of the multifunctional Ca^{2+}/calmodulin-dependent protein kinase II. *Biochem J*.; 364(Pt 3):593-611.

Hudmon A, Schulman H, Kim J, Maltez JM, Tsien RW, Pitt GS. (2005). CaMKII tethers to L-type Ca^{2+} channels, establishing a local and dedicated integrator of Ca^{2+} signals for facilitation. *J Cell Biol*.; 171(3):537-47.

Hwang JM, Weng YJ, Lin JA, Bau DT, Ko FY, Tsai FJ, Tsai CH, Wu CH, Lin PC, Huang CY, Kuo WW. (2008). Hypoxia-induced compensatory effect as related to Shh and HIF-1alpha in ischemia embryo rat heart. *Mol Cell Biochem*; 311(1-2):179-87.

Inserte J, Barba I, Hernando V, Garcia-Dorado D. (2009). Delayed recovery of intracellular acidosis during reperfusion prevents calpain activation and determines protection in postconditioned myocardium. *Cardiovasc Res*.; 81(1):116-22.

Ishida A, Kameshita I, Okuno S, Kitani T, Fujisawa H. (1995). A novel highly specific and potent inhibitor of calmodulin-dependent protein kinase II. *Biochem Biophys Res Commun*. 26; 212(3):806-12.

Ishida A, Sueyoshi N, Shigeri Y, Kameshita I. (2008). Negative regulation of multifunctional Ca^{2+}/calmodulin-dependent protein kinases: physiological and pharmacological significance of protein phosphatases. *Br J Pharmacol*.; 154(4):729-40.

Jama AM, Fenton J, Robertson SD, Török K. (2009). Time-dependent autoinactivation of phospho-Thr^{286}-alphaCa^{2+}/calmodulin-dependent proteinkinase II. *J Biol Chem*.; 284(41):28146-55.

Javadov SA, Clarke S, Das M, Griffiths EJ, Lim KH, Halestrap AP. (2003). Ischaemic preconditioning inhibits opening of mitochondrial permeability transition pores in the reperfused rat heart. *J Physiol*.; 549(Pt 2):513-24.

Jennings RB. (2011). Commentary on selected aspects of cardioprotection. J *Cardiovasc Pharmacol Ther*.; 16(3-4):340-8.

Jennings RB, Hawkins HK, Lowe JE, Hill ML, Klotman S, Reimer KA. (1978). Relation between high energy phosphate and lethal injury in myocardial ischemia in the dog. *Am J Pathol*.; 92(1):187-214.

Jennings RB, Murry CE, Steenbergen C Jr, Reimer KA. (1990). Development of cell injury in sustained acute ischemia. *Circulation*.; 82(3 Suppl):II2-12.

Jennings RB, Reimer KA. (1991). The cell biology of acute myocardial ischemia. *Annu Rev Med*.; 42:225-46

Jiang D, Xiao B, Yang D, Wang R, Choi P, Zhang L, Cheng H, Chen SR. (2004). RyR2 mutations linked to ventricular tachycardia and sudden death reduce the threshold for store-overload-induced Ca^{2+} release (SOICR). *Proc Natl Acad Sci U S A*.; 101(35):13062-7.

Jiao JD, Garg V, Yang B, Hu K. (2008). Novel functional role of heat shock protein 90 in ATP-sensitive K^+ channel-mediated hypoxic preconditioning. *Cardiovasc Res*.; 77(1):126-33.

Jones SM, Hunt NA, Del Monte F, Harding SE. (1990). Contraction of cardiac myocytes from noradrenaline-treated rats in response to isoprenaline, forskolin and dibutyryl cAMP. *Eur J Pharmacol*.; 191(2):129-40.

Juhaszova M, Zorov DB, Kim SH, Pepe S, Fu Q, Fishbein KW, Ziman BD, Wang S, Ytrehus K, Antos CL, Olson EN, Sollott SJ. (2004). Glycogen synthase kinase-3beta mediates convergence of protection signaling to inhibit the mitochondrial permeability transition pore. *J Clin Invest*.; 113(11):1535-49.

Jung YS, Kim MY, Kim MJ, Oh KS, Yi KY, Lee S, Yoo SE, Lee BH. (2006). Pharmacological profile of KR-33028, a highly selective inhibitor of Na^+/H^+ exchanger. *Eur J Pharmacol*. 27;535(1-3):220-7.

Kabakov AE, Budagova KR, Latchman DS, Kampinga HH. (2002). Stressful preconditioning and HSP70 overexpression attenuate proteotoxicity of cellular ATP depletion. *Am J Physiol Cell Physiol*.; 283(2):C521-34.

Kashiwase K, Higuchi Y, Hirotani S, Yamaguchi O, Hikoso S, Takeda T, Watanabe T, Taniike M, Nakai A, Tsujimoto I, Matsumura Y, Ueno H, Nishida K, Hori M, Otsu K. (2005). CaMKII activates ASK1 and NF-kappaB to induce cardiomyocyte hypertrophy. *Biochem Biophys Res Commun*; 327(1):136-42.

Keeley EC, Boura JA, Grines CL. (2003). Primary angioplasty versus intravenous thrombolytic therapy for acute myocardial infarction: a quantitative review of 23 randomised trials. *Lancet*.; 361(9351):13-20.

Kemi OJ, Ellingsen O, Ceci M, Grimaldi S, Smith GL, Condorelli G, Wisløff U. (2007). Aerobic interval training enhances cardiomyocyte contractility and Ca^{2+} cycling by phosphorylation of CaMKII and Thr^{17} of phospholamban. J *Mol Cell Cardiol*.; 43(3):354-61.

Kimes BW, Brandt BL. (1976). Properties of a clonal muscle cell line from rat heart. *Exp Cell Res*.;98(2):367-81.

Kirchhefer U, Schmitz W, Scholz H, Neumann J. (1999). Activity of cAMP-dependent protein kinase and Ca^{2+}/calmodulin-dependent protein kinase in failing and nonfailing human hearts. *Cardiovasc Res*.; 42(1):254-61.

Kitakaze M, Asakura M, Kim J, Shintani Y, Asanuma H, Hamasaki T, Seguchi O, Myoishi M, Minamino T, Ohara T, Nagai Y, Nanto S, Watanabe K, Fukuzawa S, Hirayama A, Nakamura N, Kimura K, Fujii K, Ishihara M, Saito Y, Tomoike H, Kitamura S; J-WIND investigators. (2007). Human atrial natriuretic peptide and nicorandil as adjuncts to reperfusion treatment for acute myocardial infarction (J-

WIND): two randomised trials. *Lancet*.; 370(9597):1483-93. Erratum in: Lancet.; 370(9605):2102.

Klabunde, (2011). Cardiovascular Physiology Concepts. Second Edition. *Lippincott Williams & Wilkins.*

Kloner RA, Jennings RB. (2001). Consequences of brief ischemia: stunning, preconditioning, and their clinical implications: part 1. *Circulation*. 11; 104(24):2981-9.

Knight MM, Roberts SR, Lee DA, Bader DL. (2003). Live cell imaging using confocal microscopy induces intracellular calcium transients and cell death. *Am J Physiol Cell Physiol*.; 284(4):C1083-9.

Kohlhaas M, Zhang T, Seidler T, Zibrova D, Dybkova N, Steen A, Wagner S, Chen L, Brown JH, Bers DM, Maier LS. (2006). Increased sarcoplasmic reticulum calcium leak but unaltered contractility by acute CaMKII overexpression in isolated rabbit cardiac myocytes. *Circ Res*.; 98(2):235-44.

Kushnir A, Shan J, Betzenhauser MJ, Reiken S, Marks AR. (2010). Role of CaMKIIdelta phosphorylation of the cardiac ryanodine receptor in the force frequency relationship and heart failure. *Proc Natl Acad Sci USA*.; 107(22):10274-9.

Lakatta EG. (1992). Functional implications of spontaneous sarcoplasmic reticulum Ca^{2+} release in the heart. *Cardiovasc Res*.; 26(3):193-214.

Lange M, Redel A, Lotz C, Smul TM, Blomeyer C, Frank A, Stumpner J, Roewer N, Kehl F. (2009). Desflurane-induced postconditioning is mediated by beta-adrenergic signaling: role of beta 1- and beta 2-adrenergic receptors, protein kinase A, and calcium/calmodulin-dependent protein kinase II. *Anesthesiology*.; 110(3):516-28.

Lange M, Smul TM, Redel A, Lotz C, Jazbutyte V, Schnupp V, Roewer N, Kehl F. (2008). Differential role of calcium/calmodulin-dependent protein kinase II in desflurane-induced preconditioning and cardioprotection by metoprolol: metoprolol blocks desflurane-induced preconditioning. *Anesthesiology*. 109(1):72-80.

Laskey WK. (2005). Brief repetitive balloon occlusions enhance reperfsuion during percutaneous coronary intervention for acute myocardial infarction: a pilot study. *Catheter Cardiovasc Interv*.; 65(3):361-7.

Laude AJ, Simpson AW. (2009). Compartmentalized signalling: Ca^{2+} compartments, microdomains and the many facets of Ca^{2+} signalling. *FEBS J.*; 276(7):1800-16.

Lax A, Soler F, Fernández-Belda F. (2005). Intracellular Ca^{2+} pools and fluxes in cardiac muscle-derived h9c2 cells. *J Bioenerg Biomembr.*;37(4):249-59.

Lax A, Soler F, Fernández-Belda F. (2006). Cytoplasmic Ca^{2+} signals and cellular death by apoptosis in myocardiac H9c2 cells. *Biochim Biophys Acta.*; 1763(9):937-47.

Layland J, Grieve DJ, Cave AC, Sparks E, Solaro RJ, Shah AM. (2004). Essential role of troponin I in the positive inotropic response to isoprenaline in mouse hearts contracting auxotonically. *J Physiol.*; 556(Pt 3):835-47.

Lecour S. (2006). Activation of the protective Survivor Activating Factor Enhancement (SAFE) pathway against reperfusion injury: Does it go beyond the RISK pathway? *J Mol Cell Cardiol.*;47(1):32-40.

Ledoux J, Chartier D, Leblanc N. (1999). Inhibitors of calmodulin-dependent protein kinase are nonspecific blockers of voltage-dependent K^+ channels in vascular myocytes. *J Pharmacol Exp Ther.*; 290(3):1165-74.

Lee JW, Lee HK, Kim HW, Kim YH. (2007). Effects of pH, Buffer System and Lactate on the Simulated Ischaemia-Reperfusion Injury of H9c2 Cardiac Myocytes. *Korean J Physiol pharmacol.*; 11: 45-55.

Lee AG, East JM. (2001). What the structure of a calcium pump tells us about its mechanism. *Biochem J.*; 356(Pt 3):665-83.

Lee KS. (1987). Potentiation of the calcium-channel currents of internally perfused mammalian heart cells by repetitive depolarization. *Proc Natl Acad Sci U S A.*; 84(11):3941-5.

Lee KW, Ladinsky H, Stuckey JH. (1967). Decreased Ca^{2+} uptake by sarcoplasmic reticulum after coronary artery occlusion for 60 and 90 minutes. *Circ Res.*; 21(4):439-44.

Levine B, Klionsky DJ. (2004). Development by self-digestion: molecular mechanisms and biological functions of autophagy. *Dev Cell.*; 6(4):463-77.

Li H, Li W, Gupta AK, Mohler PJ, Anderson ME, Grumbach IM. (2010). Calmodulin kinase II is required for angiotensin II-mediated vascular smooth muscle hypertrophy. *Am J Physiol Heart Circ Physiol.*; 298(2):H688-98.

Li J, Marionneau C, Koval O, Zingman L, Mohler PJ, Nerbonne JM, Anderson ME. (2007). Calmodulin kinase II inhibition enhances ischemic preconditioning by augmenting ATP-sensitive K^+ current. *Channels (Austin).* 1(5):387-94.

Li J, Marionneau C, Zhang R, Shah V, Hell JW, Nerbonne JM, Anderson ME. (2006). Calmodulin kinase II inhibition shortens action potential duration by upregulation of K^+ currents. *Circ Res*. 10; 99(10):1092-9.

Li L, Chu G, Kranias EG, Bers DM. (1998). Cardiac myocyte calcium transport in phospholamban knockout mouse: relaxation and endogenous CaMKII effects. *Am J Physiol*.; 274(4 Pt 2):H1335-47.

Li L, Satoh H, Ginsburg KS, Bers DM. (1997). The effect of Ca^{2+}-calmodulin-dependent protein kinase II on cardiac excitation-contraction coupling in ferret ventricular myocytes. *J Physiol*. 15; 501 (Pt 1):17-31.

Ling H, Zhang T, Pereira L, Means CK, Cheng H, Gu Y, Dalton ND, Peterson KL,Chen J, Bers D, Heller Brown J. (2009). Requirement for Ca^{2+}/calmodulin-dependent kinase II in the transition from pressure overload-induced cardiac hypertrophy to heart failure in mice. *J Clin Invest*.; 119(5):1230-40.

Liu Y, Downey JM. (1992). Ischemic preconditioning protects against infarction in rat heart. *Am J Physiol Heart Circ Physiol*.; 263:H1107-H1112

Liu GS, Thornton J, Van Winkle DM, Stanley AW, Olsson RA, Downey JM. (1991). Protection against infarction afforded by preconditioning is mediated by A1 adenosine receptors in rabbit heart. *Circulation*.; 84(1):350-6.

Ljubojević S, Walther S, Asgarzoei M, Sedej S, Pieske B, Kockskämper J. (2011) In situ calibration of nucleoplasmic versus cytoplasmic Ca^{2+} concentration in adultcardiomyocytes. *Biophys J*.;100(10):2356-66.

Lochner A, Marais E, Genade S, Moolman JA. (2000). Nitric oxide: a trigger for classic preconditioning? *Am J Physiol Heart Circ Physiol*. ;279(6):H2752-65.

Lu YM, Shioda N, Yamamoto Y, Han F, Fukunaga K. (2010). Transcriptional upregulation of calcineurin Abeta by endothelin-1 is partially mediated by calcium/calmodulin-dependent protein kinase IIdelta3 in rat cardiomyocytes. *Biochim Biophys Acta*.; 1799(5-6):429-41.

Luqman N, Sung RJ, Wang C, Kuo C. Myocardial ischemia and ventricular fibrillation: Pathophysiology and clinical implications. *Int J Cardiol*.; 119:283–290.

Lynn EG, McLeod CJ, Gordon JP, Bao J, Sack MN. (2008). SIRT2 is a negative regulator of anoxia-reoxygenation tolerance via regulation of 14-3-3 zeta and BAD in H9c2 cells. *FEBS Lett*.; 582(19):2857-62.

Maddaford TG, Hurtado C, Sobrattee S, Czubryt MP, Pierce GN. (1999). A model of low-flow ischemia and reperfusion in single, beating adult cardiomyocytes. Am *J Physiol*.; 277(2 Pt 2):H788-98.

Maier LS, Bers DM. (2007). Role of Ca2+/calmodulin-dependant protein kinase (CaMK) in excitation-contraction coupling in the heart. *Cardiovasc Res*.; 73: 631-640.

Maier LS, Zhang T, Chen L, DeSantiago J, Brown JH, Bers DM. (2003). Transgenic CaMKIIdeltaC overexpression uniquely alters cardiac myocyte Ca^{2+} handling: reduced SR Ca^{2+} load and activated SR Ca^{2+} release. *Circ Res*.; 92(8):904-11.

Mani SK, Egan EA, Addy BK, Grimm M, Kasiganesan H, Thiyagarajan T, Renaud L, Brown JH, Kern CB, Menick DR. (2010). beta-Adrenergic receptor stimulated Ncx1 upregulation is mediated via a CaMKII/AP-1 signaling pathway in adult cardiomyocytes. *J Mol Cell Cardiol*.; 48(2):342-51.

Manintveld OC, Te Lintel Hekkert M, van den Bos EJ, Suurenbroek GM, Dekkers DH, Verdouw PD, Lamers JM, Duncker DJ. (2007). Cardiac effects of postconditioning depend critically on the duration of index ischemia. *Am J Physiol Heart Circ Physiol*.; 292(3):H1551-60.

Marban E, Kitakaze M, Koretsune Y, Yue DT, Chacko VP, Pike MM. (1990). Quantification of $[Ca^{2+}]_i$ in perfused hearts. Critical evaluation of the 5F-BAPTA and nuclear magnetic resonance method as applied to the study of ischemia and reperfusion. *Circ Res*.; 66(5):1255-67.

Marber MS. (2000). Ischemic preconditioning in isolated cells. *Circ Res*.; 86(9):926-31. Review.

Maroko PR, Kjekshus JK, Sobel BE, Watanabe T, Covell JW, Ross J Jr, Braunwald E. (1971). Factors influencing infarct size following experimental coronary artery occlusions. *Circulation*.; 43(1):67-82.

Marx SO, Gaburjakova J, Gaburjakova M, Henrikson C, Ondrias K, Marks AR. (2001).Coupled gating between cardiac calcium release channels (ryanodine recep tors). *Circ Res*.; 88(11):1151-8.

Marzilli M, Huqi A. (2010) Cardioprotective Therapy in Reperfusion Theray: Lessons from the European Myocardial Infarction Project – Free Radicals (EMIP-FR). *Heart Metabolism*; 46: 35-37.

Matsui Y, Takagi H, Qu X, Abdellatif M, Sakoda H, Asano T, Levine B, Sadoshima J. (2007). Distinct roles of autophagy in the heart during ischemia and reperfusion: roles of AMP-activated protein kinase and Beclin 1 in mediating autophagy. *Circ Res*. 30; 100(6):914-22.

Mattiazzi A, Mundiña-Weilenmann C, Guoxiang C, Vittone L, Kranias E. (2005). Role of phospholamban phosphorylation on Thr^{17} in cardiac physiological and pathological conditions. *Cardiovasc Res*.; 68(3):366-75.

Mattiazzi A, Vittone L, Mundiña-Weilenmann C. (2007). Ca^{2+}/calmodulin-dependent protein kinase: a key component in the contractile recovery from acidosis. *Cardiovasc Res*.; 73(4):648-56.

Ménard C, Pupier S, Mornet D, Kitzmann M, Nargeot J, Lory P. (1999). Modulation of L-type calcium channel expression during retinoic acid-induced differentiation of H9C2 cardiac cells. *J Biol Chem*.; 274(41):29063-70.

Meyer T, Hanson PI, Stryer L, Schulman H. (1992). Calmodulin trapping by calcium-calmodulin-dependent protein kinase. *Science*.; 256(5060):1199-202.

Miki T, Cohen MV, Downey JM. (1998). Opioid receptor contributes to ischemic preconditioning through protein kinase C activation in rabbits. *Mol Cell Biochem*.; 186(1-2):3-12.

Miklós Z, Ivanics T, Roemen TH, van der Vusse GJ, Dézsi L, Szekeres M, Kemecsei P, Tóth A, Kollai M, Ligeti L. (2003). Time related changes in calcium handling in the isolated ischemic and reperfused rat heart. *Mol Cell Biochem*.; 250(1-2):115-24.

Mishra S, Gray CB, Miyamoto S, Bers DM, Brown JH. (2011). Location matters: clarifying the concept of nuclear and cytosolic CaMKII subtypes. *Circ Res*.; 109(12):1354-62.

Mocanu MM, Baxter GF, Yellon DM. (2000). Caspase inhibition and limitation of myocardial infarct size: protection against lethal reperfusion injury. *Br J Pharmacol*.; 130(2):197-200.

Murphy E, Steenbergen C. (2008). Mechanisms underlying acute protection from cardiac ischemia-reperfusion injury. *Physiol Rev*.; 88(2):581-609.

Murry CE, Jennings RB, Reimer KA. (1986). Preconditioning with ischemia: a delay of lethal cell injury in ischemic myocardium. *Circulation*.; 74(5):1124-36.

Murry CE, Richard VJ, Reimer KA, Jennings RB. (1990). Ischemic preconditioning slows energy metabolism and delays ultrastructural damage during a sustained ischemic episode. *Circ Res*.; 66(4):913-31.

Mykytenko J, Reeves JG, Kin H, Wang NP, Zatta AJ, Jiang R, Guyton RA, Vinten-Johansen J, Zhao ZQ. (2008). Persistent beneficial effect of postconditioning against infarct size: role of mitochondrial K_{ATP} channels during reperfusion. *Basic Res Cardiol*.; 103(5):472-84.

Narayanan N, Xu A. (1997). Phosphorylation and regulation of the Ca^{2+}-pumping ATPase in cardiac sarcoplasmic reticulum by calcium/calmodulin-dependent protein kinase. *Basic Res Cardiol*.; 92 Suppl 1:25-35.

Netticadan T, Temsah R, Osada M, Dhalla NS. (1999). Status of Ca^{2+}/calmodulin protein kinase phosphorylation of cardiac SR proteins in ischemia-reperfusion. *Am J Physiol*.; 277:C384-91.

Odagiri K, Katoh H, Kawashima H, Tanaka T, Ohtani H, Saotome M, Urushida T, Satoh H, Hayashi H. (2009). Local control of mitochondrial membrane potential, permeability transition pore and reactive oxygen species by calcium and calmodulin in rat ventricular myocytes. *J Mol Cell Cardiol*.; 46(6):989-97.

Odermatt A, Kurzydlowski K, MacLennan DH. (1996). The vmax of the Ca^{2+}-ATPase of cardiac sarcoplasmic reticulum (SERCA2a) is not altered by Ca^{2+}/calmodulin-dependent phosphorylation or by interaction with phospholamban. *J Biol Chem*.; 271(24):14206-13.

Office for National Statistics (2010). Population estimates for UK, England and Wales, Scotland and Northern Ireland, Mid-2010.

Okamoto F, Allen BS, Buckberg GD, Bugyi H, Leaf J. (1986). Reperfusion conditions: importance of ensuring gentle versus sudden reperfusion during relief ofcoronary occlusion. *J Thorac Cardiovasc Surg*.; 92 (3 Pt 2):613-20.

Orchard C, Brette F. (2008). t-Tubules and sarcoplasmic reticulum function in cardiac ventricular myocytes. *Cardiovasc Res*.; 77(2):237-44.

Orchard CH, Houser SR, Kort AA, Bahinski A, Capogrossi MC, Lakatta EG. (1987). Acidosis facilitates spontaneous sarcoplasmic reticulum Ca^{2+} release in rat myocardium. *J Gen Physiol*.; 90(1):145-65.

Osada M, Netticadan T, Kawabata K, Tamura K, Dhalla NS. (2000). Ischemic preconditioning prevents I/R-induced alterations in SR calcium-calmodulin protein kinase II. *Am J Physiol Heart Circ Physiol*.; 278(6):H1791-8.

Overbaugh KJ. (2009). Acute coronary syndrome. *Am J Nurs*.; 109(5):42-52.

Overend CL, Eisner DA, O'Neill SC. (2001). Altered cardiac sarcoplasmic reticulum function of intact myocytes of rat ventricle during metabolic inhibition. *Circ Res*; 88(2):181-7.

Ovize M, Baxter GF, Di Lisa F, Ferdinandy P, Garcia-Dorado D, Hausenloy DJ, Heusch G, Vinten-Johansen J, Yellon DM, Schulz R. (2010). Postconditioning and protection from reperfusion injury: where do we stand? Position paper from the Working Group of Cellular Biology of the Heart of the European Society of Cardiology. *Cardiovasc Res*.; 87(3):406-23.

Palomeque J, Rueda OV, Sapia L, Valverde CA, Salas M, Petroff MV, Mattiazzi A. (2009). Angiotensin II-induced oxidative stress resets the Ca^{2+} dependence of Ca^{2+}-calmodulin protein kinase II and promotes a death pathway conserved across different species. *Circ Res*.; 105(12):1204-12.

Parsons M, Young L, Lee JE, Jacobson KA, Liang BT. (2000). Distinct cardioprotective effects of adenosine mediated by differential coupling of receptor subtypes to phospholipases C and D. *FASEB J*.;14(10):1423-31.

Pedersen TH, Gurung IS, Grace A, Huang CL. (2009). Calmodulin kinase II initiates arrhythmogenicity during metabolic acidification in murine hearts. *Acta Physiol* (Oxf); 197(1):13-25.

Peng W, Zhang Y, Zheng M, Cheng H, Zhu W, Cao CM, Xiao RP. (2010). Cardioprotection by CaMKII-deltaB is mediated by phosphorylation of heat shock factor 1 and subsequent expression of inducible heat shock protein 70. *Circ Res*.; 106(1):102-10.

Perc M, Green AK, Dixon CJ, Marhl M. (2008). Establishing the stochastic nature of intracellular calcium oscillations from experimental data. *Biophys Chem*.; 132(1):33-8.

Piper HM, Abdallah Y, Schäfer C. (2004). The first minutes of reperfusion: a window of opportunity for cardioprotection. *Cardiovasc Res*. 15; 61(3):365-71.

Piper HM, García-Dorado D. (1999). Prime causes of rapid cardiomyocyte death during reperfusion. *Ann Thorac Surg*. ;68(5):1913-9.

Piper HM, García-Dorado D, Ovize M. (1998). A fresh look at reperfusion injury. *Cardiovasc Res*.;38(2):291-300.

Piper HM, Kasseckert S, Abdallah Y. (2006). The sarcoplasmic reticulum as the primary target of reperfusion protection. *Cardiovasc Res*.; 70(2):170-3.

Powell T, Twist V. (1976). A rapid technique for the isolation and purification of adult cardiac muscle cells having respiratory control and a tolerance to calcium. *Biochem Biophys Res Commun*; 72:327-33.

Prasad A, Stone GW, Holmes DR, Gersh B. (2009). Reperfusion injury, microvascular dysfunction, and cardioprotection: the "dark side" ofreperfusion. Circulation. 24;120(21):2105-12. *Review*.

Qin Q, Downey JM, Cohen MV. (2003). Acetylcholine but not adenosine triggers preconditioning through PI3-kinase and a tyrosine kinase. *Am J. Physiol Heart Circ Physiol*.; 284(2):H727-34.

Ramirez S, Ait-Si-Ali S, Robin P, Trouche D, Harel-Bellan A. (1997). The CREB-binding protein (CBP) cooperates with the serum response factor for transactivation of the c-fos serum response element. *J Biol Chem*.; 272(49):31016-21. Erratum in: J Biol Chem; 274(25):18140.

Reimer KA. (1996). The slowing of ischemic energy demand in preconditioned myocardium. *Ann N Y Acad Sci*.; 793:13-26.

Reimer KA, Murry CE, Yamasawa I, Hill ML, Jennings RB. (1986). Four brief periods of myocardial ischemia cause no cumulative ATP loss of necrosis. *Am J. Physiol*.; 251(6 Pt 2):H1306-15.

Rellos P, Pike AC, Niesen FH, Salah E, Lee WH, von Delft F, Knapp S. (2010). Structure of the CaMKIIdelta/calmodulin complex reveals the molecular mechanism of CaMKII kinase activation. *PLoS Biol*.; 8(7):e1000426.

Rezazadeh S, Claydon TW, Fedida D. (2006) KN-93 (2-[N-(2-hydroxyethyl)]-N-(4-methoxybenzenesulfonyl)]amino-N-(4-chlorocinnamyl)-N-methylbenzylamine), a calcium/calmodulin-dependent protein kinase II inhibitor, is a direct extracellular blocker of voltage-gated potassium channels. *J. Pharmacol Exp Ther*.;317(1):292-9.

Rodrigues MA, Gomes DA, Nathanson MH, Leite MF. (2009). Nuclear calcium signaling: a cell within a cell. *Braz J Med Biol Res*.; 42(1):17-20.

Rodríguez-Sinovas A, Cabestrero A, García del Blanco B, Inserte J, García A, García-Dorado D. (2009). Intracoronary acid infusion as an alternative to ischemic postconditioning in pigs. *Basic Res Cardiol*.; 104(6):761-71.

Rosenberg OS, Deindl S, Comolli LR, Hoelz A, Downing KH, Nairn AC, Kuriyan J. (2006). Oligomerization states of the association domain and the holoenyzme of Ca^{2+}/CaM kinase II. *FEBS J*.; 273(4):682-94.

Ruiz-Meana M, Fernandez-Sanz C, Garcia-Dorado D. (2010). The SR-mitochondria interaction: a new player in cardiac pathophysiology. *Cardiovasc Res*.; 88(1):30-9.

Sag CM, Wadsack DP, Khabbazzadeh S, Abesser M, Grefe C, Neumann K, Opiela MK, Backs J, Olson EN, Brown JH, Neef S, Maier SK, Maier LS. (2009). Calcium/calmodulin-dependent protein kinase II contributes to cardiac arrhythmogenesis in heart failure. *Circ Heart Fail*.; 2(6):664-75.

Said M, Becerra R, Palomeque J, Rinaldi G, Kaetzel MA, Diaz-Sylvester PL, Copello JA, Dedman JR, Mundiña-Weilenmann C, Vittone L, Mattiazzi A. (2008). Increased intracellular Ca^{2+} and SR Ca^{2+} load contribute to arrhythmias after acidosis in rat heart. Role of Ca^{2+}/calmodulin-dependent protein kinase II. *Am J Physiol Heart Circ Physiol*.; 295(4):H1669-83.

Sakamoto J, Miura T, Goto M, Iimura O. (1995). Limitation of myocardial infarct size by adenosine A1 receptor activation is abolished by protein kinase C inhibitors in the rabbit. *Cardiovasc Res*.; 29(5):682-8.

Sakamoto K, Urushidani T, Nagao T. (1998). Translocation of HSP27 to cytoskeleton by repetitive hypoxia-reoxygenation in the rat myoblast cell line, H9c2. *Biochem Biophys Res Commun*.; 251(2):576-9.

Salas MA, Valverde CA, Sánchez G, Said M, Rodriguez JS, Portiansky EL, Kaetzel MA, Dedman JR, Donoso P, Kranias EG, Mattiazzi A. (2010). The signalling pathway of CaMKII-mediated apoptosis and necrosis in the ischemia/reperfusion injury. *J Mol Cell Cardiol*.; 48(6):1298-306.

Sandhu R, Diaz RJ, Mao GD, Wilson GJ. (1997). Ischemic preconditioning: differences in protection and susceptibility to blockade with single-cycle versus multicycle transient ischemia. *Circulation*.; 96(3):984-95.

Sandow A. (1952). Excitation-contraction coupling in muscular response. Y*ale J Biol Med*.; 25(3):176-201.

Sapia L, Palomeque J, Mattiazzi A, Petroff MV. (2010). Na^{+}/K^{+}-ATPase inhibition by ouabain induces CaMKII-dependent apoptosis in adult rat cardiac myocytes. *J Mol Cell Cardiol*.; 49(3):459-68.

Sardão VA, Oliveira PJ, Holy J, Oliveira CR, Wallace KB. (2007). Vital imaging of H9c2 myoblasts exposed to tert-butylhydroperoxide--characterization of morphological features of cell death. *BMC Cell Biol*.16; 8:11.

Satoh N, Kitada Y. (2004). Cardioprotective effect of MCC-135 is associated with inhibition of Ca^{2+} overload in ischemic/reperfused hearts. *Eur J Pharmacol*. 19;499(1-2):179-87.

Satoh N, Sato T, Shimada M, Yamada K, Kitada Y. (2001). Lusitropic effect of MCC135 is associated with improvement of sarcoplasmic reti culum function inventricular muscles of rats with diabetic cardiomyopathy. *J Pharmacol Exp Ther*.;298(3):1161-6.

Saucerman JJ, Bers DM. (2012). Calmodulin binding proteins provide domains of local Ca^{2+} signaling in cardiac myocytes. *J Mol Cell Cardiol*.; 52(2):312-6.

Schmidt MR, Smerup M, Konstantinov IE, Shimizu M, Li J, Cheung M, White PA, Kristiansen SB, Sorensen K, Dzavik V, Redington AN, Kharbanda RK. (2007). Intermittent peripheral tissue ischemia during coronary ischemia reduces myocardial infarction through a K_{ATP}-dependent mechanism: first demonstration of remote ischemic perconditioning. *Am J Physiol Heart Circ Physiol*.; 292(4):H1883-90.

Schwartz LM, Lagranha CJ. (2006). Ischemic postconditioning during reperfusion activates Akt and ERK without protecting against lethal myocardial ischemia-reperfusion injury in pigs. *Am J Physiol Heart Circ Physiol*. ; 290(3):H1011-8.

Schworer CM, Rothblum LI, Thekkumkara TJ, Singer HA. (1993). Identification of novel isoforms of the delta subunit of Ca^{2+}/calmodulin-dependent protein kinase II. Differential expression in rat brain and aorta. *J Biol Chem*.; 268(19):14443-9.

Sebbag L, Katsuragawa M, Verbinski S, Jennings RB, Reimer KA. (1996). Intracoronary administration of the alpha 1-receptor agonist, methoxamine, does not reproduce the infarct-limiting effect of ischemic preconditioning in dogs. *Cardiovasc Res*.; 32(5):830-8.

Shan J, Kushnir A, Betzenhauser MJ, Reiken S, Li J, Lehnart SE, Lindegger N, Mongillo M, Mohler PJ, Marks AR. (2010). Phosphorylation of the ryanodine receptor mediates the cardiac fight or flight response in mice. *J Clin Inves*t.; 120(12):4388-98.

Sharma A, Singh M. (2001). Protein kinase C activation and cardioprotective effect of preconditioning with oxidative stress in isolated rat heart. *Mol Cell Biochem*.; 219(1-2):1-6.

Sheu SS, Fozzard HA. (1982). Transmembrane Na^+ and Ca^{2+} electrochemical gradients in cardiac muscle and their relationship to force development. *J Gen Physio*l.; 80(3):325-51.

Shintani-Ishida K, Yoshida K. (2011). Ischemia induces phospholamban dephosphorylation via activation of calcineurin, PKC-α, and protein phosphatase 1, thereby inducing calcium overload in reperfusion. *Biochim Biophys Acta*.; 1812(7):743-51.

Singla SI, Hudmon A, Goldberg JM, Smith JL, Schulman H. (2001). Molecular characterization of calmodulin trapping by calcium/calmodulin-dependent protein kinase II. *J Biol Chem*.; 276(31):29353-60.

Sipido KR, Marban E. (1991). L-type calcium channels, potassium channels, and novel nonspecific cation channels in a clonal muscle cell line derived from embryonic rat ventricle. *Circ Res*.; 69(6):1487-99.

Skrzypiec-Spring M, Grotthus B, Szelag A, Schulz R. (2007). Isolated heart perfusion according to Langendorff- still viable in the new millennium. *J Pharmacol Toxicol Methods*.; 55(2):113-26.

Song Q, Saucerman JJ, Bossuyt J, Bers DM. (2008). Differential integration of Ca^{2+}-calmodulin signal in intact ventricular myocytes at low and high affinity Ca^{2+}-calmodulin targets. *J Biol Chem*.; 283(46):31531-40.

Sossalla S, Fluschnik N, Schotola H, Ort KR, Neef S, Schulte T, Wittköpper K, Renner A, Schmitto JD, Gummert J, El-Armouche A, Hasenfuss G, Maier LS. (2010). Inhibition of Elevated Ca^{2+}/Calmodulin-Dependent Protein Kinase II Improves Contractility in Human Failing Myocardium. *Circ Res*. 29;107(9):1150-61.

Srinivasan M, Edman CF, Schulman H. (1994). Alternative splicing introduces a nuclear localization signal that targets multifunctional CaM kinase to the nucleus. *J Cell Biol*.; 126(4):839-52.

Staat P, Rioufol G, Piot C, Cottin Y, Cung TT, L'Huillier I, Aupetit JF, Bonnefoy E, Finet G, André-Fouët X, Ovize M. (2005). Postconditioning the human heart. *Circulation*; 112(14):2143-8.

Stephanou A, Brar B, Liao Z, Scarabelli T, Knight RA, Latchman DS. (2001). Distinct initiator caspases are required for the induction of apoptosis in cardiac myocytes during ischaemia versus reperfusion injury. *Cell Death Differ*.; 8(4):434-5.

Sumi M, Kiuchi K, Ishikawa T, Ishii A, Hagiwara M, Nagatsu T, Hidaka H. (1991). The newly synthesized selective Ca^{2+}/calmodulin dependent protein kinase II inhibitor KN-93 reduces dopamine contents in PC12h cells. *Biochem Biophys Res Commun.*;181(3):968-75.

Sun HY, Wang NP, Kerendi F, Halkos M, Kin H, Guyton RA, Vinten-Johansen J, Zhao ZQ. (2005). Hypoxic postconditioning reduces cardiomyocyte loss by inhibiting ROS generation and intracellular Ca^{2+} overload. *Am J Physiol Heart Circ Physiol*.; 288(4):H1900-8.

Sutherland FJ, Hearse DJ. (2000). The isolated blood and perfusion fluid perfused heart. *Pharmacol Res*.; 41(6):613-27.

Tada M, Katz AM. (1982). Phosphorylation of the sarcoplasmic reticulum and sarcolemma. *Annu Rev Physiol*.; 44:401-23.

Takano H, Fukushi H, Morishima Y, Shirasaki Y. (2003). Calmodulin and calmodulin-dependent kinase II mediate neuronal cell death induced by depolarization. *Brain Res*.; 962(1-2):41-7.

Talukder MA, Zweier JL, Periasamy M. (2009). Targeting calcium transport in ischaemic heart disease. *Cardiovasc Res*.; 84(3):345-52.

Tan HL, Kupershmidt S, Zhang R, Stepanovic S, Roden DM, Wilde AAM, Anderson ME, Balser JR. (2002). A calcium sensor in the sodium channel modulates cardiac excitability. *Nature*; 415(6870):442.

Tanaka M, Fujiwara H, Yamasaki K, Sasayama S. (1994). Superoxide dismutase and N-2-mercaptopropionyl glycine attenuate infarct size limitation effect of ischaemic preconditioning in the rabbit. *Cardiovasc Res*.; 28(7):980-6.

Tandon N, Cannizzaro C, Chao PH, Maidhof R, Marsano A, Au HT, Radisic M, Vunjak-Novakovic G. (2009). Electrical stimulation systems for cardiac tissue engineering. *Nat Protoc*.; 4(2):155-73.

Tani M, Neely JR. (1989). Role of intracellular Na^{+} in Ca^{2+} overload and depressed recovery of ventricular function of reperfused ischemic rat hearts. Possible involvement of H^{+}-Na^{+} and Na^{+}-Ca^{2+} exchange. *Circ Res*.; 65(4):1045-56.

Temsah RM, Netticadan T, Chapman D, Takeda S, Mochizuki S, Dhalla NS. (1999). Alterations in sarcoplasmic reticulum function and gene expression in ischemic-reperfused rat heart. *Am J Physiol*.; 277(2 Pt 2):H584-94.

Temsah RM, Netticadan T, Kawabata K, Dhalla NS. (2002). Lack of both oxygen and glucose contributes to I/R-induced changes in cardiac SR function. *Am J Physiol Cell Physiol*; 283(4):C1306-12.

Tessier S, Karczewski P, Krause EG, Pansard Y, Acar C, Lang-Lazdunski M, Mercadier JJ, Hatem SN. (1999). Regulation of the transient outward K^+ current by Ca^{2+}/calmodulin-dependent protein kinases II in human atrial myocytes. *Circ Res*.; 85(9):810-9.

Thibault H, Piot C, Staat P, Bontemps L, Sportouch C, Rioufol G, Cung TT, Bonnefoy E, Angoulvant D, Aupetit JF, Finet G, André-Fouët X, Macia JC, Raczka F, Rossi R, Itti R, Kirkorian G, Derumeaux G, Ovize M. (2008). Long-term benefit of postconditioning. *Circulation*; 117(8):1037-44.

Toba K, Katagiri T, Takeyama Y. (1978). Studies of the cardiac sarcoplasmic reticulum in myocardial infarction. *Jpn Circ J*.; 42(4):447-53.

Tobimatsu T, Fujisawa H. (1989). Tissue-specific expression of four types of rat calmodulin-dependent protein kinase II mRNAs. *J Biol Chem*.; 264(30):17907-12.

Toischer K, Rokita AG, Unsöld B, Zhu W, Kararigas G, Sossalla S, Reuter SP, Becker A, Teucher N, Seidler T, Grebe C, Preuss L, Gupta SN, Schmidt K, Lehnart SE, Krüger M, Linke WA, Backs J, Regitz-Zagrosek V, Schäfer K, Field LJ, Maier LS, Hasenfuss G. (2010). Differential cardiac remodeling in preload versus afterload. *Circulation*; 122(10):993-1003.

Tomai F, Crea F, Chiariello L, Gioffrè PA. (1999). Ischemic preconditioning in humans: models, mediators, and clinical relevance. *Circulation.*; 100(5):559-63.

Tombes RM, Faison MO, Turbeville JM. (2003). Organization and evolution of multifunctional Ca^{2+}/CaM-dependent protein kinase genes. *Gene*.; 322:17-31.

Towbin H, Staehelin T, Gordon J. (1979). Electrophoretic transfer of proteins from polyacrylamide gels to nitrocellulose sheets: procedure and some applications. *Proc Natl Acad Sci U S A*.; 76(9):4350-4.

Trafford AW, Díaz ME, Eisner DA. (2001). Coordinated control of cell Ca^{2+} loading and triggered release from the sarcoplasmic reticulum underlies the rapid inotropic response to increased L-type Ca^{2+} current. *Circ Res*.; 88(2):195-201.

Tsang A, Hausenloy DJ, Mocanu MM, Yellon DM. (2004). Postconditioning: a form of "modified reperfusion" protects the myocardium by activating the phosphatidylinositol 3-kinase-Akt pathway. *Circ Res*.; 95(3):230-2.

Tsuji Y, Hojo M, Voigt N, El-Armouche A, Inden Y, Murohara T, Dobrev D, Nattel S, Kodama I, Kamiya K. (2011). Ca^{2+}-related signaling and protein phosphorylation abnormalities play central roles in a new experimental model of electrical storm. *Circulation*.; 123(20):2192-203.

Tsung A, Klune JR, Zhang X, Jeyabalan G, Cao Z, Peng X, Stolz DB, Geller DA, Rosengart MR, Billiar TR. (2007). HMGB1 release induced by liver ischemia involves Toll-like receptor 4 dependent reactive oxygen species production and calcium-mediated signaling. *J Exp Med*. 26; 204(12):2913-23.

Tunwell RE, Wickenden C, Bertrand BM, Shevchenko VI, Walsh MB, Allen PD, Lai FA. (1996). The human cardiac muscle ryanodine receptor-calcium release channel: identification, primary structure and topological analysis. *Biochem J*.; 318 (Pt 2):477-87.

Tyers GF, Williams EH, Hughes HC, Todd GJ. (1977). Effect of perfusate temperature on myocardial protection from ischemia. *J Thorac Cardiovasc Surg*.; 73(5):766-71.

Tzivoni D, Balkin J, Bär FW, Hibberd M, Reiber JH, Cowing G. (2009). Effect of caldaret on the incidence of severe left ventricular dysfunction in patients with ST-elevation myocardial infarction undergoing primary coronary intervention. *Am J Cardiol*.; 103(1):1-4.

Uchiyama T, Engelman RM, Maulik N, Das DK. (2004). Role of Akt signaling in mitochondrial survival pathway triggered by hypoxic preconditioning. *Circulation*.; 109(24):3042-9.

Uemura A, Naito Y, Matsubara T. (2002). Dynamics of Ca^{2+}/calmodulin-dependent protein kinase II following acute myocardial ischemia-translocation and autophosphorylation. *Biochem Biophys Res Commun*.; 297(4):997-1002.

Uetani T, Nakayama H, Okayama H, Okura T, Higaki J, Inoue H, Higashiyama S. (2009). Insufficiency of pro-heparin-binding epidermal growth factor-like growth factor shedding enhances hypoxic cell death in H9c2 cardiomyoblasts via the activation of caspase-3 and c-Jun N-terminal kinase. *J Biol Chem*.; 284(18):12399-409.

Unal B., Critchley J.A., Capewell S. (2004) Explaining the decline in coronary heart disease mortality in England and Wales between 1981 and 2000. *Circulation*; 109 (9): 1101-7.

Valverde CA, Kornyeyev D, Ferreiro M, Petrosky AD, Mattiazzi A, Escobar AL. (2010). Transient Ca^{2+} depletion of the sarcoplasmic reticulum at the onset of reperfusion. *Cardiovasc Res*.; 85(4):671-80.

Valverde CA, Mundiña-Weilenmann C, Reyes M, Kranias EG, Escobar AL, Mattiazzi A. (2006). Phospholamban phosphorylation sites enhance the recovery of intracellular Ca^{2+} after perfusion arrest in isolated, perfused mouse heart. *Cardiovasc Res*.; 70(2):335-45.

Valverde CA, Mundiña-Weilenmann C, Said M, Ferrero P, Vittone L, Salas M, Palomeque J, Petroff MV, Mattiazzi A. (2005). Frequency-dependent acceleration of relaxation in mammalian heart: a property not relying on phospholamban and SERCA2a phosphorylation. *J Physiol*.; 562(Pt 3):801-13.

Verdouw PD, van den Doel MA, de Zeeuw S, Duncker DJ. (1998). Animal models in the study of myocardial ischaemia and ischaemic syndromes. *Cardiovasc Res*.; 39(1):121-35.

Vest RS, Davies KD, O'Leary H, Port JD, Bayer KU. (2007). Dual mechanism of a natural CaMKII inhibitor. *Mol Biol Cell*.; 18(12):5024-33.

Vila-Petroff M, Mundiña-Weilenmann C, Lezcano N, Snabaitis AK, Huergo MA, Valverde CA, Avkiran M, Mattiazzi A. (2010). Ca^{2+}/calmodulin-dependent protein kinase II contributes to intracellular pH recovery from acidosisvia Na^{+}/H^{+} exchanger activation. *J Mol Cell Cardiol*.; 49(1):106-12.

Vila-Petroff M, Salas MA, Said M, Valverde CA, Sapia L, Portiansky E, Hajjar RJ, Kranias EG, Mundiña-Weilenmann C, Mattiazzi A. (2007). CaMKII inhibition protects against necrosis and apoptosis in irreversible ischemia-reperfusion injury. *Cardiovasc Res*.; 73(4):689-98.

Vinten-Johansen J, Shi W. (2011). Perconditioning and postconditioning: current knowledge, knowledge gaps, barriers to adoption, and future directions. *J Cardiovasc Pharmacol Ther*.; 16(3-4):260-6.

Vittone L, Mundiña-Weilenmann C, Said M, Ferrero P, Mattiazzi A. (2002). Time course and mechanisms of phosphorylation of phospholamban residues in ischemia-reperfused rat hearts. Dissociation of phospholamban phosphorylation pathways. *J Mol Cell Cardiol*.; 34(1):39-50.

Wagner S, Dybkova N, Rasenack EC, Jacobshagen C, Fabritz L, Kirchhof P, Maier SK, Zhang T, Hasenfuss G, Brown JH, Bers DM, Maier LS. (2006). Ca^{2+}/calmodulin-dependent protein kinase II regulates cardiac Na^{+} channels. *J Clin Invest*; 116(12):3127-38.

Wayman GA, Tokumitsu H, Davare MA, Soderling TR. (2011). Analysis of CaM-kinase signaling in cells. *Cell Calcium.*; 50(1):1-8.

Weber CR, Ginsburg KS, Bers DM. (2003). Cardiac submembrane [Na^{+}] transients sensed by Na^{+}-Ca^{2+} exchange current. *Circ Res*.; 92(9):950-2.

Wehrens XH, Lehnart SE, Reiken SR, Marks AR. (2004). Ca^{2+}/calmodulin-dependent protein kinase II phosphorylation regulates the cardiac ryanodine receptor. *Circ Res*.; 94(6):e61-70.

WHO (2011). Global Atlas on cardiovascular disease prevention and control. Mendis S, Puska P, Norrving B editors. World Health organization, Geneva 2011.

Witcher DR, Kovacs RJ, Schulman H, Cefali DC, Jones LR. (1991). Unique phosphorylation site on the cardiac ryanodine receptor regulates calcium channel activity. *J Biol Chem*.; 266(17):11144-52.

Woischwill C, Karczewski P, Bartsch H, Luther HP, Kott M, Haase H, Morano I. (2005). Regulation of the human atrial myosin light chain 1 promoter by Ca^{2+}-calmodulin-dependent signaling pathways. *FASEB J*; 19(6):503-11.

Wu X, Zhang T, Bossuyt J, Li X, McKinsey TA, Dedman JR, Olson EN, Chen J, Brown JH, Bers DM. (2006). Local InsP3-dependent perinuclear Ca^{2+} signaling in cardiac myocyte excitation-transcription coupling. *J Clin Invest*.; 116(3):675-82.

Wu Y, MacMillan LB, McNeill RB, Colbran RJ, Anderson ME. (1999). CaM kinase augments cardiac L-type Ca^{2+} current: a cellular mechanism for long Q-T arrhythmias. *Am J Physiol*.; 276(6 Pt 2):H2168-78.

Xie F, Qu Z, Garfinkel A, Weiss JN. (2001). Effects of simulated ischemia on spiral wave stability. *Am J Physiol Heart Circ Physiol*.; 280(4):H1667-73.

Xie Y, Zhu WZ, Zhu Y, Chen L, Zhou ZN, Yang HT. (2004). Intermittent high altitude hypoxia protects the heart against lethal Ca^{2+} overload injury. *Life Sci*.; 76(5):559-72.

Xu L, Mann G, Meissner G. (1996). Regulation of cardiac Ca^{2+} release channel (ryanodine receptor) by Ca^{2+}, H^{+}, Mg^{2+}, and adenine nucleotides under normal and simulated ischemic conditions. *Circ Res.*; 79(6):1100-9.

Yaglom JA, Ekhterae D, Gabai VL, Sherman MY. (2003). Regulation of necrosis of H9c2 myogenic cells upon transient energy deprivation. Rapid deenergization of mitochondria precedes necrosis and is controlled by reactive oxygen species, stress kinase JNK, HSP72 and ARC. *J Biol Chem*.; 278(50):50483-96.

Yan X, Gao S, Tang M, Xi J, Gao L, Zhu M, Luo H, Hu X, Zheng Y, Hescheler J, Liang H. (2011). Adenylyl cyclase/cAMP-PKA-mediated phosphorylation of basal L-type Ca^{2+} channels in mouse embryonic ventricular myocytes. *Cell Calcium*.; 50(5):433-43.

Yan XS, Ma JH, Zhang PH. (2009). Modulation of K_{ATP} currents in rat ventricular myocytes by hypoxia and a redox reaction. *Acta Pharmacol Sin*.; 30(10):1399-414.

Yang D, Zhu WZ, Xiao B, Brochet DX, Chen SR, Lakatta EG, Xiao RP, Cheng H. (2007). Ca^{2+}/calmodulin kinase II-dependent phosphorylation of ryanodine receptors suppresses Ca^{2+} sparks and Ca^{2+} waves in cardiac myocytes. *Circ Res*.; 100(3):399-407.

Yang X, Cohen MV, Downey JM. (2010). Mechanism of cardioprotection by early ischemic preconditioning. *Cardiovasc Drugs Ther*.; 24(3):225-34.

Yang XM, Proctor JB, Cui L, Krieg T, Downey JM, Cohen MV. (2004). Multiple, brief coronary occlusions during early reperfusion protect rabbit hearts by targeting cell signalling pathways. *J Am Coll Cardiol*.; 44(5):1103-10.

Yang Z, Steele DS. (2001). Effects of cytosolic ATP on Ca^{2+} sparks and SR Ca^{2+} content in permeabilized cardiac myocytes. *Circ Res*.; 89(6):526-33.

Yellon DM, Alkhulaifi AM, Pugsley WB. (1993). Preconditioning the human myocardium. *Lancet*.; 342(8866):276-7.

Yellon DM, Downey JM. (2003). Preconditioning the myocardium: from cellular physiology to clinical cardiology. *Physiol Rev*. ;83(4):1113-51.

Yetgin T, Manintveld OC, Duncker DJ, van der Giessen WJ. (2010). Postconditioning against ischaemia-reperfusion injury: ready for wide application in patients? *Neth Heart J*.; 18(7-8):389-92.

Youn HJ, Kim HS, Jeon MH, Lee JH, Seo YJ, Lee YJ, Lee JH. (2005). Induction of caspase-independent apoptosis in H9c2 cardiomyocytes by adriamycin treatment. *Mol Cell Biochem*.; 270(1-2):13-9.

Yu Z, Wang ZH, Yang HT. (2009). Calcium/calmodulin-dependent protein kinase II mediates cardioprotection of intermittent hypoxia against ischemic-reperfusion-induced cardiac dysfunction. *Am J Physiol Heart Circ Physiol*.; 297(2):H735-42.

Yurukova S, Kilić A, Völker K, Leineweber K, Dybkova N, Maier LS, Brodde OE, Kuhn M. (2007). CaMKII-mediated increased lusitropic responses to beta-adrenoreceptor stimulation in ANP-receptor deficient mice. *Cardiovasc Res*.; 73(4):678-88.

Zalewska T, Zabłocka B, Domańska-Janik K. (1996). Changes of Ca^{2+}/calmodulin-dependent protein kinase-II after transient ischemia in gerbil hippocampus. *Acta Neurobiol Exp* (Wars).; 56(1):41-8.

Zaza and Rosen, (2000). An introduction to cardiac electrophysiology. *Informa Healthcare*

Zhang R, Khoo MS, Wu Y, Yang Y, Grueter CE, Ni G, Price EE Jr, Thiel W, Guatimosim S, Song LS, Madu EC, Shah AN, Vishnivetskaya TA, Atkinson JB, Gurevich VV, Salama G, Lederer WJ, Colbran RJ, Anderson ME. (2005). Calmodulin kinase II inhibition protects against structural heart disease. *Nat Med*.; 11(4):409-17.

Zhang T, Johnson EN, Gu Y, Morissette MR, Sah VP, Gigena MS, Belke DD, Dillmann WH, Rogers TB, Schulman H, Ross J Jr, Brown JH. (2002). The cardiac-specific nuclear $delta_B$ isoform of Ca^{2+}/calmodulin-dependent protein kinase II induces hypertrophy and dilated cardiomyopathy associated with increased protein phosphatase 2A activity. *J Biol Chem*.; 277(2):1261-7.

Zhang T, Kohlhaas M, Backs J, Mishra S, Phillips W, Dybkova N, Chang S, Ling H, Bers DM, Maier LS, Olson EN, Brown JH. (2007). CaMKIIdelta isoforms differentially affect calcium handling but similarly regulate HDAC/MEF2 transcriptional responses. *J Biol Chem*.; 282(48):35078-87.

Zhang T, Maier LS, Dalton ND, Miyamoto S, Ross J Jr, Bers DM, Brown JH. (2003). The deltaC isoform of CaMKII is activated in cardiac hypertrophy and induces dilated cardiomyopathy and heart failure. *Circ Res*.; 92(8):912-9.

Zhao ZQ, Corvera JS, Halkos ME, Kerendi F, Wang NP, Guyton RA, Vinten-Johansen J. (2003). Inhibition of myocardial injury by ischemic postconditioning during reperfusion: comparison with ischemic preconditioning. *Am J Physiol Heart Circ Physiol*.; 285(2):H579-88.

Zheng M, Reynolds C, Jo SH, Wersto R, Han Q, Xiao RP. (2005). Intracellular acidosis-activated p38 MAPK signaling and its essential role in cardiomyocyte hypoxic injury. *FASEB J*.; 19(1):109-11.

Zhu HL, Wei X, Qu SL, Zhang C, Zuo XX, Feng YS, Luo Q, Chen GW, Liu MD, Jiang L, Xiao XZ, Wang KK. (2011). Ischemic postconditioning protects cardiomyocytes against ischemia/reperfusion injury by inducing MIP2. *Exp Mol Med*.; 43(8):437-45.

Zhu W, Woo AY, Yang D, Cheng H, Crow MT, Xiao RP. (2007). Activation of CaMKIIdeltaC is a common intermediate of diverse death stimuli-induced heart muscle cell apoptosis. *J Biol Chem*. ; 282(14):10833-9.

Zhu W, Zou Y, Shiojima I, Kudoh S, Aikawa R, Hayashi D, Mizukami M, Toko H, Shibasaki F, Yazaki Y, Nagai R, Komuro I. (2000). Ca^{2+}/calmodulin-dependent kinase II and calcineurin play critical roles in endothelin-1-induced cardiomyocyte hypertrophy. *J Biol Chem*.; 275(20):15239-45.

Zhu WZ, Wang SQ, Chakir K, Yang D, Zhang T, Brown JH, Devic E, Kobilka BK, Cheng H, Xiao RP. (2003). Linkage of beta1-adrenergic stimulation to apoptotic heart cell death through protein kinase A-independent activation of Ca^{2+}/calmodulin kinase II. *J Clin Invest*; 111(5):617-25.

Zima AV, Blatter LA. (2006). Redox regulation of cardiac calcium channels and transporters. *Cardiovasc Res*.;71(2):310-21.

Zimmer HG (1998). The Isolated Perfused Heart and Its Pioneers. *News Physiol Sci*.; 13:203-210.

Zou Y, Yao A, Zhu W, Kudoh S, Hiroi Y, Shimoyama M, Uozumi H, Kohmoto O, Takahashi T, Shibasaki F, Nagai R, Yazaki Y, Komuro I. (2001). Isoproterenol activates extracellular signal-regulated protein kinases in cardiomyocytes through calcineurin. *Circulation*.; 104(1):102-8.